

5-2010

SYNTHESIS OF META-TERPHENYL SCAFFOLDED MOLECULES FOR CATALYSIS AND SENSOR APPLICATIONS

Brad Morgan

Clemson University, bradm@clemson.edu

Follow this and additional works at: https://tigerprints.clemson.edu/all_dissertations



Part of the [Inorganic Chemistry Commons](#)

Recommended Citation

Morgan, Brad, "SYNTHESIS OF META-TERPHENYL SCAFFOLDED MOLECULES FOR CATALYSIS AND SENSOR APPLICATIONS" (2010). *All Dissertations*. 555.

https://tigerprints.clemson.edu/all_dissertations/555

This Dissertation is brought to you for free and open access by the Dissertations at TigerPrints. It has been accepted for inclusion in All Dissertations by an authorized administrator of TigerPrints. For more information, please contact kokeefe@clemson.edu.

SYNTHESIS OF META-TERPHENYL SCAFFOLDED MOLECULES FOR
CATALYSIS AND SENSOR APPLICATIONS

A Dissertation
Presented to
the Graduate School of
Clemson University

In Partial Fulfillment
of the Requirements for the Degree
Doctor of Philosophy
Chemistry

by
Brad P. Morgan
May 2010

Accepted by:
Dr. Rhett C. Smith, Committee Chair
Dr. Gautam Bhattacharyya
Dr. Julia L. Brumaghim
Dr. William T. Pennington

ABSTRACT

The utility of the *m*-terphenyl has been observed in a wide variety of applications since its first discovery. The tunable conformational flexibility contributes to the unique properties and resulting applications thereof. Chapter 1 goes into detail about the concepts used throughout and defines the tools needed to understand the chemistry in the resulting chapters.

The primary use of the *m*-terphenyl herein is as a canopy that shields a pocket created underneath the central ring. Functionalization within this pocket allows metal binding in defined coordination environments, with the use of donor ligands attached to the flanking rings. The applications of these metal complexes are discussed throughout Chapters 2, 3 and 4.

Chapters 5 and 6 describe a different approach wherein the focus was on exploiting the defined pocket shape to enhance sensing mechanisms. A good sensor must be selective for one analyte over others; this is typically achieved through electronic or steric considerations. The *m*-terphenyl canopy can be used to sterically control what analytes can interact with the molecule. Applications of *m*-terphenyl dizinc complexes that selectively sense pyrophosphates over other analytes are discussed in Chapter 5. The use of a *m*-terphenyl scaffold in a poly(*p*-phenylene ethynylene) derivative discussed in Chapter 6 shows how steric porosity control can enhance the rate of nitroaromatic detection by polymer films.

Our eyesight is a test to see if we can see beyond it.

Matter is here as a test for our curiosity.

Examine the nature of everything you observe.

-Waking Life

DEDICATION

To those who believe in me.

ACKNOWLEDGMENTS

I first wish to thank my research advisor Dr. Rhett C. Smith for his guidance and encouragement throughout. He is an exceptional mentor and his enthusiasm for the field of chemistry and his example has allowed me to become a better chemist. I will forever look back with pride for having worked with Dr. Smith. I would not have developed into the person I am today without his influence in my life. I am also grateful for the encouragement and support I have received from the Smith group. I would like to thank Anshuman Mangalum, Susan He and Ellie Tennyson in particular for making our work environment enjoyable and productive. I was fortunate to have the ability to guide several undergraduates through a part of their experience in chemistry and I am grateful for their continued work ethic and inquisitive minds, which continually kept me on my toes. The undergraduate students that helped produce the data within this dissertation are listed as co-authors in the footnotes of each chapter.

I would also like to thank Dr. Don VanDerveer for his input and great discussions on crystallography. The Chemistry Department at Clemson has been a great facility to work within and I appreciate everything the department has provided for both me and the Smith group. I would like to express gratitude to my committee members Dr. Gautam Bhattacharyya, Dr. Julia L. Brumaghim and Dr. William T. Pennington for their time and encouraging support.

My parents, Charles and Donna Morgan, have played a vital part of developing me into the man I am today, and I am grateful for their continued love and support throughout my life. My brother has been a great confidant and I appreciate his

encouragement. Lindsay's wonderful family has been so accepting of me and I am thankful for their moral support. I would have never believed that a soul mate as wonderful as Lindsay existed, much less that we would somehow find each other. I feel so blessed to have such a wonderful encourager and supporter throughout my graduate studies. I appreciate everything you do and I am lucky to have you.

TABLE OF CONTENTS

	Page
TITLE PAGE	i
ABSTRACT	ii
DEDICATION	iv
ACKNOWLEDGMENTS	v
LIST OF TABLES	x
LIST OF FIGURES	xii
LIST OF SCHEMES.....	xix
CHAPTER	
I. GENERAL INTRODUCTION.....	1
1. Ligands.....	3
1. Phosphines	8
2. Carbenes.....	12
2. meta-Terphenyl	14
1. Synthesis of <i>m</i> -Terphenyls.....	16
3. Catalysts	20
4. Chemical Sensing	22
5. Aim and Scope.....	29
6. References.....	33
II. 1,4-CONJUGATE ADDITION OF ARYLBORONIC ACIDS TO ENONES UTILIZING TERPHSPAN COMPLEXES	38
1. Introduction.....	38
2. Synthesis, Structure and Catalytic Activity	44
3. Conclusion	52
4. Experimental Details.....	53
5. Selected Spectra	55
6. References.....	61

Table of Contents (Continued)

III.	SYNTHESIS, TRANSFER REAGENTS AND CATALYTIC APPLICATIONS OF BIS N-HETEROCYCLIC CARBENES BASED ON TERPHENYL SCAFFOLDS.....	67
	1. Introduction.....	67
	2. Synthesis and reactivity	72
	3. Structure.....	81
	4. Suzuki Cupling.....	90
	5. Conclusions.....	97
	6. Experimental.....	98
	7. Selected Spectra.....	102
	8. References.....	111
IV.	HYDROFORMYLATION OF STYRENE USING PHOSPHINES WHICH INCLUDE A META-TERPHENYL	119
	1. Introduction.....	119
	2. Results and Discussion	128
	3. Conclusions.....	136
	4. Experimental Details.....	137
	5. Selected Spectra.....	140
	6. References.....	144
V.	PHOSPHORUS OXYANION DETECTION BASED ON CANOPIES WITH SCAFFOLDED DIMETALLIC SITES FOR SENSING APPLICATIONS	148
	1. Overview of Phosphorus Oxyanions	148
	2. Results and Discussion	158
	3. Conclusions.....	164
	4. Experimental Details.....	165
	5. Selected Spectra.....	166
	6. References.....	189

Table of Contents (Continued)

VI.	POLY(PARA-PHENYLENE ETHYNYLENE) INCORPORATING STERICALLY ENSHROUDING META-TERPHENYL OXACYCLOPHANE CANOPIES	195
	1. Introduction.....	195
	2. Results and Discussion	201
	3. Experimental Details.....	210
	4. Conclusions.....	214
	5. Selected Spectra.....	215
	6. References.....	219
. VII.	CONCLUSIONS AND FURTHER DIRECTIONS.....	223
	BIBLIOGRAPHY.....	224

LIST OF TABLES

Table	Page
1.1	Examples of ligands commonly used in organometallic compounds..... 6
1.2	Gutmann donor and acceptor numbers and dielectric constants for selected solvents 25
2.1	Select Bond Lengths and Angles for 1-DMF 48
2.2	Crystal Data and Structure Refinement Details for 1-DMF 49
2.3	Catalytic 1,4-addition of boronic acids to α,β -unsaturated enones 50
3.1	Yields of Suzuki-Miyaura coupling reactions in the presence of $[\text{Cl}_2\text{Pd}(\mathbf{1})]$ 84
3.2	Selected bond lengths and angles for $\{[\text{Ag}(\mathbf{1})]\text{AgBr}_2\}_2$ 85
3.3	Selected bond lengths and angles for $[\text{PdX}_2(\mathbf{1})] \cdot \text{PhCH}_3$ 88
3.4	Crystal data and structure refinement details of $[\text{PdX}_2(\mathbf{1})] \cdot \text{PhCH}_3$ 89
3.5	Yields of Suzuki-Miyaura coupling reactions in the presence of $[\text{Cl}_2\text{Pd}(\mathbf{1})]$ 90
3.6	Selected bond lengths and angles for $[\mu\text{-ClPd}(\text{PPh}_2\text{OH})(\text{PPh}_2\text{O})]_2$ 92
3.7	Yields of Suzuki-Miyaura coupling reactions in the presence of $[\text{Cl}_2\text{Pd}(\mathbf{L})]$ 93
3.8	Crystal data and structure refinement details of $[\mu\text{-ClPd}(\text{PPh}_2\text{OH})(\text{PPh}_2\text{O})]_2$ 96
4.1	Refinement details for $\text{IrCl}(\text{COD})(\text{L1})$ 130
4.2	Refinement details for L4 133
4.5	Catalytic Results for the Hydroformylation of styrene using terphspan ligands 134

List of Tables (Continued)

Table	Page
5.1 Absorption data and photos demonstrating the range of colorimetric responses observed in free, bound and pyrophosphate-displaced states....	160
6.1 Select photophysical properties of P1 and P2 solutions in THF.....	203
6.2 Refinement details for M1	218

LIST OF FIGURES

Figure		Page
1.1	Examples of ligand interactions.....	3
1.2	Examples of electron donating ability (Δv)	8
1.3	Tolman cone angles (θ) for tertiary phosphines and Natural bite angle (β) for diphosphines.....	9
1.4	Steric and electronic map of electronic parameter (v) and cone angle (θ)...	10
1.5	Examples of ligand bite angles of some common phosphines.	11
1.6	Examples of singlet and triplet carbenes.	12
1.7	Structures and orbital representations of the first Fischer & Schrock carbene complexes and the first structurally characterized “free” Arduengo carbenes.....	13
1.8	Two representations of the conformation of <i>m</i> -terphenyl.....	14
1.9	Various means to aryl-aryl bond formation that lead to the one pot synthesis of <i>m</i> -Terphenyls.	16
1.10	Synthetic routes to <i>m</i> -terphenyl scaffolds used herein	19
1.11	Example of catalyzed reactions by lowering the energy of the transition state or by finding alternate pathways to intermediates.....	20
1.12	Example of catalysis by raising the energy of the reactant.....	21
1.13	“Lock and Key” model of molecular recognition.....	23
1.14	Conceptual representation of a guest-induced signal transduction event	26
1.15	General representation of an indicator displacement assay.	27
2.1	Example of steric repulsion from the generation of 1,4 addition reactions	39

List of Figures (Continued)

Figure	Page
2.2 Ligands used for 1,4 conjugate addition of enones and some examples of some wide bite angle diphosphines.	42
2.3 ORTEP drawing (50% probability ellipsoids) of the molecular structure of 1.	47
2.4 Proton NMR spectrum of 1·DMF (CDCl ₃ , 500 MHz) referenced to residual CHCl ₃ . Note that peaks at 2.94, 2.88, and 8.06 are attributable to cocrystallized DMF.....	55
2.5 Aromatic region, proton NMR spectrum of 1·DMF (CDCl ₃ , 500 MHz)	55
2.6 Inset above 7.5 ppm, proton NMR spectrum of 1·DMF (CDCl ₃ , 500 MHz).....	56
2.7 Region from 4.5 ppm to 6.5 ppm, proton NMR spectrum of 1·DMF (CDCl ₃ , 500 MHz).....	56
2.8 Aliphatic region, proton NMR spectrum of 1·DMF (CDCl ₃ , 500 MHz).....	57
2.9 Carbon-13 NMR spectrum of 1·DMF (CDCl ₃ , 126 MHz). Referenced to CDCl ₃	57
2.10 Aromatic region, carbon-13 NMR spectrum of 1·DMF (CDCl ₃ , 126 MHz).....	58
2.11 Region above 140 ppm, carbon-13 NMR spectrum of 1·DMF (CDCl ₃ , 126 MHz).....	58
2.12 Aliphatic region, carbon-13 NMR spectrum of 1·DMF (CDCl ₃ , 126 MHz).....	59
2.13 Phosphorus-31 NMR spectrum of 1·DMF (CDCl ₃ , 121 MHz)	59
2.14 Inset, phosphorus-31 NMR spectrum of 1·DMF (CDCl ₃ , 121 MHz).....	60
3.1 Exemplary examples of N-heterocyclic carbenes (NHCs)	67

List of Figures (Continued)

Figure	Page
3.2 Variants of Grubb's catalyst for olefin metathesis.	69
3.3 Examples of crystallographically characterized bidentate bis(NHC) complexes with C–M–C angles of $\geq 170^\circ$	71
3.4 Structures of canopied ligands that chelate metals via carbene, phosphine, and diphosphinite moieties..	72
3.5 ^1H - ^1H Correlated Spectrum (COSY) of $[\text{Ag}(1)]\text{AgBr}_2$ (DMSO, 300 MHz)	77
3.6 Nuclear Overhauser Effect Difference (NOE-DIFF) Spectrum of $[\text{Ag}(1)]\text{AgBr}_2$ (DMSO, 300 MHz) for protons resonating at 3.96 ppm.	79
3.7 Some binding modes of silver(I) complexes featuring mono- (top) and bis- (bottom) N-heterocyclic carbene ligands that have been observed in the solid state by Xray diffraction.	81
3.8 ORTEP drawing (50% probability ellipsoids) of the molecular structure of $\{[\text{Ag}(1)]\text{AgBr}_2\}_2$	82
3.9 ORTEP drawing (50% probability ellipsoids) of the molecular structure of $[\text{X}_2\text{Pd}(1)]$	87
3.10 ORTEP drawing (50% probability ellipsoids) of the molecular structure of $[\mu\text{-ClPd}(\text{PPh}_2\text{OH})(\text{PPh}_2\text{O})]_2$	95
3.11 Proton NMR spectrum of $[\text{Ag}(1)]\text{AgBr}_2$ (DMSO, 300 MHz).....	102
3.12 Aromatic Region of the ^1H NMR spectrum of $[\text{Ag}(1)]\text{AgBr}_2$ (DMSO , 300 MHz).....	102
3.13 Aliphatic Region of the ^1H NMR spectrum of $[\text{Ag}(1)]\text{AgBr}_2$ (DMSO, 300 MHz).....	103
3.14 Nuclear Overhauser Effect Difference (NOE-DIFF) Spectrum of $[\text{Ag}(1)]\text{AgBr}_2$ (DMSO, 300 MHz) for protons resonating at 5.43 ppm. ...	103
3.15 Carbon-13 NMR spectrum of $[\text{Ag}(1)]\text{AgBr}_2$ (DMSO, 75 MHz)	104

List of Figures (Continued)

Figure	Page
3.16 Aromatic region of the ^{13}C NMR spectrum of $[\text{Ag}(1)]\text{AgBr}_2$ (DMSO, 75 MHz).....	104
3.17 Heteronuclear Multiple Quantum Coherence (HMQC) spectrum of $[\text{Ag}(1)]\text{AgBr}_2$ (300 MHz for ^1H , 75 MHz for ^{13}C , in DMSO).....	105
3.18 Distortionless Enhancement by Polarization Transfer (DEPT-135) spectrum of $[\text{Ag}(1)]\text{AgBr}_2$ (DMSO, 75 MHz).....	105
3.19 Aromatic region of DEPT-135 spectrum of $[\text{Ag}(1)]\text{AgBr}_2$ (DMSO, 75 MHz).....	106
3.20 Proton NMR spectrum of $[\text{H}_2\text{1}]\text{Br}_2$ (DMSO, 300 MHz).....	106
3.21 Aromatic Region of the ^1H NMR spectrum of $[\text{H}_2\text{1}]\text{Br}_2$ (DMSO, 300 MHz).....	107
3.22 ^{13}C NMR spectrum of $[\text{H}_2\text{1}]\text{Br}_2$ (CD_3CN , 75 MHz).....	107
3.23 Aromatic region of the ^{13}C NMR spectrum of $[\text{H}_2\text{1}]\text{Br}_2$ (CD_3CN , 75 MHz).....	108
3.24 ^1H NMR spectrum of $[\text{Cl}_2\text{Pd}(1)]$ (CDCl_3 , 300 MHz).....	108
3.25 Alliphatic region of the ^1H NMR spectrum of $[\text{Cl}_2\text{Pd}(1)]$ (CDCl_3 , 300 MHz).....	109
3.26 Aromatic region of the ^1H NMR spectrum of $[\text{Cl}_2\text{Pd}(1)]$ (CDCl_3 , 300 MHz).....	109
3.27 ^{13}C NMR spectrum of $[\text{Cl}_2\text{Pd}(1)]$ (CDCl_3 , 75 MHz).....	110
3.28 Aromatic region of the ^{13}C NMR spectrum of $[\text{Cl}_2\text{Pd}(1)]$ (CDCl_3 , 75 MHz).....	110
4.1 Dewar Chatt Duncanson model of pi back bonding of metal to a carbonyl ligand. used to measure electron donating ability of phosphines.....	120
4.2 Difference between the solid angle (Ω) and cone angle (Θ) as seen by trimethylphosphine.....	121

List of Figures (Continued)

Figure	Page
4.3	Some bidentate P-donor ligands for Rh-catalyzed hydroformylation 125
4.4	The generally accepted mechanism for the hydroformylation reaction of an olefin. 126
4.5	A proposed mechanism for the explanation of the preference for the linear aldehydes with the use of larger bite angles (120° and 180°) compared to (90°). 128
4.6	ORTEP drawing (50% probability ellipsoids) of the molecular structure of [IrCl(COD)(L1)]. 129
4.7	ORTEP drawing (50% probability ellipsoids) of the molecular structure of L4. 140
4.8	Proton NMR spectrum of L4 (CDCl ₃ , 300 MHz) referenced to residual CHCl ₃ 140
4.9	Phosphorus-31 NMR spectrum of L4 (CDCl ₃ , 121 MHz) 141
4.10	Carbon-13 NMR spectrum of L4 (CDCl ₃ , 75 MHz). Referenced to CDCl ₃ 141
4.11	Aromatic region, carbon-13 NMR spectrum of L4 (CDCl ₃ , 75 MHz)..... 142
4.12	Phosphorus-31 NMR spectrum of [IrCl(COD)(L1)] (CDCl ₃ , 121 MHz).. 142
4.13	Proton NMR spectrum of [IrCl(COD)(L1)] (CDCl ₃ , 300 MHz) referenced to residual CHCl ₃ 143
4.14	Phosphorus-31 NMR spectrum of L5 (CDCl ₃ , 121 MHz) 143
5.1	Examples of some phosphorus oxyanions 149
5.2	Dinucleating ligand and complexometric dyes used in the current study 153
5.3	Titration of ZC with Zn ₂ L1 , followed by UV-vis spectroscopy 162
5.4	Titration of alizarin red S (ARS). 166

List of Figures (Continued)

Figure	Page
5.5 Titration of bromo pyrogallol red (BPR).....	167
5.6 Titration of dithizone (DT).	168
5.7 Titration of eriochrome blue black B (EBBB).....	169
5.8 Titration of eriochrome red B (ERB).....	170
5.9 Titration of galloxyanine (GC).....	171
5.10 Titration of mordant blue 9 (MB9).	172
5.11 Titration of murexide (MX).....	173
5.12 Titration of 4-(pyridin-2-ylazo)resorcinol (PAR).....	174
5.13 Titration of pyrocatechol violet (PV).....	175
5.14 Titration of zincon (ZC).....	176
5.15 Proton NMR spectrum of H-L1 (CDCl ₃ , 300 MHz).....	177
5.16 Carbon-13 NMR spectrum of H-L1 (CDCl ₃ , 75 MHz).	177
5.17 Phosphate and pyrophosphate displacement tests for alizarin red S (ARS).....	178
5.18 Phosphate and pyrophosphate displacement tests for bromo pyrogallol red (BPR).....	179
5.19 Phosphate and pyrophosphate displacement tests for dithizone (DT).....	180
5.20 Phosphate and pyrophosphate displacement tests for eriochrome blue black B (EBBB).....	181
5.21 Phosphate and pyrophosphate displacement tests for eriochrome red B (ERB)	182

List of Figures (Continued)

Figure	Page
5.22 Phosphate and pyrophosphate displacement tests for gallocyanine (GC).....	183
5.23 Phosphate and pyrophosphate displacement tests for mordant blue 9 (MB9).....	184
5.24 Phosphate and pyrophosphate displacement tests for murexide (MX).	185
5.25 Phosphate and pyrophosphate displacement tests for 4-(pyridin-2-ylazo)resorcinol (PAR).	186
5.26 Phosphate and pyrophosphate displacement tests for pyrocatechol violet (PV).....	187
5.27 Phosphate and pyrophosphate displacement tests for zincon (ZC).....	188
6.1 Examples of sterically-insulated CPs (I-III) and of covalently-scaffolded π -systems (IV-VII), and the oxacyclophane scaffold VIII used in the current work.	195
6.2 ORTEP drawing, numbering scheme for M1 and optimized geometry indicating possible arrangements of canopy substituents around the backbone in a section of polymer P1	202
6.3 Absorption spectra in THF (1.0×10^{-6} M, left); and photoluminescence spectra of both films and THF solutions (right) for P1 and P2.....	207
6.4 ^1H NMR spectra of M1 in CDCl_3 at 500 MHz.....	215
6.5 Aromatic region of ^1H NMR spectra of M1 in CDCl_3 at 500 MHz	215
6.6 ^{13}C NMR spectra of M1 in CDCl_3 at 125.7 MHz.....	216
6.7 Aromatic region of ^{13}C NMR spectra of M1 in CDCl_3 at 125.7 MHz	216
6.8 ^1H NMR spectra of P1 in CDCl_3 at 500 MHz	217
6.9 ^1H NMR spectra of P2 in CDCl_3 at 500 MHz	217

LIST OF SCHEMES

Scheme	Page
1.1 Chelate effects as seen by dissociation of a ligand from metal for monodentate ligands and bidentate ligands	4
1.2 Synthetic route to Arduengo “free” carbene	13
1.3 Synthesis of <i>m</i> -terphenyls via two aryne intermediates.....	17
1.4 First step towards the synthesis of <i>m</i> -terphenyls via the lithiation of 1,3-dichlorobenzene.	19
1.5 Generalized sensing ensemble in which an analyte concentration is determined via transduction followed by signal processing.	22
2.1 Equilibrium of Terphspan ligand to demonstrate flexibility in coordination compounds.	40
2.2 Two possible mechanisms for 1,4 conjugate addition of enones.....	41
2.3 1-4 Conjugate Addition of the R ₃ on the boronic acid to the enone... ..	43
2.4 Preparation of (1) from RhCl ₃ and Terphspan ligand L1	44
3.1 Carbene and ylide resonance forms of free N-Heterocyclic carbenes (NHCs).....	68
3.2 Preparation of [1H ₂](Br) ₂	73
3.3 Preparation of [Ag(1)]AgBr ₂ and [PdCl ₂ (1)].....	75
3.4 First step towards the synthesis of <i>m</i> -terphenyls via the lithiation of 1,3-dichlorobenzene.	94
4.1 General Scheme for hydrofomylation wherein the desired linear aldehyde is shown in red.....	124
4.2 Synthetic route using 1 to prepare phosphines	131

List of Scheme (Continued)

Scheme	Page
5.1 Generalized representation of the signal transduction mechanism for indicator displacement assays	151
6.1 Synthetic route to P1 and P2.....	201

CHAPTER 1

GENERAL INTRODUCTION

Chemistry is the study of matter and the components that make up this matter. Unique properties are held within these components and they are amalgamated to form the world in which we live. The materials of today are made up of molecules which consist of atoms that are made up of subatomic particles. Synthetic chemists depend upon atomic properties to provide molecules their assets. A synthetic chemist could be referred to as an artist who uses different atoms as the palette and the overall painting is the desired molecule. Just like an artist, a chemist can be inspired from nature and the vast molecular designs, such as enzymes.

The use of a diverse palette as a chemist increases the number of potential molecules that can be devised. Organometallic chemistry takes advantage of this principle in that it lies at the interface of both organic and inorganic chemistry. The first organometallic compound prepared was the organoarsenic compound cacodyl ($\text{As}_2(\text{CH}_3)_4$) in 1757 by Louis-Claude de Gassicourt.² Organometallic chemistry did not experience a large growth in interest, however, until the late 20th century.³⁻⁵ Specific areas in which organometallic chemistry has gained widespread recognition include catalyst design, bioinorganic chemistry and ligand design for various material science applications.

Organometallic compounds consist of an organic component typically referred to as a ligand which is bound to a metal. Ligand design is a crucial part of organometallic chemistry given that the ligands can strongly influence the electronic and steric

parameters about the metal. Ligands may be divided into three classes; cationic, anionic and neutral. Cationic ligands are the least common and include nitrosyl⁶ (NO^+) and phosphonium⁷ (PR_2^+). Anionic and neutral ligands are more common and often feature pnictogen or chalcogen donor atoms and give coordination complexes. Another common feature of ligands is the use of sterically encumbered ligands to enforce specific geometries on the metal. This is a common theme in catalyst design and will thus be examined in further detail (*vide infra*).

1.1 Ligands

The word ligand comes from the Latin for “to tie or bind”. In metal ligand coordination the bonding is accomplished through the donation of one or more electrons to a metal center and potentially back donation from metal-centered orbitals to the ligand. This in turn “binds” the metal and the formation of a sigma bond is achieved. The ligand may act as a pi donor or acceptor to form up to three formal bonds with the metal. Metals have a tendency to contain eighteen electrons within their valence s, p and d orbitals. This can help in the prediction of the environment around a metal by coordinating the number of electrons the metal provides as well as the number of electrons donated by the various ligands. Ligands can form various interactions with metals such as variable denticity, hapticity (η^x) and bridging effects (μ^x) (**Figure 1.1**). Denticity refers to the number of donor atoms within a given ligand attached to the same central atom typically referred to as monodentate or polydentate. Hapticity is the number of electrons in a ligand that are directly coordinated to a metal. Bridging is observed when a ligand binds two or more metals acting as a bridge between the two metals. Synthetic design of ligands can result in preferences towards one of these ligand effects.

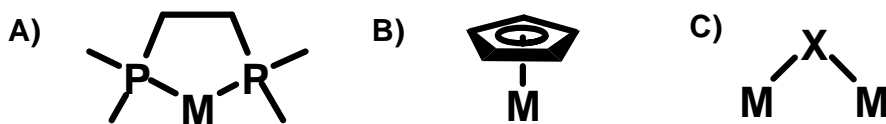
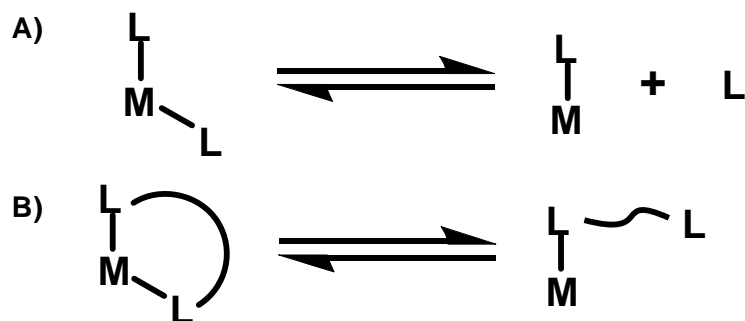


Figure 1.1 Examples of ligand interactions a) bidentate ligand to demonstrate denticity b) η^5 -cyclopentadiene (Cp) for hapticity and c) μ^2 halide as a bridging ligand.

The preference for metals to bind multidentate ligands, called chelate effect is derived from entropic arguments. Kinetically, when a ligand acts as a chelator to a metal, even when the ligand begins to dissociate away from the metal, its close proximity allows rapid reassociation in preference to exchange for a different ligand (**Scheme 1.1**). The coordination of chelating ligands can also be of particular interest when designing a ligand. A chelating ligand can bind the metal in different geometries. In a square planar complex, the first made is *cis*, where the two coordinating atoms approach the metal on the same side and bind in this manner. Another option is to span over the metal and bind from opposite sides in what is called the *trans* mode. The rigidity or flexibility of the ligand can allow for preference of a single binding mode; a ligand that binds preferentially to two sites *trans*- to one another may be called *trans*-spanning, for example. Catalysis typically requires that various coordination geometries be attainable in the course of a reaction, so flexibility should be of great concern when designing ligands. This will be covered in more detail (*vide infra*).



Scheme 1.1 Chelate effects as seen by dissociation of a ligand (L) from metal (M) for a) monodentate ligands and b) bidentate ligands.

Bonding is a principle of chemistry that has been actively studied practically since the dawn of atomic theory. Linus Pauling described many aspects of how we now see the nature of a chemical bond, for which he was awarded the Nobel Prize in Chemistry in 1954.⁸ A great deal of research has been dedicated to elucidating the different types of bonding and the extent to which bonding occurs.^{9,10} Bonding can become complicated and describing bonding can be complex when all parameters are considered, as exemplified by the classification of oxidation states for atoms. Oxidation states are commonly used when an atom is considered to withhold electron sharing to an appreciable amount. Therein lies a problem as to when this effect becomes enough to consider an oxidation state an appropriate model. Green suggests a solution for this known as the “covalent bond classification” (CBC) method where ligands are thought of as being one of three types and formal oxidation states are abandoned.¹¹

Metal complexes include the use of one s orbital, three p orbitals and five d orbitals as valence orbitals, each of which have the capacity of two electrons. This gives a total of 18 electrons, which when interacting with ligands these atomic orbitals become molecular orbitals and then the electrons can come from the metal or ligands bound to it. The “18 electron rule” states that most complexes tend to form with a total of 18 valence electrons. This rule can help predict the reactivity of various metals and ligands. Organometallic complexes in particular consist of similar classes of ligands that allow one to predict structural features prior to synthesis. As stated before, the use of oxidation states is common, but not necessary. This is highlighted in **Table 1.1** where common ligands in organometallic chemistry can be classified by a neutral or oxidation state electron counting method.

Table 1.1 Examples of ligands commonly used in organometallic compounds. Adapted from *Inorganic Chemistry: Principles of Structure and Reactivity* by Huheey et. al.¹

Ligand	Neutral Electron Count	Oxidation State Electron Count
Carbonyl(M–CO)	2	2
Phosphine (M–PR ₃)	2	2
Amine (M–NR ₃)	2	2
Alkene (M–II)	2	2
Isocyanide (M–CNR)	2	2
Halogen (M–X)	1	2
Hydrogen (M–H)	1	2
Alkyl (M–R)	1	2
Amide (M–NR ₂)	1	2
Phosphide (M–PR ₂)	1	2
Alkylidene (M=CR ₂)	2	4
Carbene (M–CR ₂)	2	2

Phosphines and carbenes are essential ligands for many contemporary types of catalysts, as will be discussed in later sections. The current widespread use of phosphines and carbenes attests to their robust utility as ligands for organometallic complexes. For

this reason phosphines and carbenes will be the focus of the ligand design within the following chapters.

1.1.1 Phosphines

Phosphine ligands have been used in catalysis since the mid 1950's because of their ability to engage in efficient two electron sigma donation to metals and to support efficient catalysts. These ligands also have the ability to act as pi acceptors due to the empty d orbitals in phosphorus. Phosphines also act as soft donor ligands allowing for coordination with low oxidation state metals with late transition metals. Phosphines are synthesized with a wide variety of functionalization that allows researchers to tune their steric and electronic properties. The most common phosphine ligand in catalysis and other applications is triphenylphosphine due to its relative air stability, and affordability.

With the emergence of phosphines in catalysis came the desire to quantify the steric¹² and electronic¹³ parameters that impact their efficacy as supporting ligands. Chadwick Tolman was a pioneer in such efforts, summarizing his methods in a 1977 *Chemical Reviews* article.¹⁴ The electron donating ability ($\Delta\nu$) of phosphine ligands was determined by measuring the change in the C–O stretch of $\text{Ni}(\text{CO})_3(\text{PR}_3)$ (**Figure 1.2**). If the phosphine is a strong electron donor, the increased electron density on Ni facilitates more pi backbonding to the carbonyl C–O antibonding orbital, thus weakening the carbonyl bond and lowering the C–O stretch frequency.

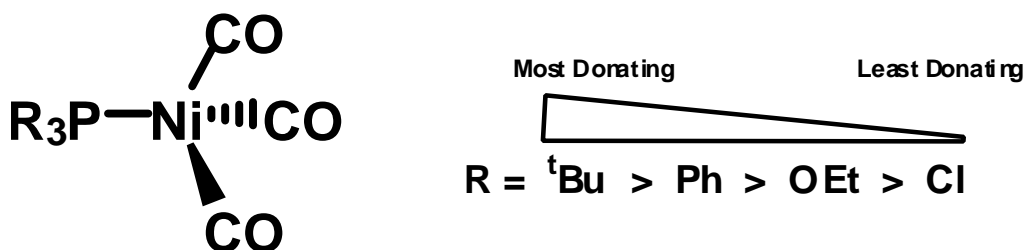


Figure 1.2 Examples of electron donating ability ($\Delta\nu$).

Tolman also created a systematic classification for steric bulk known as the cone angle (θ). The Tolman cone angle (**Figure 1.3a**) is defined as the apex angle centered at 2.86 Å from the center of the M–P bond based on CPK models. This simple parameter is still one of the most commonly used to quantify phosphine sterics.^{14, 15} Other parameters have been developed to characterize phosphine sterics, including the solid angle^{16,17}, pocket angle,¹⁸ repulsive energy¹⁹⁻²¹ and the accessible molecular surface.²²

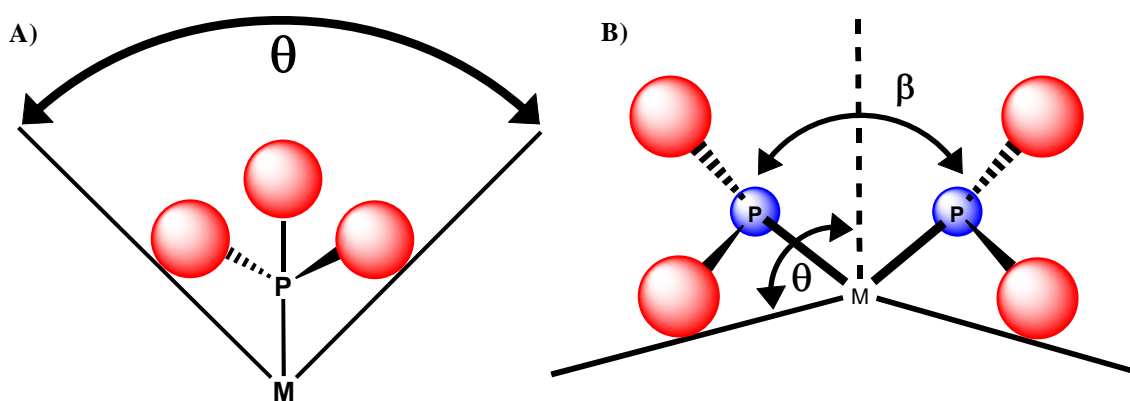


Figure 1.3 a) Tolman cone angles (θ) for tertiary phosphines b) Natural bite angle (β) for diphosphines.

The use of the electron donating ability ($\Delta\nu$) and the Tolman cone angle (θ) for classification of phosphines is an active area of phosphine ligand design. Prediction of various unknown parameters can be accomplished if a relationship is shown between a measurable criterion such as the electron donating ability or Tolman cone angle. The Tolman cone angle has a dependence on ligand binding ability as well as the degree of substitution. Other parameters such as catalytic activity have a dependence on both electronics and sterics effects, therefore a plot of electron donating ability against the Tolman cone angle would be useful (**Figure 1.4**). If a catalyst requires a strong electron donor with a large amount of steric bulk, the plot conveniently displays which ligands fit

these criteria. This steric and electronic map has the practical advantage of allowing one to quickly read steric and electron parameters in one convenient graph.

Following early studies on monophosphines, it was found that diphosphines can also support efficient catalysts, and thus the development of additional parameters to describe chelation properties of diphosphines became important. Casey and Whiteker introduced the natural bite angle (β), a ligand preferred P–M–P angle by using a dummy metal atom to allow for the proper alignment of the phosphorus lone pair, with the M–P length constrained to 2.315 Å and the force constant of the P–M–P angle constrained to 0 kcal (Figure 1.3b).²³ They also introduced a flexibility range by allowing 3 kcal/mol flexibility and to measure the range of bite angles produced from this simulation. The natural bite angle provides an idea of the P–M–P angle preferred by the diphosphine

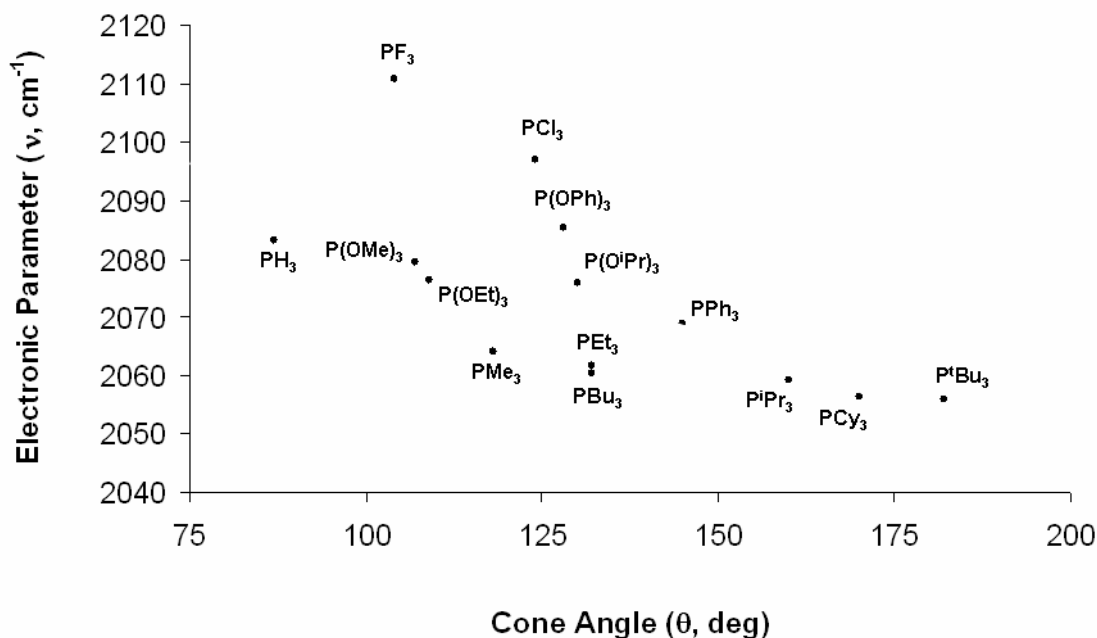


Figure 1.4 Steric and electronic map of electronic parameter (ν) and cone angle (θ).

without influence of metal-preferred geometries or steric repulsion of other ligands on the complex (**Figure 1.5**). A definite, sometimes profound correlation between bite angle and catalytic activity has been noted for numerous industrially important processes. This aspect is a central motivating force behind the work described in Chapters 2, 3 and 4.

Ligand	β (°)	
dppm	72	
dppe	85	
dppp	91	
dppb	98	
BINAP	92	
Xantphos	112	

Figure 1.5. Examples of ligand bite angles of some common phosphines.

1.1.2 Carbenes

Carbenes ($:\text{CR}_2$) are molecular entities with a divalent carbon that only has six valence electrons, making these species generally unstable. The simplest example of this would be methylene. Depending on the spin distribution of the unbinding electrons, there are two different forms of carbenes, singlet and triplet carbenes (**Figure 1.6**). Singlet carbenes have an electron pair while the triplet state carbenes exhibit two lone electrons. For this reason the singlet carbenes are typically substantially more stable than triplet carbenes. Although the typical half life of a triplet state carbene is on the order of seconds, a triplet carbene with a 40 minute half life was observed recently.²⁴

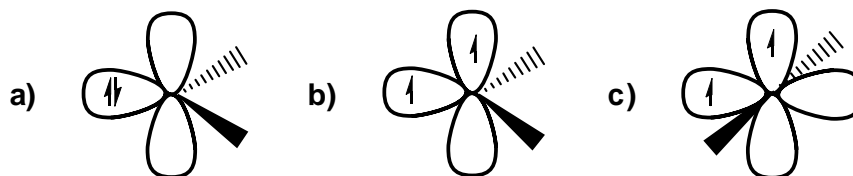


Figure 1.6 Examples of singlet (a) and triplet (b and c) carbenes.

Carbenes have an extensive history including the ubiquitous Fischer and Schrock type carbenes (**Figure 1.7**), both of which require a metal for stabilization. The Fischer carbenes typically are complexes to low oxidation state metals from the middle to late transition metals. Fischer carbenes also tend to be good pi acceptor ligands, and they usually display pi donor substituents on the methylene group. Fischer carbenes are sometimes referred to as singlet carbenes.

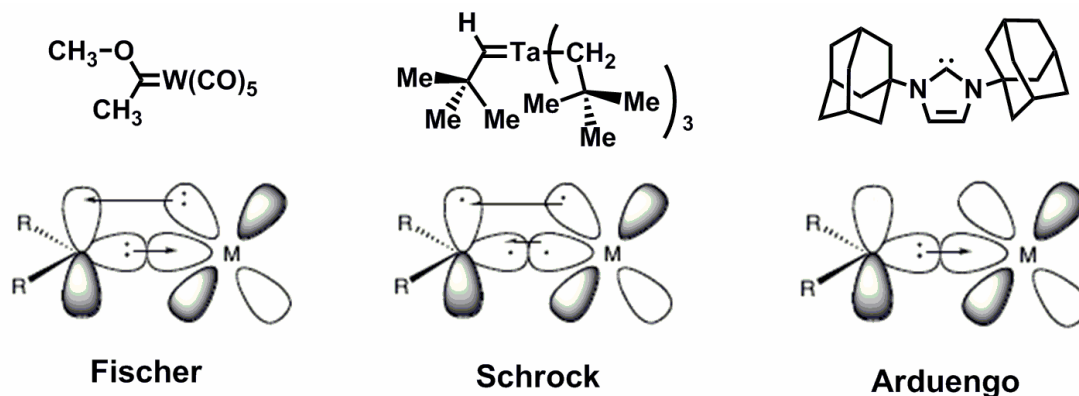
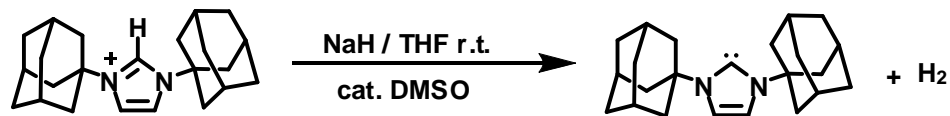


Figure 1.7. Structures and orbital representations of the first Fischer & Schrock carbene complexes and the first structurally characterized “free” Arduengo carbenes.

Schrock carbenes contain high oxidation state early transition metals and are not good pi acceptor ligands and are often referred to as triplet carbenes. The isolation of carbenes without stabilization by coordination with a metal was unheard of until Arduengo developed a synthetic route to the first stable “free” carbene (**Scheme 1.2**).²⁵ The carbene was stable in the solid state and the crystal structure was determined; however the absence of oxygen and moisture were necessary. These carbenes derive their stability from nitrogen donors that effectively stabilize the singlet carbene.

The isolation of the first “free” *N*-heterocyclic carbenes (NHCs) by Arduengo has provided a renewed interest in the field of carbenes. Like Fischer and Schrock carbenes, NHCs can coordinate to metal ions. In this regard, NHCs are very similar to phosphines; they are good σ donor ligands and therefore have been studied as ligands to support catalytic activity.



Scheme 1.2 Synthetic route to Arduengo “free” carbene.

1.2 The *meta*-Terphenyl

A *m*-terphenyl consists of a 1,3-diphenyl benzene core (**Figure 1.8**). All of the carbons within the terphenyl are sp^2 hybridized, and the rings have the potential for rotation about the single bond between the central aryl and the flanking phenyl rings. This freedom of rotation allows for different conformations of terphenyls. The two conformations with the most energetic difference would be one in which all three aryl rings are coplanar versus the conformation in which the flanking rings twist out of the plane to become perpendicular to the central ring. When all three rings are coplanar, the hydrogens attached to carbons (a), (c) and (e) in **Figure 1.8** experience the most steric repulsion. To minimize this repulsion the preferred conformation should be where the flanking rings twist out of this plane. The *m*-terphenyl where the attached phenyl rings are arranged *meta* to one another on the central aryl ring when exhibiting this conformation allows a pocket within the molecule.

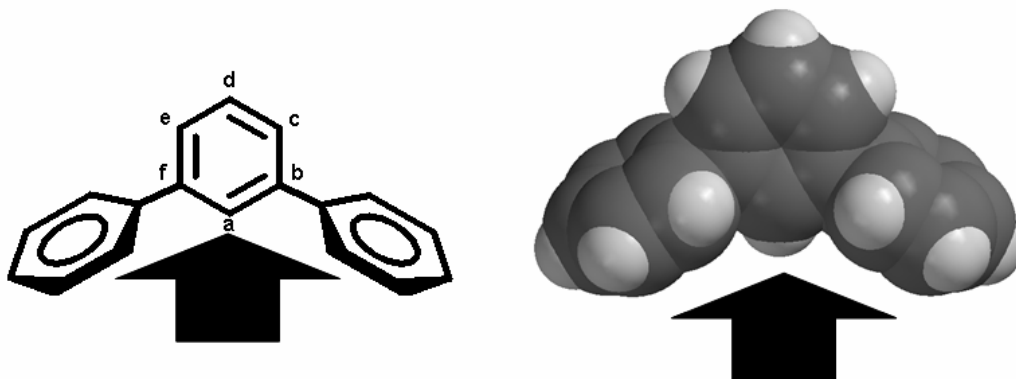


Figure 1.8 Two representations of the conformation of *m*-terphenyl. Arrows indicate the sterically enshrouded cleft that is the most often exploited feature of the *m*-terphenyl scaffold.

This pocket also acts as a steric shield for specific applications, and various substituents can be utilized to alter the function. The use of *m*-terphenyls can also afford a rigid backbone that incorporates the *m*-terphenyl component as a scaffold for ligand design. The widespread utility of *m*-terphenyl ligands has been demonstrated in the large number of ligands that incorporate the *m*-terphenyl into their design.²⁶ Particularly the use of phosphorus donor atoms appended to the *m*-terphenyl are of interest and will be covered in further detail in Chapters 2, 3 and 4.

1.2.1 Synthesis of *m*-Terphenyls

Aryl-aryl bond formation is an important component of organic chemistry. Many improvements have been made to this area since pioneering work by Ullmann utilizing the direct oxidative dehydrodimerization of aryl halides in the presence of copper reported in 1901.^{27, 28} The Ullmann reaction (**Figure 1.9a**) required extremely harsh conditions including temperatures typically above 200 °C.^{27, 29} In 1912 Scholl discovered the occurrence of aryl coupling in the presence of a Lewis acid³⁰ (**Figure 1.9b**); however, this reaction suffers from low yields. It wasn't until 1972, when Kumada discovered the cross coupling of aryl Grignard reagents catalyzed by a nickel phosphine complex that gives high yields (>80%) with reasonable conditions (refluxing diethyl ether), that aryl-aryl bond formation was commonly used (**Figure 1.9c**).³¹

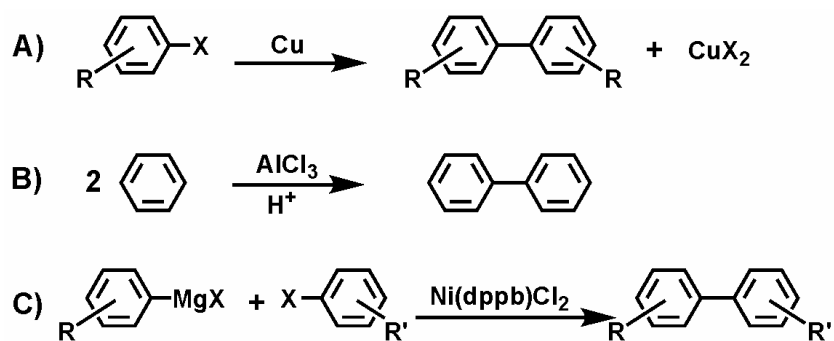
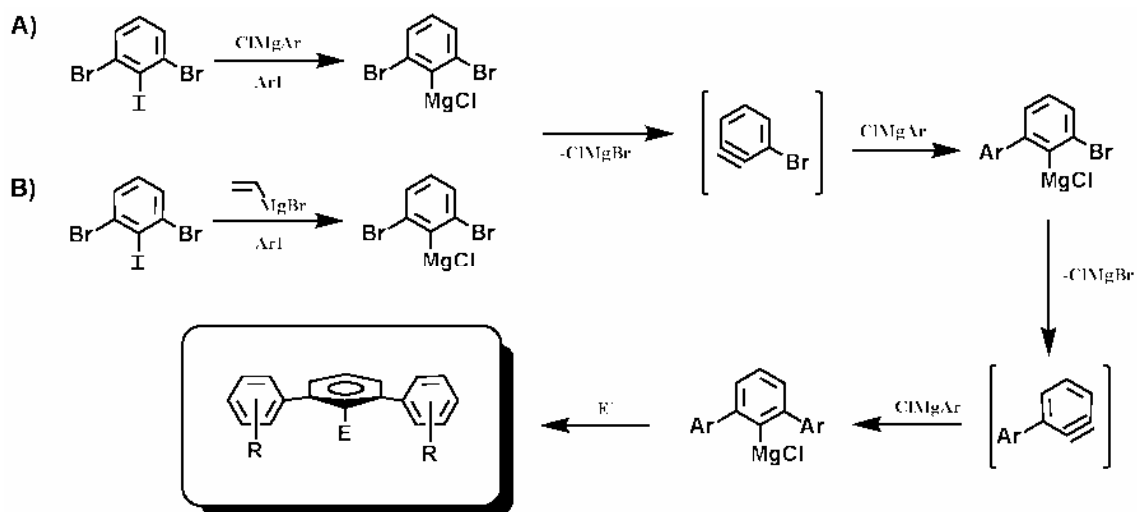


Figure 1.9 Various means to aryl-aryl bond formation that lead to the one pot synthesis of *m*-Terphenyls. a) Ullmann b) Scholl c) Kumada.

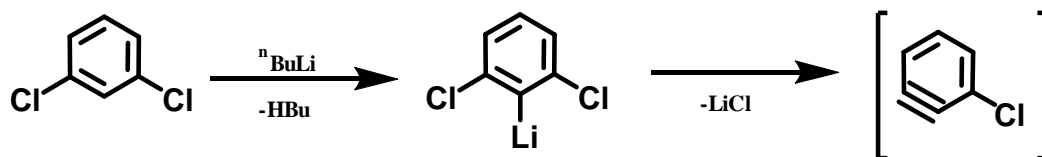
Hart initiated the one pot synthesis of *m*-terphenyls via an aryne intermediate from an aryl Grignard in 1986 with the use of 2,6-dibromiodobenzene which allows metal halogen exchange followed by elimination of ClMgBr to yield a benzyne (dehydrobenzene) intermediate (**Scheme 1.3a**).³² This key aryne intermediate then undergoes the first nucleophilic addition via the Grignard followed by another elimination of ClMgBr then the second nucleophilic addition. The reaction is then quenched using an electrophile to yield the functionalized *m*-terphenyl. The use of this synthetic route to *m*-terphenyls was utilized for a variety of purposes including the synthesis of cyclophanes such as cuppedophanes and cappedophanes.³³ This reaction has many advantages compared to previous aryl-aryl bond forming reactions. The primary drawback was the demand for an excess of Grignard that was needed due to the initial metal halogen exchange. To compensate for the requirement of activation of the 2,6-dibromiodobenzene the use of vinyl magnesium bromide was employed (**Scheme 1.3b**).³³



Scheme 1.3 Synthesis of *m*-terphenyls via two aryne intermediates.

A plethora of papers followed these initial studies that demonstrated the versatility of the *m*-terphenyls prepared following Hart's two aryne intermediates which included the use of various electrophiles to quench the central ring Grignard during the last step.³⁴⁻³⁶ Luening thoroughly explored the capability of this freedom of electrophile functionality which is highlighted in a series of papers on concave reagents.³⁷⁻⁴² The use of electrophiles needs to be approached with caution because any excess Grignard used also gets quenched and some electrophiles can lead to mixtures that are difficult to purify. This can be avoided by first quenching with molecular iodine followed by a simple purification step. Isolation of the desired compound allows subsequent preparation of a Grignard which can then be quenched with the desired electrophile.

In 1940 the lithiation of benzene was utilized to synthesize *m*-terphenyls by reacting with various halobenzenes.⁴³ This reaction led to the proposal of the aryne or benzyne intermediate originally known as dehydrobenzene. This later inspired Kress to discover that 1,3-dichlorobenzene could undergo selective metal-halogen exchange at the 2 position with ⁿBuLi at low temperatures followed by self coupling to prepare a *m*-terphenyl when heated to -50 °C.⁴⁴ These discoveries led to the use of the lithiation of 1,3-dichlorobenzene as the first step in the synthesis of *m*-terphenyls in place of the metal halogen exchange of 2,6-dibromiodobenzene (**Scheme 1.4**).⁴⁵ This is advantageous for the synthesis of *m*-terphenyls in that the current cost of 5 g of 2,6-dibromiodobenzene (\$30) is currently the same price as 250 g of 1,3-dichlorobenzene.



Scheme 1.4 First step towards the synthesis of *m*-terphenyls via the lithiation of 1,3-dichlorobenzene.

The one pot synthesis of compounds employing a *m*-terphenyl scaffold and subsequent functionalization is an efficient and valuable means to materials with various applications. The various ways in which *m*-terphenyls are synthesized within this thesis are highlighted in **Figure 1.10a**. The uses of materials incorporating various *m*-terphenyl scaffolds (**Figure 1.10b**) are exemplified by catalysis and scaffolded chromophores for sensing and other optoelectronic applications. The utilization of *m*-terphenyls for various other applications is an ongoing area of research in many other groups, particularly their use as sterically encumbering units to enforce multiple bonding of heavier main group elements⁴⁶⁻⁴⁸ as well as their use in conjugated polymers^{49,50}.

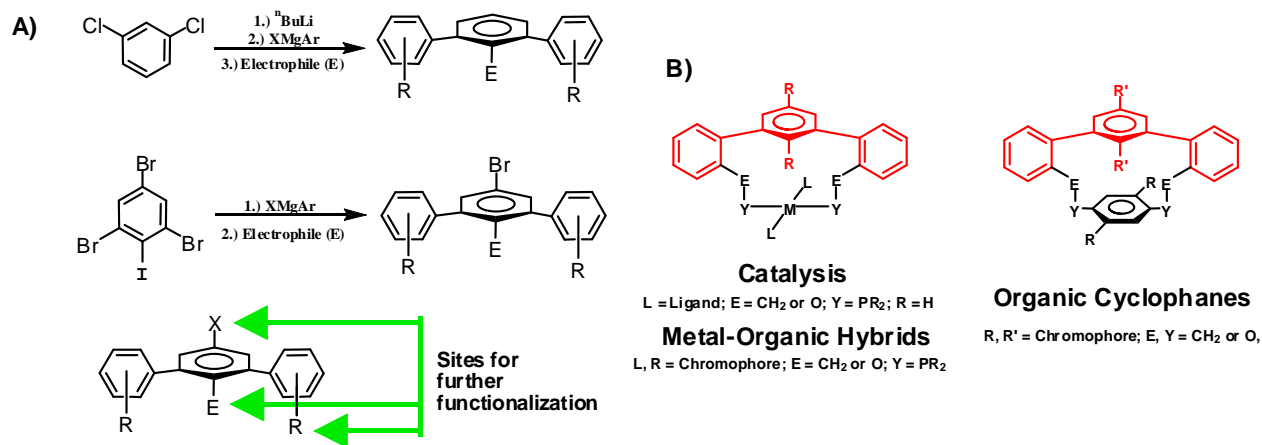


Figure 1.10. a) Synthetic routes to *m*-terphenyl scaffolds used herein b) examples of various functionality and uses for the *m*-terphenyl scaffold (shown in red).

1.3 Catalysis

Catalysis is the process by which a chemical reaction's rate is increased. A catalyst is not consumed during the reaction and is typically only required in a small quantity. A catalyst must lower the energy of activation (E_a) and there are two typical modes of action through which a catalyst can achieve this. The first would be to lower the energy of the transition state or find alternate pathways to intermediates that are more stable, therefore lowering the E_a (**Figure 1.11**). A second method would be to raise the energy of the starting material by making it less stable (**Figure 1.12**). This would then lower the energy needed to reach the intermediate, allowing the chemical equilibrium to be reached more quickly.

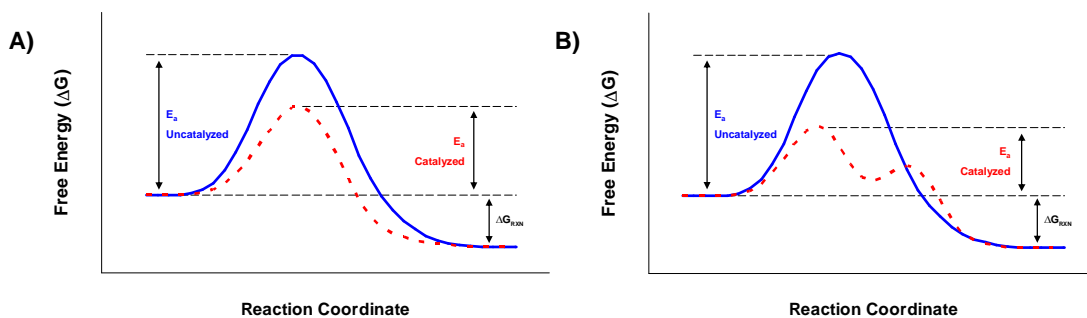


Figure 1.11. Example of catalyzed reactions by a) lowering the energy of the transition state or by b) finding alternate pathways to intermediates.

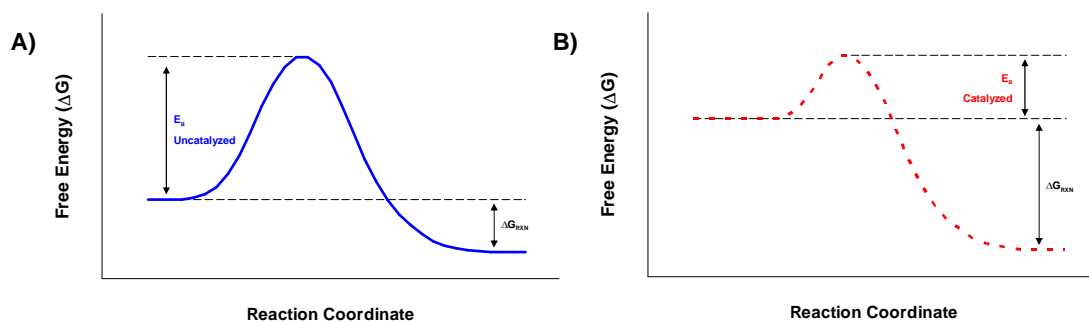
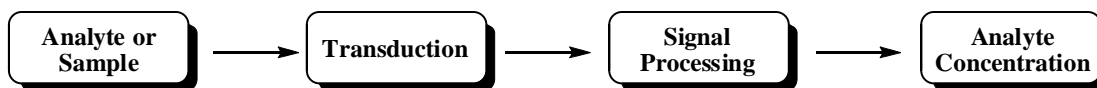


Figure 1.12. Example of catalysis by raising the energy of the reactant. a) Uncatalyzed reaction b) Catalyzed reaction.

Industrialization has been a primary component in making the world's demand for an ever increasing supply of chemical feed stocks evident. The materials of today demand chemical manufacturing that has an astounding effect on the environment through energy consumption and waste production. The need for alternate methods to chemical manufacturing using "green" production methods is apparent. In this context, "green chemistry" can be defined as a chemical conversion that consumes a minimal amount of energy and resources, which in turn produces less waste. The use of a catalyst in this regard would be advantageous in that less energy is required and less waste production is achieved by high atom efficiency during chemical conversion.

1.4 Chemical Sensing

Sensing is a crucial part of life and we depend upon it. Everyday we use the senses of sight, hearing, touch, smell and taste to perceive and evaluate the world. The ability to understand and mimic these senses has been the goal of an immense amount of research and continues to be a significant area of research. The means by which sensing ensembles are mimicked requires an understanding in the way a signal is recognized then perceived (**Scheme 1.5**). This occurs via signal transduction where the signal is received as a stimulus and then converted into a message the body can interpret. This concept of signal transduction is an imperative part of sensing and scientists have devised a variety of transduction methods including but not limited to chemical, electrical, thermal, mechanical and optical. Optical methods are commonly preferred due to many factors, including a fast response time, non-invasive capabilities and the potentials for a two dimensional experiment.⁵¹



Scheme 1.5. Generalized sensing ensemble in which an analyte concentration is determined via transduction followed by signal processing.

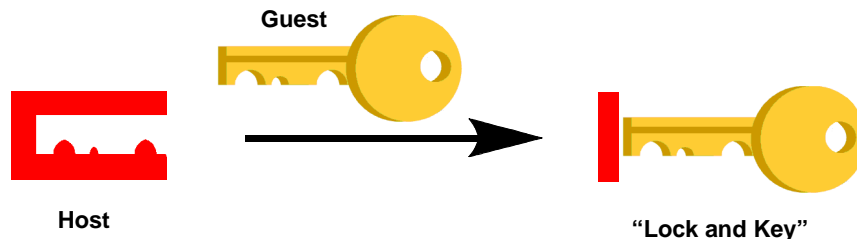
Chemical sensing is commonly referred to as molecular recognition and refers to a host or sensing ensemble to which a particular guest or analyte can become associated with to form a host-guest complex. These host-guest complexes are held together by inter and/or intra-molecular forces that consist of non-covalent bonds such as hydrogen bonding, dispersion (van der Waals) forces, pi-pi interactions, electrostatics and hydrophobic forces.⁵²⁻⁵⁵ Some quintessential examples of these types of interactions are

those involved in the base pairing of DNA, antibody-antigen interactions and substrate-enzyme complexes.

It is essential that interactions of this type can be substantial as would be seen in the binding of many biological systems. This was understood over a century ago; as illustrated by the observations of Hermann Emil Fischer, the Nobel Prize laureate of chemistry in 1902, who noted that configurational changes drastically impacted the action of enzymes.^{56, 57} Fischer proposed that the guest was like a “key” and the host was the “lock”, leading to the familiar “lock and key” model (**Figure 1.13A**). Today the induced fit model is used due to the ability to describe enzymes as flexible structures that continually reshape when coming in contact with the substrate (**Figure 1.13B**).⁵⁸

Strong association of the host and guest ensures that specificity is achieved which in turn allows for proper functioning in biological systems. For a chemical sensor the guest, which is an analyte of importance you are attempting to sense, is determined based on practical applications. Therefore, as a synthetic chemist the rational design of a host that has favorable interactions with the guest is essential. Inspiration is commonly drawn

(A)



(B)

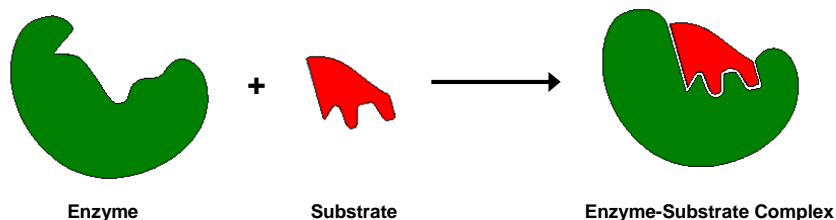


Figure 1.13. (A) “Lock and Key” model of molecular recognition. (B) Induced-fit model of enzyme-substrate binding. Adapted from *Biochemistry* by Berg et. al.⁵⁸

from nature, in the form of enzymes or other bioconstructs that can overcome the entropically unfavorable association of a host with a guest.⁵⁹ Another common means of overcoming this entropic barrier is to create a host that incorporates units that rigidly extend in three dimensions.⁶⁰ However, a host should not be too rigid; there needs to be a balance between rigidity and flexibility to allow for dynamic binding to occur.

The interactions between guest and host depend upon many factors. Solvent effects are commonly discussed due to the relatively large amount of data pertaining to the treatment of various parameters that affect the host-guest interactions. The donor number (DN) measures the Lewis basicity and is experimentally determined by forming a 1:1 adduct with SbCl_5 in 1,2-dichloroethane, which is given a value of zero. This value is used to determine the ability the solvent has to solvate cations. The acceptor number (AN), as would be expected, is a characteristic to describe how the solvent solvates anions. The ability to solvate ions is an important part of sensing as well as a useful tool to remember when choosing an appropriate solvent for analytes. If the analyte is detained by the solvent and cannot interact with the receptor in an appreciable amount, the binding constant can be drastically affected. This was exemplified by Schneider when he observed a greater than 10^4 difference in binding constants of potassium to a 18-crown-6 from solvent effects.⁶¹ The dielectric constant of a solvent can strongly affect the electrostatic forces between components of a sensing ensemble. Solvents with large dipole moments interact more with the charged species in which some molecular recognition can be based on. This results in a shielding effect from the guest-host complex being formed. These effects can be predicted based on an observation of the Gutmann donor and acceptor numbers and the dielectric constant (**Table 1.2**).

Table 1.2 Gutmann donor and acceptor numbers and dielectric constants for selected solvents.

Solvent	Donor Number	Acceptor Number	Dielectric Constant
Acetone (CH ₃ COCH ₃)	17.0	12.5	20.56
Acetonitrile (CH ₃ CN)	14.1	18.9	35.94
Chloroform (CHCl ₃)	0	23.1	4.89
Dichloromethane (CH ₂ Cl ₂)	0	20.4	8.93
Diethyl Ether (CH ₃ CH ₂ OCH ₂ CH ₃)	19.2	3.9	4.20
<i>N,N</i> -dimethyl formamide (CH ₃) ₂ NCOH	26.6	16.0	36.71
Dimethyl sulfoxide (CH ₃ SOCH ₃)	29.8	20.4	46.45
1,4-dioxane (C ₄ H ₈ O ₂)	14.8	10.8	2.21
Ethanol (CH ₃ CH ₂ OH)	31.5	37.1	24.55
Ethyl Acetate (CH ₃ COOCH ₂ CH ₃)	17.1	9.3	6.02
Methanol (CH ₃ OH)	19.0	41.5	32.66
Tetrahydrofuran (C ₄ H ₈ O)	20.0	8.0	7.58
Triethylamine (CH ₃ CH ₂) ₃ N	61.0	1.4	2.42
Water (H ₂ O)	33.0	54.8	78.36

Optical detection for analytes can be utilized in a fairly straightforward manner by the attachment of a chromophore or fluorophore to the host/receptor. The methods in which this can be done vary and allow for variable sensitivity. When the chromophore or fluorophore itself comprises a portion of the host, the efficiency of the signal transduction event is better than if a linker is used to attach the two pieces. The interaction of the guest to the host causes the chromophore or fluorophore to respond resulting in a measurable change (**Figure 1.14**). The ability to synthetically change the host and use the same response mechanism makes for easy variability.

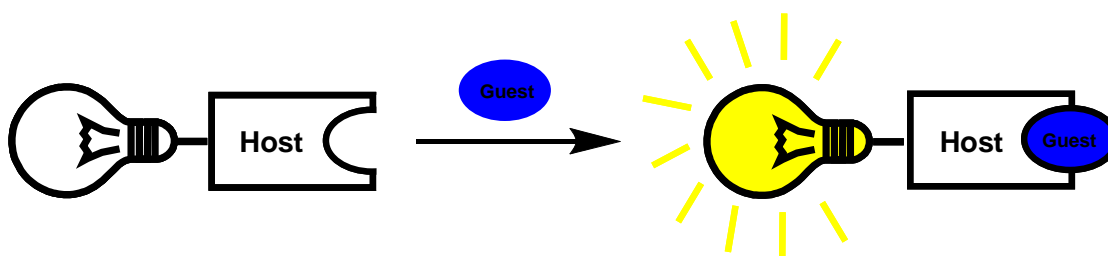


Figure 1.14. Conceptual representation of a guest-induced signal transduction event.

The design of covalent architecture to attach chromophores and fluorophores can be a time consuming process. The direct use of the host is an advantageous method of detection; however, a transduction method still needs to be developed. The use of displacement methods fulfills this need. In the displacement method, the indicator is initially bound to the receptor/host and after introduction of an analyte/guest the indicator becomes released, changing the optical properties of the indicator (**Figure 1.15**). The use of the analyte detection via a displacement method is commonly referred to as an indicator displacement assay. The need for an indicator that gives a response when introduced to a receptor requires the receptor to become associated with the indicator.

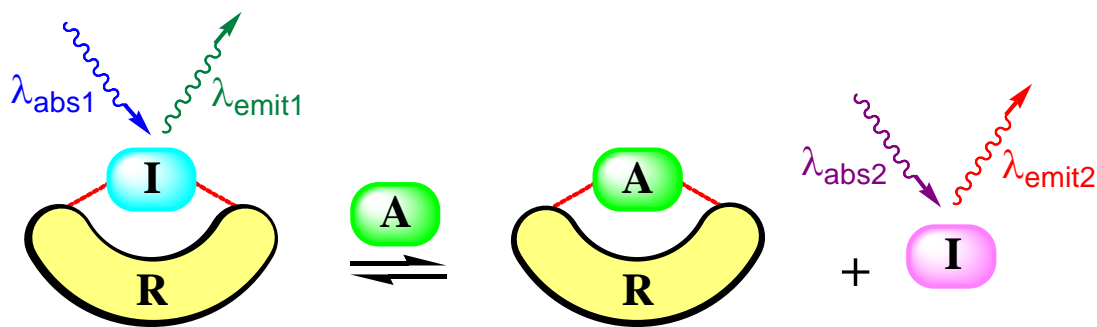


Figure 1.15. General representation of an indicator displacement assay. R = Receptor, I = Indicator and A = Analyte

Selectivity can thus be achieved if the indicator's binding constant lies between the two analytes to which the receptor can associate.

The direct detection of analytes without the use of an indicator is also of interest for many sensors. The design of the receptor/host, however, must naturally account for the signal detection method if a direct method is to be used. NMR spectroscopy is a common means in which the detection of analytes is monitored via direct methods. The need for well resolved chemical shifts must be met for proper function of the sensor. The association of the guest with the host must also alter the chemical shift of the host nuclei of interest, typically ^1H spectroscopy (^{31}P is occasionally seen) and be measurable.⁶² A drawback to the use of NMR for sensing is that a limited working range for concentrations must be used; consequently NMR is only reliable for association constants in the range of $10^1 - 10^4 \text{ M}^{-1}$.^{63,64}

The design of receptors can accommodate a variety of sensing ensembles. The incorporation of *m*-terphenyl units as a scaffold with a pocket in it allows for binding of analytes of specific size and shape. The uses of the *m*-terphenyl scaffold for sensing

represents the foundation of a new receptor for a variety of analytes. The variable functionality of *m*-terphenyl units allows for the improvement of receptor design to be achieved with ease.

1.5 Aim and Scope

The research described herein was sponsored by the Clemson University chemistry department and the American Chemical Society Petroleum Research Fund (ACS-PRF Grant #45992-G3). There are two central themes of research described in this thesis; catalysis and sensing. The use of various *m*-terphenyl ligands as scaffolds for catalytic applications, with expectations to improve yields and atom efficiency at lower temperature or pressure, is covered in *Chapters 2-4*. These improvements guide catalysts towards “green” production of chemical feedstock. The utility of *m*-terphenyl scaffolded ligands in catalytic reactions is still a young area of research and many other studies would be fruitful in furthering understanding in this area of chemistry. An immense variety of ligands can be synthetically designed using this scaffold which exponentially increases the probability for success.

The second theme utilizes various sensing ensembles for various analytes, discussed within *Chapters 5 and 6*. The use of the *m*-terphenyl is a vital part of the molecular design of sensors in that the pocket made from the twisting of the flanking rings is used to hold analytes in close proximity. The use of various substituents allows for various intermolecular attractions to be utilized for sensing. The analytes in these sections were all detected based on optical response. The importance for selective sensing remains a crucial part of chemistry and the following studies add to the current literature and improve on previous designs. The uses of materials similar to ones discussed have potential for a variety of applications which are currently being explored within the Rhett C. Smith group.

In *Chapter 2*, the synthesis structure and characterization of a rhodium complex featuring a wide bite angle diphosphine ligand is discussed. The ligand supports a bite angle (P–M–P angle, β) of 171.37° in the *trans*-square planar complex and was tested in Rh-catalyzed 1,4-addition reactions of arylboronic acids (six examples) to α,β -unsaturated ketones (five examples). In mixed aqueous/cyclohexane solution at 60°C , addition reactions proceed in up to quantitative yield with a 1:1 arylboronic acid/enone ratio. Yields as high as 77% were acquired even when one of the coupling partners was sterically encumbered 2,4,6-trimethylphenylboronic acid.

In *Chapter 3* a *bis*(*N*-heterocyclic carbene) (NHC) ligand that provided a *m*-terphenyl canopy over one side of its metal complexes is discussed. The *bis*(NHC) was utilized for catalytic applications. Single crystal X-ray diffraction studies on a silver complex employing the *bis*(NHC) revealed an unusual tetranuclear silver core with a Ag–Ag bond distance of $3.0241(8)\text{ \AA}$ as a *trans*-chelating ligand (C–Ag–C = 171°). A preliminary X-ray structure of pseudo-square planar palladium procatalyst showed a similar binding mode as previously synthesized complexes (C–Pd–C = 177°). High yields were obtained in Suzuki-Miyaura coupling reactions utilizing the procatalyst and results compared with analogous complexes of *trans*-spanning diphosphine and diphosphinite complexes. The diphosphinite complex was found to decompose at room temperature.

In *Chapter 4* the synthesis of a series of ligands with various substituents appended to the *m*-terphenyl backbone are discussed. The uses of the ligands for the hydroformylation of styrene was explored under various conditions to examine the effect of electron donating ability and steric effects on catalysis. The increase in amount of linear aldehyde compared to branched aldehyde produced was monitored to test ability to

favor one regioisomer over the other. The conditions were optimized for temperature, pressure and molar concentrations. The isolation of various coordination modes of the ligands employed suggest the ease for catalytic cycle completion.

In *Chapter 5* a dizinc phosphohydrolase enzyme model complex employing a dinucleating ligand based on a *m*-xylyl scaffold was initially tested for binding to a series of eleven commercially available complexometric indicators in aqueous HEPES buffer at pH 7.4, with the aim of determining the applicability of these indicators in indicator displacement assays (IDAs) under physiological conditions. Dissociation constants (K_d) were determined for eleven indicator-dizinc complexes, spanning two orders of magnitude. Phosphate and pyrophosphate were tested for their ability to displace the bound indicators and produce a detectable colorimetric response. Three indicators were found to act as indicator displacement assays selective for pyrophosphate over phosphate. The selection of indicator/analyte pairs having appropriate relative K_d values are critical for successful application in IDAs as seen in the results obtained.

In *Chapter 6* a sterically encumbered *m*-terphenyl oxacyclophane substituted with two aryl iodide substituents was prepared as a versatile monomer for the preparation of π -conjugated polymers. The monomer was then used to prepare a poly(*p*-phenylene ethynylene) derivative incorporating the oxacyclophane units as canopies that shield one side of the π -system from interchain interactions. The photophysical properties of the polymer compares well to those of a reference poly(*p*-phenylene ethynylene) derivative that lacks the canopy. The presence of the steric canopy leads to diminished interchain interaction in the solid state and enhances the kinetic response of the canopied polymer to

vapors of nitroorganics such as TNT, presumably by increasing the permeability to analytes.

1.6 References

1. Huheey, J. E.; Keiter, E. A.; Keiter, R. L., *Inorganic Chemistry*. 4th ed.; HarperCollins College Publishers: New York, 1993.
2. Withers, H. P., Jr.; Seyferth, D.; Fellmann, J. D.; Garrou, P. E.; Martin, S., *Organometallics* **1982**, *1*, 1283-1288.
3. Gevorgyan, V.; Radhakrishnan, U.; Takeda, A.; Rubina, M.; Rubin, M.; Yamamoto, Y., *Journal of Organic Chemistry* **2001**, *66*, 2835-2841.
4. Thayer, J. S., *Advances in Organometallic Chemistry* **1975**, *13*, 1-45.
5. Parshall, G. W., *Accounts of Chemical Research* **1970**, *3*, 139-144.
6. Rothfuss, H.; Barry, J. T.; Huffman, J. C.; Caulton, K. G.; Chisholm, M. H., *Inorganic Chemistry* **1993**, *32*, 4573-4577.
7. Cowley, A. H.; Norman, N. C.; Pakulski, M., *Journal of the Chemical Society, Dalton Transactions* **1985**, 383-386.
8. Pauling, L., *The nature of the chemical bond, and the structure of molecules and crystals : an introduction to modern structural chemistry*. 2nd ed.; Cornell University Press: Ithaca, N.Y., 1948; p 450.
9. Kutzelnigg, W., *Angewandte Chemie* **1984**, *96*, 262-286.
10. Boehme, C.; Frenking, G., *Journal of the American Chemical Society* **1996**, *118*, 2039-2046.
11. Green, M. L. H., *Journal of Organometallic Chemistry* **1995**, *500*, 127-148.
12. Tolman, C. A., *Journal of the American Chemical Society* **1970**, *92*, 2956-2965.
13. Tolman, C. A., *Journal of the American Chemical Society* **1970**, *92*, 2953-2956.

14. Tolman, C. A., *Chemical Reviews* **1977**, 77, 313-348.
15. Tolman, W. B.; Que, L., Jr., *Journal of the Chemical Society, Dalton Transactions* **2002**, 653-660.
16. Lee, T. R.; Carey, R. I.; Biebuyck, H. A.; Whitesides, G. M., *Langmuir* **1994**, 10, 741-749.
17. Tour, J. M.; Jones, L., II; Pearson, D. L.; Lamba, J. J. S.; Burgin, T. P.; Whitesides, G. M.; Allara, D. L.; Parikh, A. N.; Atre, S., *Journal of the American Chemical Society* **1995**, 117, 9529-9534.
18. Koide, Y.; Bott, S. G.; Barron, A. R., *Organometallics* **1996**, 15, 2213-2226.
19. Brown, T. L., *Inorganic Chemistry* **1992**, 31, 1286-1294.
20. Choi, M.-G.; White, D.; Brown, T. L., *Inorganic Chemistry* **1994**, 33, 5591-5594.
21. Cha, J. S.; Brown, H. C., *Journal of Organic Chemistry* **1993**, 58, 4727-4731.
22. Angermund, K.; Baumann, W.; Dinjus, E.; Fornika, R.; Goerls, H.; Kessler, M.; Krueger, C.; Leitner, W.; Lutz, F., *Chemistry--A European Journal* **1997**, 3, 755-764.
23. Casey, C. P.; Whiteker, G. T., *Israel Journal of Chemistry* **1990**, 30, 299-304.
24. Liang, T.-T.; Naitoh, Y.; Horikawa, M.; Ishida, T.; Mizutani, W., *Journal of the American Chemical Society* **2006**, 128, 13720-13726.
25. Arduengo, A., *Journal of the American Chemical Society* **1991**, 113, 361-362.
26. Clyburne, J. A. C.; McMullen, N., *Coord. Chem. Rev.* **2000**, 210, 73-99.
27. Liu, T.; Han, W.-G.; Himo, F.; Ullmann, G. M.; Bashford, D.; Toutchkine, A.; Hahn, K. M.; Noodleman, L., *Journal of Physical Chemistry A* **2004**, 108, 3545-3555.

28. Hassan, J.; Sevignon, M.; Gozzi, C.; Schulz, E.; Lemaire, M., *Chemical Reviews* **2002**, *102*, 1359-1470.
29. Carre, F.; Chuit, C.; Corriu, R. J. P.; Fanta, A.; Mehdi, A.; Reye, C., *Organometallics* **1995**, *14*, 194-198.
30. Scholl, R.; Seer, C., *Monatshefte fuer Chemie* **1912**, *33*, 1-8.
31. Tamao, K.; Sumitani, K.; Kumada, M., *Journal of the American Chemical Society* **1972**, *94*, 4374-4376.
32. Du, C. J. F.; Hart, H.; Ng, K. K. D., *Journal of Organic Chemistry* **1986**, *51*, 3162-3165.
33. Vinod, T. K.; Hart, H., *Journal of Organic Chemistry* **1990**, *55*, 5461-5466.
34. Grewal, R. S.; Hart, H.; Vinod, T. K., *Journal of Organic Chemistry* **1992**, *57*, 2721-2726.
35. Hart, H., *Pure and Applied Chemistry* **1993**, *65*, 27-34.
36. Hart, H.; Rajakumar, P., *Tetrahedron* **1995**, *51*, 1313-1336.
37. Luening, U.; Baumstark, R.; Wangnick, C.; Mueller, M.; Schyja, W.; Gerst, M.; Gelbert, M., *Pure and Applied Chemistry* **1993**, *65*, 527-532.
38. Luening, U.; Baumgartner, H., *Synlett* **1993**, 571-572.
39. Luening, U.; Baumgartner, H.; Manthey, C.; Meynhardt, B., *Journal of Organic Chemistry* **1996**, *61*, 7922-7926.
40. Luening, U.; Baumbartner, H.; Wangnick, C., *Tetrahedron* **1996**, *52*, 599-604.
41. Luening, U., *Journal of Materials Chemistry* **1997**, *7*, 175-182.
42. Abbass, M.; Kuehl, C.; Manthey, C.; Mueller, A.; Luening, U., *Collection of Czechoslovak Chemical Communications* **2004**, *69*, 1325-1344.

43. Wittig, G.; Geissler, G., *Justus Liebigs Annalen der Chemie* **1953**, 580, 44-57.
44. Kress, T. H.; Leanna, M. R., *Synthesis* **1988**, 803-805.
45. Saednya, A.; Hart, H., *Synthesis* **1996**, 1455-1458.
46. Clyburne, J. A. C.; McMullen, N., *Coordination Chemistry Reviews* **2000**, 210, 73-99.
47. Shah, S.; Eichler, B. E.; Smith, R. C.; Power, P. P.; Protasiewicz, J. D., *New Journal of Chemistry* **2003**, 27, 442-445.
48. Power, P. P., *Chemical Reviews* **1999**, 99, 3463-3503.
49. Morgan, B. P.; Gilliard, R. J., Jr.; Loungani, R. S.; Smith, R. C., *Macromolecular Rapid Communications* **2009**, 30, 1399-1405.
50. Annan, K. O.; Scherf, U.; Mullen, K., *Synthetic Metals* **1999**, 99, 9-16.
51. Armstrong, N.; Hoft, R. C.; McDonagh, A.; Cortie, M. B.; Ford, M. J., *Nano Letters* **2007**, 7, 3018-3022.
52. Schmidtchen, F. P.; Berger, M., *Chemical Reviews* **1997**, 97, 1609-1646.
53. Antonisse, M. M. G.; Reinhoudt, D. N., *Chemical Communications* **1998**, 443-448.
54. Hartley, J. H.; James, T. D.; Ward, C. J., *Perkin 1* **2000**, 3155-3184.
55. Beer, P. D.; Gale, P. A., *Angewandte Chemie, International Edition* **2001**, 40, 486-516.
56. Fischer, E., *Ber.* **1894**, 27, 2985-2993.
57. Behr, J.-P. Y. O. N.; Ed. By Jean-Paul, B., *The lock-and-key principle : the state of the art--100 years on*. Wiley & Sons: Chichester; New York, 1994; p 325.

58. Berg, J. M.; Tymoczko, J. L.; Stryer, L.; Stryer, L., *Biochemistry*. 5th ed.; W.H. Freeman: New York, 2002.
59. Kyba, E. P.; Helgeson, R. C.; Madan, K.; Gokel, G. W.; Tarnowski, T. L.; Moore, S. S.; Cram, D. J., *Journal of the American Chemical Society* **1977**, *99*, 2564-2571.
60. Cram, D. J.; Cram, J. M., *Accounts of Chemical Research* **1978**, *11*, 8-14.
61. Solov'ev, V. P.; Strakhova, N. N.; Raevsky, O. A.; Ruediger, V.; Schneider, H.-J., *Journal of Organic Chemistry* **1996**, *61*, 5221-5226.
62. Green, D. P.; Balcom, B. J.; Lees, T. J., *Review of Scientific Instruments* **1996**, *67*, 102-107.
63. Fielding, L., *Tetrahedron* **2000**, *56*, 6151-6170.
64. Okada, T.; Katou, K.; Hirose, T.; Yuasa, M.; Sekine, I., *Chemistry Letters* **1998**, 841.

CHAPTER 2

1,4-CONJUGATE ADDITION OF ARYLBORONIC ACIDS TO ENONES UTILIZING TERPHSPAN COMPLEXES[#]

2.1 Introduction

Due to high atom efficiency (few atoms are wasted), versatility and cheap feedstock, conjugate addition reactions have been studied extensively since Arthur Michael pioneered conjugative addition reactions in the late 19th century.^{3,4} The plethora of publications involving Stork enamine reactions,⁵ which involve enamines as the nucleophile, the Nagata reactions,⁶ which use hydrogen cyanide to make 1,4-keto-nitriles and the Michael reaction,⁷ which uses enolates, are testaments to the longstanding recognition and importance of 1,4-conjugate addition reactions as synthetic tools. The development of asymmetric catalysts utilizing the Michael reaction has been of recent interest due to the synthetic ease and large chemical databank of conjugate unsaturated reagents capable of producing viable products for direct pharmaceutical applications. The growing need for higher enantiomeric excess in these types of reactions has caused a shift from reagents such as cuprates,⁸ to more viable reagents that have been thoroughly studied.

The use of 1,4-conjugate addition of enones to give substituted carbonyl compounds has potential for further synthetic use through retrosynthetic techniques. The common use of moisture and air stable reagents, such as organoboronic acids, allows water to be used as a solvent, which is crucial for cost efficiency and environmental

[#] Adapted from Morgan, B. P.; Smith, R. C. *J. Organomet. Chem.* **2008**, 693, 11-16

concerns. Other advantages of using organoboronic acids is the prevention of 1,2-addition to enones as is observed when organomagnesium or organolithium reagents have been used instead.^{2,9,10} One concern, however, is noted in cases when bulky substituents are present at the four position in conjugative addition: the 1,2-addition product is less crowded and would be expected to be the favored product (**Figure 2.1**).

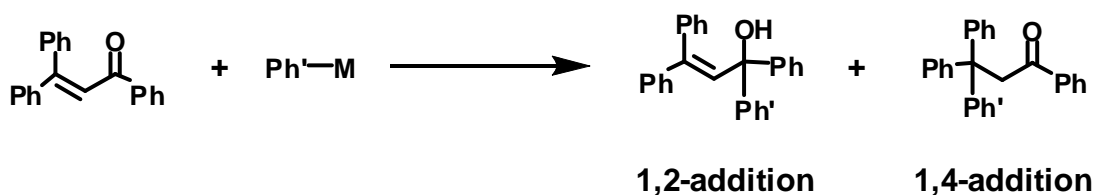


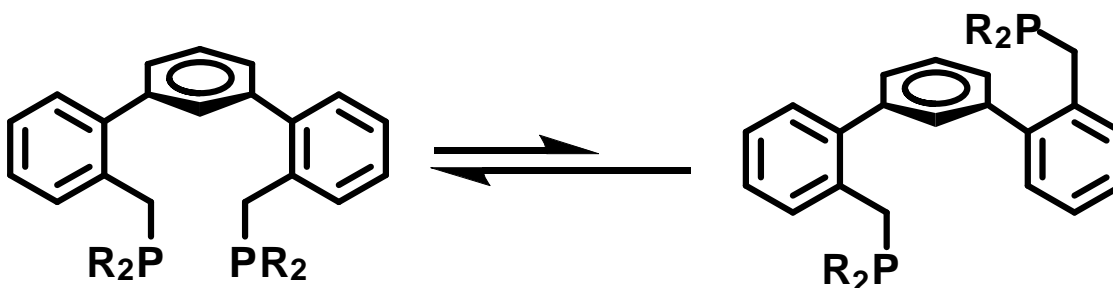
Figure 2.1 Example of steric repulsion from the generation of 1,4 addition reactions.

Organoboronic acids are generally less reactive towards enones than are other organometallic reagents. Less reactive species are less likely to undergo uncatalyzed 1,2-addition, so regioselectivity towards 1,4-addition can be accomplished. The use of phosphine transition metal complexes as catalysts can afford additional advantages to 1,4-conjugate addition reactions. Exhaustive investigations utilizing phosphines as chiral ligands have also lent themselves to asymmetric 1,4-addition to enones.^{9,11}

Catalytic processes are dramatically influenced by supporting ligands, such as phosphines, which have been of great interest since the initial discovery that phosphines can influence the efficiency of catalyzed reactions in the early 20th century. Advantages to phosphines as supporting ligands are demonstrated by their use in numerous functional group tolerant C–C bond-forming reactions.¹² The ease of access to functionally diverse phosphines increases the number of parameters that can be tuned to optimize their role in catalysis. The Tolman cone angle, as discussed in Chapter 1 (**Figure 1.3**), is one parameter that is used to quantify phosphine sterics.

The use of bidentate phosphorus donor ligands has been of recent interest, resulting in the introduction of a bite angle (P–M–P angle, β) parameter, also discussed in Chapter 1 (**Figure 1.3**), that can be applied to predict coordination modes.¹³ The ability for a ligand to stabilize various coordination modes is essential for metals in the course of a catalytic cycle. A definite correlation between bite angle and catalytic activity has been observed for numerous industrially important processes, notably hydroformylation,¹⁴⁻¹⁷ hydrocyanation,^{15, 18} allylic alkylation¹⁹⁻²¹ and cross coupling,²²⁻²⁵ and various trends have been summarized by van Leeuwen in several reviews.²⁶⁻³⁰

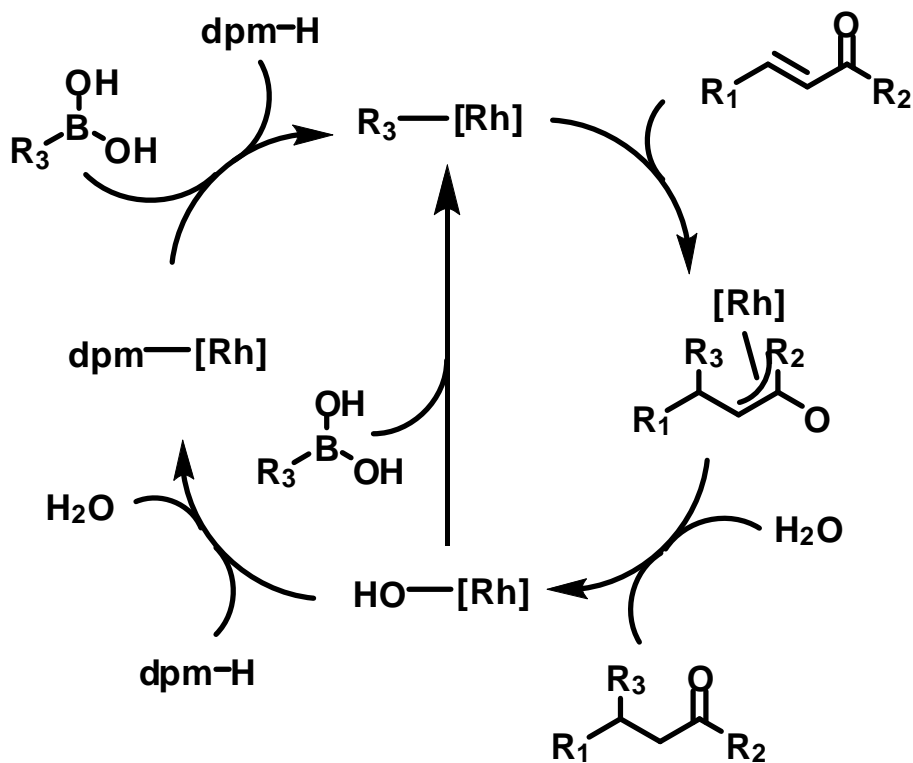
The design of a flexible scaffold involving a *m*-terphenyl scaffold that can accommodate different geometries has been studied and a critical evaluation of catalytic activity and structural features was achieved (**Scheme 2.1**).¹² Flexibility may be beneficial when a catalytic process requires transmetalation or ligand exchange wherein the metal complex must rearrange to accommodate intermediate geometries in the course of the mechanistic cycle. Crystallographically characterized pseudo-square planar palladium and nickel complexes were reported previously in which Terphspan diphosphines displayed a *trans*-spanning binding mode with P–M–P angles of 174.77° and 172.97° for their Pd and Ni complexes, respectively. The ability for Terphspan ligands to accommodate different geometries was anticipated on the basis of the



Scheme 2.1 Equilibrium of Terphspan ligand to demonstrate flexibility in coordination compounds.

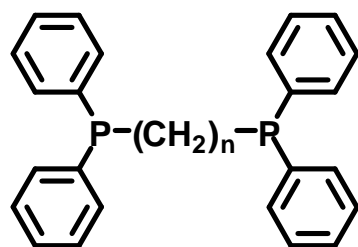
scaffold's flexibility. This property may be beneficial in catalytic cycles that involve various oxidation states and coordination modes in their mechanistic pathways.

The addition of aryl groups via organoboron compounds to enones was recently reported in the presence of palladium acetate catalyst with sodium acetate and antimony (III) chloride.³¹ It was proposed that the oxidative addition of the C–B bond to the Pd (0) species was required for the reaction to proceed. In 1997, however, it was proposed that organoboron compounds can undergo transmetalation with transition metals such as rhodium as an alternate catalytic pathway (**Scheme 2.2**).³² A more thoroughly examined C–C bond forming reaction, Suzuki-Miyaura coupling involving aryl halides and organoboron compounds, has amply demonstrated the efficacy of transmetalation from boron to palladium.³³

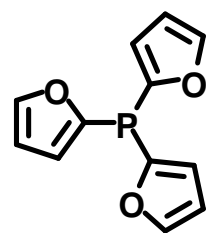


Scheme 2.2 Two possible mechanisms for 1,4 conjugate addition of enones.²

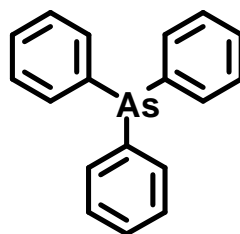
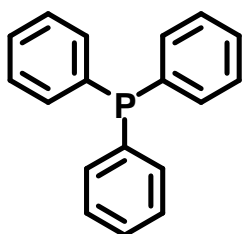
A)



n = 2 (dppe)
 n = 3 (dppp)
 n = 4 (dppb)



trifuran-2-ylphosphine



B)

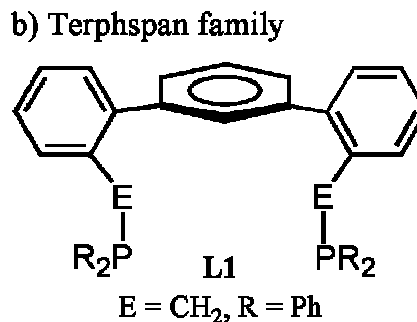
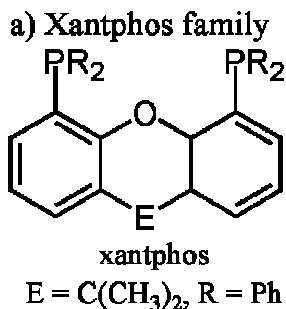
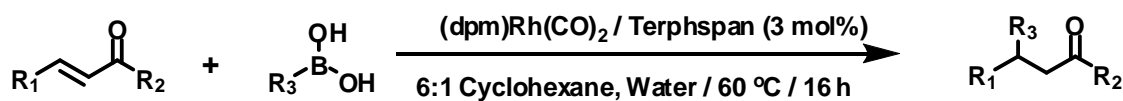


Figure 2.2 a) Ligands used for 1,4 conjugate addition of enones and b) some examples of some wide bite angle diphosphines.

A recent study by Miyaura took advantage of the ability for boronic acids to undergo transmetalation with rhodium to study the 1,4 conjugate addition of aryl- or alkenylboronic acids to enones (**Scheme 2.3**). Miyaura elucidated the observed trend in catalytic activity of diphosphine-mediated Rh-catalyzed 1,4-addition of phenylboronic acid to 2-octen-4-one, where the activity followed the trend: diphenylphosphinobutane (dppb) > diphenylphosphinopropane (dppp) > tri-(2-furyl)phosphine (TFP) > diphenylphosphinoethane (dppe) (**Figure 2.2**).

This trend was attributed to the increasing P–M–P bite angle, spurring subsequent studies on wide bite angle diphosphines. Terphspan diphosphine ligands, the ligands used in the current work, have been known to accommodate wide bite angles (greater than $\sim 110^\circ$). The preference of the Terphspan scaffold for larger bite angles led us to explore its use in 1,4-conjugate addition. This initial study focused on the development of reaction conditions including reaction temperature, solvent and substrates. Other significant reactions and conditions to obviously pursue include the use of an asymmetric catalyst designed using a functionalized Terphspan ligand; however, time has not yet allowed this study to be completed.

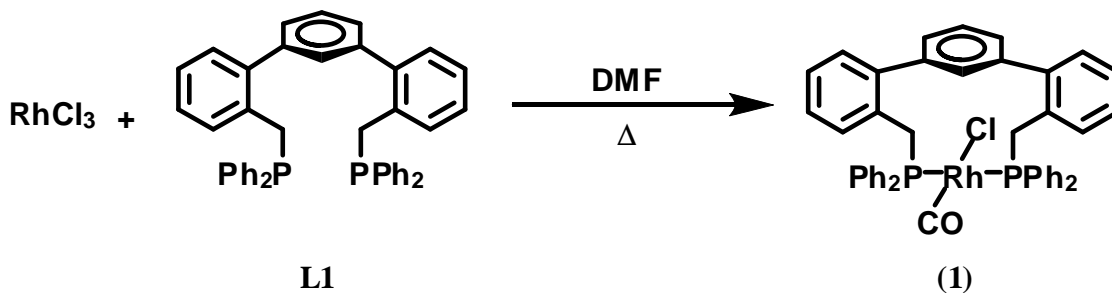


Scheme 2.3 1-4 Conjugate Addition of the R₃ on the boronic acid to the enone.

The catalytic activity of rhodium catalyzed 1,4 conjugate addition of aryl boronic acids to α,β -unsaturated ketones utilizing Terphspan was shown to give up to quantitative yields with 1:1 arylboronic acid/enones ratios (**Scheme 2.1**). With these initial studies the use of Terphspan ligand as an asymmetric catalyst can be envisioned by making use of various cyclometallated palladacycles with C₂ symmetry.³⁴

2.2 Synthesis, Structure and Catalytic Activity

The ability for *m*-terphenyl ligands within the Terphspan family to chelate metals was first pioneered by Smith *et al.* in 2004,³⁵ followed by its use in catalysis in the following year.³⁶ The ability for Terphspan complexes to form with other metals, especially rhodium, was of keen interest due to its established catalytic ability. The synthesis of rhodium carbonyl complex [ClRh(CO)(L1)] (**1**) was the first targeted complex to elucidate the coordination mode of a rhodium complex involving the Terphspan ligand L1 (Scheme 2.4).



Scheme 2.4 Preparation of (**1**) from RhCl₃ and Terphspan ligand L1.

The preparation of **1** was achieved following a modified procedure for the preparation of *trans*-[RhCl(CO)(PPh₃)₂] by Serp *et al.*³⁷ This procedure involves a convenient one-pot synthesis with the use of refluxing dimethyl formamide (DMF) as the source of the carbonyl ligand. The general pathway in which the decarbonylation of DMF occurs can be monitored by infrared (IR) spectroscopy due to the distinct sharp carbonyl band (ν_{CO}) which will exhibit changes upon formation of a complex. The preparation of **1** was achieved in 43% yield by reacting RhCl₃·3H₂O with L1 in the presence of 120 °C DMF to give a yellow powder. Compound **1** exhibits a C–O stretch in the IR spectrum at $\nu_{\text{CO}} = 1966 \text{ cm}^{-1}$, which compares well with the values observed in *trans*-

[RhCl(CO)(PR₃)₂] complexes such as *trans*-[RhCl(CO)(PPh₃)₂] (1960 cm⁻¹)³⁷ and *trans*-[RhCl(CO)(P(*t*-Bu)₂H)₂] (1965 cm⁻¹).³⁸

NMR spectra of molecules in solution that exhibit fluxionality can be difficult to analyze. Unexpectedly, complex spectra can be attributable to various anomalies within the structure such as two molecular structures that do not interconvert or a less rigid structure that allows slow interconversion of two conformational isomers (i.e atropisomers) in solution. These differences are typically temperature and solvent dependent. Fluxionality of this type was observed in palladium and nickel complexes of the Terphspan ligand **L1** via proton NMR spectra.³⁵ The analogous rhodium structure [RhCl(CO)(**L1**)] (**1**), however, did not exhibit this fluxionality, which was attributed to a more rigid **L1** scaffold for the rhodium complex (**1**) in solution.

The broad distribution of aromatic protons on the central terphenyl ring of **1** is a notable feature within its ¹H NMR spectrum. This large dispersion occurs as a result of the close proximity of the central terphenyl ring protons to the metal center. For **1** the aromatic protons span a range of more than 2 ppm from δ 6.18 to 8.04 ppm which is similar to those effects observed for the Pd and Ni complexes of **L1**.³⁵ The ability of the metal to affect these protons can be initially evaluated based on the internuclear distance from the metal center to hydrogen. For **1** the rhodium metal sits 3.37 Å from H(1) which is closer than both the Pd and Ni complexes (3.48 and 3.51 Å respectively), but is still not within the sum of van der Waals radii for C (1.20Å) and Rh (2.00Å).

Coordination chemistry has a variety of characterization techniques to determine the environment around the metal. Ligands with donor atoms that have nuclei that contain an odd number of nucleons create advantageous characterization techniques. The use of

NMR spectroscopy of the nuclei of interest can be used to obtain coordination environments as well as other structural information. A common use for this technique is the use of phosphorus donor ligands which are NMR active nuclei and can be measured readily due to the high natural isotopic abundance of phosphorus-31 (^{31}P , an NMR active isotope). In particular the difference in ^{31}P NMR chemical shift ($\Delta\delta$) between free ligand and complexed states can be used to determine whether the molecule of interest has formed.³⁹ The $\Delta\delta$ between the free ligand **L1** (-8.8 ppm) and the coordination compound **1** (27.3 ppm) is 36.1 ppm. This is in close agreement to the $\Delta\delta$ for *trans*-[RhCl(CO)(PPh₃)₂] (37.3 ppm) as calculated from the difference of the free ligand PPh₃ (-4.8 ppm) to the *trans*-[RhCl(CO)(PPh₃)₂] complex (32.5 ppm).³⁷

Another useful tool for predicting the coordination environment around a metal is the use of the coupling constant of the metal with the donor ligands; however, not all metals have NMR active nuclei, so this method has limitations. The coordination compound **1** utilizes rhodium as the metal center, which does allow for this technique to be employed and the P-Rh coupling constant is calculated to be 137 Hz. This is relatively low and indicative of the coordination environment of a *trans*-diphosphine complex. The typical values for $J_{\text{Rh-P}}$ coupling constants for *trans*-diphosphine Rh(I) complexes are ~140-145 Hz and are normally smaller than *cis*-isomers which range from ~190-195 Hz. Other effects that can effect the coupling constants are the electronegativity of the other atoms attached to the metal in which the Cl and CO of **1** account for the slightly lower coupling constant.⁴⁰⁻⁴⁵

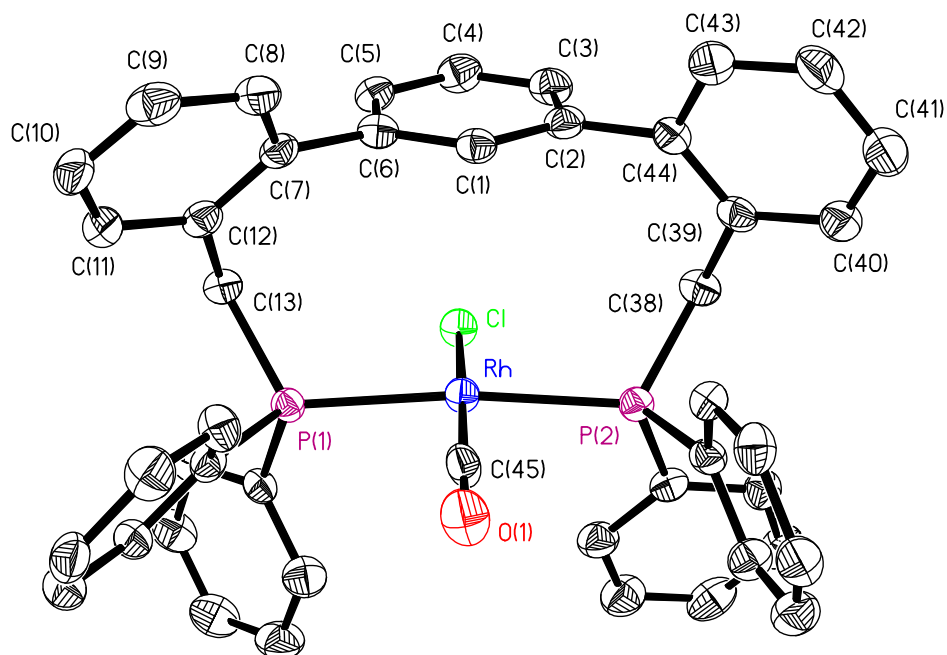


Figure 2.3 ORTEP drawing (50% probability ellipsoids) of the molecular structure of **1**. Hydrogen atoms and the cocrystallized DMF solvent molecule are omitted for clarity.

The confirmation of the proposed structure for $[\text{ClRh}(\text{CO})(\mathbf{L1})]$ (**1**) was revealed by the use of single crystal X-ray crystallography, an excellent technique to obtain detailed structural information including bond lengths and angles. The growth of high quality crystals by cooling a saturated 60 °C DMF solution to room temperature over 12 hours provided the structure **1**-DMF after single crystal X-ray diffraction analysis (**Figure 2.3**). Select bond lengths and angles are provided in **Table 2.1** and include P–M–P angle of 171.37° which is comparable to those observed in $[\text{PdCl}_2(\mathbf{L1})]$ and $[\text{NiCl}_2(\mathbf{L1})]$ (172.97° and 174.78°, respectively).³⁵ DMF free crystals were also obtained by the diffusion of tetramethylsilane into a saturated dichloromethane solution of **1**, however the **1**-DMF crystals gave superior refinement details (**Table 2.2**). Another noteworthy feature of **1**-DMF is the preferential orientation in which the chlorine atom attached to the rhodium resides on the less sterically crowded side of the terphenyl. This

Table 2.1 Select Bond Lengths (Å) and Angles (deg) for **1**·DMF.

Rh–Cl	2.3839 (5)
Rh–P(1)	2.3146 (4)
Rh–P(2)	2.3228 (4)
Rh–C(45)	1.7978 (4)
C(45)–O(1)	1.1515 (3)
P(1)–Rh–P(2)	171.372 (10)
P(1)–Rh–Cl	87.887 (10)
P(1)–Rh–C(45)	91.104 (11)
P(2)–Rh–Cl	89.332 (9)
P(2)–Rh–C(45)	90.819 (11)
Cl–Rh–C(45)	174.048 (16)

sterically-gearred selective synthesis could be exploited in additional manipulations of Terphspan complexes.

The full characterization of the *trans*-spanning rhodium complex (**1**), which exhibits air and thermal stability, was proposed to exhibit catalytic activity. To investigate the ability of **L1** to display catalytic activity, the use of **L1** for support within Rh-catalyzed C-C bond formation was probed. The initial catalytic reaction investigated was the 1,4-conjugate addition of aryl boronic acids to α,β -unsaturated ketones which was first introduced in the introduction of Chapter 2 (*vide supra*).^{2,9,31,46-63} Miyaura and coworkers discovered the use of Rh complexes to catalyze reactions of this type in 1997, and it has been an active area of research ever since.³² Miyaura's initial study explored the use of many phosphines of which the greatest activity was observed with dppb (1,4-bis(diphenylphosphino)butane), a flexible diphosphine capable of supporting large bite angle complexes (**Figure 2.2**). The high activity of dppb suggests that the use of *trans*-

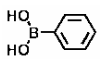
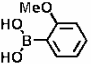
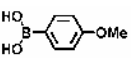
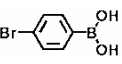
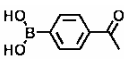
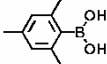
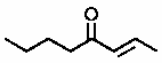
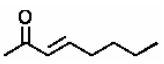
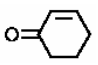
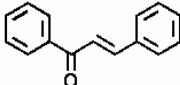
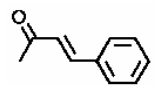
Table 2.2 Crystal Data and Structure Refinement Details for **1**·DMF.

Empirical formula	C ₄₅ H ₃₆ ClOP ₂ Rh · C ₃ H ₇ NO
Formula weight (g/mol)	866.13
Temperature (K)	153 (2)
Wavelength (Å)	0.71073
Crystal system	Monoclinic
Space group	P2 ₁ /c (# 14)
Unit cell dimensions	
<i>a</i> (Å)	18.623(4)
<i>b</i> (Å)	11.779(2)
<i>c</i> (Å)	18.629(4)
<i>α</i> (deg)	90.00
<i>β</i> (deg)	98.05(3)
<i>γ</i> (deg)	90.00
Volume (Å ³)	4046.1(14)
<i>Z</i>	4
Calculated density (Mg/m ³)	1.422
Absorption coefficient (mm ⁻¹)	0.608
<i>F</i> (000)	1784
Crystal size (mm)	0.36 × 0.29 × 0.14
Crystal color and shape	yellow plate
<i>θ</i> range for data collection (deg)	2.05 – 25.10
Limiting indices	-22 < <i>h</i> < 20 -14 < <i>k</i> < 14 -22 < <i>l</i> < 22
Reflections collected	7182
Independent reflections	6016
Completeness to <i>θ</i>	25.10 (99.6 %)
Max. transmission	0.9197
Min. transmission	0.8108
Refinement method	Full-matrix least-squares on <i>F</i> ²
Data / restraints / parameters	7182/1/666
Goodness of fit on <i>F</i> ²	1.144
<u>Final R indices (<i>I</i> > 2σ(<i>I</i>))</u>	
R1	0.0489
wR2	0.1182
<u>R indices (all data)</u>	
R1	0.0604
wR2	0.1273

spanning ligands such as **L1** could exhibit superior activity. To investigate this activity the use of six arylboronic acids and five enones (**Table 2.3**) were examined for C-C bond formation with the use of **L1** as the supporting ligand. The use of a variety of substituents allows for information about the effects of sterics and electronics which allow for vital information for further studies.

The initial reaction conditions used for the reactions explored were chosen to mimic those in the original study by Miyaura.³² This similarity in conditions allowed for direct correlation of results to those previously reported by Miyaura. The initial trials were carried out at 60 °C in 6:1 cyclohexane/water with a 1:2 enone/arylboronic acid ratio and are summarized in **Table 2.3**. The yields of the substrates employed showed results that were as good or better than those observed with dppb under the current reaction conditions.³²

Table 2.3 Catalytic 1,4-addition of boronic acids to α,β -unsaturated enones. Conditions are described in the Experimental section. (Adapted from Morgan et. al.¹)

Boronic Acid : Enone												
	2:1	1:1	2:1	1:1	2:1	1:1	2:1	1:1	2:1	1:1	1:1	
	89	88	68	32	95	41	63	25	23	20	77	
	91	98	58	46	98	~100	~100	32	~100	13	47	
	84	90	90	83	98	9	~100	46	97	38	24	
	98	77	34	23	83	36	62	30	36	27	6	
	93	70	41	36	98	40	41	24	36	26	31	

The use of excess arylboronic acid is often necessary to reach acceptable yields for 1,4-addition reactions. This demand for wasted materials sparked the interest to improve atom efficiency employing a 1:1 arylboronic acid/enone ratio as well as encompassing sterically encumbered 2,4,6-trimethylphenylboronic acid as a coupling partner (**Table 2.3**). The use of 1:1 ratios gave similar yields in 10 out of the 25 trials as those utilizing 2:1 ratios. Sterically demanding enones and boronic acids, however, demanded the need for 2:1 ratios as seen by the depressed yields for enones such as 4-phenyl-3-butene-2-one and phenyl styryl ketone. Coupling of sterically encumbered 2,4,6-trimethylphenylboronic acid was moderately successful only with 2-octene-4-one and 3-octene-2-one (77% and 47%, respectively), while lower yields of 6-31% for the other enones was achieved. The 1,4-conjugate addition of boronic acids to less sterically demanding enones employing the Terphspan scaffold holds promise for the expansion of ligand parameters such as chiral phosphine moieties to explore asymmetric coupling reactions of commercially relevant reactions.

2.3 Conclusions

The preparation of the first Terphspan rhodium complex (**1**) was achieved. This material was fully characterized and was shown to exhibit air and thermal stability. The coordination environment of (**1**) was shown to exhibit a *trans*-spanning mode similar to that previously reported for Ni and Pd complexes of **L1**. The single crystal x-ray diffraction of crystals of **1**·DMF showed a P-M-P angle of 171.37° which was similar to previously reported structures of **L1**. The use of the Terphspan ligand **L1** in rhodium-catalyzed 1,4-addition of aryl boronic acids to α,β -unsaturated ketones was studied to initially test the catalytic ability of rhodium Terphspan complexes. Moderate to high yields were achieved with many substrate pairs which illustrates the use of complexes incorporating Terphspan ligands as important catalysts. The enhancement of atom efficiency in the use of 1:1 arylboronic acid/enone ratios was employed with improved yields to the current literature. The modification of **L1** to design an asymmetric catalyst would accommodate the increasing demand for asymmetric catalysis employing reactions involving C-C bond formations of α,β -unsaturated ketones.

2.4 Experimental Details

All synthesis was carried out in an inert atmosphere of nitrogen using an MBraun dry box or with standard Schlenk techniques. Ligand **L1**³⁵ and Rh(CO)₂(dpm) (dpm = dipivaloylmethanoate)⁶⁴ were prepared as reported previously. Solvents were purified by passage through alumina columns under a N₂ atmosphere employing an Mbraun solvent purification system. All other reagents were used as received from TCI and Alfa Aesar. ³¹P NMR spectra were collected using a Bruker Avance 300 instrument operating at 121.4 MHz, while proton and ¹³C spectra were collected using a Bruker Avance 500 instrument operating at 500MHz for proton and 125.7 MHz for carbon. Infrared spectra were collected using a Thermo Nicolet IR-100 FT-IR utilizing the EZ OMNIC analysis program. Gas Chromatographs and Mass Spectra were collected using a Shimadzu GCMS-QP2010 and analyzed using the GCMSsolution software.

Preparation of [ClRh(CO)(L1)] (1)

A solution of RhCl₃·3H₂O (0.150 g, 0.570 mmol) and **L1** (0.393 g, 0.627 mmol) in 15 mL of *N,N*-dimethylformamide (DMF) was heated to 120 °C under nitrogen for 2.5 h. The resultant yellow solution was reduced to half its volume by vacuum distilling away some of the solvent. The solution was then cooled to 0° C and 20 mL of cold methanol was added to produce a yellow precipitate. The precipitate was collected by filtration, washed with cold methanol three times and dried *in vacuo* to yield the target compound (0.196 g, 43.1 %). An analytically pure sample of **1**·DMF was obtained by crystallization via slowly cooling a saturated DMF solution from 60 °C to room temperature overnight. IR: (CH₂Cl₂) ν_{CO} = 1966 cm⁻¹. ¹H NMR (500 MHz, CDCl₃): δ 2.88 (s, 3H, from cocrystallized DMF), 2.94 (s, 3H, from cocrystallized DMF), 3.36-3.39

(m, 2H), 4.82 (d, 2H, $J = 12$ Hz), 6.16 (d, 2H, $J = 8$ Hz), 6.79-6.83 (m, 6H), 7.05 (t, 4H, $J = 8$ Hz), 7.20-7.45 (m, 15H), 7.78-7.79 (m, 4H), 8.02 (s, 1H), 8.04 (s, 1H from cocrystallized DMF). ^{31}P NMR (121.4 MHz, CDCl_3): 27.4 (d, $J_{\text{Rh-P}} = 137$ Hz). ^{13}C NMR (125.7 MHz, CDCl_3): 31.4 (m, CH_2 partially overlapping cocrystallized DMF), 36.4 (from cocrystallized DMF, 126.2, 126.6, 127.1 (t, $J = 5$ Hz), 127.7 (t, $J = 5$ Hz) 128.5, 128.9, 129.5, 129.7, 130.1, 131.6, 132.3, 133.5 (t, $J = 6$ Hz), 134.1 (t, $J = 6$ Hz), 142.0, 143.8, 162.5 (from cocrystallized DMF), (carbonyl not observed). Anal. Calcd. for $\text{C}_{45}\text{H}_{36}\text{ClOP}_2\text{Rh}$: C, 68.15 H, 4.58. N, 0.00; Found: C, 67.84 H, 4.36 N <0.5.

General conditions for catalysis

To a preloaded conical vial containing the arylboronic acid (0.50 or 1.0 mmol) were sequentially added a solution of $\text{Rh}(\text{dpm})(\text{CO})_2$ (0.015 mmol) in 1 mL cyclohexane and **L1** (0.015 mmol in 1 mL 9:1 cyclohexane/ CH_2Cl_2). This mixture was allowed to stir at room temperature for 15 min prior to addition of the enone (0.50 mmol) solution in 1 mL cyclohexane followed by 0.5 mL of water. The mixture was heated to 60 °C with stirring for 16 h. The mixture was collected and diluted with 10 mL THF for immediate GC/MS analysis.

X-ray crystallography

Intensity data were collected using a Rigaku Mercury CCD detector and an AFC8S diffractometer. Data reduction and absorbance corrections were achieved using CrystalClear.⁶⁵ The structure was solved by direct methods and subsequent Fourier difference techniques, and refined anisotropically, by full-matrix least squares, on F^2 using SHELXTL 6.10.⁶⁶ C(13) – H(13B) was constrained to 1.083 Å.

2.5 Selected Spectra

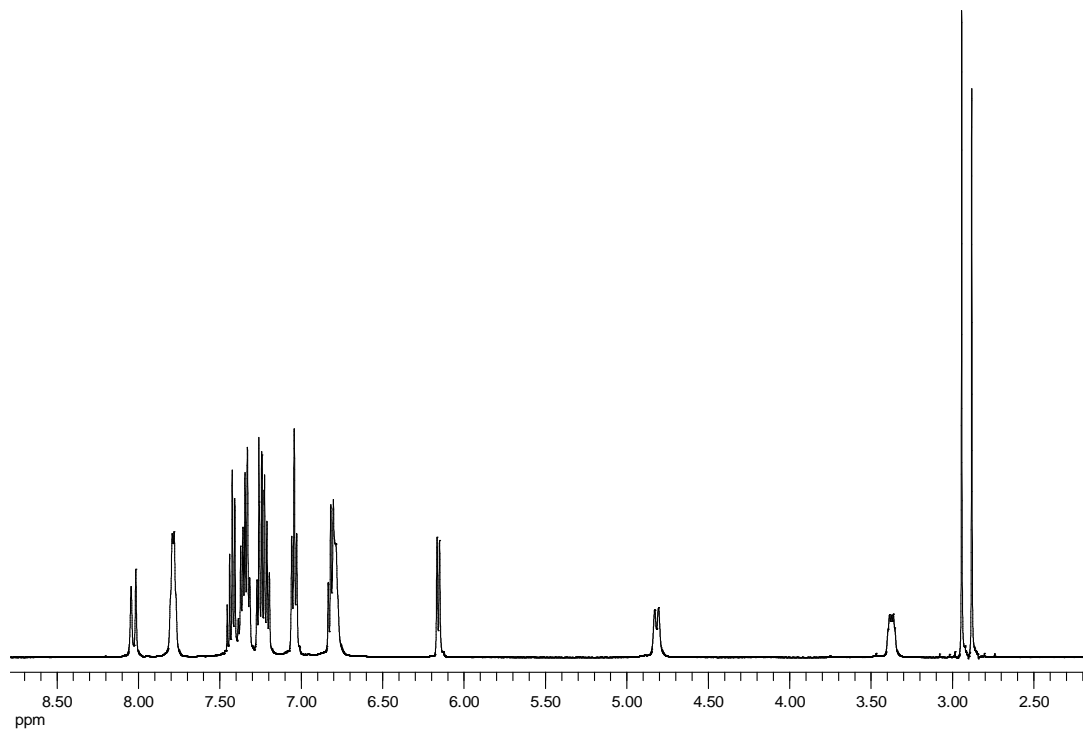


Figure 2.4 Proton NMR spectrum of **1**·DMF (CDCl_3 , 500 MHz) referenced to residual CHCl_3 . Note that peaks at 2.94, 2.88, and 8.06 are attributable to cocrystallized DMF.

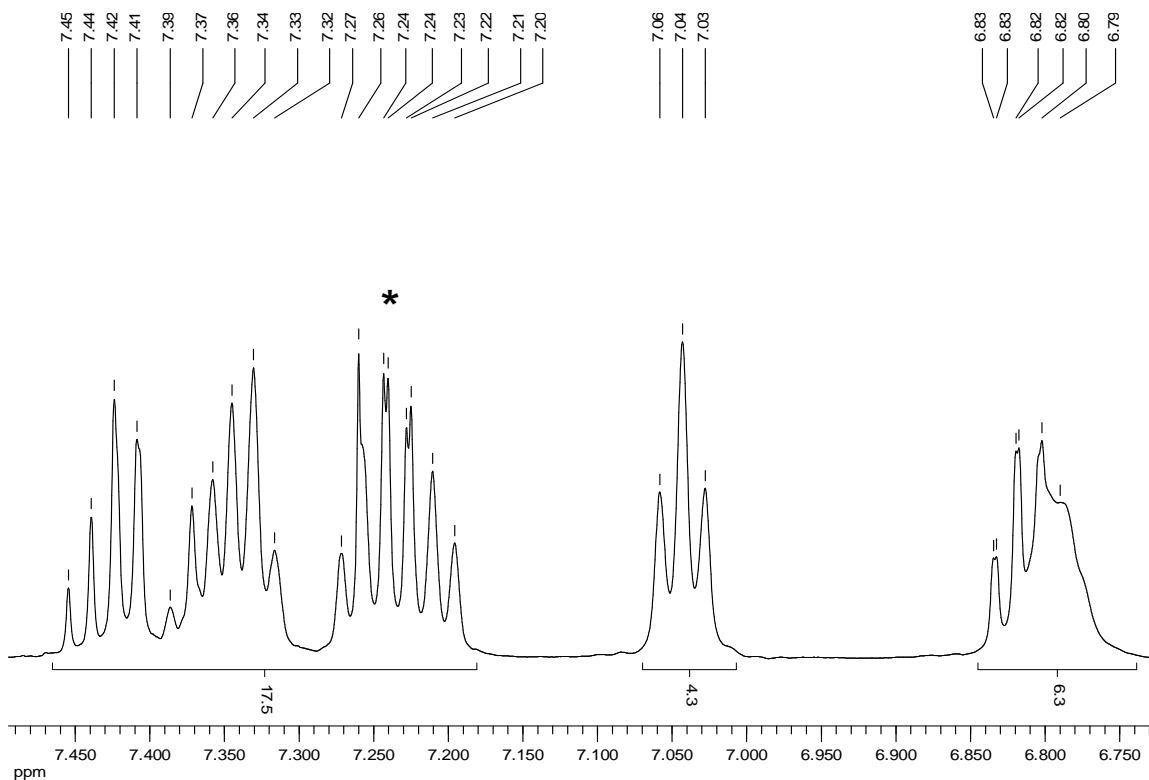


Figure 2.5 Aromatic region, proton NMR spectrum of **1**·DMF (CDCl_3 , 500 MHz).

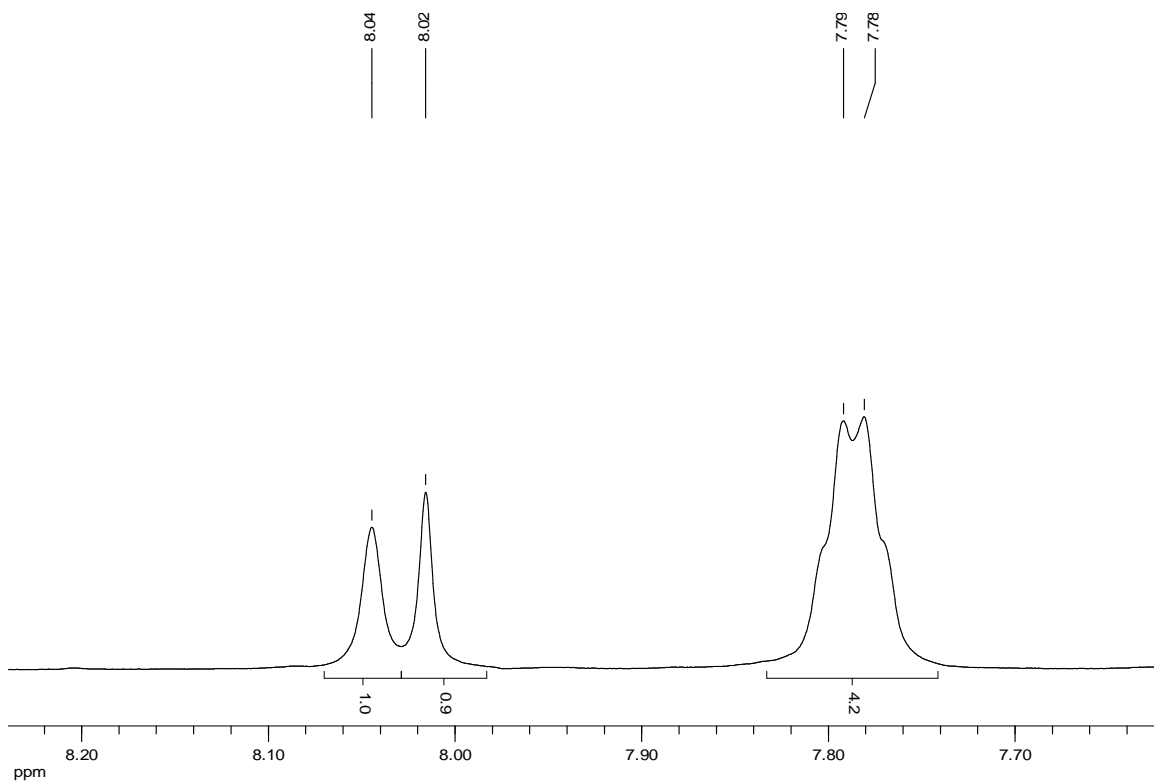


Figure 2.6 Inset above 7.5 ppm, proton NMR spectrum of **1**·DMF (CDCl₃, 500 MHz).

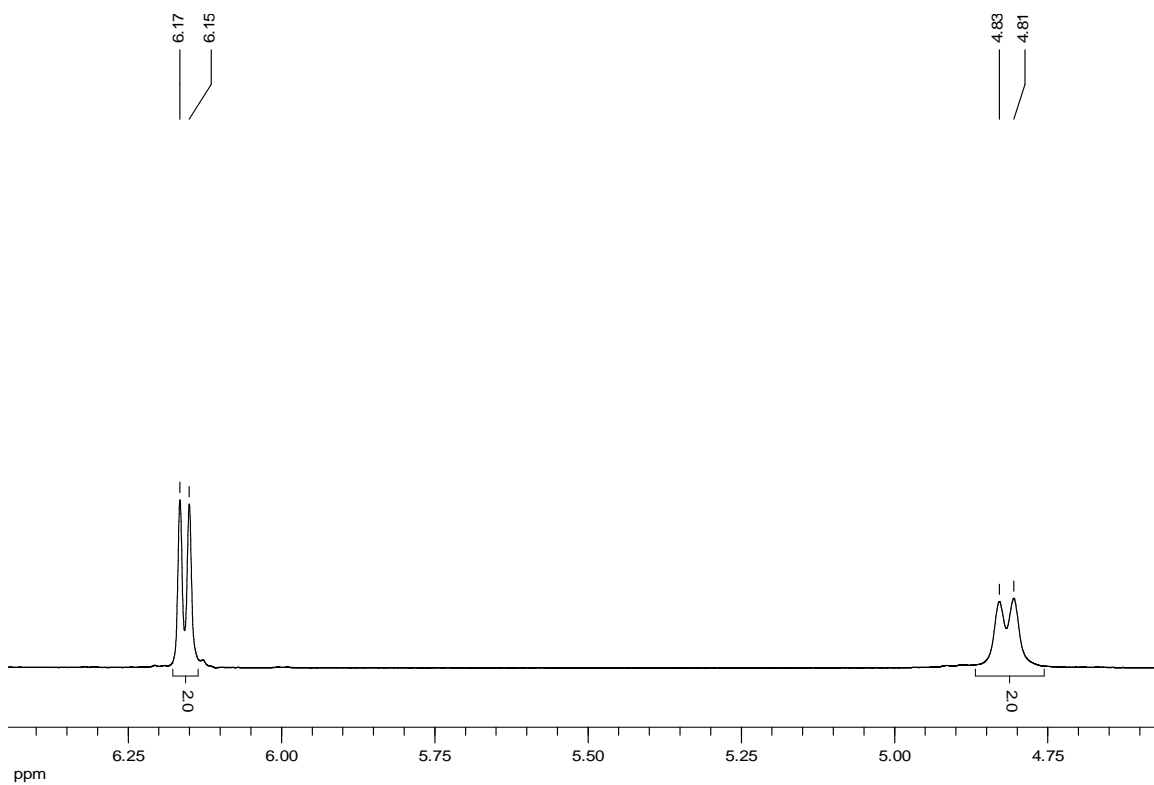


Figure 2.7 Region from 4.5 ppm to 6.5 ppm, proton NMR spectrum of **1**·DMF (CDCl₃, 500 MHz).

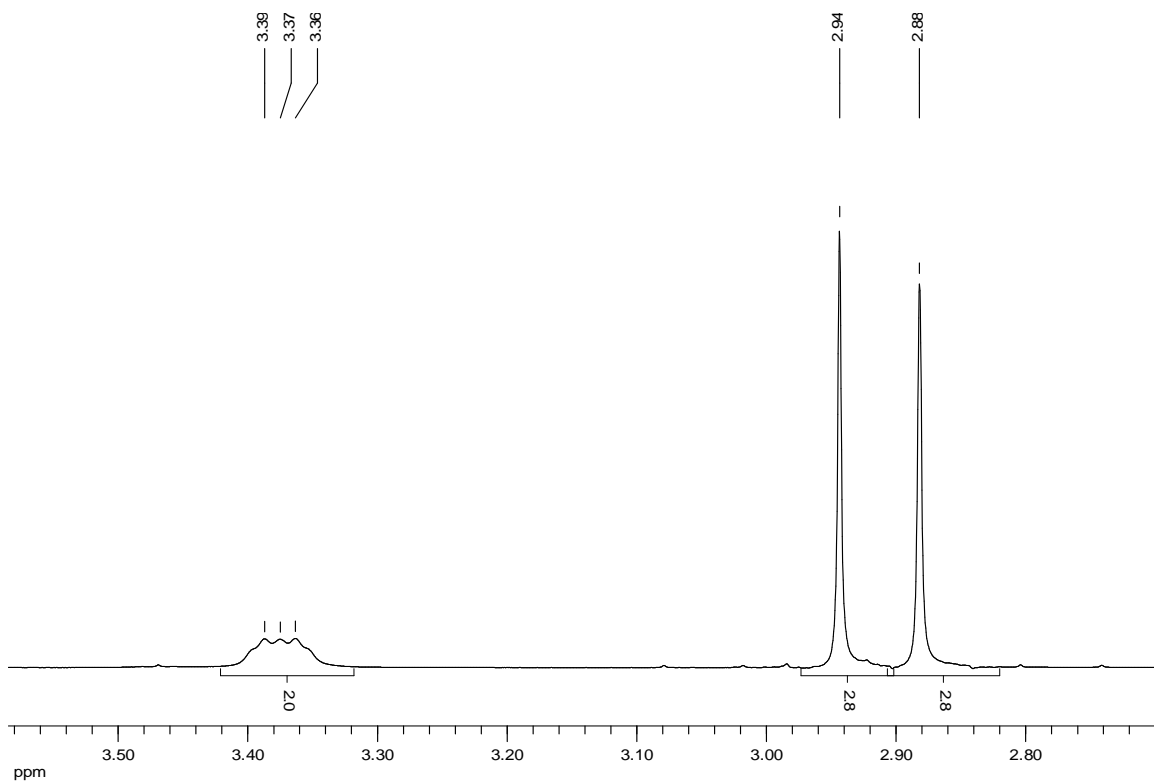


Figure 2.8 Aliphatic region, proton NMR spectrum of **1**·DMF (CDCl₃, 500 MHz).

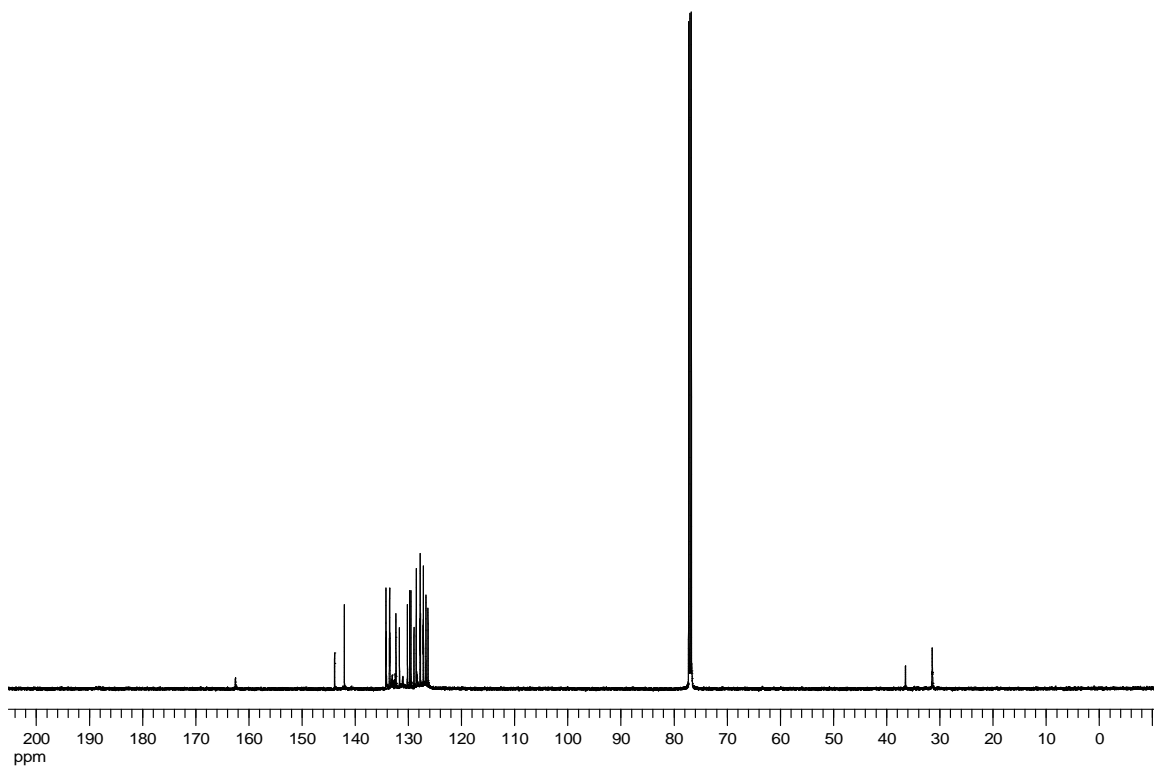


Figure 2.9 Carbon-13 NMR spectrum of **1**·DMF (CDCl₃, 126 MHz). Referenced to CDCl₃.

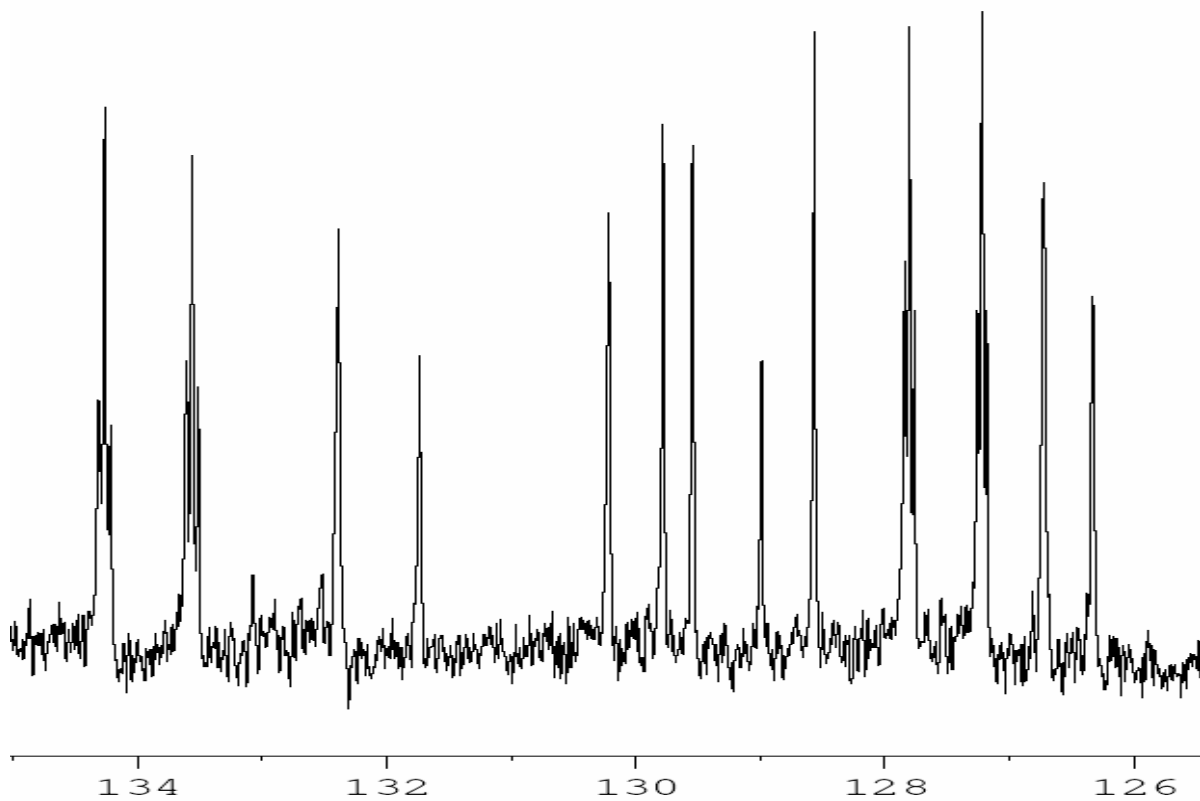


Figure 2.10 Aromatic region, carbon-13 NMR spectrum of **1**·DMF (CDCl₃, 126 MHz).

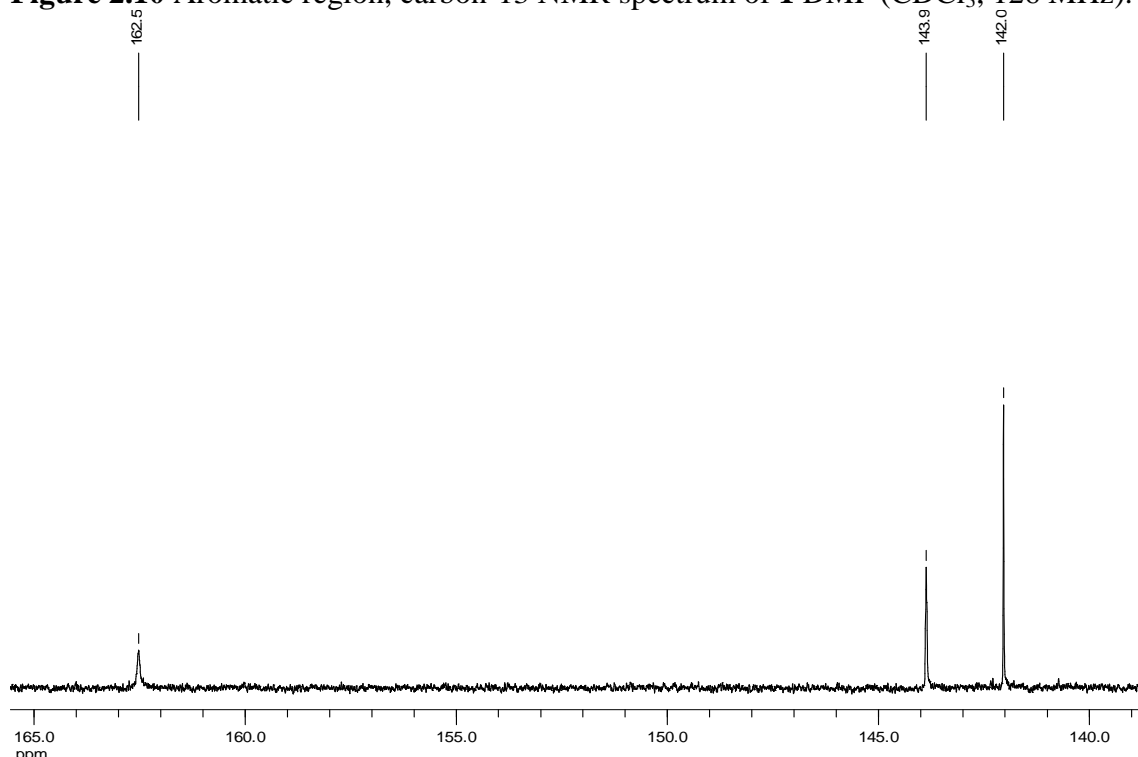


Figure 2.11 Region above 140 ppm, carbon-13 NMR spectrum of **1**·DMF (CDCl₃, 126 MHz).

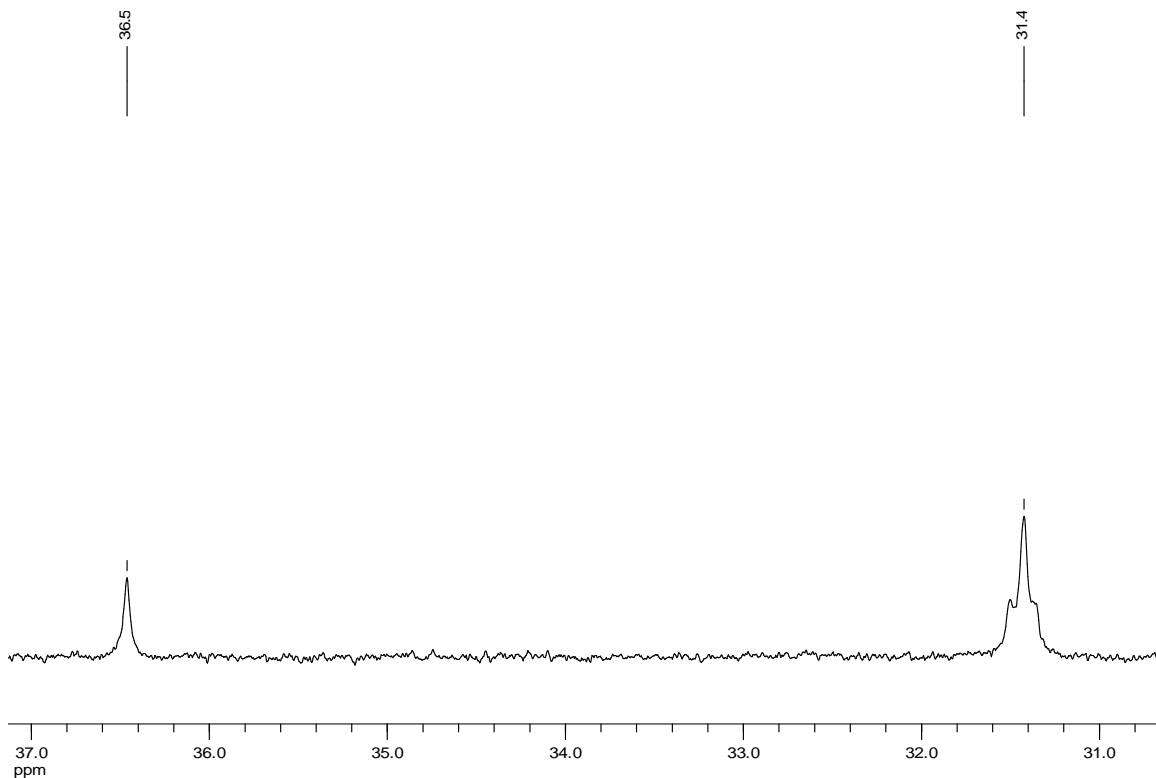


Figure 2.12 Aliphatic region, carbon-13 NMR spectrum of **1**·DMF (CDCl₃, 126 MHz).

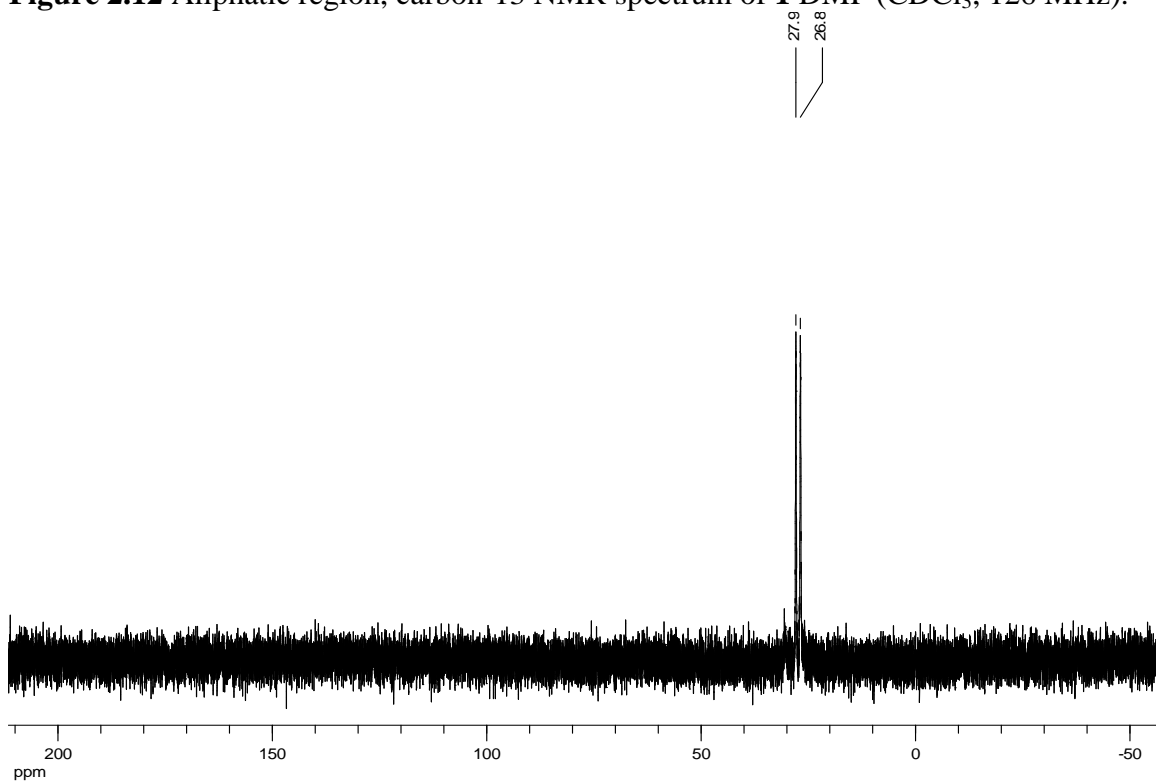


Figure 2.13 Phosphorus-31 NMR spectrum of **1**·DMF (CDCl₃, 121 MHz).

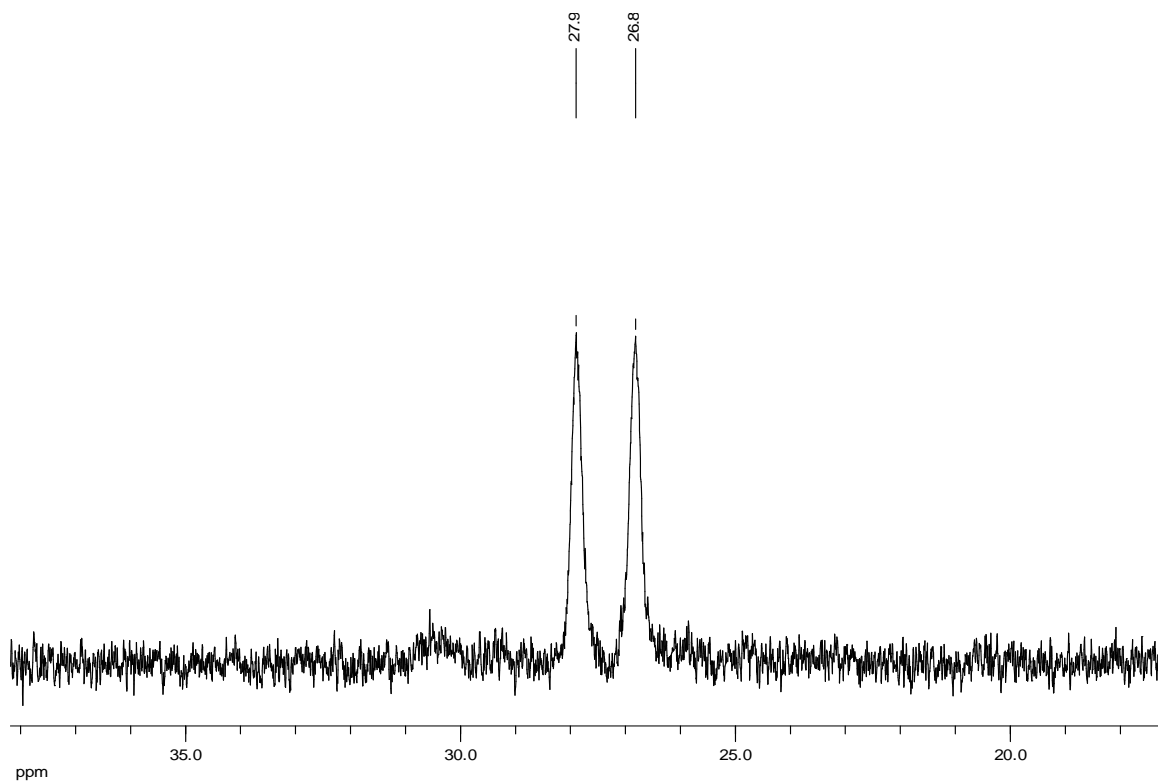


Figure 2.14 Inset, phosphorus-31 NMR spectrum of **1**•DMF (CDCl_3 , 121 MHz).

2.6 References

1. Morgan, B. P.; Smith, R. C., *Journal of Organometallic Chemistry* **2008**, *693*, 11-16.
2. Hayashi, T.; Takahashi, M.; Takaya, Y.; Ogasawara, M., *Journal of the American Chemical Society* **2002**, *124*, 5052-5058.
3. Michael, A., *Journal für Praktische Chemie* **1887**, *35*, 349-356.
4. Michael, A., *Journal für Praktische Chemie* **1894**, *49*, 20-25.
5. Silvestri, M. A.; Bromfield, D. C.; Lepore, S. D., *Journal of Organic Chemistry* **2005**, *70*, 8239-8241.
6. Andres, J. M.; Martinez, M. A.; Pedrosa, R.; Perez-Encabo, A., *Tetrahedron: Asymmetry* **2001**, *12*, 347-353.
7. Fan, Q.-H.; Li, Y.-M.; Chan, A. S. C., *Chemical Reviews* **2002**, *102*, 3385-3465.
8. Schlosser, M., *Organometallics in synthesis : a manual*. John Wiley & Sons: Chichester, West Sussex, England ; New York, 1994; p 603 p.
9. Hayashi, T.; Yamasaki, K., *Chemical Reviews* **2003**, *103*, 2829-2844.
10. Kazuhiro Yoshida, T. H., Rhodium(I)-Catalyzed Asymmetric Addition of Organometallic Reagents to Electron-Deficient Olefins. In *Modern Rhodium-Catalyzed Organic Reactions*, Prof, P. A. E., Ed. 2005; pp 55-77.
11. Rossiter, B. E.; Swingle, N. M., *Chemical Reviews* **1992**, *92*, 771-806.
12. Crabtree, R. H., *The organometallic chemistry of the transition metals*. 4th ed.; John Wiley: Hoboken, NJ, 2005; p xiii, 546 p.
13. Casey, C. P.; Whiteker, G. T., *Israel Journal of Chemistry* **1990**, *30*, 299-304.

14. Casey, C. P.; Whiteker, G. T.; Melville, M. G.; Petrovich, L. M.; Gavney, J. A., Jr.; Powell, D. R., *Journal of the American Chemical Society* **1992**, *114*, 5535-5543.
15. Kranenburg, M.; Kamer, P. C. J.; Vanleeuwen, P.; Vogt, D.; Keim, W., *Journal of the Chemical Society-Chemical Communications* **1995**, 2177-2178.
16. Van der Veen, L. A.; Boele, M. D. K.; Bregman, F. R.; Kamer, P. C. J.; Van Leeuwen, P. W. N. M.; Goubitz, K.; Fraanje, J.; Schenk, H.; Bo, C., *Journal of the American Chemical Society* **1998**, *120*, 11616-11626.
17. van der Veen, L. A.; Keeven, P. K.; Kamer, P. C. J.; van Leeuwen, P. W. N. M., *Dalton Transactions* **2000**, 2105-2112.
18. Marcone, J. E.; Moloy, K. G., *Journal of the American Chemical Society* **1998**, *120*, 8527-8528.
19. Trost, B. M.; Breit, B.; Peukert, S.; Zambrano, J.; Ziller, J. W., *Angewandte Chemie, International Edition* **1995**, *34*, 2386-2388.
20. Kranenburg, M.; Kamer, P. C. J.; Van Leeuwen, P. W. N. M., *European Journal of Inorganic Chemistry* **1998**, 25-27.
21. Van Haaren, R. J.; Oevering, H.; Coussens, B. B.; Van Strijdonck, G. P. F.; Reek, J. N. H.; Kamer, P. C. J.; Van Leeuwen, P. W. N. M., *European Journal of Inorganic Chemistry* **1999**, 1237-1241.
22. Portnoy, M.; Milstein, D., *Organometallics* **1993**, *12*, 1655-1664.
23. Hayashi, T.; Konishi, M.; Kumada, M., *Tetrahedron Letters* **1979**, 1871-1874.
24. Hayashi, T.; Konishi, M.; Kobori, Y.; Kumada, M.; Higuchi, T.; Hirotsu, K., *Journal of the American Chemical Society* **1984**, *106*, 158-163.

25. Kranenburg, M.; Kamer, P. C. J.; Van Leeuwen, P. W. N. M., *European Journal of Inorganic Chemistry* **1998**, 155-157.
26. van Leeuwen, P.; Kamer, P. C. J.; Reek, J. N. H., *Pure and Applied Chemistry* **1999**, *71*, 1443-1452.
27. Dierkes, P.; van Leeuwen, P. W. N. M., *Journal of the Chemical Society, Dalton Transactions* **1999**, 1519-1530.
28. van Leeuwen, P. W. N. M.; Kamer, P. C. J.; Reek, J. N. H.; Dierkes, P., *Chemical Reviews* **2000**, *100*, 2741-2769.
29. Kamer, P. C. J.; van Leeuwen, P. W. N. M.; Reek, J. N. H., *Accounts of Chemical Research* **2001**, *34*, 895-904.
30. Freixa, Z.; Van Leeuwen, P. W. N. M., *Dalton Transactions* **2003**, 1890-1901.
31. Levy, S. M.; Kohout, F. J.; Guha-Chowdhury, N.; Kiritsy, M. C.; Heilman, J. R.; Wefel, J. S., *Journal of Dental Research* **1995**, *74*, 1399-1407.
32. Sakai, M.; Hayashi, H.; Miyaura, N., *Organometallics* **1997**, *16*, 4229-4231.
33. Miyaura, N.; Suzuki, A., *Chemical Reviews* **1995**, *95*, 2457-2483.
34. Desimoni, G.; Faita, G.; Jorgensen, K. A., *Chemical Reviews* **2006**, *106*, 3561-3651.
35. Smith, R. C.; Protasiewicz, J. D., *Organometallics* **2004**, *23*, 4215-4222.
36. Smith, R. C.; Bodner, C. R.; Earl, M. J.; Sears, N. C.; Hill, N. E.; Bishop, L. M.; Sizemore, N.; Hehemann, D. T.; Bohn, J. J.; Protasiewicz, J. D., *Journal of Organometallic Chemistry* **2005**, *690*, 477-481.
37. Serp, P.; Hernandez, M.; Richard, B.; Kalck, P., *European Journal of Inorganic Chemistry* **2001**, 2327-2336.

38. Goel, R. G.; Ogini, W. O., *Organometallics* **1982**, *1*, 654-658.
39. Shaw, B. L.; Mann, B. E.; Masters, C., *Journal of the Chemical Society A: Inorganic, Physical, Theoretical* **1971**, 1104-1106.
40. Verkade, J. G.; Quin, L. D., *Phosphorus-31 NMR Spectroscopy in Stereochemical Analysis*. VCH: Deerfield Beach, 1987; Vol. 8, p 717.
41. Tolman, C. A.; Meakin, P. Z.; Lindner, D. I.; Jesson, J. P., *Journal of the American Chemical Society* **1974**, *96*, 2762-2774.
42. Brown, T. H.; Green, P. J., *Journal of the American Chemical Society* **1970**, *92*, 2359-2362.
43. Chiu, J. J.; Hart, H.; Ward, D. L., *Journal of Organic Chemistry* **1993**, *58*, 964-966.
44. Diesveld, J. W.; Menger, E. M.; Edzes, H. T.; Veeman, W. S., *Journal of the American Chemical Society* **1980**, *102*, 7935-7936.
45. Maerten, E.; Hassouna, F.; Couve-Bonnaire, S.; Mortreux, A.; Carpentier, J.-F.; Castanet, Y., *Synlett* **2003**, 1874-1876.
46. Kuriyama, M.; Nagai, K.; Yamada, K.; Miwa, Y.; Taga, T.; Tomioka, K., *Journal of the American Chemical Society* **2002**, *124*, 8932-8939.
47. Reetz, M. T.; Moulin, D.; Gosberg, A., *Organic Letters* **2001**, *3*, 4083-4085.
48. Kuriyama, M.; Tomioka, K., *Tetrahedron Letters* **2001**, *42*, 921-923.
49. Laeng, F.; Breher, F.; Stein, D.; Gruetzmacher, H., *Organometallics* **2005**, *24*, 2997-3007.
50. Otomaru, Y.; Kina, A.; Shintani, R.; Hayashi, T., *Tetrahedron: Asymmetry* **2005**, *16*, 1673-1679.

51. Otomaru, Y.; Okamoto, K.; Shintani, R.; Hayashi, T., *Journal of Organic Chemistry* **2005**, *70*, 2503-2508.
52. Yuan, W.-C.; Cun, L.-F.; Gong, L.-Z.; Mi, A.-Q.; Jiang, Y.-Z., *Tetrahedron Letters* **2005**, *46*, 509-512.
53. Moss, R. J.; Wadsworth, K. J.; Chapman, C. J.; Frost, C. G., *Chemical Communications* **2004**, 1984-1985.
54. Otomaru, Y.; Senda, T.; Hayashi, T., *Organic Letters* **2004**, *6*, 3357-3359.
55. Ma, Y.; Song, C.; Ma, C.; Sun, Z.; Chai, Q.; Andrus, M. B., *Angewandte Chemie, International Edition* **2003**, *42*, 5871-5874.
56. Boiteau, J.-G.; Minnaard, A. J.; Feringa, B. L., *Journal of Organic Chemistry* **2003**, *68*, 9481-9484.
57. Zou, G.; Wang, Z.; Zhu, J.; Tang, J., *Chemical Communications* **2003**, 2438-2439.
58. Itooka, R.; Iguchi, Y.; Miyaura, N., *Journal of Organic Chemistry* **2003**, *68*, 6000-6004.
59. Tsuboyama, A.; Iwawaki, H.; Furugori, M.; Mukaide, T.; Kamatani, J.; Igawa, S.; Moriyama, T.; Miura, S.; Takiguchi, T.; Okada, S.; Hoshino, M.; Ueno, K., *Journal of the American Chemical Society* **2003**, *125*, 12971-12979.
60. Boiteau, J.-G.; Imbos, R.; Minnaard, A. J.; Feringa, B. L., *Organic Letters* **2003**, *5*, 681-684.
61. Metivier, R.; Amengual, R.; Leray, I.; Michelet, V.; Genet, J.-P., *Organic Letters* **2004**, *6*, 739-742.
62. Pucheault, M.; Darses, S.; Genet, J.-P., *Tetrahedron Letters* **2002**, *43*, 6155-6157.

63. Ingleson, M.; Patmore, N. J.; Ruggiero, G. D.; Frost, C. G.; Mahon, M. F.; Willis, M. C.; Weller, A. S., *Organometallics* **2001**, *20*, 4434-4436.
64. Coolen, H. K. A. C.; van Leeuwen, P. W. N. M.; Nolte, R. J. M., *Journal of Organic Chemistry* **1996**, *61*, 4739-4747.
65. Hart, H.; Takehira, Y., *Journal of Organic Chemistry* **1982**, *47*, 4370-4372.
66. Hart, H.; Ward, D. L.; Tanaka, K.; Toda, F., *Tetrahedron Letters* **1982**, *23*, 2125-2128.

CHAPTER 3
SYNTHESIS, TRANSFER REAGENTS AND CATALYTIC APPLICATIONS
OF BIS N-HETEROCYCLIC CARBENES BASED ON TERPHENYL
SCAFFOLDS*

3.1 Introduction

Exploration of the reactivity and synthetic complexities of carbenes has been a vital role within organic chemistry since the pioneering development of carbene complexes by Fisher and Schrock. There are many differences in the properties and stability of these initial carbenes, which were discussed in detail in Chapter 1. The susceptibility of these initial carbenes to oxidation and ready decomposition was a primary drawback to these materials; however, in 1968 Öfele¹ and Wanzlick² isolated the first *N*-heterocyclic carbene (NHC) complexes which are stable to air oxidation and rapid decomposition.³ The advantageous stability of NHCs spurred a renewed interest in carbenes, resulting in the discovery of the first uncoordinated, stable, free carbene that was crystallographically characterized by Arduengo in 1991 (**Figure 3.1**).⁴

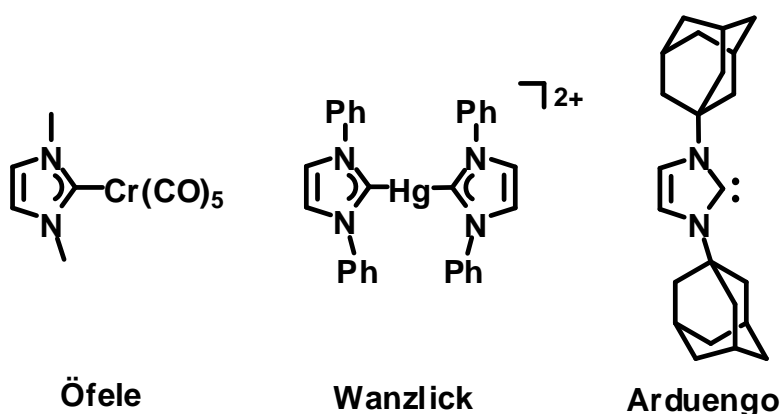
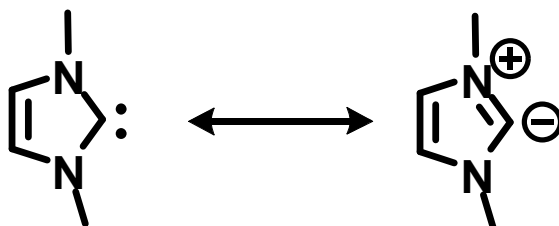


Figure 3.1 Exemplary examples of *N*-heterocyclic carbenes (NHCs).

* Adapted from Morgan, Brad P.; Galdamez, Gabriela A.; Gilliard Jr., Robert J.; Smith, Rhett C. "Canopied *trans*-chelating bis(*N*-heterocyclic carbene) ligand: synthesis, structure and catalysis" *Dalton Transactions* **2009**, 11, 2020-2028.

The surprising stability of NHCs arise from the multitude of beneficial electronic and steric properties which also allow free carbenes to be crystallographically isolated. The electronic effects that stabilize NHCs are both inductive wherein the more electronegative nitrogen atoms pull electron density from the lone pair on the carbene carbon and mesomeric where the lone pairs on the nitrogen can be accepted by the empty p orbital of the carbene carbon, forming an ylide (**Scheme 3.1**).⁵ The NHC also exhibits some aromaticity when the free carbene is generated, leading to additional stabilization.^{6,7} Another noteworthy attribute to free NHCs is the requirement for steric protection of the carbene to allow kinetic stabilization against dimerization.⁴ The construction of a new class of π -conjugated materials for opto/electronic applications, drug delivery and self-healing polymers, however, rely upon the ability for NHCs to dimerize.⁸⁻¹² Conversely, Robinson has utilized the steric demand for stabilization of free carbenes to prevent dimerization and to enforce multiple bonds within main group elements such as an Si=Si bond.¹³



Scheme 3.1 Carbene and ylide resonance forms of free N-Heterocyclic carbenes (NHCs).

The utility of NHC complexes has spurred extensive investigation into their value in the catalysis of a large number of reactions.¹⁴⁻¹⁸ The investigation of the ability for this unique ligand to be used as a catalyst has been of interest since 1977 when it was first explored for hydrosilylation.¹⁹ It was noted that the activity of the rhodium NHC complex

was comparable to that of phosphines, thus initializing a surge in a variety of catalytic applications including Heck,²⁰⁻²² Suzuki,^{21,23} Sonogashira,^{24,25} Stille²⁶⁻²⁸ and other C-C coupling reactions.²⁹⁻³¹

One of the most important examples of a catalytic process that features a sterically encumbered NHC is olefin metathesis, for which the 2005 Nobel Prize in chemistry was awarded to Grubbs, Schrock and Chauvin for their ground breaking work in this area.³²⁻³⁵ The design of an active catalyst for olefin metathesis consisted of two phosphorus ligands which was later termed Grubb's first generation catalyst (**Figure 3.2a**). The replacement of one of the phosphorus ligands with a NHC was found to be more active for both ring-opening and ring-closing metathesis as well as the ability to performing ring-closing metathesis on sterically hindered olefins whereas the first generation catalyst could not (**Figure 3.2b**).³³ In 1999 Grubbs discovered that saturation of the imidazolium ring was beneficial in that the catalyst became even more active for metathesis (**Figure 3.2c**).³⁶ These steps towards improved performance and thermal stability with a NHC in place of a phosphine has made these the preferred next generation for catalyst design in many cases.

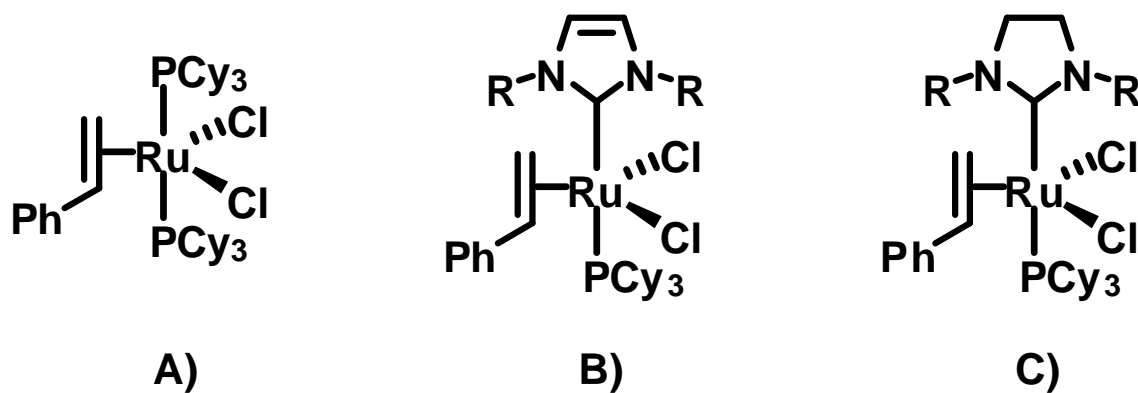


Figure 3.2 Variants of Grubbs' catalyst for olefin metathesis.

The ability for NHCs to donate a lone pair from the carbene to metals resembles that of phosphines in that both ligands are good σ -donors. Consequently, the ability for a supporting ligand to be a good σ -donor has been attributable to the high activity of various catalytic transformations in which phosphines have long proven their value. Phosphine ligands have been systematically studied for many years and a variety of characterization techniques provide vital information on the activity and selectivity of reactions as discussed in Chapter 1. The ability for control of these parameters, such as the diphosphine bite angle (P–M–P angle, β) allows tuning of selectivity to favor one isomer.³⁷⁻⁴⁰ Specifically, there is an ongoing interest in wide bite angle (β greater than $\sim 110^\circ$) or *trans*-spanning diphosphine ligands, which can provide superior regioselectivity in industrially important catalytic processes, notably rhodium catalyzed hydroformylation.⁴¹⁻⁴³

The versatility of this same principle to other ligand systems can easily be envisioned; however, current literature involving chelating bis(NHC)s is relatively young and the first chelating bis(NHC) was reported was only two decades ago; furthermore, the first chiral chelating NHC complex was not reported until 2000.⁴⁴ The ability for the correlations to be derived are a vital part of chemistry and corresponding studies on the tunable parameters of NHCs and their dependence for supported catalysis remain in their early stages of development. The lack of literature involving bis(NHC)s is apparent when a literature survey of the available crystallographically characterized structures with *trans*-chelating binding modes (shown in red in **Figure 3.3**) for bis(NHC)s was examined using the Cambridge Structure Database (CSD) version 5.29 which are shown in **Figure 3.3** (CSD version 5.29 Nov. 2007).⁴⁵⁻⁴⁹

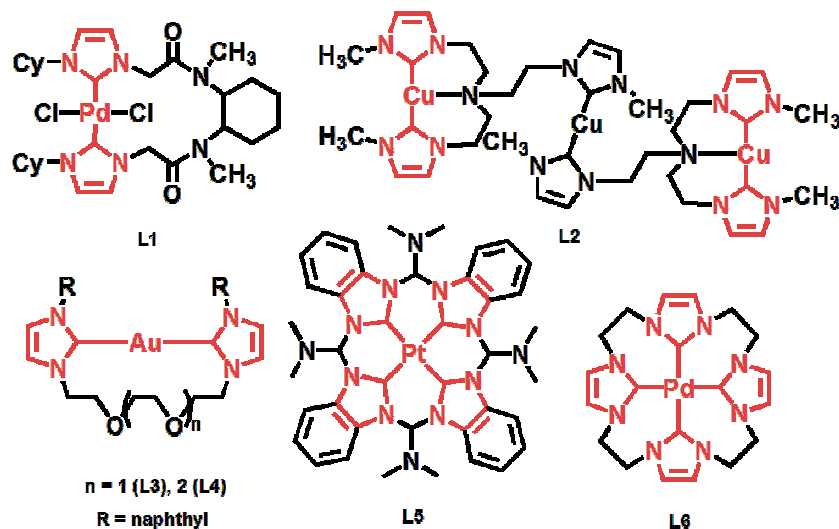


Figure 3.3 Examples of crystallographically characterized bidentate bis(NHC) complexes with C–M–C angles of $\geq 170^\circ$. *Trans*-chelating binding modes are shown in red.

Terphspan-scaffolded ligands have good activity for use in Pd-catalyzed Suzuki-Miyaura and Mizoroki-Heck couplings⁵⁰ and in Chapter 2 the Terphspan diphosphine supported rhodium catalyzed 1,4-conjugate addition of arylboronic acids to α,β -unsaturated ketones was shown to have promise.⁵¹ The use of Terphspan diphosphines, diphosphinites and bis(imines) has been utilized to produce cyclometallated C_2 -symmetric Terpincer ligands which have demonstrated asymmetric catalysis and hold promise for use of Terphspan scaffolds utilizing bis(NHC) complexes for asymmetric functions.⁵²⁻⁵⁴

The use of *trans*-chelating bis(NHC) complexes built on the Terphspan scaffolds was shown to demonstrate Pd-catalyzed C–C bond-formation via Suzuki-Miyaura coupling followed by the comparison of its analogous diphosphine and diphosphinite ligands.

3.2 Synthesis and reactivity

The design of various donor ligands has been the focus of many research groups in recent years. The comparison of donor ability as well as catalytic activity can provide critical information towards the understanding of catalytic cycles. The synthesis of a series of *m*-terphenyl scaffolded ligands will be the primary focus of this section, with the design of a new bis *N*-heterocyclic carbene (NHC) ligand **1** and comparison to analogous diphosphine **2** and diphosphinite **3** also discussed in the current chapter (**Figure 3.4**).

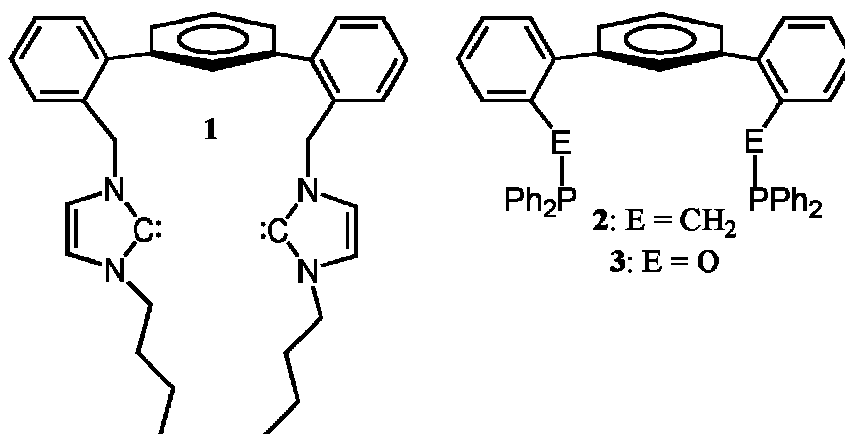
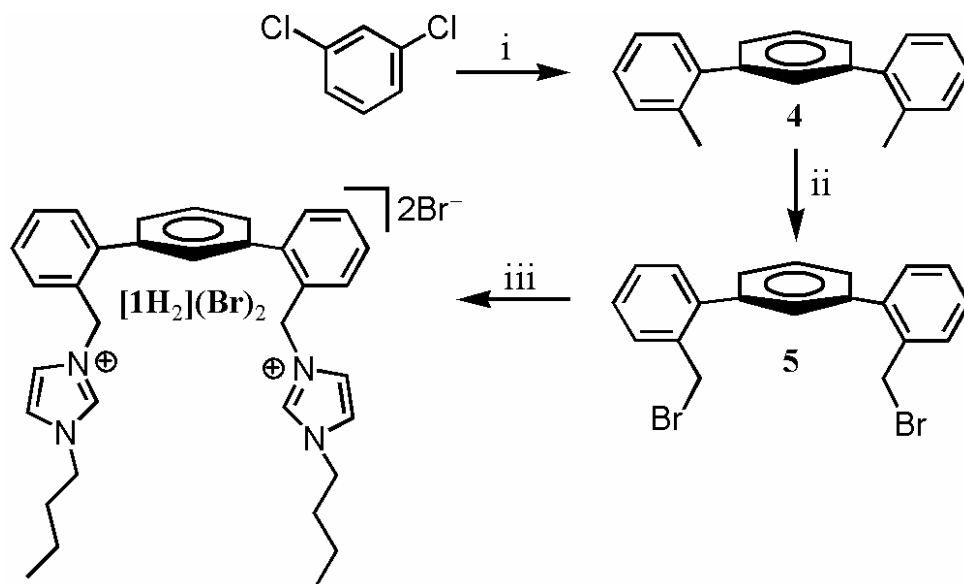


Figure 3.4 Structures of canopied ligands that chelate metals via carbene (**1**), phosphine (**2**), and diphosphinite (**3**) moieties.

The preparation of the diphosphine **2** and diphosphinite **3** used throughout this chapter were carried out by a modification of the literature reports.^{55,56} The preparation of the NHC **1** proceed from the easily accessible bis(imidazolium) salt **[1H₂](Br)₂** via the commonly employed precursor 2,2'-bis(bromomethyl)-*m*-terphenyl **5** as shown in **Scheme 3.2**. The imidazolium salt **[1H₂](Br)₂** was initially isolated as a hygroscopic, thick, viscous oil that melted near room temperature when the reaction was first completed; however the purification of this material was achieved via the precipitation of a white powder by dropwise addition of a saturated dichloromethane solution into diethyl ether at

–40 °C under a dry nitrogen atmosphere followed by cold filtration and found to be pure by NMR spectroscopy. It was later found that $[\mathbf{1H}_2](\mathbf{Br})_2$ could also be purified via trituration using refluxing pentane to give a white solid. The resulting white solid was then used for subsequent preparations.

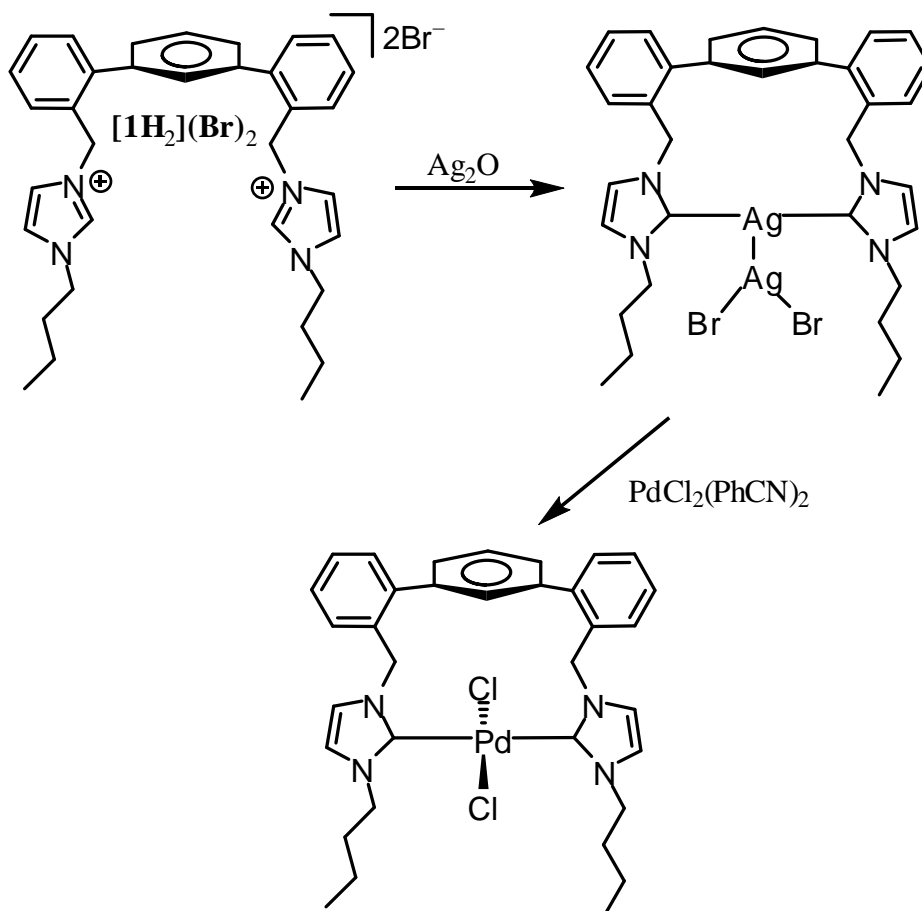


Scheme 3.2 Preparation of $[\mathbf{1H}_2](\mathbf{Br})_2$. i) 1) $n\text{-BuLi}$ -78 °C THF 2) 2-tolylmagnesium bromide -78 °C THF 6h. 3) Δ 12 h. 4) HCl, 0 °C ii) *N*-bromosuccinimide / benzoylperoxide CHCl_3 Δ 48 h. iii) *N*-(*n*-butyl)imidazole, CH_3CN , Δ 12 h.

The ability for two carbene fragments to dimerize to form tetrafulvalene units has been reported in literature previously with enhancement as a result of scaffolded bis(NHC)s.^{57, 58} The ability for free carbene **1** to dimerize in this manner was explored by the reaction of the imidazolium salt $[\mathbf{1H}_2](\mathbf{Br})_2$ with 2 equiv NaH in anhydrous $\text{DMSO-}d^6$ at room temperature under a nitrogen atmosphere which was then monitored by ^1H and ^{13}C NMR spectroscopy. The ^1H NMR resonance at 9.07 ppm attributable to the NCHN proton rapidly disappeared from the ^1H NMR spectrum, and a new resonance at 210.9 ppm was observed in the ^{13}C NMR spectrum. The latter peak is comparable to that observed in Arduengo's initial report on an isolable NHC (211.4 in C_6D_6),⁴ and was

attributed to the free carbene unit in **1**. Crystallization attempts of free **1** were unsuccessful in a variety of different solvent systems. Although the bis(NHC) **1** appears to be predisposed to intramolecular dimerization due to potential for close proximity of the two carbene units as seen by the scaffold in **Figure 3.4**, molecular modeling at a semi-empirical PM3 level revealed that dimerization would place significant strain on the central aryl ring of the *m*-terphenyl scaffold. The ability for **1** to undergo intermolecular dimerization to produce polymers is conceivable as well; however, no increase in viscosity of reaction solutions with concentrations as high as 100 mg/mL or evidence from NMR spectroscopy for polymerization such as broadening of resonances and disruption of molecular symmetry was observed.

The use of the imidazolium salt $[\mathbf{1H}_2](\text{Br})_2$ to cleanly convert the precursor to the Ag(I) complex $[\text{Ag}(\mathbf{1})]\text{AgBr}_2$, was simple with the use of silver oxide. Transmetalation via bis(benzonitrile)palladium(II) chloride to give the pertinent complex $[\text{PdCl}_2(\mathbf{1})]$ is highlighted in **Scheme 3.3**. The synthesis and isolation of $[\text{Ag}(\mathbf{1})]\text{AgBr}_2$ following a modified literature procedure⁵⁹ was a convenient one step synthesis and the material was confirmed to exist as the dimer $\{[\text{Ag}(\mathbf{1})]\text{AgBr}_2\}_2$ in the solid state, as detailed later in the current chapter. $[\text{Ag}(\mathbf{1})]\text{AgBr}_2$ was found to be a hygroscopic, light-sensitive material that started off white, but upon exposure to light became brown. Attempts to isolate and



Scheme 3.3 Preparation of $[\text{Ag}(\mathbf{1})]\text{AgBr}_2$ and $[\text{PdCl}_2(\mathbf{1})]$.

determine the identity of this brown material have been unsuccessful thus far. Analytically pure crystals of [Ag(**1**)]AgBr₂ were obtained either by slow diffusion of pentane into a saturated methylene chloride solution, or by slow evaporation of a saturated solution in acetone. The complete assignment of ¹H and ¹³C NMR resonances for [Ag(**1**)]AgBr₂ were determined through a variety of NMR spectrometric techniques. The ability for unique coupling and the variety of spin systems incorporated in [Ag(**1**)]AgBr₂ made complete assignment difficult, but the use of ¹H-¹H correlation spectroscopy (COSY), heteronuclear multiple quantum coherence (HMQC), distortionless enhancement by polarization transfer (DEPT) and differential nuclear overhauser effect (NOE) proved useful in the determination of peak assignments. The preliminary ¹H NMR spectrum showed resolution of the aromatic peaks which was not observed for a variety of other *m*-terphenyl scaffolded metal complexes, allowing for the complete assignment of all protons.

The ¹H-¹H correlation spectroscopy (**Figure 3.5**) was vital in determining the complete proton assignment in that the protons in different spin systems could be differentiated. The central ring has three different types of protons in which the only spin system observed to have three cross peaks was that of 7.38, 7.34 and 6.95 ppm which from integrations and splitting pattern the known identity of each can be determined. The same applies for the protons attached to the backbone of the NHC in which only two unique protons should be in the spin system in which 7.47 and 7.38 are seen to have the same spin system. The identity of these cannot be differentiated by COSY, however.

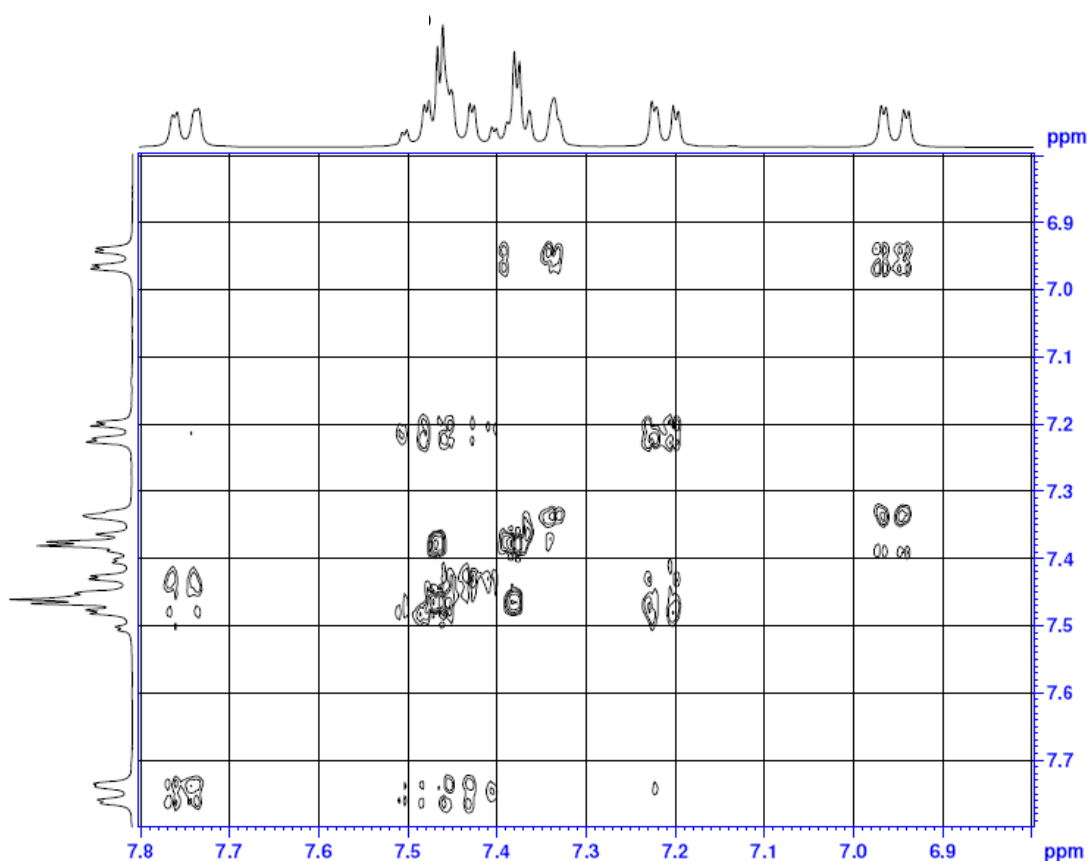


Figure 3.5 ^1H - ^1H Correlated spectrum (COSY) of $[\text{Ag}(\mathbf{1})]\text{AgBr}_2$ (DMSO, 300 MHz).

Differential nuclear overhauser effect (NOE) was explored to determine the differentiation between the two protons attached to the backbone of the NHC. The irradiation of the methylene protons at 3.96 ppm should result in the attenuation of all peaks except those within an interatomic distance of 6 Å regardless of spin systems, which should result in the proton farthest from the *m*-scaffold and closest to the butyl side chain to interact with a positive NOE effect (**Figure 3.6**). The proton that exhibited this effect resonated at 7.47, allowing conclusive differentiation of the two protons attached to the NHC backbone.

The convenient transmetallation of [Ag(**1**)]AgBr₂ to catalytically pertinent late transition metal complexes was advantageous in that a variety of metals could be easily explored. The use of Pd catalyzed C-C coupling reactions commonly incorporates NHC ligands, so the utility of the Pd NHC utilizing the *m*-terphenyl scaffold was of particular interest. The synthesis of [PdCl₂(**1**)] was achieved at room temperature in dichloromethane followed by filtering of the silver salts to give the desired compound in moderate yields. The ¹H NMR showed sharp, well-resolved resonances unlike that of the phosphine analogue [PdCl₂(**2**)] which displays broad resonances due to fluxionality. Crystalline [PdCl₂(**1**)]·PhCH₃ was obtained by diffusion of toluene into a saturated solution in chlorobenzene and was shown to relate closely to that of the phosphine analogue [PdCl₂(**2**)] however even in ¹H and ¹³C NMR spectra of the crystalline material, small side peaks were visible on some of the resonances attributable to atoms nearest the metal coordination site.

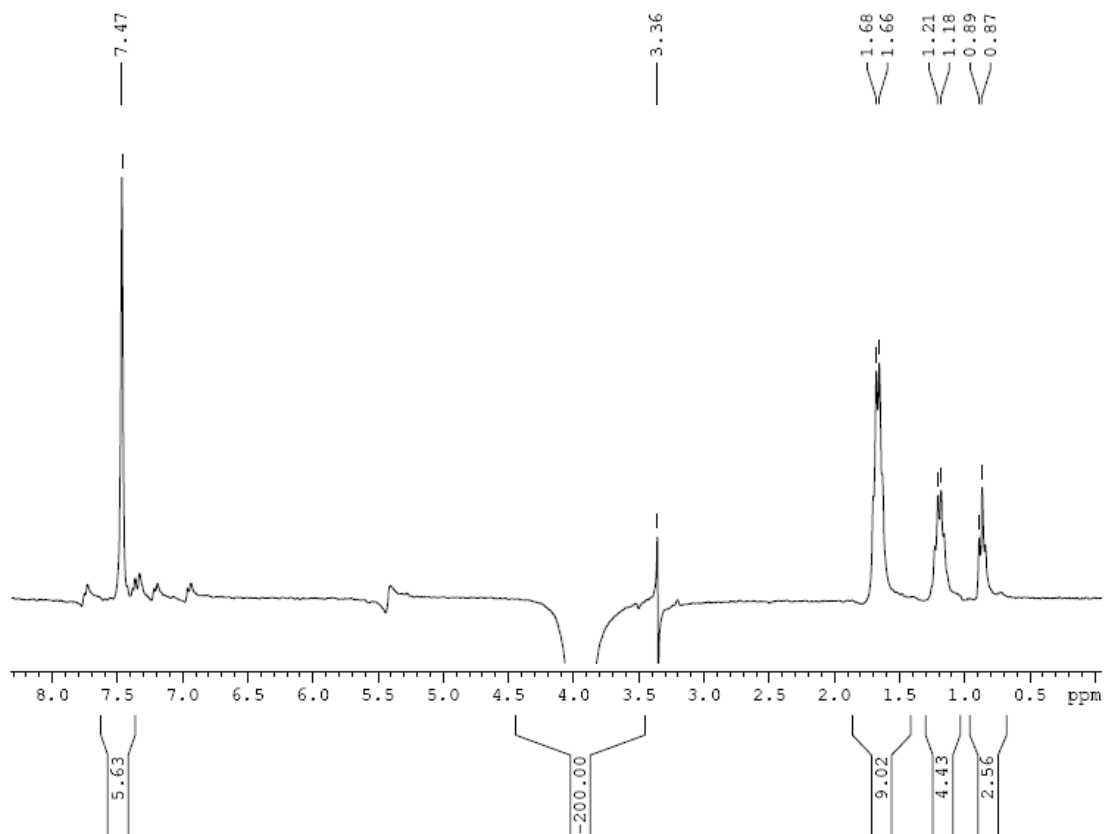


Figure 3.6. Nuclear Overhauser Effect Difference (NOE-DIFF) Spectrum of [Ag(1)]AgBr₂ (DMSO, 300 MHz) for protons resonating at 3.96 ppm.

The attributes of the small side peaks observed in both the ¹H and ¹³C NMR spectra were initially thought to be indicative of two isomers that could possibly interconvert through various conformations of the 14-membered ring that includes the Pd atom, analogous to that reported for the phosphine analogue [PdCl₂(**2**)].⁵⁶ The determination of the rationale for these small side peaks was later determined to arise from the partial occupancy of the halogen sites by both chlorine and bromine on the palladium, which was confirmed by single crystal X-ray diffraction studies. The complete discussion of this observation will be covered later in the chapter. The two isomers could not be separated by preparative TLC or crystallization methods; therefore, the material

was utilized as a mixture of isomers without separation. The use of bis(benzonitrile)palladium (II) bromide would be a possible exclusion method of these isomers in that the elimination of chloride would afford only bromides bound to the palladium. The carbene ^{13}C NMR signal of the carbene carbon within $[\text{PdCl}_2(\mathbf{1})]$ was observed at 168.9 ppm in CDCl_3 which was found to be comparable to that of other *trans*- $[\text{PdCl}_2(\text{bis}(\text{NHC}))]$ complexes (165.6-171.7 ppm).⁶⁰⁻⁶²

3.3 Structure

The use of silver for isolation of NHC complexes has shown its utility in the wide array of complexes crystallographically characterized within the literature. The plethora of single crystal X-ray diffraction data on these silver (I) NHC complexes have proven to demonstrate an extensive range of possible metal environments, which are highlighted in **Figure 3.7**. In particular, the use of bis(NHC)s has been limited in scope, with the primary focus more directed to the more understood mono(NHC)s.

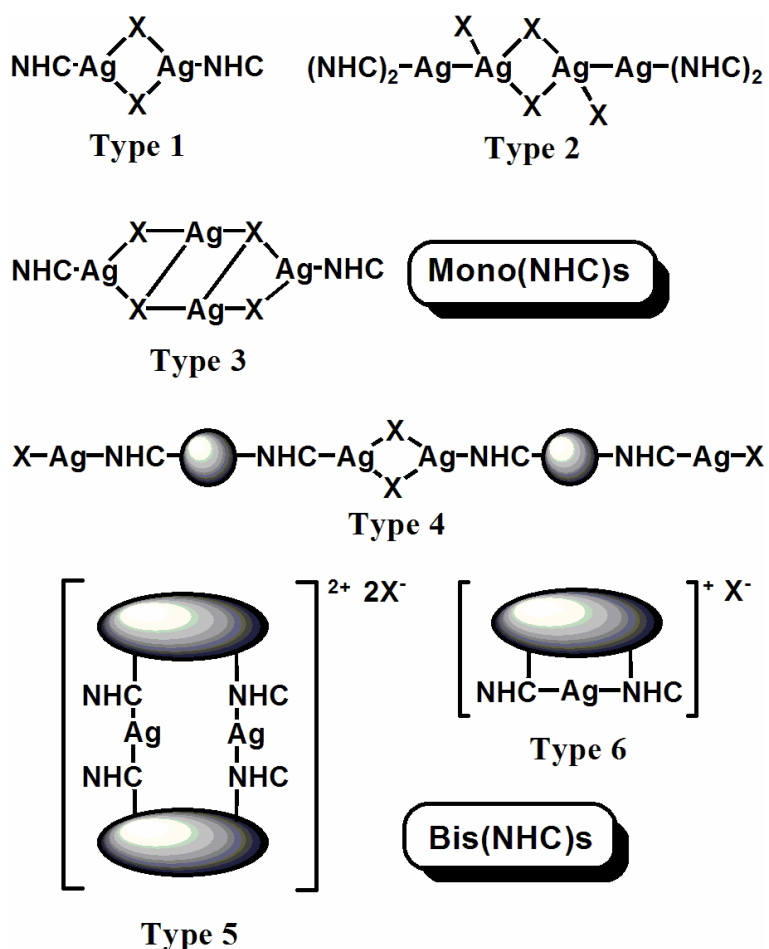


Figure 3.7 Some binding modes of silver(I) complexes featuring mono- (top) and bis- (bottom) *N*-heterocyclic carbene ligands that have been observed in the solid state by X-ray diffraction.

The structure of the silver (I) bis(NHC) complex scaffolded by a *m*-terphenyl canopy {[Ag(1)]AgBr₂}₂ was observed to exhibit a Type 2 binding mode as seen in **Figure 3.7** with a unique tetranuclear bridging AgAg-(μ -Br)₂AgAg core (**Figure 3.8**) within the solid state. Refinement details (**Table 3.1**) and selected bond angles and distances listed in **Table 3.2** with the most important features being the Ag(1)–Ag(2)

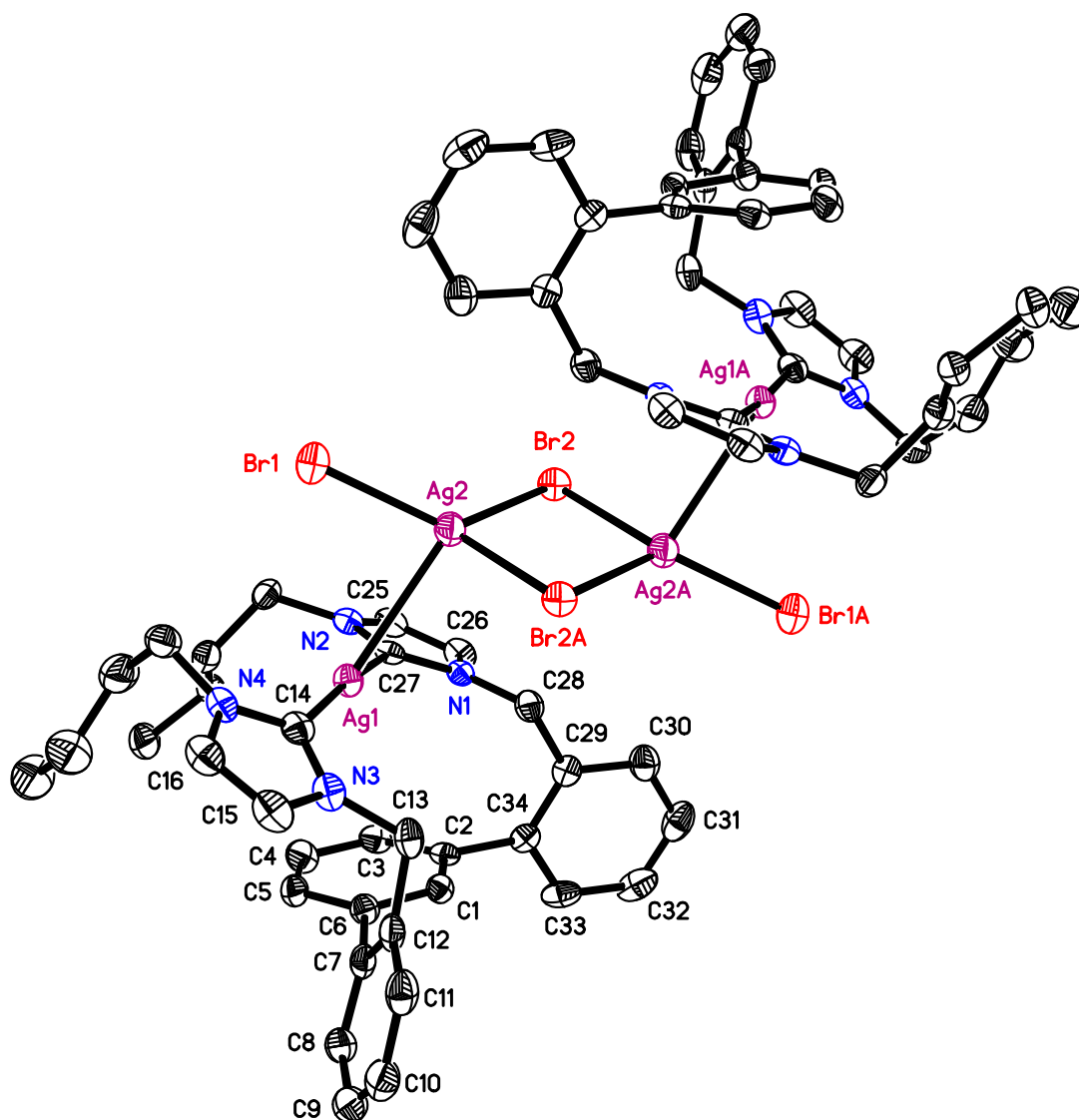


Figure 3.8 ORTEP drawing (50% probability ellipsoids) of the molecular structure of {[Ag(1)]AgBr₂}₂. Hydrogen atoms are omitted for clarity.

distance of 3.0241(8) Å which is indicative of Ag–Ag bonding, and a cross-core Ag–Ag distance of 3.504 Å which is close to the sum of the van der Waals radii (3.44 Å),⁶³ attributable to argentophilic effects, similar to the more commonly explored aureophilic effects with use of gold. The unusual bis- μ -Br tetrametallic core of {[Ag(**1**)]AgBr₂}₂ (Type 2 in **Figure 3.7**) has only been observed in a select few Ag(I) NHC complexes previously,⁶⁴⁻⁷⁰ and {[Ag(**1**)]AgBr₂}₂ has emerged as the first instance of a crystallographically characterized *chelating* NHC complex implementing a Type 2 mode in the solid state.

It has been previously reported that ligands showing a Type 2 binding mode (**Figure 3.7**) can adopt other conformations and strongly depends on the crystallization conditions, suggesting that different coordination modes may exist in solution versus the solid state.⁶⁴ Specifically, the recrystallization of a Type 2 crystal in the presence a potentially coordinating solvent such as acetone has been shown to allow the isolation of a Type 1 binding mode (**Figure 3.7**).⁶⁴ This principle was tested for {[Ag(**1**)]AgBr₂}₂ by growing crystals from both the diffusion of pentane into a CH₂Cl₂ solution of the silver complex and by slow evaporation of acetone. The structure of both crystals was shown to exhibit the same binding mode from both types of crystals, but only the data from crystals grown in acetone will be discussed due to the better refinement. The inability for {[Ag(**1**)]AgBr₂}₂ to show evidence of other binding types is likely a result of the scaffolds preference for this unusual binding motif.

Table 3.1 Crystal data and structure refinement details for {[Ag(1)]AgBr₂}₂

Molecular formula	C ₆₈ H ₇₆ Ag ₄ Br ₄ N ₈
Formula weight (g/mol)	1756.49
Temperature (K)	153 (2)
Wavelength (Å)	0.71073
Crystal system	Monoclinic
Space group	<i>P</i> 2 ₁ / <i>n</i> (#14)
Unit cell dimensions	
<i>a</i> (Å)	15.262(3)
<i>b</i> (Å)	10.348(2)
<i>c</i> (Å)	21.561(4)
α (deg)	90.00
β (deg)	103.32(3)
γ (deg)	90.00
Volume (Å ³)	3316.2(12)
<i>Z</i>	2
Calculated density (Mg/m ³)	1.759
Absorption coefficient (mm ⁻¹)	3.620
<i>F</i> (000)	1736
Crystal size (mm)	0.46 × 0.22 × 0.12
Crystal color and shape	colorless chip
θ range for data collection (deg)	2.74 - 25.10
Limiting indices	-18 < <i>h</i> < 18 -12 < <i>k</i> < 12 -25 < <i>l</i> < 25
Reflections collected	21729
Independent reflections	2510 (99.2 %)
Max. transmission	0.6504
Min. transmission	0.2781
Refinement method	Full-matrix least-squares on <i>F</i> ²
Data / restraints / parameters	5901/0/381
Goodness of fit on <i>F</i> ²	1.013
Final R indices (<i>I</i> > 2σ(<i>I</i>))	
R1	0.0389
wR2	0.0732
R indices (all data)	
R1	0.0465
wR2	0.0779

Table 3.2 Selected bond lengths (Å) and angles (°) for {[Ag(**1**)]AgBr₂]₂.

Ag(1)–Ag(2)	3.0241 (8)
Ag(2)–Br(1)	2.5486 (8)
Ag(2)–Br(2)	2.6965 (11)
Ag(2)–Br(2)A ^a	2.7231 (8)
Ag(1)–C(14)	2.100 (5)
Ag(1)–C(27)	2.104 (5)
C(27)–Ag(1)–C(14)	171.16 (18)
C(27)–Ag(1)–Ag(2)	62.88 (12)
C(14)–Ag(1)–Ag(2)	125.84 (13)
Br(1)–Ag(2)–Br(2)	129.40 (3)
Br(1)–Ag(2)–Br(2)A ^a	122.82 (3)
Br(2)–Ag(2)–Br(2)A ^a	99.45 (2)
Br(1)–Ag(2)–Ag(1)	80.86 (3)
Br(2)–Ag(2)–Ag(1)	134.14 (2)
Br(2)A ^a –Ag(2)–Ag(1)	84.37 (2)
Ag(2)–Br(2)–Ag(2)A ^a	80.55 (2)

a) Symmetry transformations used to generate equivalent atoms:

-x + 1, -y + 1, -z

The ability for [Ag(**1**)]AgBr₂ to exhibit other modes in solution was considered. The possibilities of commonly seen Ag (I) coordination environments, Type 1 and 3 binding modes, require too far a separation between carbene fragments to be accommodated by a single **1** unit as gauged by simple modeling using molecular mechanics. These modes are also inconsistent with the NMR data. The other binding modes may all be accommodated by the flexible terphenyl scaffold, but Type 4 binding is ruled out by NMR spectrometry, which reveals a symmetry plane through the central aryl ring of the *m*-terphenyl unit. The ability for Type 5 binding is a viable mode in which one carbene fragment from each unit of **1** binds to each of the two Ag(I) ions. The NMR data of Type 5 binding would still reveal a symmetry plane through the central aryl ring therefore it cannot be ruled out on the basis of NMR data. The ability for the analogous phosphine **2** to exhibit this mode also seems to suggest the possibility of Type 5 binding due to their similar structures.⁵⁶ In diphosphine complexes employing the same scaffold

such as [RhCl(CO)(2)] and [MCl₂(2)] (M = Ni, Pd, or Pt), as well as in [PdCl₂(1)], which is discussed later in this chapter, the ligand incorporates a *trans*-spanning mode. The chelate effect makes the formation of a Type 5 core entropically unfavorable in the presence of coordinating bromide anions unless argentophilic interactions are strong enough to provide the necessary stabilization. The Type 6 core is the most likely species to be present in solution on the basis of NMR and X-ray diffraction data however there still remains the possibility for the ligand-preferred *trans*-spanning mode within the Type 2 core can predominate when concentrated without much reorganization needed within the core.

The diffusion of toluene into a saturated solution of [PdCl₂(1)] in chlorobenzene gave a preliminary structure of a bis-NHC palladium carbene which demonstrates a *trans*-chelating structure (**Figure 3.9**). The X-ray diffraction analysis of one of these colorless crystals exposed that both halogen sites are partially occupied by Br in addition to the expected Cl (**Figure 3.9**: X(1) = 61.63 % Cl, 38.37 % Br and X(2) = 81.18 % Cl, 18.82 % Br). Mixed halogen occupancy has been observed before through the use of a [PdCl₂(NHC)] complex prepared by the same method used to prepare [PdCl₂(1)].⁶² The denotation of the partial occupancy in [PdCl₂(1)] is easily observed by the difference in bond distances and angles as represented in **Table 3.3**. For example, the Pd – X(1) (2.377(2) Å) and Pd – X(2) (2.347(2) Å) interatomic distances are longer than the standard Pd – Cl bond (2.31 Å) which can be accredited to the larger van der Waals radius of bromide. The larger amount of bromide in X1 is expected due to the less steric hindrance and is seen in the larger of the two bond distances. The C(14) - Pd(1) - C(25) angle of 176.8(3)° is rather similar to the P–Pd–P angle observed in the Terphspan

phosphine complex [PdCl₂(**2**)] 172.97(7)° which demonstrates a *trans*-spanning square planar coordination environment.⁵⁶

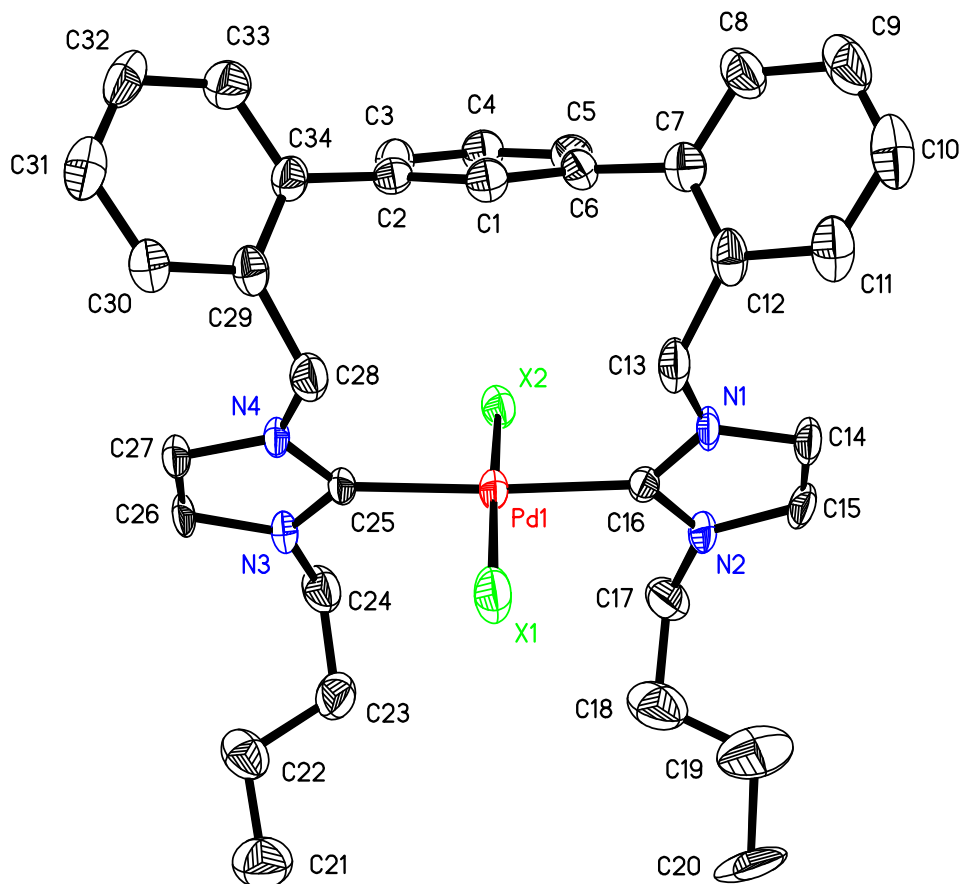


Figure 3.9 ORTEP drawing (50% probability ellipsoids) of the molecular structure of [X₂Pd(**1**)]. Hydrogen atoms and the cocrystallized toluene solvent are omitted for clarity. C18, C19 and C20 show only one of the representative examples of the butyl partial occupancy observed. X1 = 61.63 % Cl, 38.37 % Br and X2 = 81.18 % Cl, 18.82 % Br.

The use of NMR spectroscopy also uncovered significant differences in the structural aspects of the Terphspan carbene (**1**) and phosphine (**2**) complexes. The phosphine analogue [PdCl₂(**2**)] has shown broad ¹H NMR resonances resulting from structural fluxionality,⁵⁶ however [PdCl₂(**1**)] demonstrates sharp, well-resolved

resonances in both ^1H and ^{13}C NMR spectra. The proton spectra of the analogous phosphine complex $[\text{PdCl}_2(\mathbf{2})]$ has a broad range of aromatic protons from 5.96-8.02 ppm due to interaction between the metal and the aryl ring, however the carbene complex $[\text{PdCl}_2(\mathbf{1})]$ proton resonances attributable to H atoms on the central *m*-terphenyl ring do not exhibit this characteristic trait. The plausible reason for this is the expansion of the Pd-containing ring size from 12 atoms in $[\text{PdCl}_2(\mathbf{2})]$ to 14 atoms for $[\text{PdCl}_2(\mathbf{1})]$ which increases the interatomic distance of the closest solid state Pd–Cl \cdots H_{aryl} distance from 3.48 to 3.69 Å. This increase in distance apparently positions the metal center too far from the central ring to engage in this type of interaction.

Table 3.3 Selected bond lengths (Å) and angles (°) for $[\text{PdX}_2(\mathbf{1})] \cdot \text{PhCH}_3$.

Pd(1) – C(16)	2.015 (6)
Pd(1) – C(25)	2.031 (5)
Pd(1) – X(1)	2.377 (2)
Pd(1) X(2)	2.347 (2)
N(1) – C(16)	1.343 (8)
N(2) – C(16)	1.360 (8)
N(3) – C(25)	1.353 (7)
N(4) – C(25)	1.343 (7)
C(16) – Pd(1) – C(25)	176.8 (3)
X(1) – Pd(1) – X(2)	175.75(6)
C(16) – Pd(1) – X(1)	90.69(18)
C(25) – Pd(1) – X(1)	90.26(17)
C(16) – Pd(1) – X(2)	88.08 (18)
C(25) – Pd(1) – X(2)	91.19 (17)
N(1) – C(16) – N(2)	105.3(5)
N(3) – C(25) – N(4)	105.2(4)

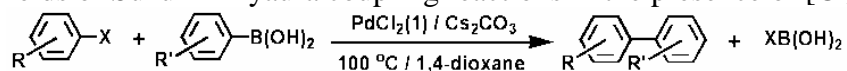
Table 3.4 Crystal data and structure refinement details of [PdX₂(1)]·PhCH₃.

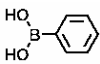
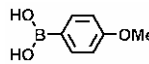
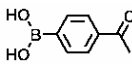
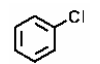
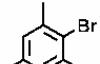
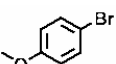
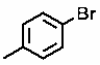
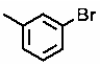
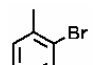
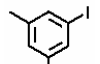
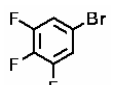
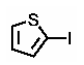
Molecular formula	C ₃₄ H ₃₈ Cl _{1.43} Br _{0.57} N ₄ Pd•C ₇ H ₈
Formula weight (g/mol)	797.46
Temperature (K)	153(2)
Wavelength (Å)	0.71073
Crystal system	Triclinic
Space group	<i>P</i> $\bar{1}$ (#2)
Unit cell dimensions	
<i>a</i> (Å)	10.392(2)
<i>b</i> (Å)	13.675(3)
<i>c</i> (Å)	15.092(3)
α (deg)	109.66(3)
β (deg)	91.31(3)
γ (deg)	111.21(3)
Volume (Å ³)	1857.2(6)
<i>Z</i>	2
Calculated density (Mg/m ³)	1.426
Absorption coefficient (mm ⁻¹)	1.250
<i>F</i> (000)	940
Crystal size (mm)	0.22 × 0.17 × 0.10
Crystal color and shape	colorless chip
θ range for data collection (deg)	2.43 – 25.10
Limiting indices	-10 < <i>h</i> < 12 -16 < <i>k</i> < 14 -18 < <i>l</i> < 18
Reflections collected	13822
Independent reflections	6539
Completeness to θ	25.10 (98.8 %)
Max. transmission	0.8852
Min. transmission	0.7705
Refinement method	Full-matrix least-squares on <i>F</i> ²
Data / restraints / parameters	6539/6/473
Goodness of fit on <i>F</i> ²	1.024
Final R indices (<i>I</i> > 2 σ (<i>I</i>))	
R1	0.0583
wR2	0.1073
R indices (all data)	
R1	0.0922
wR2	0.1196

3.4 Suzuki Coupling

The canopied Terphspan diphosphine **2** produces moderately active catalysts for Pd-catalyzed Suzuki-Miyaura coupling.⁵⁰ Chelating NHC Pd complexes, however, have produced a wide range of yields, from poor to excellent for this coupling reaction^{22, 60, 71-83} and thus Suzuki-Miyaura coupling was the first reaction examined with Terphspan carbene **1**. Because the coupling partners reported for reactions supported by **2** were

Table 3.5 Yields of Suzuki-Miyaura coupling reactions in the presence of [Cl₂Pd(**1**)].



			
	96	83	99 ^b
	81	52	28
	97	33	0
	82	90 ^{a,b}	60
	90 ^a	89 ^{a,b}	8
	90 ^a	96 ^a	43
	~100	~100	65 ^a
	~100	~100	57 ^a
	95 ^{a,b}	~100	39 ^a

a) Aryl halide self coupling was observed. b) Boronic acid self coupling was observed

rather limited in scope (PhB(OH)_2 was the only boronic acid employed), we expanded the set to include electron rich and electron deficient boronic acids as well as a heteroatom-containing aryl halide (2-iodothiophene) to gauge the compatibility of these species with reaction conditions (**Table 3.5**).

That $[\text{PdCl}_2(\mathbf{1})]$ supports high yields employing 2-iodothiophene illustrates the use of heteroatom-containing aryl halides as successful reagents for coupling reactions. It is also noteworthy that **1** exhibits high yields in all cases ($\geq 81\%$) when phenyl boronic acid is a coupling partner, while both electron donating (4-methoxyphenylboronic acid) and withdrawing (4-acetylphenylboronic acid) group substituted boronic acids sacrifice some efficiency, though modest yields are still achievable. The 4-acetylphenylboronic acid has substantially lower yields than reactions employing phenylboronic acid or 4-methoxyphenylboronic acid. Good to excellent yields are achievable utilizing a variety of aryl halides including aryl chlorides, bromides and iodides.

This represents an improvement over coupling reactions employing diphosphine **2** under identical conditions, in which the highest yields achievable for coupling aryl chlorides and phenylboronic acid was 5%.⁵⁰ Modest to good yields (28–81%) were also observed utilizing $[\text{PdCl}_2(\mathbf{1})]$ for sterically encumbered aryl halides such as 2,4,6-trimethylbromobenzene.

Table 3.6 Selected bond lengths (Å) and angles (°) for $[\mu\text{-ClPd}(\text{PPh}_2\text{OH})(\text{PPh}_2\text{O})]_2$.

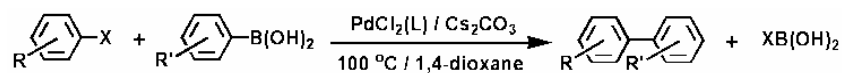
Pd(1) – P(1)	2.2578 (10)
Pd(1) – P(2)	2.2510 (12)
Pd(1) – Cl(1)	2.4198 (10)
Pd(1) – Cl(1)A ^a	2.4284 (12)
P(1) – O(1)	1.537 (3)
P(2) – O(2)	1.539 (3)
P(1)-Pd(1)-P(2)	92.56 (4)
P(1)-Pd(1)-Cl(1)	171.87 (3)
P(1)-Pd(1)-Cl(1)A ^a	89.77 (4)
P(2)-Pd(1)-Cl(1)	93.85 (4)
P(2)-Pd(1)-Cl(1)A ^a	177.06 (3)
Cl(1)-Pd(1)-Cl(1)A ^a	83.99 (4)
Pd(1)-Cl(1)-Pd(1)A ^a	96.01 (4)
Pd(2) – P(3)	2.2410 (13)
Pd(2) – P(4)	2.2449 (11)
Pd(2) – Cl(2)	2.4251 (13)
Pd(2) – Cl(2)A ^b	2.4297 (10)
P(3) – O(3)	1.542 (3)
P(4) – O(4)	1.536 (3)
P(3)-Pd(2)-P(4)	91.69 (5)
P(3)-Pd(2)-Cl(2)	168.14 (4)
P(3)-Pd(2)-Cl(2)A ^b	91.09 (4)
P(4)-Pd(2)-Cl(2)	93.84 (4)
P(4)-Pd(2)-Cl(2)A ^b	175.05 (3)
Cl(2)-Pd(2)-Cl(2)A ^b	84.19 (4)
Pd(2)-Cl(2)-Pd(2)A ^b	95.81 (4)

Symmetry transformations used to generate equivalent atoms:

a) $-x, -y + 1, -z + 1$ b) $-x, -y + 2, -z + 2$

Having demonstrated that complexes of **1** can participate in efficient catalytic reactions, it was of interest to compare the relative efficiency of canopied carbene (**1**), diphosphine (**2**) and diphosphinite (**3**) ligands under identical reaction conditions. We therefore selected a subset of the reactions listed in **Table 3.5** for testing with each of the three ligands (**Table 3.7**). As anticipated, catalytic reactions employing the diphosphinite ligand were generally much less efficient than analogous bis(NHC)- and diphosphine-supported reactions.

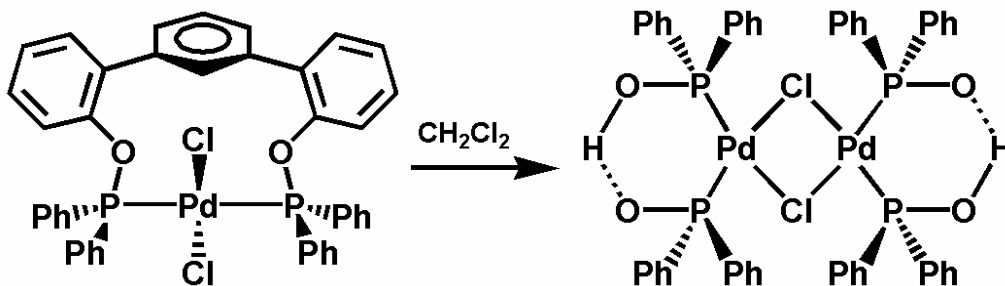
Table 3.7 Yields of Suzuki-Miyaura coupling reactions in the presence of $[\text{Cl}_2\text{Pd}(\text{L})]$, where $\text{L} = \mathbf{1}$, $\mathbf{2}$, or $\mathbf{3}$.



<u>ArB(OH)₂; Ar =</u>	<u>ArX</u>	<u>Ligand</u>	<u>Yield</u>
4-methoxyphenyl	PhCl	1	83
4-methoxyphenyl	PhCl	2	100
4-methoxyphenyl	PhCl	3	82
4-acetylphenyl	PhCl	1	99
4-acetylphenyl	PhCl	2	2
4-acetylphenyl	PhCl	3	2
Ph	2-bromotoluene	1	90
Ph	2-bromotoluene	2	100
Ph	2-bromotoluene	3	100

Depressed yields of reactions employing the diphosphinite may be due to Pd-mediated decomposition of the ligand to species such as $[\text{ClPd}(\mu\text{-Cl})(\text{PPh}_2\text{OH})_2]$ or $[\mu\text{-ClPd}(\text{PPh}_2\text{OH})(\text{PPh}_2\text{O})_2]$ (**Scheme 3.4**), though such species have also been employed in Stille-Miyaura coupling,⁸⁴⁻⁸⁷ and related diphosphinite hydrolysis products have proven active in a variety of catalytic processes.⁸⁸⁻⁹⁰ To determine whether ligand decomposition could be occurring in the current case, a solution of $[\text{PdCl}_2(\text{NCPh})_2]$ and **3** in a 1:2 ratio was allowed to stand at room temperature under nitrogen in the absence of other reagents. Crystals of $[\mu\text{-ClPd}(\text{PPh}_2\text{OH})(\text{PPh}_2\text{O})_2]$ were indeed isolated from this mixture after 18 h (**Figure 3.10 Table 3.6** and **Table 3.8**), and the initial yellow color attributable to the putative $[\text{PdCl}_2(\mathbf{3})]$ complex slowly fades to colorless. As seen in Table 4, the data referring to 4-acetylphenylboronic acid has considerable differences in yields depending on ligand substrate. The NHC ligand **1** emerges as an obvious choice for coupling due to the advantageous yields achieved. It is also noteworthy that while diphosphine **2** provides poor (<5%) yields for coupling of aryl chlorides with either phenylboronic acid or 4-acetylphenylboronic acid, near quantitative coupling is achieved when 4-

methoxyphenylboronic acid is employed. The generally good yields observed for all ligands used in this study for the coupling of phenylboronic acid with aryl bromides and iodides are also noteworthy.



Scheme 3.4 Decomposition of $[Cl_2Pd(3)]$ to form $[\mu-ClPd(PPh_2OH)(PPh_2O)]_2$

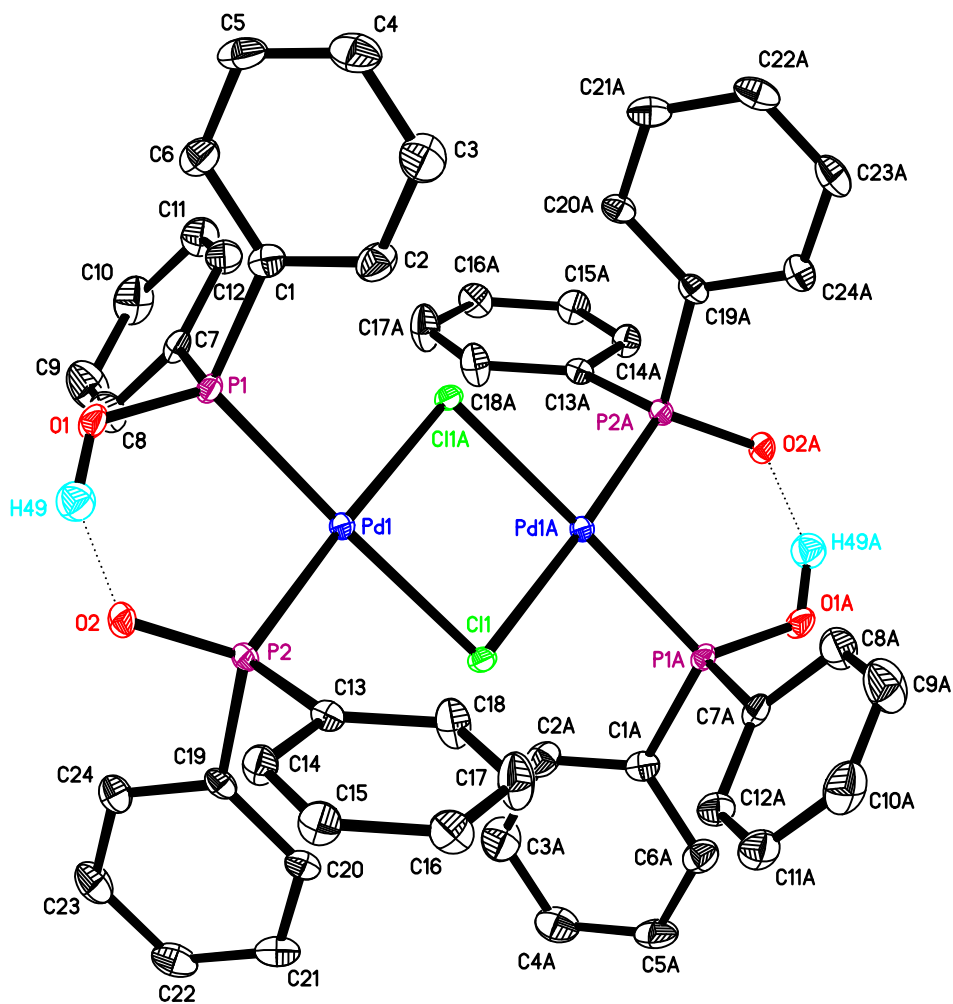


Figure 3.10 ORTEP drawing (50% probability ellipsoids) of the molecular structure of $[\mu\text{-ClPd}(\text{PPh}_2\text{OH})(\text{PPh}_2\text{O})]_2$. Hydrogen atoms are omitted for clarity, except for H49 and H49A, which are shown to demonstrate hydrogen bonding.

Table 3.8 Crystal data and structure refinement details of $[\mu\text{-ClPd}(\text{PPh}_2\text{OH})(\text{PPh}_2\text{O})]_2$

Molecular formula	$\text{C}_{48}\text{H}_{42}\text{Cl}_2\text{O}_4\text{P}_4\text{Pd}_2$
Formula weight (g/mol)	1090.40
Temperature (K)	153 (2)
Wavelength (\AA)	0.71073
Crystal system	Triclinic
Space group	$P\bar{1}$ (#2)
Unit cell dimensions	
a (\AA)	11.855(2)
b (\AA)	13.167(3)
c (\AA)	17.352(4)
α (deg)	68.76(3)
β (deg)	78.84(3)
γ (deg)	63.27(3)
Volume (\AA^3)	2253.2(8)
Z	2
Calculated density (Mg/m^3)	1.607
Absorption coefficient (mm^{-1})	1.103
$F(000)$	1096
Crystal size (mm)	$0.53 \times 0.48 \times 0.36$
Crystal color and shape	yellow prism
θ range for data collection (deg)	$3.15 - 25.10.43 - 25.10$
Limiting indices	$-14 < h < 14$ $-15 < k < 14$ $-20 < l < 18$
Reflections collected	16023
Independent reflections	7784
Completeness to θ	25.10 (97.0 %)
Max. transmission	0.6923
Min. transmission	0.5926
Refinement method	Full-matrix least-squares on F^2
Data / restraints / parameters	7784/0/567
Goodness of fit on F^2	1.004
Final R indices ($I > 2\sigma(I)$)	
R1	0.0375
wR2	0.0715
R indices (all data)	
R1	0.0436
wR2	0.0759

3.5 Conclusions

The preparation of various ligands can be a versatile tool for the design of complexes with a variety of properties and functions. The development of the synthetic route to $[\mathbf{1H}_2](\mathbf{Br})_2$ allows for easy modification of a previously reported ligand to allow for versatility in the ability of the scaffold. The use of $[\mathbf{1H}_2](\mathbf{Br})_2$ as a precursor to the carbene was a versatile tool as seen by the clean conversion to the silver NHC complex via silver oxide. Isolation and full characterization of the *trans*-chelating bis(NHC) silver complex $\{[\text{Ag}(\mathbf{1})]\text{AgBr}_2\}_2$ demonstrates a unique tetranuclear core in the solid state and is to our knowledge the first silver complex with a *trans*-chelating bis(NHC) whose X-ray structure has been reported (CSD version 5.29 Nov. 2007).

The transmetalation of the silver (I) NHC complex $[\text{Ag}(\mathbf{1})]\text{AgBr}_2$ to the palladium NHC complex $[\text{PdCl}_2(\mathbf{1})]$ was shown to exhibit similar binding as $[\text{PdCl}_2(\mathbf{2})]$. The catalytic activity of canopied *trans*-chelating bis(NHC) ligands were compared that that of its phosphine and diphosphinite analogues utilizing C-C bond formation reactions such as Suzuki-Miyaura coupling. The ability to demonstrate moderate to high yields and distinct differences in catalytic activity demonstrates the importance *trans*-chelating complexes have within catalytic processes. The utility of a variety of wide bite angle bis(NHC) ligands encompassing the *m*-terphenyl scaffold would prove to be a vital study in determining the relationship of catalytic applications and bite angles within bis(NHC) ligands.

3.6 Experimental Details

All air sensitive procedures were carried out in an inert atmosphere of nitrogen using an MBraun dry box or with standard Schlenk techniques. Compounds **2**,⁵⁶ **3**,⁵⁵ **4**,⁹¹ and **5**,⁹² were prepared as reported previously. Solvents were purified by passage through alumina columns under a N₂ atmosphere employing an MBraun solvent purification system. All other reagents were used as received from Aldrich Chemical Company, Acros, TCI and Alfa Aesar. NMR spectra were collected using a Bruker Avance 300 instrument operating at 300 MHz for proton and 75.4 MHz for ¹³C. Gas chromatographs and mass spectra were collected using a Shimadzu GCMS-QP2010 and analyzed using the GCMSsolution software.

Preparation of [IH₂](Br)₂

A solution of 1,3-bis[2-(bromomethyl)phenyl]benzene (1.00 g, 2.40 mmol) and *N*-(*n*-butyl)imidazole (0.656 g, 5.28 mmol) in acetonitrile (200 mL) was refluxed for 15 h. Once cooled to room temperature, the solvent was removed under reduced pressure to give an oily residue. Further purification was affected by reprecipitation from a saturated DCM solution into ethyl ether at -40 °C followed by cold filtration. The resulting solid was then dried in vacuo to yield a white powder that was used without further purification (1.46 g, 91.6 %). ¹H NMR (300 MHz, DMSO-*d*₆) δ = 9.07 (s, 2H), 7.81 (s, 2H), 7.63-7.44 (m, 7H), 7.44-7.33 (m, 4H), 7.33-7.24 (m, 2H), 7.21 (s, 1H), 5.50 (s, 4H), 4.12 (t, 9.0 Hz, 4H), 1.69 (quintet, 6.0 Hz, 4H), 1.19 (sextet, 6.0 Hz, 4H), 0.85 (t, 7.5Hz, 6H). ¹³C{H} NMR (CD₃CN, 75.4 MHz): δ 12.6, 18.9, 31.5, 49.4, 51.3, 122.4, 122.5, 128.1, 128.7, 128.8, 129.1, 129.6, 130.0, 130.8, 130.9, 135.3, 140.1, 141.7.

Preparation of [Ag(I)]AgBr₂

To a solution of 0.556 g (0.837 mmol) [**1H₂**](**Br**)₂ in 25 mL dichloromethane 0.239 g (1.03 mmol) silver(I) oxide was added. The suspension was refluxed for 24 h in the absence of light. The resulting solution was filtered through Celite and the filtrate was concentrated under reduced pressure then vacuum dried for 3 hours to afford the product as a white powder. A minimal amount of DCM was used to dissolve the material and pentane was diffused into the vial at 0 °C to afford the pure complex as clear colorless crystals (0.632 g, 86.0 %). High quality crystals for single crystal X-ray diffraction were also attainable by slow evaporation of acetone. ¹H NMR (300 MHz, DMSO-*d*⁶) δ = 7.75 (dd, 6.0 Hz, 2H), 7.48 (t, 7.5 Hz, 2H), 7.47 (d, 3.0 Hz, 2H), 7.43 (t, 7.5 Hz, 2H), 7.38 (t, 9 Hz, 1H), 7.38 (d, 3.0 Hz, 2H), 7.34 (bs, 1H), 7.21 (dd, 6.0 Hz, 2H), 6.95 (dd, 6.0 Hz, 2H), 5.43 (s, 4H), 3.96 (t, 7.5 Hz, 4H), 1.66 (quintet, 6.0 Hz, 4H), 1.20 (sextet, 9.0 Hz, 4H), 0.87 (t, 7.5 Hz, 6H) ¹³C{H} NMR (75.4 MHz, DMSO-*d*⁶) δ = 179.8, 142.2, 140.8, 134.1, 131.2, 131.2, 129.6, 129.1, 129.1, 128.6, 128.6, 122.8, 121.5, 53.1, 51.0, 33.6, 19.6, 13.9. Elemental analysis calculated for C₆₈H₇₆Ag₄Br₂N₈·C₄H₈O: (fw 1662.13) C, 47.29; H, 4.63; N, 6.13. Found: C, 47.77; H, 4.28; N, 6.31.

Preparation of [PdCl₂(I)]

To a vigorously stirring solution of 0.0646 g (0.168 mmol) bis(benzonitrile) palladium (II) chloride (10 mM in dichloromethane) a 10 mM solution of 0.1493 g (0.157 mmol) [Ag(**1**)]AgBr₂ in dichloromethane was added dropwise. This solution was allowed to stir overnight then filtered and the filtrate was concentrated in vacuo then washed with hexane to afford a light yellow powder (0.0863 g, 80.9%) that was used immediately for coupling reactions. ¹H NMR (300 MHz, CDCl₃) δ = 7.63-7.30 (m, 10H) (dd, 6.0 Hz, 2H),

7.24 (dd, 7.7 Hz, 2H), 6.86 (d, 1.8 Hz, 2H), 6.76 (d, 2.1 Hz, 2H), 6.11 (s, 4H), 4.42 (t, 7.5 Hz, 4H), 2.03 (quintet, 7.5 Hz, 4H), 1.45 (sextet, 7.8 Hz, 4H), 1.00 (t, 7.2 Hz, 6H)
 $^{13}\text{C}\{\text{H}\}$ NMR (75.4 MHz, CDCl_3) δ = 168.9, 143.5, 140.1, 132.6, 132.4, 131.6 (131.7), 131.0, 130.8, 130.2, 128.5, 128.4, 120.8 (120.9), 119.1 (119.2), 52.4 (52.8), 50.4 (50.6), 33.4 (33.2), 20.1, 13.8. (peaks attributable to minor isomers are provided in parentheses; see ESI for original NMR spectra). ESI-MS: m/z 689, (100%) $[\text{BrPd}(\mathbf{1})]^+$; m/z 645 (73.3%) $[\text{ClPd}(\mathbf{1})]^+$; m/z 608 (49.5%) $[\text{Pd}(\mathbf{1})]^+$.

General conditions for Suzuki coupling reactions

Conditions were identical to those reported for Suzuki coupling reactions utilizing ligand **2**.⁵⁰ A 5 mL vial equipped with a spin vane was charged with the requisite aryl halide (0.30 mmol), phenylboronic acid (0.45 mmol), Cs_2CO_3 (0.90 mmol), and 1 mol% of $[\text{PdCl}_2(\mathbf{1})]$. The components were then taken up in 2 mL 1,4-dioxane and heated at 100 °C under nitrogen for 25 h. Following the reaction, the crude reaction mixtures were diluted with diethyl ether for direct GC-MS analysis.

X-ray crystallography

Intensity data were collected using a Rigaku Mercury CCD detector and an AFC8S diffractometer. Data collection and cell refinements were achieved using CrystalClear.⁹³ Data reduction and absorbance corrections were attained using REQAB.⁹⁴ The structures were solved by direct methods and subsequent Fourier difference techniques, and refined anisotropically, by full-matrix least squares, on F^2 using SHELXTL 6.10⁹⁵ All molecular graphics were generated using SHELXTL 6.10. Hydrogen atom positions were calculated from ideal geometry with coordinates riding on the parent atom however H49 and H50 in $[\mu\text{-ClPd}(\text{PPh}_2\text{OH})(\text{PPh}_2\text{O})]_2$ were located in the

Fourier difference map, then refined. Partial occupancy was used to account for disorder observed in C47 and C48 of a phenyl ring in this structure. Disorder was observed in [PdX₂(**1**)]·C₇H₈ on one of the n-butyl functionalities and accounted for using partial occupancies of C18, C19 and C20 with their counterparts being C18A, C19A and C20A respectively. The disorder in the cocrystallized toluene molecule in [PdX₂(**1**)]·C₇H₈ was accounted for using partial occupancy of C41 with its counterpart being C41A.

3.7 Selected Spectra

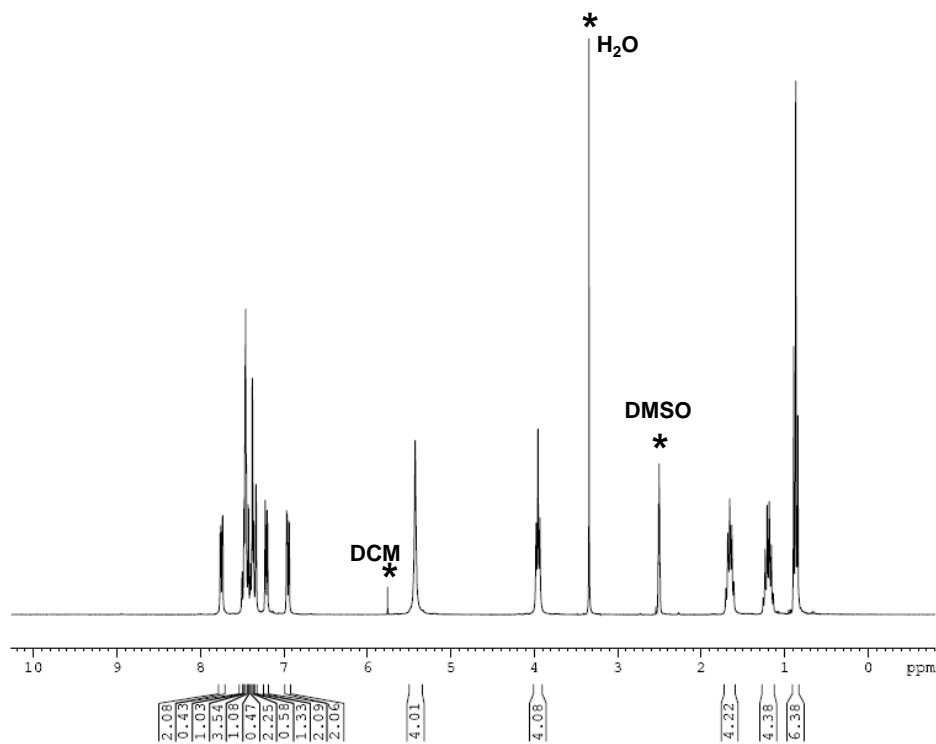


Figure 3.11. ^1H NMR spectrum of $[\text{Ag}(\mathbf{1})]\text{AgBr}_2$ (DMSO, 300 MHz).

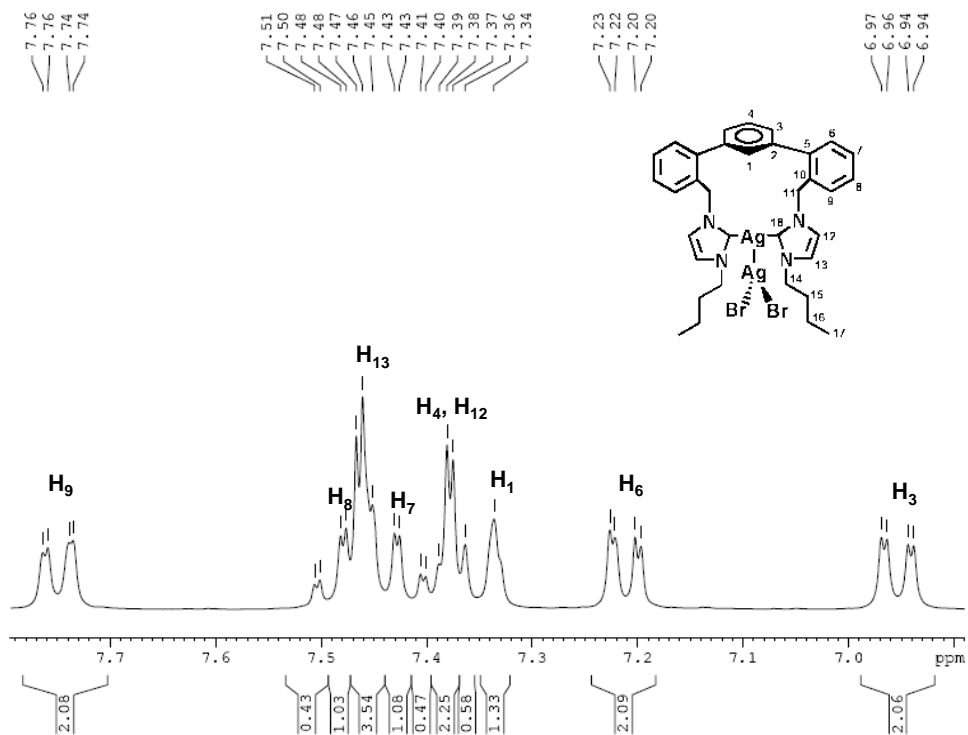


Figure 3.12. Aromatic region of the ^1H NMR spectrum of $[\text{Ag}(\mathbf{1})]\text{AgBr}_2$ (DMSO, 300 MHz).

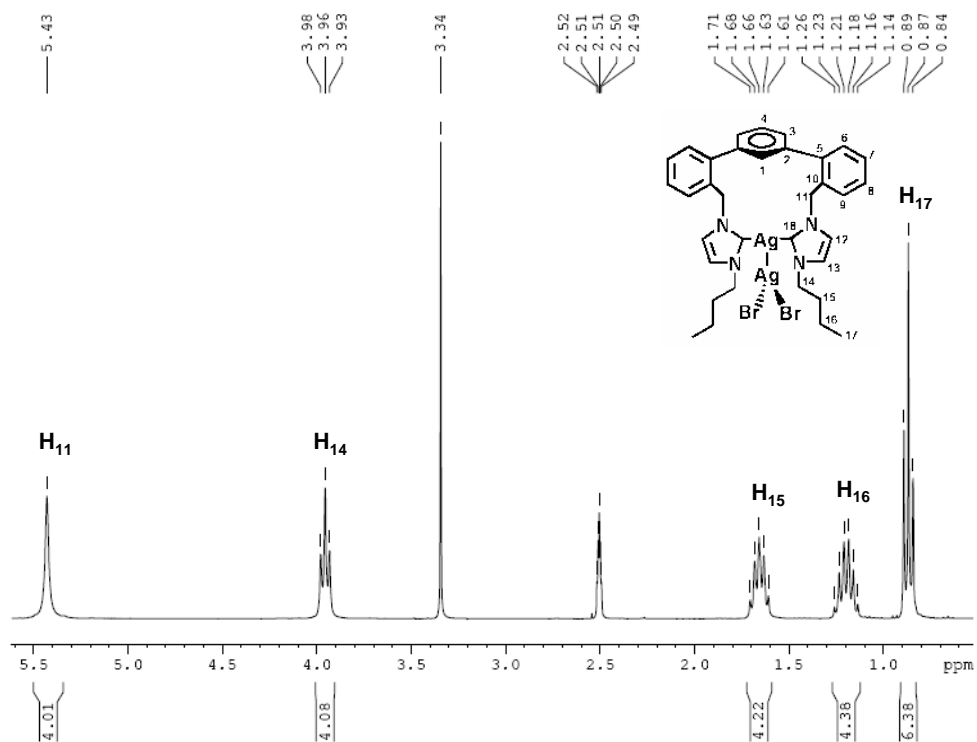


Figure 3.13. Aliphatic region of the ^1H NMR spectrum of $[\text{Ag}(\mathbf{1})]\text{AgBr}_2$ (DMSO, 300 MHz).

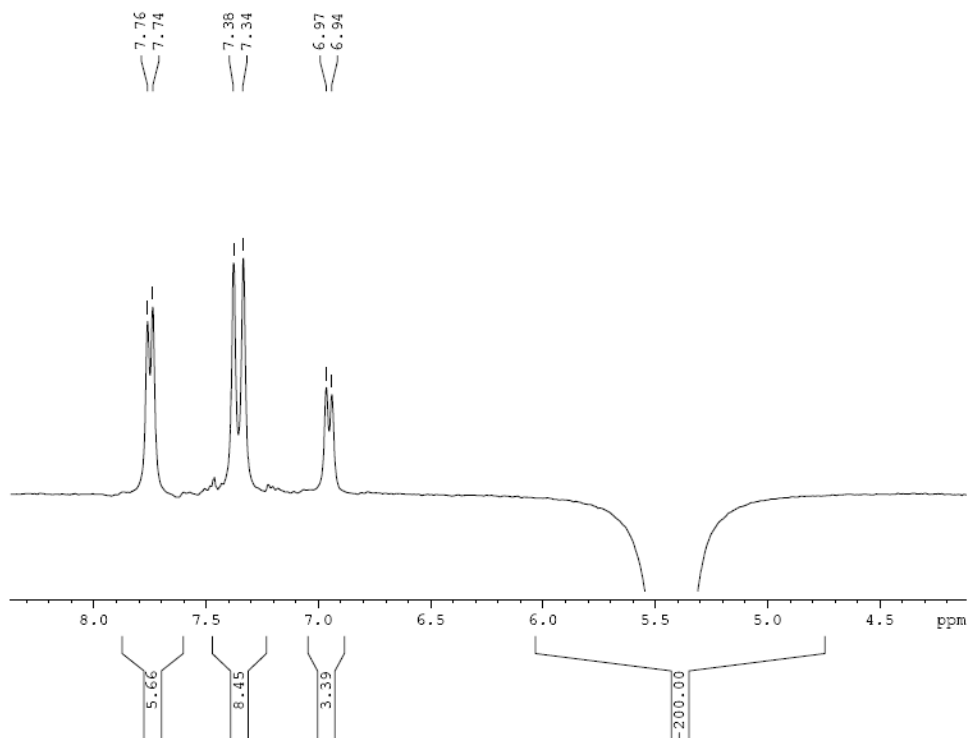


Figure 3.14. Nuclear overhauser effect difference (NOE-DIFF) spectrum of $[\text{Ag}(\mathbf{1})]\text{AgBr}_2$ (DMSO, 300 MHz) for protons resonating at 5.43 ppm.

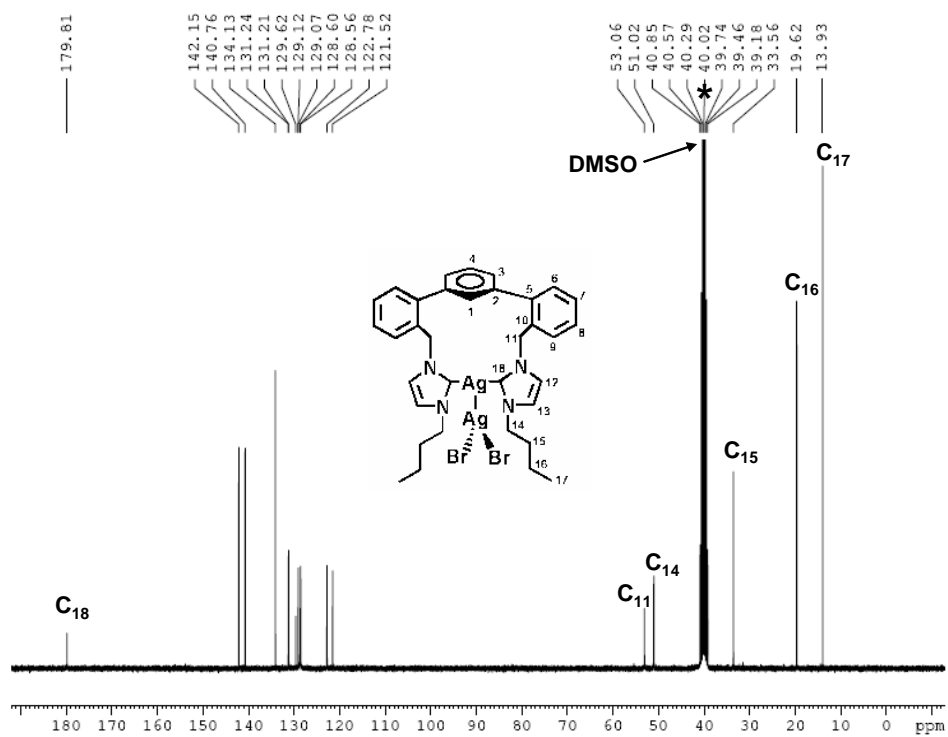


Figure 3.15. ^{13}C NMR spectrum of $[\text{Ag}(\mathbf{1})]\text{AgBr}_2$ (DMSO, 75 MHz).

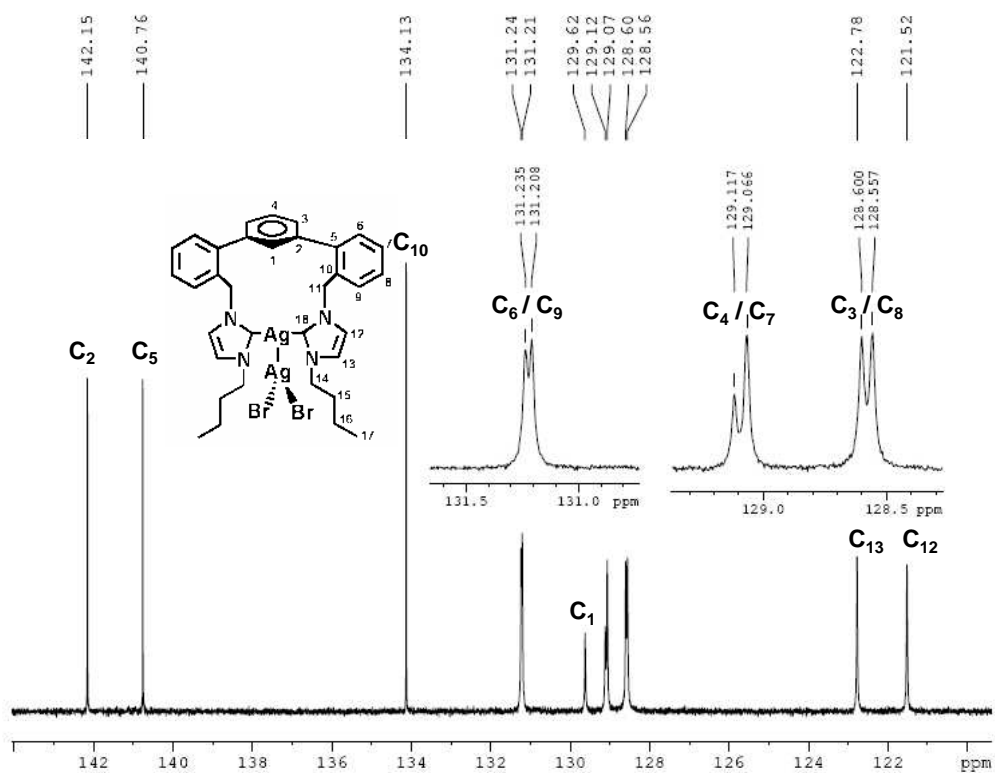


Figure 3.16. Aromatic region of the ^{13}C NMR spectrum of $[\text{Ag}(\mathbf{1})]\text{AgBr}_2$ (DMSO, 75 MHz).

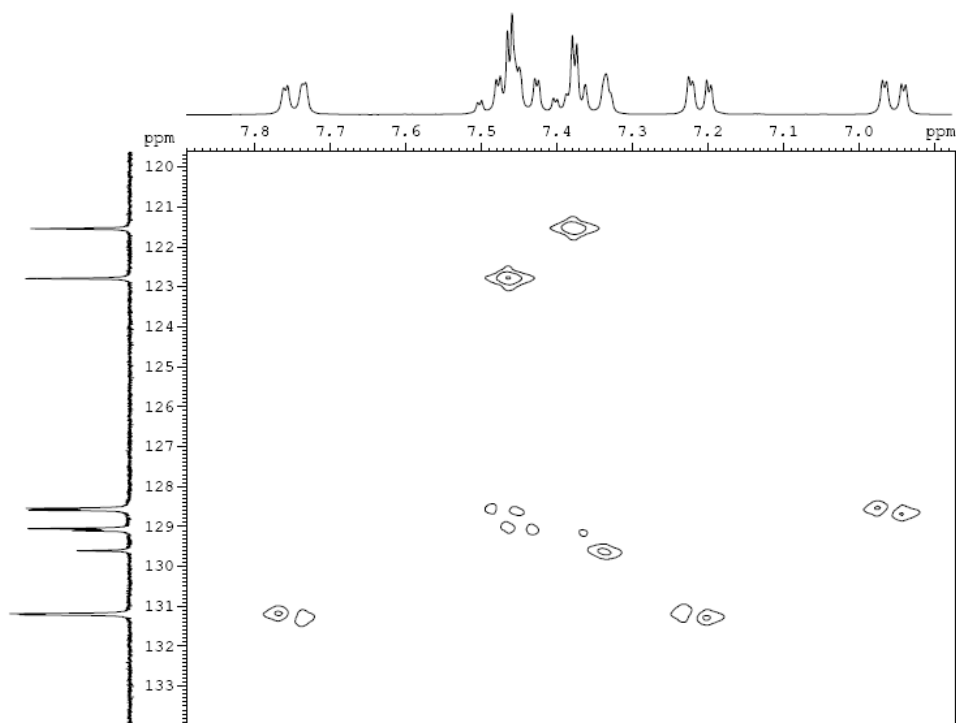


Figure 3.17. Heteronuclear multiple quantum coherence (HMQC) spectrum of $[\text{Ag}(\mathbf{1})]\text{AgBr}_2$ (300 MHz for ^1H , 75 MHz for ^{13}C , in DMSO).

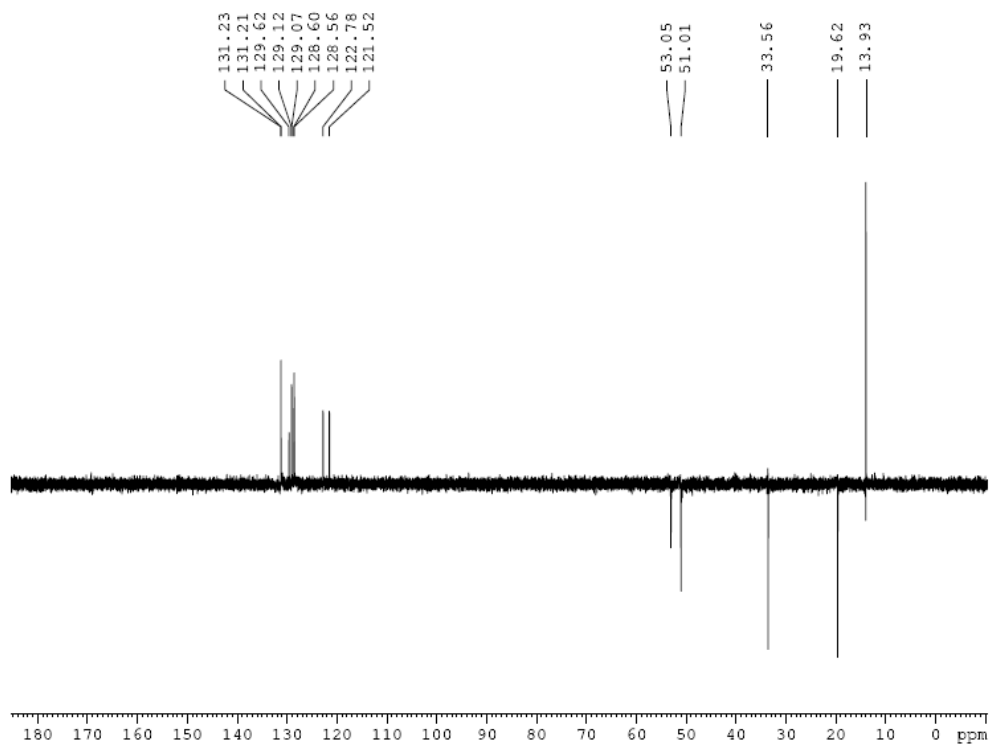


Figure 3.18. Distortionless enhancement by polarization transfer (DEPT-135) spectrum of $[\text{Ag}(\mathbf{1})]\text{AgBr}_2$ (DMSO, 75 MHz).

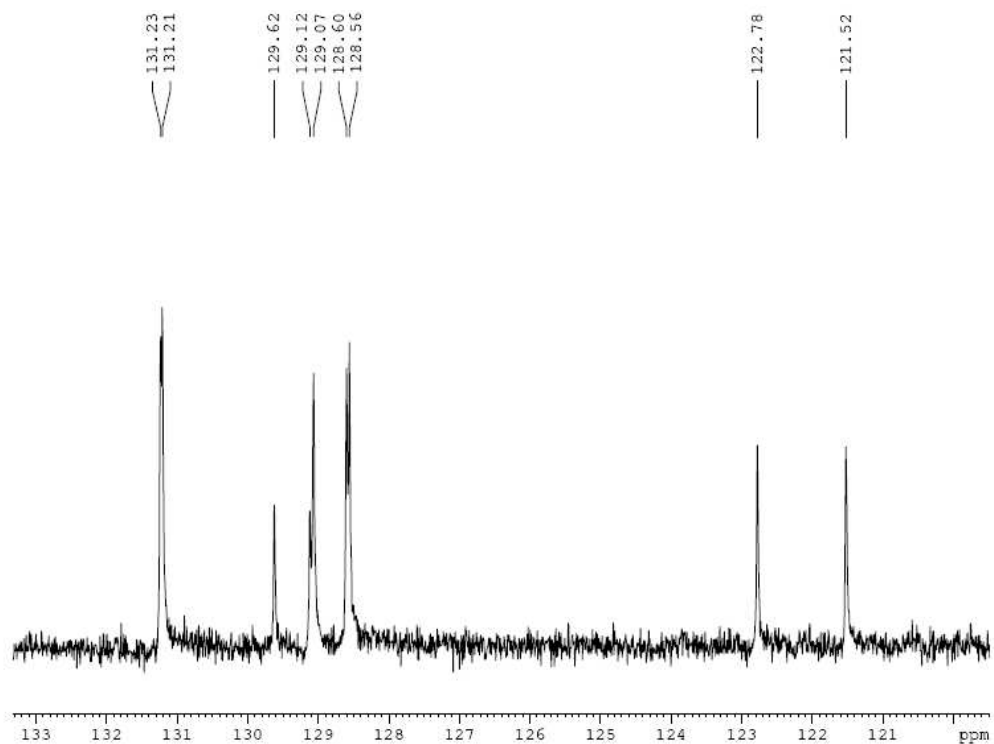


Figure 3.19. Aromatic region of DEPT-135 spectrum of [Ag(1)]AgBr₂ (DMSO, 75 MHz).

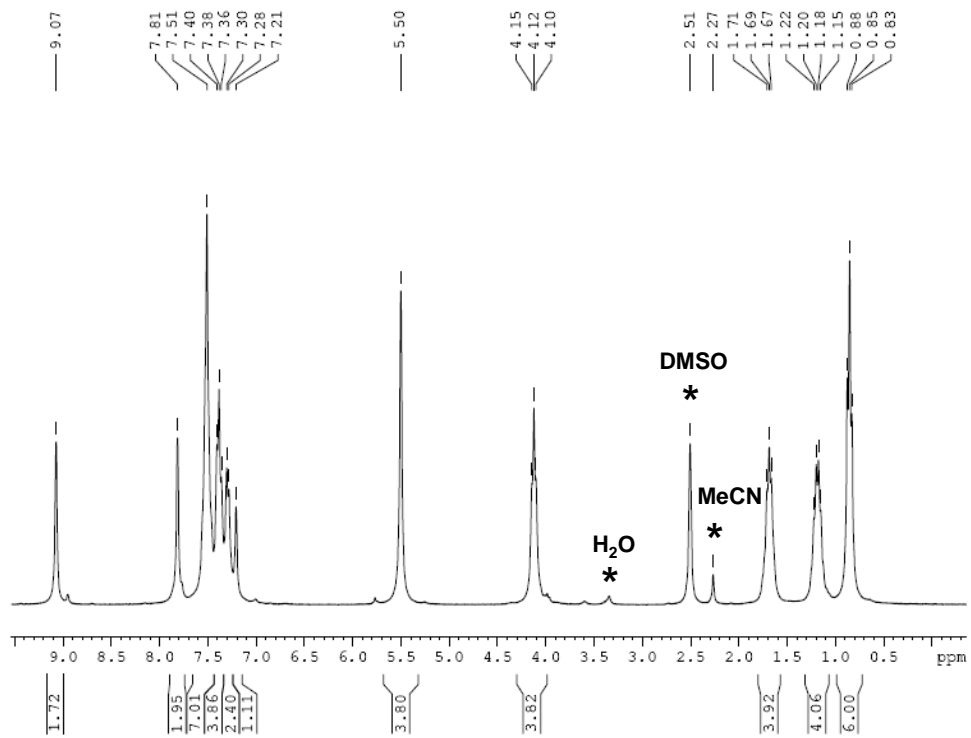


Figure 3.20. ¹H NMR spectrum of [H₂1]Br₂ (DMSO, 300 MHz).

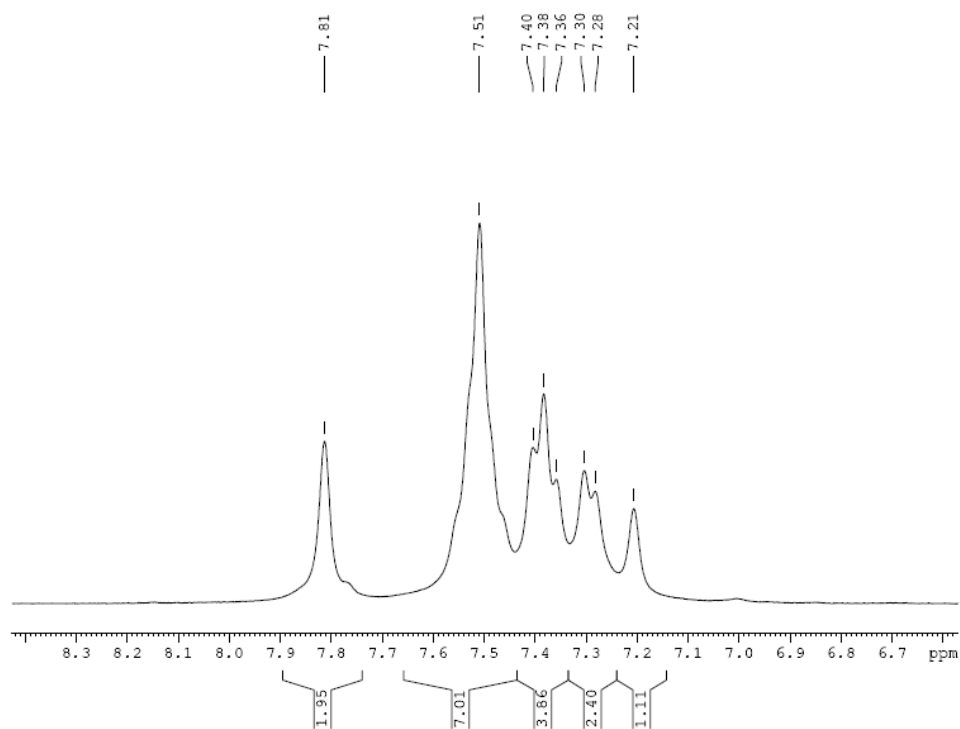


Figure 3.21. Aromatic region of the ^1H NMR spectrum of $[\text{H}_2\text{1}]\text{Br}_2$ (DMSO, 300 MHz).

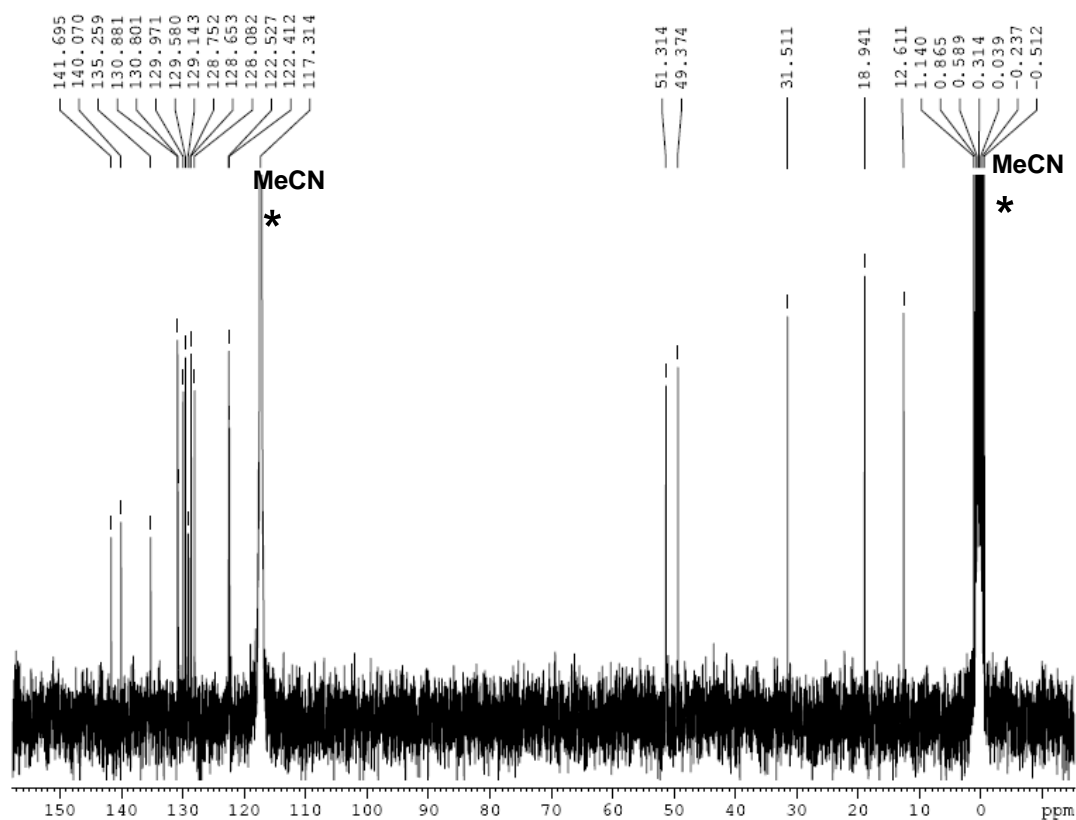


Figure 3.22. ^{13}C NMR spectrum of $[\text{H}_2\text{1}]\text{Br}_2$ (CD_3CN , 75 MHz).

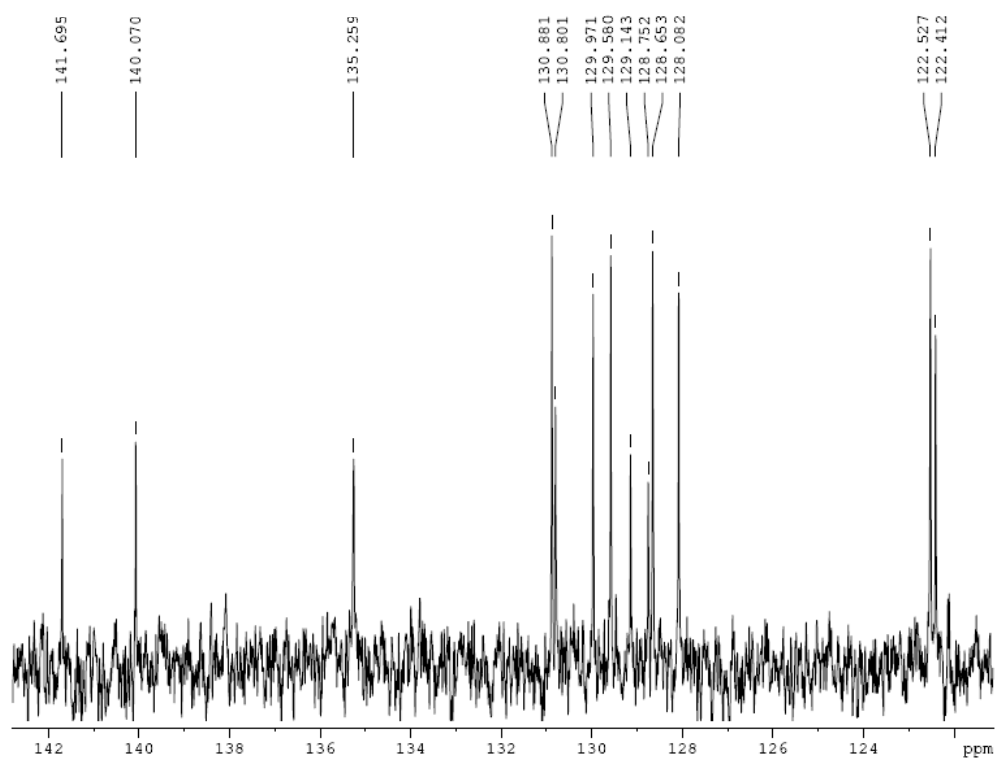


Figure 3.23. Aromatic region of the ^{13}C NMR spectrum of $[\text{H}_2\mathbf{1}]\text{Br}_2$ (CD_3CN , 75 MHz).

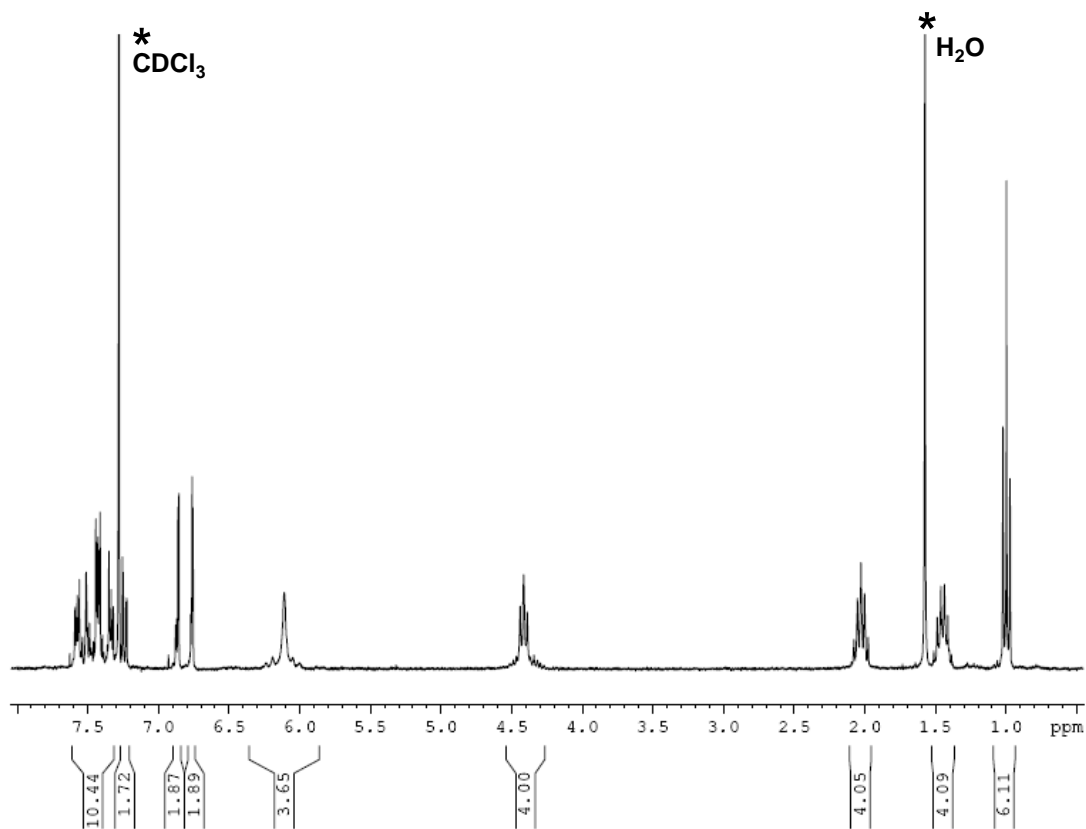


Figure 3.24. ^1H NMR spectrum of $[\text{Cl}_2\text{Pd}(\mathbf{1})]$ (CDCl_3 , 300 MHz).

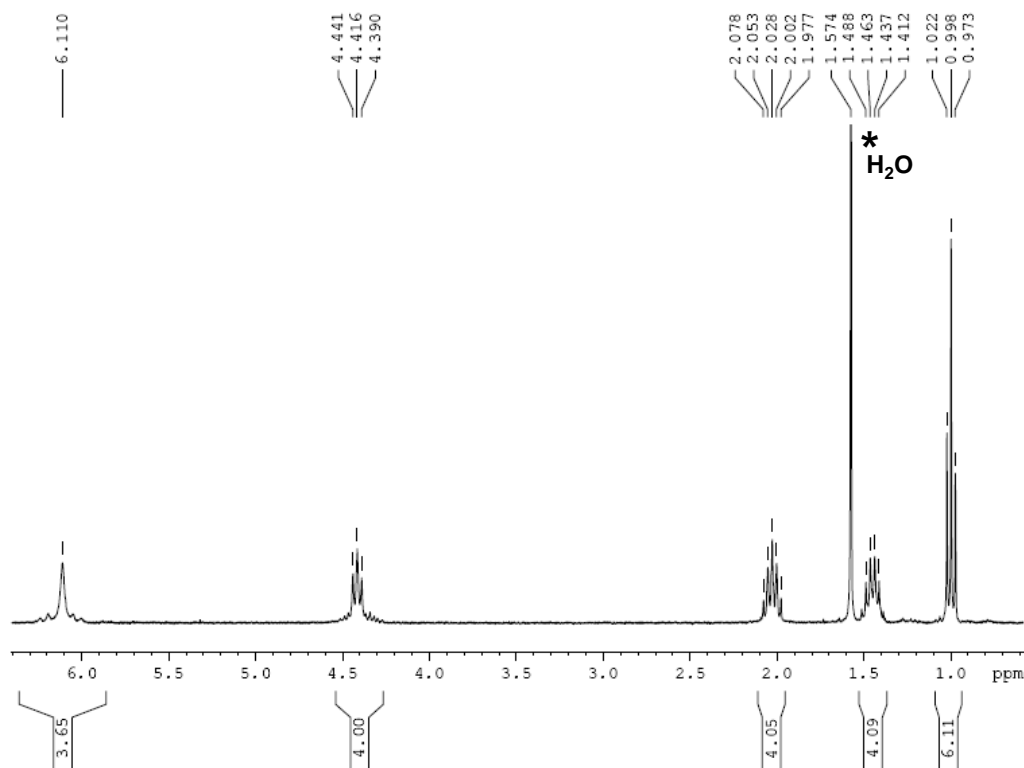


Figure 3.25. Aliphatic region of the ^1H NMR spectrum of $[\text{Cl}_2\text{Pd}(\mathbf{1})]$ (CDCl_3 , 300 MHz).

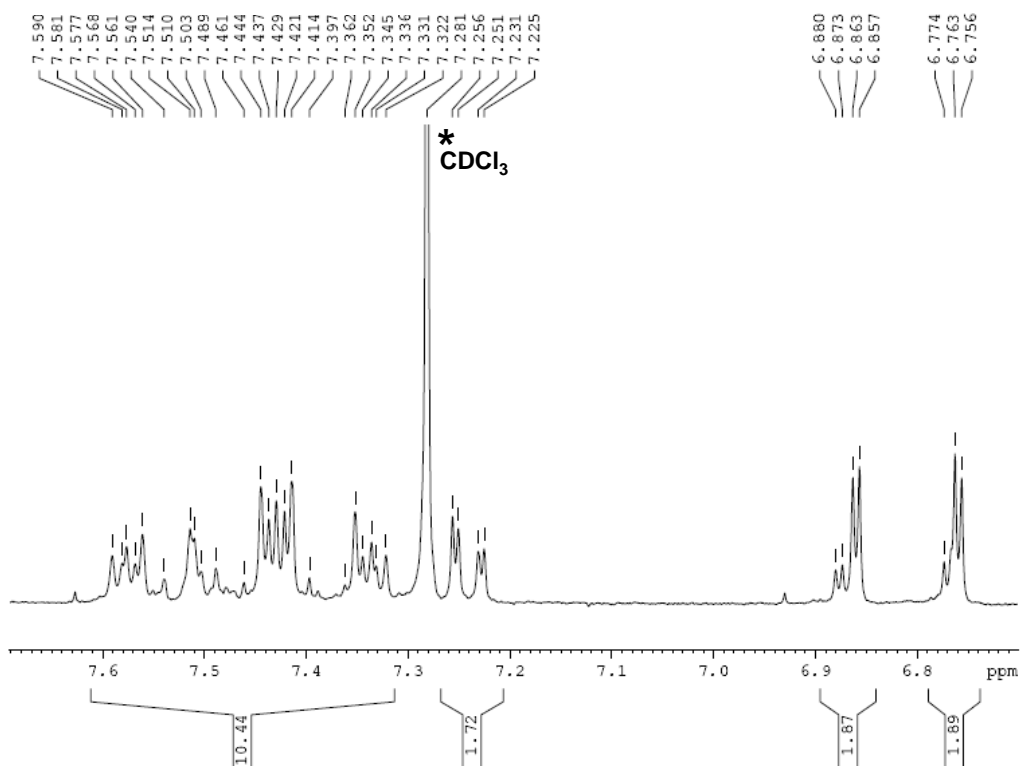


Figure 3.26. Aromatic region of the ^1H NMR spectrum of $[\text{Cl}_2\text{Pd}(\mathbf{1})]$ (CDCl_3 , 300 MHz).

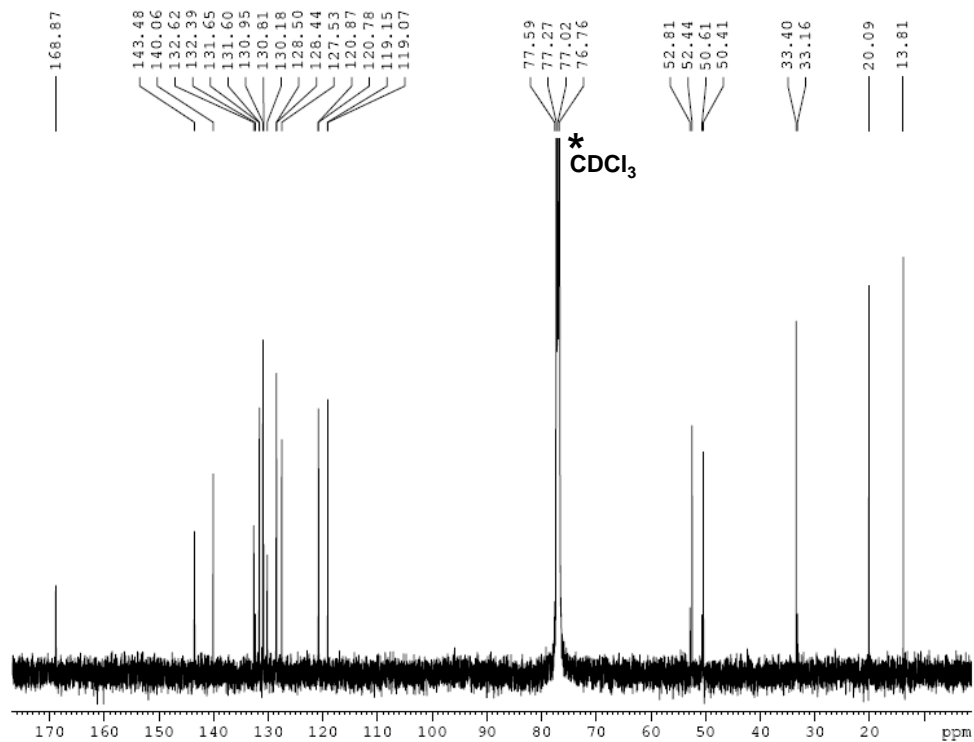


Figure 3.27. ^{13}C NMR spectrum of $[\text{Cl}_2\text{Pd}(\mathbf{1})]$ (CDCl_3 , 75 MHz).

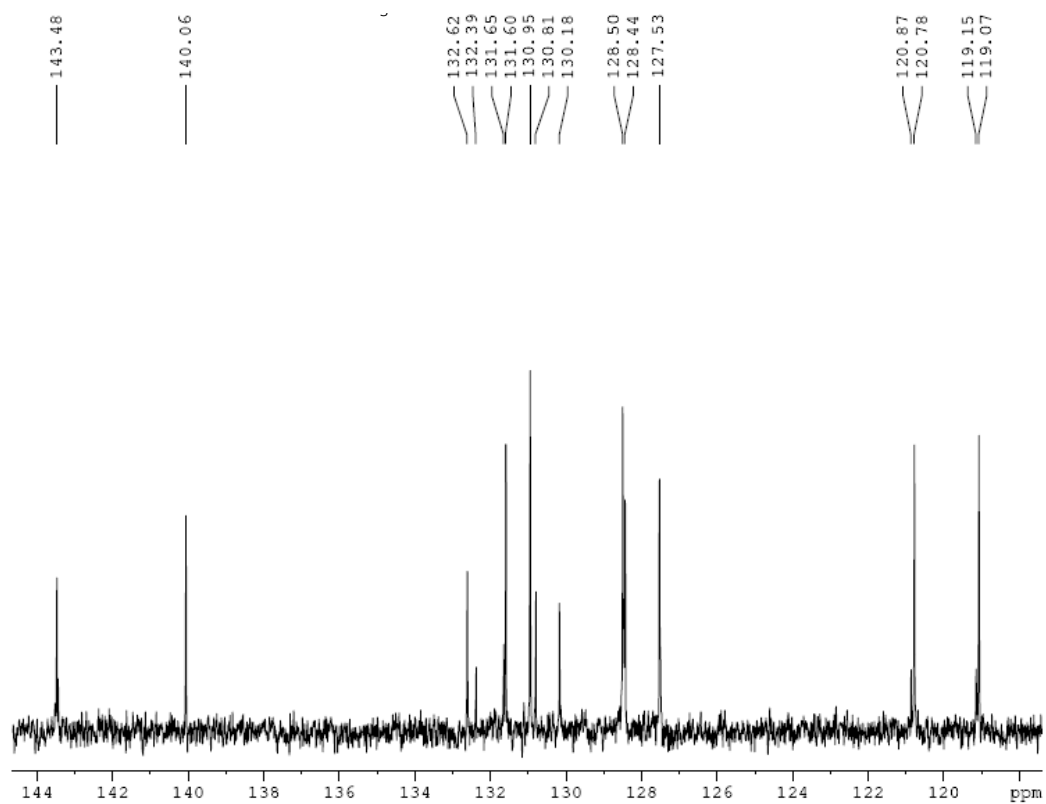


Figure 3.28. Aromatic region of the ^{13}C NMR spectrum of $[\text{Cl}_2\text{Pd}(\mathbf{1})]$ (CDCl_3 , 75 MHz).

3.8 References

1. Oefele, K., *Journal of Organometallic Chemistry* **1968**, *12*, P42-P43.
2. Wanzlick, H. W.; Schoenherr, H. J., *Angewandte Chemie, International Edition* **1968**, *7*, 141-142.
3. Schmitz, M.; Leininger, S.; Bergstrasser, U.; Regitz, M., *Heteroatom Chemistry* **1998**, *9*, 453-460.
4. Arduengo, A., *Journal of the American Chemical Society* **1991**, *113*, 361-362.
5. Bourissou, D.; Guerret, O.; Gabbai, F. P.; Bertrand, G., *Chemical Reviews* **2000**, *100*, 39-91.
6. Boehme, C.; Frenking, G., *Journal of the American Chemical Society* **1996**, *118*, 2039-2046.
7. Heinemann, C.; Mueller, T.; Apeloig, Y.; Schwarz, H., *Journal of the American Chemical Society* **1996**, *118*, 2023-2038.
8. Boydston, A. J.; Williams, K. A.; Bielawski, C. W., *Journal of the American Chemical Society* **2005**, *127*, 12496-12497.
9. Boydston, A. J.; Bielawski, C. W., *Dalton Transactions* **2006**, 4073-4077.
10. Khramov, D. M.; Boydston, A. J.; Bielawski, C. W., *Angewandte Chemie, International Edition* **2006**, *45*, 6186-6189.
11. Kamplain, J. W.; Bielawski, C. W., *Chemical Communications* **2006**, 1727-1729.
12. Williams, K. A.; Boydston, A. J.; Bielawski, C. W., *Journal of the Royal Society Interface* **2007**, *4*, 359-362.
13. Zhang, T.; Wang, W.; Gu, X.; Shi, M., *Organometallics* **2008**, *27*, 753-757.

14. Nolan, S. P., *N-Heterocyclic Carbenes in Synthesis*. Wiley-VCH: Weinheim, Germany, 2006; p 47.
15. Peris, E.; Crabtree, R. H., *Coordination Chemistry Reviews* **2004**, *248*, 2239-2246.
16. Lin, I. J. B.; Vasam, C. S., *Coordination Chemistry Reviews* **2007**, *251*, 642-670.
17. Garrison, J. C.; Youngs, W. J., *Chemical Reviews* **2005**, *105*, 3978-4008.
18. Glorius, F., *N-Heterocyclic Carbenes in Transition Metal Catalysis*. Springer-Verlag: Berlin Germany, 2007; p 21.
19. Hill, J. E.; Nile, T. A., *J. Organomet. Chem.* **1977**, *137*, 293-300.
20. Herrmann, W. A.; Elison, M.; Fischer, J.; Koecher, C.; Artus, G. R. J., *Angewandte Chemie, International Edition* **1995**, *34*, 2371-2374.
21. Herrmann, W. A.; Reisinger, C.-P.; Spiegler, M., *Journal of Organometallic Chemistry* **1998**, *557*, 93-96.
22. Loch, J. A.; Albrecht, M.; Peris, E.; Mata, J.; Faller, J. W.; Crabtree, R. H., *Organometallics* **2002**, *21*, 700-706.
23. Miyaura, N.; Suzuki, A., *Chemical Reviews* **1995**, *95*, 2457-2483.
24. Sonogashira, K.; Tohda, Y.; Hagihara, N., *Tetrahedron Letters* **1975**, 4467-4470.
25. McGuinness, D. S.; Cavell, K. J., *Organometallics* **2000**, *19*, 741-748.
26. Stille, J. K., *Angewandte Chemie, International Edition* **1986**, *98*, 504-519.
27. Herrmann, W. A.; Bohm, V. P. W.; Gstottmayr, C. W. K.; Grosche, M.; Reisinger, C. P.; Weskamp, T., *Journal of Organometallic Chemistry* **2001**, *617-618*, 616-628.

28. Weskamp, T.; Bohm, V. P. W.; Herrmann, W. A., *Journal of Organometallic Chemistry* **1999**, *585*, 348-352.
29. Frisch, A. C.; Rataboul, F.; Zapf, A.; Beller, M., *Journal of Organometallic Chemistry* **2003**, *687*, 403-409.
30. Mas-Marza, E.; Segarra, A. M.; Claver, C.; Peris, E.; Fernandez, E., *Tetrahedron Letters* **2003**, *44*, 6595-6599.
31. Hillier, A. C.; Grasa, G. A.; Viciu, M. S.; Lee, H. M.; Yang, C.; Nolan, S. P., *Journal of Organometallic Chemistry* **2002**, *653*, 69-82.
32. Cao, D. R.; Schollmeyer, D.; Meier, H., *European Journal of Organic Chemistry* **1999**, 791-795.
33. Scholl, M.; Trnka, T. M.; Morgan, J. P.; Grubbs, R. H., *Tetrahedron Letters* **1999**, *40*, 2247-2250.
34. Hsu, J.-H.; Fann, W.; Tsao, P.-H.; Chuang, K.-R.; Chen, S.-A., *Journal of Physical Chemistry A* **1999**, *103*, 2375-2380.
35. Frenzel, U.; Weskamp, T.; Kohl, F. J.; Schattenmann, W. C.; Nuyken, O.; Herrmann, W. A., *Journal of Organometallic Chemistry* **1999**, *586*, 263-265.
36. Scholl, M.; Ding, S.; Lee, C. W.; Grubbs, R. H., *Organic Letters* **1999**, *1*, 953-956.
37. Casey, C. P.; Whiteker, G. T., *Israel Journal of Chemistry* **1990**, *30*, 299-304.
38. Kamer, P. C. J.; van Leeuwen, P. W. N. M.; Reek, J. N. H., *Accounts of Chemical Research* **2001**, *34*, 895-904.
39. Freixa, Z.; Van Leeuwen, P. W. N. M., *Dalton Transactions* **2003**, 1890-1901.

40. Kranenburg, M.; Kamer, P. C. J.; Van Leeuwen, P. W. N. M., *European Journal of Inorganic Chemistry* **1998**, 25-27.
41. van Leeuwen, P. W. N. M.; Kamer, P. C. J.; Reek, J. N. H.; Dierkes, P., *Chemical Reviews* **2000**, *100*, 2741-2769.
42. van der Veen, L. A.; Keeven, P. K.; Kamer, P. C. J.; van Leeuwen, P. W. N. M., *Dalton Transactions* **2000**, 2105-2112.
43. Dierkes, P.; van Leeuwen, P. W. N. M., *Journal of the Chemical Society, Dalton Transactions* **1999**, 1519-1530.
44. Clyne, D. S.; Jin, J.; Genest, E.; Gallucci, J. C.; RajanBabu, T. V., *Organic Letters* **2000**, *2*, 1125-1128.
45. Hu, X.; Castro-Rodriguez, I.; Meyer, K., *Journal of the American Chemical Society* **2003**, *125*, 12237-12245.
46. Perry, M. C.; Cui, X.; Burgess, K., *Tetrahedron: Asymmetry* **2002**, *13*, 1969-1972.
47. Wang, J.-W.; Li, Q.-S.; Xu, F.-B.; Song, H.-B.; Zhang, Z.-Z., *European Journal of Organic Chemistry* **2006**, 1310-1316.
48. Hahn, F. E.; Langenhahn, V.; Luegger, T.; Pape, T.; Le Van, D., *Angewandte Chemie, International Edition*. **2005**, *44*, 3759-3763.
49. Chan, K. L.; Watkins, S. E.; Mak, C. S. K.; McKiernan, M. J.; Towns, C. R.; Pascu, S. I.; Holmes, A. B., *Chemical Communications* **2005**, 5766-5768.
50. Smith, R. C.; Bodner, C. R.; Earl, M. J.; Sears, N. C.; Hill, N. E.; Bishop, L. M.; Sizemore, N.; Hehemann, D. T.; Bohn, J. J.; Protasiewicz, J. D., *Journal of Organometallic Chemistry* **2005**, *690*, 477-481.

51. Morgan, B. P.; Smith, R. C., *Journal of Organometallic Chemistry* **2008**, *693*, 11-16.
52. Ma, L.; Wobser, S. D.; Protasiewicz, J. D., *Journal of Organometallic Chemistry* **2007**, *692* 5331-5338
53. Ma, L.; Imbesi, P. M.; Updegraff, J. B., III; Hunter, A. D.; Protasiewicz, J. D., *Inorganic Chemistry* **2007**, *46*, 5220-5228.
54. Ma, L.; Woloszynek, R. A.; Chen, W.; Ren, T.; Protasiewicz, J. D., *Organometallics* **2006**, *25*, 3301-3304.
55. Ma, L. Synthesis and Characterization of Ligands and Transition Metal Complexes Containing m-Terphenyl Scaffolds. Ph.D. Dissertation, Case Western Reserve University, Cleveland, OH, 2007.
56. Smith, R. C.; Protasiewicz, J. D., *Organometallics* **2004**, *23*, 4215-4222.
57. Taton, T. A.; Chen, P., *Angewandte Chemie, International Edition* **1996**, *35*, 1011-1013.
58. Poater, A.; Ragone, F.; Giudice, S.; Costabile, C.; Dorta, R.; Nolan, S. P.; Cavallo, L., *Organometallics*, **2008**, *27*, 2679-2681.
59. De Fremont, P.; Scott, N. M.; Stevens, E. D.; Ramnial, T.; Lightbody, O. C.; Macdonald, C. L. B.; Clyburne, J. A. C.; Abernethy, C. D.; Nolan, S. P., *Organometallics* **2005**, *24*, 6301-6309.
60. Dinares, I.; Garcia de Miguel, C.; Font-Bardia, M.; Solans, X.; Alcalde, E., *Organometallics* **2007**, *26*, 5125-5128.
61. Cottrell, I. F.; Hands, D.; Houghton, P. G.; Humphrey, G. R.; Wright, S. H. B., *Journal of Heterocyclic Chemistry* **1991**, *28*, 301-304.

62. Hannig, F.; Kehr, G.; Froehlich, R.; Erker, G., *Journal of Organometallic Chemistry* **2005**, *690*, 5959-5972.
63. Bondi, A., *Journal of Physical Chemistry* **1964**, *68*, 441-451.
64. Lee, C. K.; Lee, K. M.; Lin, I. J. B., *Organometallics* **2002**, *21*, 10-12.
65. Corberan, R.; Ramirez, J.; Poyatos, M.; Peris, E.; Fernandez, E., *Tetrahedron: Asymmetry* **2006**, *17*, 1759-1762.
66. Ramirez, J.; Corberan, R.; Sanau, M.; Peris, E.; Fernandez, E., *Chemical Communications* **2005**, 3056-3058.
67. Chen, W.; Liu, F., *Journal of Organometallic Chemistry* **2003**, *673*, 5-12.
68. Lee, C. K.; Vasam, C. S.; Huang, T. W.; Wang, H. M. J.; Yang, R. Y.; Lee, C. S.; Lin, I. J. B., *Organometallics* **2006**, *25*, 3768-3775.
69. Burling, S.; Mahon, M. F.; Reade, S. P.; Whittlesey, M. K., *Organometallics* **2006**, *25*, 3761-3767.
70. Roseblade, S. J.; Ros, A.; Monge, D.; Alcarazo, M.; Alvarez, E.; Lassaletta, J. M.; Fernandez, R., *Organometallics* **2007**, *26*, 2570-2578.
71. Lee, H. M.; Lu, C. Y.; Chen, C. Y.; Chen, W. L.; Lin, H. C.; Chiu, P. L.; Cheng, P. Y., *Tetrahedron* **2004**, *60*, 5807-5825.
72. Baker, M. V.; Brown, D. H.; Simpson, P. V.; Skelton, B. W.; White, A. H.; Williams, C. C., *Journal of Organometallic Chemistry* **2006**, *691*, 5845-5855.
73. Baker, M. V.; Skelton, B. W.; White, A. H.; Williams, C. C., *Journal of the Chemical Society, Dalton Transactions* **2001**, 111-120.
74. Chiu, P. L.; Lai, C.-L.; Chang, C.-F.; Hu, C.-H.; Lee, H. M., *Organometallics* **2005**, *24*, 6169-6178.

75. Churruca, F.; SanMartin, R.; Ines, B.; Tellitu, I.; Dominguez, E., *Advance Synthesis and Catalysis* **2006**, *348*, 1836-1840.
76. Frank, M.; Maas, G.; Schatz, J., *European Journal of Organic Chemistry* **2004**, 607-613.
77. Hahn, F. E.; Jahnke, M. C.; Pape, T., *Organometallics* **2007**, *26*, 150-154.
78. Magill, A. M.; McGuinness, D. S.; Cavell, K. J.; Britovsek, G. J. P.; Gibson, V. C.; White, A. J. P.; Williams, D. J.; White, A. H.; Skelton, B. W., *Journal of Organometallic Chemistry* **2001**, *617-618*, 546-560.
79. Nonnenmacher, M.; Kunz, D.; Rominger, F.; Oeser, T., *Journal of Organometallic Chemistry* **2007**, *692*, 2554-2563.
80. Saito, S.; Yamaguchi, H.; Muto, H.; Makino, T., *Tetrahedron Letters* **2007**, *48*, 7498-7501.
81. Shi, M.; Qian, H.-X., *Applied Organometallic Chemistry* **2005**, *19*, 1083-1089.
82. Tu, T.; Assenmacher, W.; Peterlik, H.; Weisbarth, R.; Nieger, M.; Doetz, K. H., *Angew. Chem., Int. Ed.* **2007**, *46*, 6368-6371.
83. Xu, Q.; Duan, W.-L.; Lei, Z.-Y.; Zhu, Z.-B.; Shi, M., *Tetrahedron* **2005**, *61*, 11225-11229.
84. Pryjomska, I.; Bartosz-Bechowski, H.; Ciunik, Z.; Trzeciak, A. M.; Zi'olkowski, J. o. J., *Dalton Transactions* **2006**, 213-220.
85. Li, G. Y., *Angewandte Chemie, International Edition* **2001**, *40*, 1513-1516.
86. Fairlamb, I. J. S.; Grant, S.; Tommasi, S.; Lynam, J. M.; Bandini, M.; Dong, H.; Lin, Z.; Whitwood, A. C., *Advanced Synthesis and Catalysis* **2006**, *348*, 2515-2530.

87. Wolf, C.; Lerebours, R., *Journal of Organic Chemistry* **2003**, *68*, 7077-7084.
88. Bedford, R. B.; Hazelwood, S. L.; Limmert, M. E.; Brown, J. M.; Ramdeehul, S.; Cowley, A. R.; Coles, S. J.; Hursthouse, M. B., *Organometallics* **2003**, *22*, 1364-1371.
89. Bedford, R. B.; Hazelwood, S. L.; Horton, P. N.; Hursthouse, M. B., *Dalton Transactions* **2003**, 4164-4174.
90. Bedford, R. B.; Welch, S. L., *Chemical Communications* **2001**, 129-130.
91. Saednya, A.; Hart, H., *Synthesis* **1996**, 1455-1458.
92. Vinod, T. K.; Hart, H., *Journal of Organic Chemistry* **1990**, *55*, 5461-5466.
93. Rigaku/MSD *CrystalClear*, MSD, The Woodlands, Texas, USA, and Rigaku Corporation, Tokyo, Japan, 2006.
94. Jacobson, R. *REQAB*, 1.1; Molecular Structure Corporation, The Woodlands, Texas, USA, 1998.
95. Sheldrick, G. M., *Acta Crystallographica, Section A: Foundations of Crystallography* **2008**, *A64*, 112-122.

CHAPTER 4

HYDROFORMYLATION OF STYRENE USING PHOSPHINES WHICH INCLUDE A META-TERPHENYL MOIETY

4.1 Introduction

Phosphine ligands have been employed in catalysts for over 60 years dating back to the use of triphenylphosphine in the complex $\text{NiBr}_2(\text{PPh}_3)_2$, which led to a more efficient catalyst in Reep Chemistry than the commonly used NiBr_2 .¹ The petrochemical industry became interested in this discovery and started using triphenylphosphine in cobalt catalysts for the Shell process (hydroformylation), which required a higher temperature than phosphine-free processes, but the product contained more of the desired linear aldehyde than did phosphine-free processes.^{2, 3} The use of phosphine ligands in catalysts became widespread with applications in hydrocyanation using nickel catalysts containing arylphosphines.⁴⁻⁶ Hydrogenation reactions initially showed diminished reactivity upon addition of phosphine ligands to platinum and tin complexes.⁷ Wilkinson, however, pioneered rhodium catalyzed hydrogenation processes in the 1960's using $\text{RhCl}(\text{PPh}_3)_3$, which gave a much higher activity and renewed the interest in phosphine ligands in hydrogenation catalysts. Vaska furthered this research by studying rhodium and iridium phosphine complexes in hydrogenation. An extreme effect on rates and selectivities was first noted by Pruett using a phosphite instead of the common phosphine. This relatively rapid series of events initiated an era of ligand design, leading to another significant advance in which Chatt and Hieber developed the first bidentate phosphine ligand (dppe). Early studies employing bidentate phosphines seemed to stabilize complexes rather than allowing them to undergo the series of reactions involved in

catalytic cycles, and it became widely held that bidentate phosphines generally lead to slower reactions and less efficiency. A further complication arose when Sanger discovered that bidentate ligands can bridge bimetallic complexes instead of simply chelating a single metal center.⁸ Despite the perceived drawbacks, this era saw many patents on diphosphines. It was not until Kagen studied the hydrogenation of styrene at room temperature using a methodical range of diphosphines with various bridge lengths from one to six methylene units, that the effect of bite angle variation was considered. Kagen discovered that 1,3-bis(diphenylphosphino)propane (dppp) did not follow the trends of the previous diphosphines.^{9,10} This led to the conclusion that bidentate ligands do not necessarily lead to slower rates.¹¹

Even the simplest phosphines (monodentate phosphines) display a wide range of steric and electronic properties that have a decided impact on their complexes' catalytic performance. Chadwick Tolman carried out much of the groundbreaking work to quantify these effects, and summarized his findings in a 1977 *Chemical Reviews* article.⁶ The electron donating ability of phosphine ligands was determined by measuring the change in C–O stretch of Ni(CO)₃(phosphine). If the phosphine is a strong electron

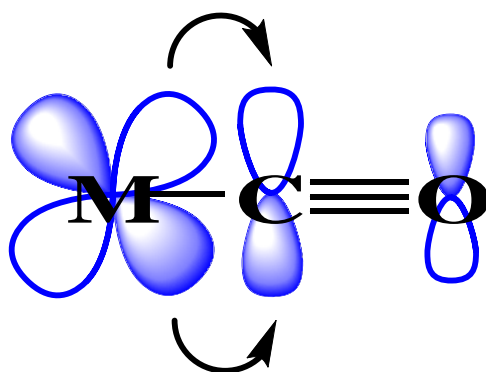


Figure 4.1 Dewar Chatt Duncanson model of pi back bonding of metal to a carbonyl ligand. used to measure electron donating ability of phosphines.

donor, the increased electron density on Ni facilitates more pi back bonding (**Figure 4.1**) to the carbonyl C–O antibonding orbital, thus weakening the carbonyl bond. Tolman also created a systematic classification of steric bulk in the form of the cone angle (Θ).

Tolman studied ligand effects in terms of the electronic parameter (ρ) and the cone angle (Θ). Other methods are available, however, this review has become the standard.^{12, 13} The cone angle is defined as the apex angle centered at 2.28 Å from the center of the P atom based on CPK (Corey Pauling Koltun) models. The cone angles observed in crystal structures of the same ligands have been determined to actually be smaller than the calculated cone angles due to intermeshing of the substituents.¹⁴ Methods for ranking steric and electronic properties of bidentate phosphines, as well as to further refine Tolman's early treatment, continued to be pursued. Other parameters that have been developed including the solid angle, pocket angle, repulsive energy and the accessible molecular surface (*vide infra*).

The solid angle (Ω) was defined to be the integral of the scalar product of the vector r , where r is the distance to the cone formed with a vector element of surface

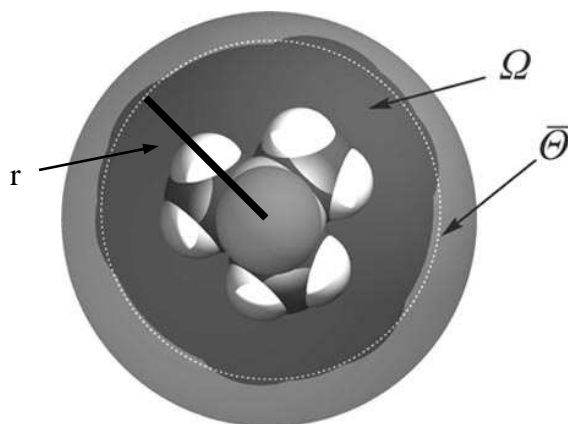


Figure 4.2 Difference between the solid angle (Ω) and cone angle (Θ) as seen by trimethylphosphine. Adapted from Niksch, T.; Goerls, H.; Weigand, W. *Eur. J. Inorg. Chem.*, 95-105.¹⁷

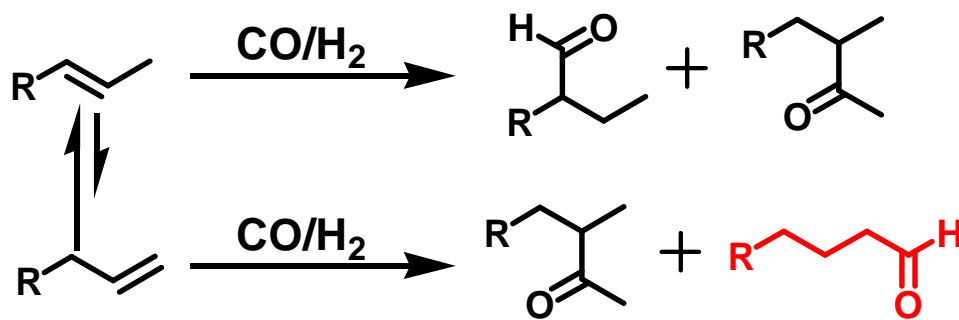
divided by the cube of the magnitude r .¹⁵⁻¹⁷ For simplicity the solid angle can be thought of as the sphere that forms when a shadow is cast upon the molecule which differs from the cone formed from a plane within the Tolman cone angle (Θ) (**Figure 4.2**).¹⁸ The pocket angle, developed by Barron, is based on the crystal structures of complexes and is defined as the space available for other substrates in the complex.¹⁹ The pocket angle can be simplistically viewed as 360° minus the cone angle, but using X-ray diffraction data rather than CPK models.

A more accurate method of determining steric bulk, termed the repulsive energy (E_R), was developed by Brown using molecular mechanics calculations.^{20,21} Good correlation between the cone angle and repulsive energy were noted. The accessible molecular surface (AMS) is a useful approach to describe the catalytic properties of complexes in that a pseudodynamic approach is used.²² This allows for the calculation of the relative penetration towards the metal center that a sphere of diameter 1.4 Å can attain upon coming within the van der Waals radii of ligand atoms. A similar treatment, known as the Connolly surface, has also been used in biochemistry to describe the active centers of enzymes.²³⁻²⁵

Transitions between different coordination modes are sometimes needed in catalytic processes. Therefore, a ligand with flexibility is desirable to allow for stabilization or destabilization of initial, transition or final states, which then accelerate the catalytic cycle. For example, the most common transition metal coordination modes (tetrahedral, trigonal bipyramidal, square planar, and octahedral) favor P–M–P angles of 109° , 120° and 90° respectively, so diphosphines favoring one or two of these angles can be utilized to drive desired reaction pathways and complex formation. In light of the

complex interplay of metal-dictated geometric preferences, requirements of the catalytic cycle, and steric / electronic ligand parameters, additional simplifying themes were sought for systematic experimental study of the influence of P–M–P angles on reactivity. Casey and Whiteker introduced the ligand preferred P–M–P angle (bite angle, β) by using a dummy metal atom to allow for the proper alignment of the phosphorus lone pair, keeping the M–P length constrained to 2.315 Å and the force constant of the P–M bond set to 0 kcal.²⁶⁻²⁸ Their treatment also introduced a convention for describing flexibility by reporting the range of angles accessible within 3 kcal/mol of strain from the natural bite angle.

All of the fundamental underpinnings related in this chapter thus far led to our research into hydroformylation. Hydroformylation was first discovered by Otto Roelen in 1938 when he observed the reaction of ethylene with hydrogen and carbon monoxide to yield propynal and diethyl ketone at higher pressures.²⁹ Hydroformylation later found industrial application employing cobalt catalysts that incorporated phosphine ligands. Although the activities of these catalysts were not high, the strong demand for hydroformylation products was evident. It was not until the 1970's that rhodium catalysts began taking over the market due to their improved catalytic activity and regioselectivity, and hydroformylation quickly became one of the pinnacle catalytic reactions, with wide scale industrial applications. A large portion of these rhodium catalysts were and still are based on rhodium triarylphosphine catalysts with the intent of forming linear aldehydes. Linear aldehydes are desired due to their preferred properties and commercialized application. A large portion of these aldehydes are commonly hydrogenated to alcohols or oxidized to carboxylic acids for further treatment. The esterification of these alcohols



Scheme 4.1 General scheme for hydroformylation wherein the desired linear aldehyde is shown in red.

with phthalic anhydride produces dialkyl phthalate which is a common plasticizer used for polyvinyl chloride plastics.¹⁴

Hydroformylation is the most important homogeneously catalyzed process in industry in terms of product volume. The production of *n*-butyraldehyde from the hydroformylation of propene is an important starting material for 2-ethylhexanol, an important plasticizer, although other plasticizers are in high demands due to environmental concerns. The production of linear aldehydes by the selective hydroformylation of internal olefins is of great interest due to the lost cost of mixtures of internal and terminal olefin feedstocks. The challenge with this effort is the initial isomerization required to convert the internal olefins to terminal olefins prior to the hydroformylation (**Scheme 4.1**).

Currently a limited number of catalysts are capable of performing this isomerization. Phosphites have advantages over phosphines in that the phosphorus electron density is shared with the oxygen to allow a more electron deficient metal. Some examples of particularly successful phosphites have appeared in the patent literature. Some sterically hindered phosphites, which are sometimes used for hydroformylation

reactions, can react with the aldehyde produced in hydroformylation at higher temperature and pressures to produce unwanted side products and the termination of activity of the catalyst. The use of phosphines would be preferred due to the reactivity towards ligand decomposition phosphates and have seen (**Scheme 3.4**). There are not many phosphines used currently with the ability to efficiently convert internal olefins to linear aldehydes, although van Leeuwen's group has made important advances in this area.^{30,31}

Although hydroformylation started out as primarily a cobalt catalyzed reaction, the evolution of high-activity rhodium-centered catalysts has developed to such an extent as to compensate for the large increase in cost of rhodium in some applications. NAPHOS (**Figure 4.3**), a common ligand used in hydroformylation, has been studied by Beller for the conversion of internal olefins to linear aldehydes using 2-pentene using both cobalt and rhodium. The cobalt metal center gave a much lower selectivity towards linear aldehydes than that of rhodium with a lower activity as well.³² Selectivity for the

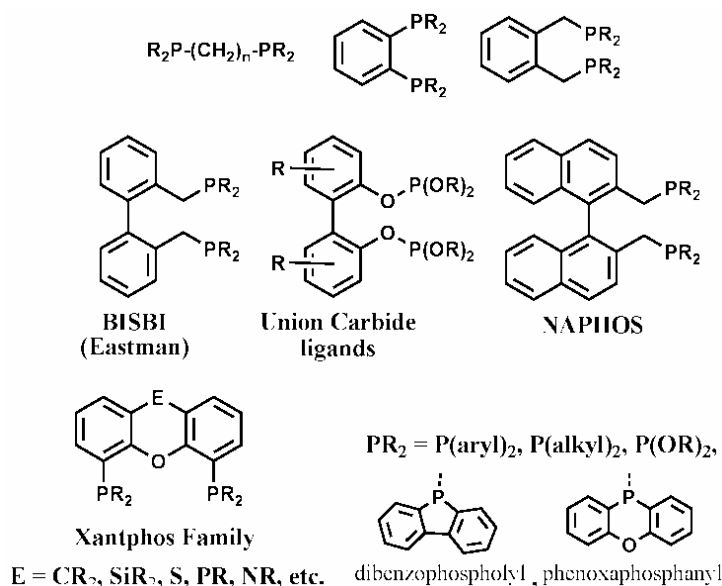


Figure 4.3 Some bidentate P-donor ligands for Rh-catalyzed hydroformylation.

linear aldehyde with rhodium was observed at 89:11 at 10 bar CO/H₂ pressure and 100°C. The yield of 2-pentene was lower at higher pressures, which was attributed to the faster isomerization of 2-pentene at lower pressures.

Beller carried out important studies into the electronic effect of the aryl groups on phosphines with a common backbone to further rationalize previous studies that had revealed higher activity and linear: branched ratios upon reaction of terminal olefins when electron deficient substituents are present on the phosphines.^{26,33} Beller's work traced the origin of these empirical observations to the increase in diequatorial complexes compared to the unfavorable equatorial axial complexes (**Figure 4.4**).³⁴ The most active catalyst at that time contained a 3,5-bis(trifluoromethyl)phenyl substituent with a TOF

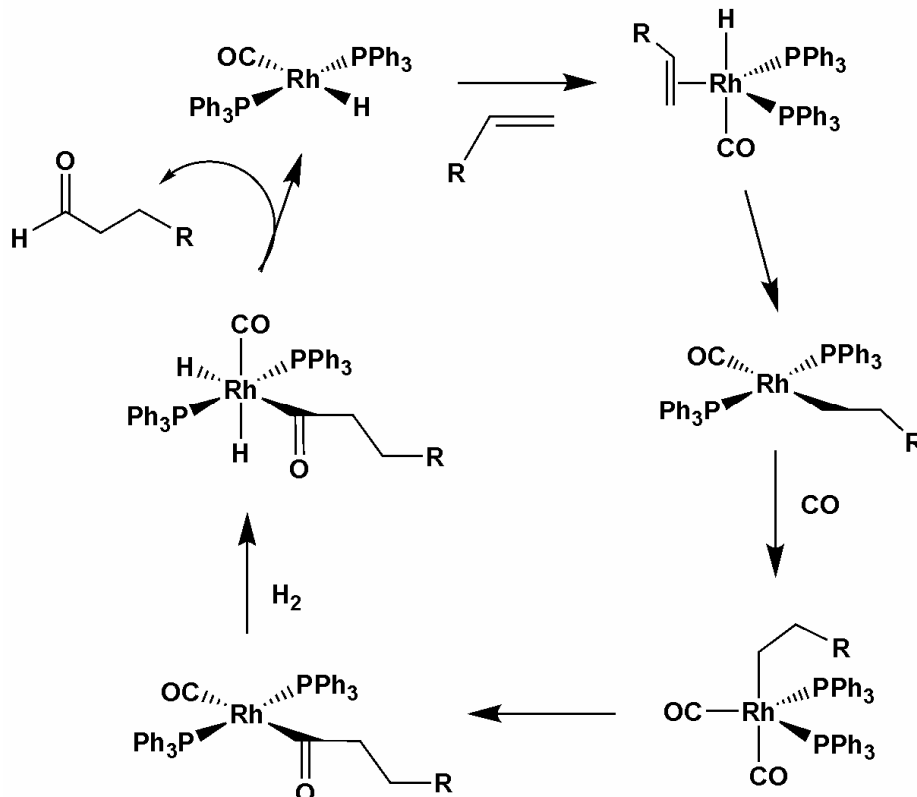


Figure 4.4 The generally accepted mechanism for the hydroformylation reaction of an olefin.

(turnover frequency) of 325 h^{-1} . The 3,5-difluorophenyl substituent also gave the highest selectivity for linear aldehydes with a 95:5 ratio. Another important insight gained from this study was that the rate of isomerization of 2-pentene was similar in rate if not faster than the hydroformylation step due to similar activities of both 1- and 2-pentene.

The ability for two isomers to form in the trigonal bipyramidal has been utilized in chemistry for many different applications. Brown observed the preference for one isomer over the other when synthesizing a rhodium hydride that contained triphenylphosphine.³⁵ This was attributed to the steric bulk the triphenylphosphine provided allowing the phosphines to favor diequatorial (ee) over the equatorial-axial (ea) with an isomer ratio of 85:15. The ability to utilize this preference has been seen in reaction including hydroformylation. The ability to quickly test for which isomer is forming was solved by the use of high pressure IR by van Leeuwen in which the absorptions at 2015 cm^{-1} and 2075 cm^{-1} were from the ee isomers and the 1990 cm^{-1} and 2030 cm^{-1} absorptions were from the ea isomers.³⁶ Since this initial discovery other methods to determine the isomer have been developed.¹⁴ Other factors besides sterics were also determined to influence the ability to form ee isomers selectively and therefore influence the hydroformylation reaction and favor linear aldehydes including the bite angle.^{28,37-39} The preference for a wide bite angle diphosphine has been determined as a large factor in increasing the selectivity towards linear aldehydes from the increases ee isomer. The relationship between ligand, complex structure and selectivity of the hydroformylation reaction is not always straightforward but the bisequatorial geometry gives higher linear branched ratios in most cases.

4.2 Results and Discussion

The ability of wide bite angle diphosphine complexes to support processes favoring linear aldehydes in the hydroformylation reaction was the inspiration for the utility of terphspan ligands (Chapters 2 and 3) in this process.^{40,41} Previous metal complexes with a *m*-terphenyl scaffold have primarily shown a *trans*-spanning square planar geometry with the two flanking aryl rings on the terphenyl allowing a bite angle of about 180°. The ability for the *m*-terphenyl scaffold to accommodate the trigonal bipyramidal (TBP) geometry required in the course of the catalytic cycle (**Figure 4.5**) was an aspect of interest that had not been demonstrated from terphspan ligands at the time we began this study. The regioselectivity of hydroformylation derives in large part from the ligand's ability to accommodate the *trans*-4-coordinate and diequatorial trigonal bipyramidal 5-coordinate binding.

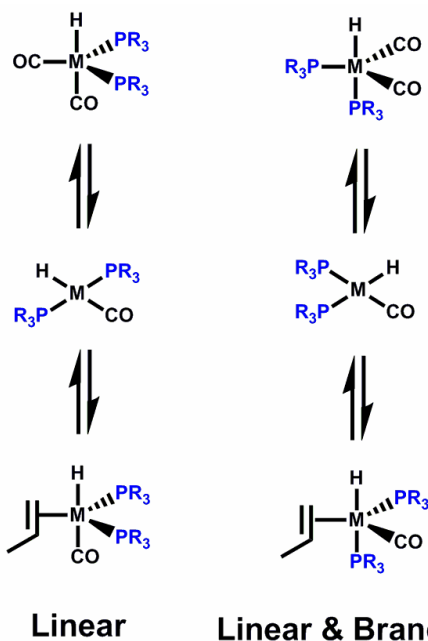


Figure 4.5 A proposed mechanism for the explanation of the preference for the linear aldehydes with the use of larger bite angles (120° and 180°) compared to (90°).

Having demonstrated the *trans*-spanning mode of a terphspan diphosphine in a square planar Rh complex (**Figure 2.3**),⁴⁰ we attempted to prepare a five coordinate Rh complex with the same ligand. Unfortunately, this effort was unsuccessful in a large number of trials, so other five-coordinate metal complexes were pursued. Satisfyingly, an iridium complex that had a coordination number of five was successful, and the coordination mode was demonstrated by single crystal X-ray diffraction of [IrCl(COD)(L1)] (COD = 1,5-cyclooctadiene. In this structure, the terphspan diphosphine L1 showed a P-Ir-P angle (bite angle) of 104.66° (**Figure 4.6**) and refinement details are listed in **Table 4.1**. The bite angle is somewhat smaller than the ideal angle of 120° for equatorial-equatorial binding. In the pseudo-trigonal bipyramidal structure, however, the two axial ligands are those with the largest L-Ir-L angle. Those are the Cl(1) and the center of the C-C bond of COD carbons C(52)-C(45) which have an angle of 168° and are in the axial positions while the P(1), P(2) and C-C bond between C(49) and C(48) are equatorial with X-M-X angles from 105° to 123°.

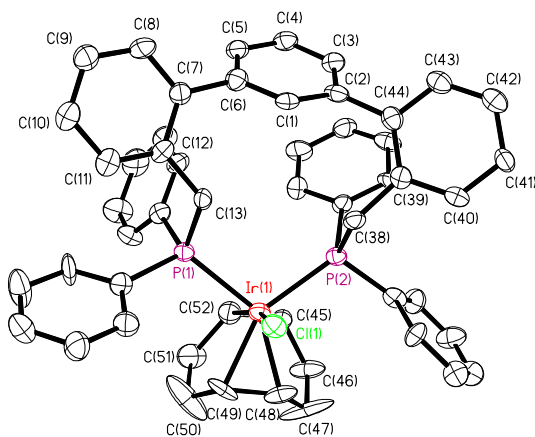
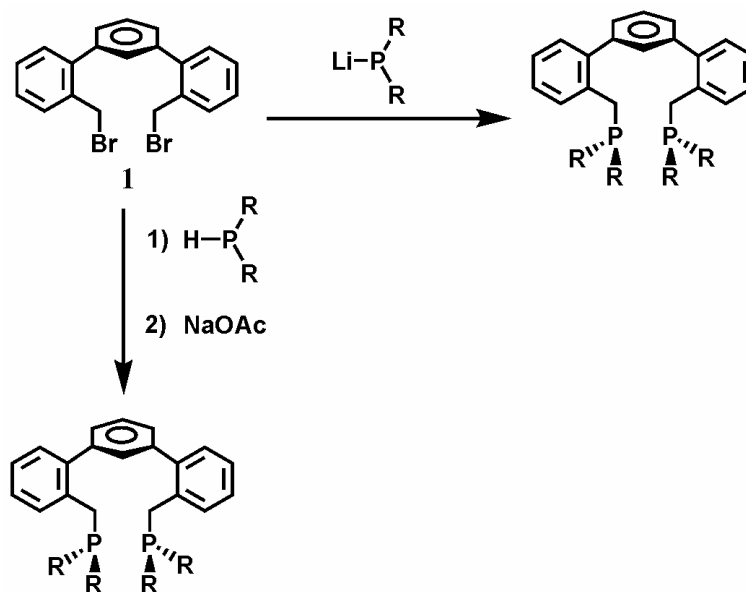


Figure 4.6 ORTEP drawing (50% probability ellipsoids) of the molecular structure of [IrCl(COD)(L1)]. Hydrogen atoms are omitted for clarity.

Table 4.1 Refinement details for IrCl(COD)(L1)].

Empirical formula	C ₅₂ H ₄₈ ClIrP ₂
Formula weight (g/mol)	962.49
Temperature (K)	153 (2)
Wavelength (Å)	0.71073
Crystal system	Triclinic
Space group	<i>P</i> $\bar{1}$ (#2)
Unit cell dimensions	
<i>a</i> (Å)	10.269(2)
<i>b</i> (Å)	11.786(2)
<i>c</i> (Å)	18.511(4)
<i>α</i> (deg)	97.54(3)
<i>β</i> (deg)	102.65(3)
<i>γ</i> (deg)	102.80(3)
Volume (Å ³)	2093.3(7)
<i>Z</i>	2
Calculated density (Mg/m ³)	1.527
Absorption coefficient (mm ⁻¹)	3.366
<i>F</i> (000)	968
Crystal size (mm)	0.26 × 0.19 × 0.04
Crystal color and shape	yellow plate
θ range for data collection (deg)	3.18 – 25.05
Limiting indices	-12 < <i>h</i> < 12 -14 < <i>k</i> < 14 -22 < <i>l</i> < 16
Reflections collected	14888
Independent reflections	7319
Completeness to θ	25.05 (98.7 %)
Max. transmission	0.8771
Min. transmission	0.4749
Refinement method	Full-matrix least-squares on <i>F</i> ²
Data / restraints / parameters	7319/0/501
Extinction coefficient	0.0015(6)
Goodness of fit on <i>F</i> ²	1.122
Final R indices (<i>I</i> > 2σ(<i>I</i>))	
R1	0.0631
wR2	0.1555
R indices (all data)	
R1	0.0791
wR2	0.1721



Scheme 4.2 Synthetic route using **1** to prepare phosphines (R = Ph (**L1**), ^tHx (**L2**), ^tBu (**L3**), ^oTol (**L4**), ^pTol (**L5**), ⁿPn (**L6**)).

Because the dependence of catalytic reactions on electronic and steric parameters has been well documented, we appended the general Terphspan scaffold with several R₂P moieties for testing in hydroformylation. Synthesis of this set of phosphines proceeded readily from *m*-terphenyl scaffold intermediate **1** (**Scheme 4.2**). The reaction of the bis(2,2'-bromomethyl)-*m*-terphenyl (**1**) with lithium diarylphosphides (freshly prepared from the respective diarylchlorophosphine) can be cleanly converted to **L1**, **L4** and **L5**. An alternative route for the conversion of **1** to diphosphines is through reaction with HPR₂, to form the phosphonium salts, followed by deprotonation with a mild base such as sodium acetate. This route was used to prepare **L2**, **L3**, **L5** and **L6**.

Phosphorus-31 NMR spectroscopy is a convenient tool for initial assessment of phosphine electronics. The similarities in ³¹P NMR shifts for **L4** and **L5** suggests that whether the methyl groups are *ortho*- or *para*- to the P center, there is very little electronic influence, though significant steric differences are obvious. These two ligands

thus provide an excellent opportunity for comparing two electronically similar but sterically different ligands based on the same scaffold. The similarities in **L2** and **L6** are also of interest; they are electronically similar to one another, sterically different from one another, and both are electronically much more donating than the tolyl-containing diphosphines.

The conformational flexibility of the scaffold is exemplified by the single crystal X-ray structure of free ligand **L4** (**Figure 4.7**), in which the two phosphine arms are anti to one another across the central aryl ring of the *m*-terphenyl unit. The crystals were obtained by the slow diffusion of pentane into a concentrated dichlororomethane solution of **L4** and the refinement details are listed in **Table 4.2**. The ability for **L4** to situate the two aryl flanking rings in an anti mode was attributed to alleviation of the extra steric strain that would be present in the syn mode.

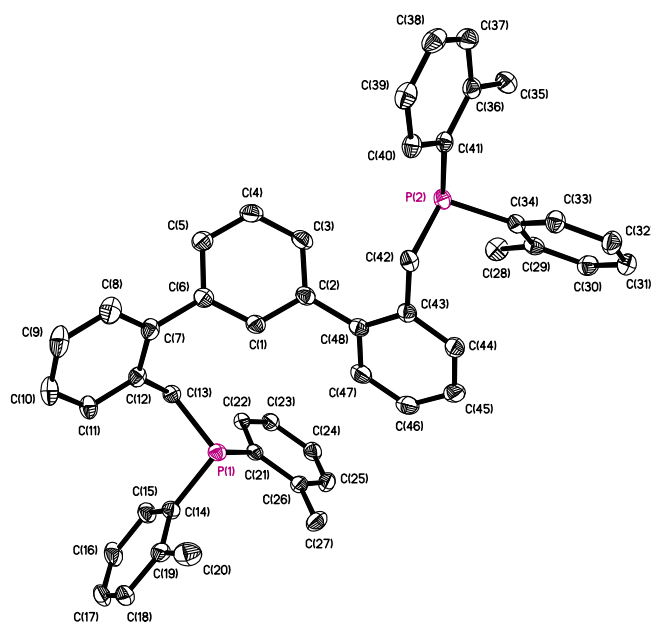


Figure 4.7 ORTEP drawing (50% probability ellipsoids) of the molecular structure of **L4**. Hydrogen atoms are omitted for clarity.

The ability of **L1** – **L6** to support Rh-catalyzed hydroformylation of styrene was the first reaction probed. The conditions used were selected to mimic those of Clark et. al. to attain a direct correlation with their results.⁴² This would give a starting point to be

Table 4.2 Refinement details for **L4**.

Empirical formula	C ₄₈ H ₄₄ P ₂
Formula weight (g/mol)	682.77
Temperature (K)	153 (2)
Wavelength (Å)	0.71073
Crystal system	Triclinic
Space group	<i>P</i> $\bar{1}$ (#2)
Unit cell dimensions	
<i>a</i> (Å)	11.537(2)
<i>b</i> (Å)	12.018(2)
<i>c</i> (Å)	15.863(3)
<i>α</i> (deg)	91.85(3)
<i>β</i> (deg)	106.32(3)
<i>γ</i> (deg)	115.16(3)
Volume (Å ³)	1881.0(7)
<i>Z</i>	2
Calculated density (Mg/m ³)	1.205
Absorption coefficient (mm ⁻¹)	0.149
<i>F</i> (000)	724
Crystal size (mm)	0.36 × 0.36 × 0.36
Crystal color and shape	colorless chip
θ range for data collection (deg)	2.72 – 25.10
Limiting indices	-13 < <i>h</i> < 11 -12 < <i>k</i> < 14 -18 < <i>l</i> < 18
Reflections collected	14183
Independent reflections	6600
Completeness to θ	25.10 (98.7 %)
Max. transmission	0.9484
Min. transmission	0.9484
Refinement method	Full-matrix least-squares on <i>F</i> ²
Data / restraints / parameters	6600/0/455
Goodness of fit on <i>F</i> ²	1.065
Final R indices (<i>I</i> > 2σ(<i>I</i>))	
R1	0.0508
wR2	0.1286
R indices (all data)	
R1	0.0632
wR2	0.1431

able to quickly evaluate the ability for **L1-L6** to catalyze styrene and the regioselectivity these ligands exert. Xantphos, a commercially available phosphine typically revered as a superior wide bite angle phosphine capable of giving high linear to branched aldehyde ratios and of the benchmark triphenylphosphine were also tested under these conditions for comparison. Up to 36.4% conversion was obtained using the ligand **L6**; however, the linear: branched ratio was relatively low. Use of **L1** led to a 1.64 l:b ratio, higher than that of Xantphos (1.32), but a 23.65 % lower conversion. These initial results give hope that optimized systems using the *m*-terphenyl scaffold could be on par with commercially available ligands for the conversion of olefins to linear aldehydes.

Table 4.5. Catalytic results for the hydroformylation of styrene using terphspan ligands All reactions were performed at 80 °C using 1:1 CO:H₂ with L : Rh = 1.2 (1.0 M in toluene with respect to Rh) total substrate : Rh = 5000 l:b is the linear to branched ratio

- L : Rh = 2.4 due to this being a monophosphine

Ligand	Time (h)	Pressure (psi)	Conversion (%)	l:b ratio
L1 (R = Ph)	3	200	6.95	1.64
L1 (R = Ph)	12	300	26.6	1.43
L1 (R = Ph)	12	200	26.8	1.18
L1 (R = Ph)	12	100	0.75	1.56
L4 (R= ^o Tol)	12	200	9.03	1.52
L6 (R = ^c Pn)	12	200	36.4	0.74
L3 (R= ^t Bu)	12	200	20.3	1.63
Xantphos	12	200	30.6	1.32
PPh ₃ *	12	200	27.3	0.96

The ability for the *m*-terphenyl scaffolded diphosphines to act as a good catalysts for the conversion of styrene to the linear aldehyde also has a dependence on the pressure in which the system is set to. When pressurized to only 100 psi the activity of the catalyst (**L1**) suffers with a less than 1% conversion however the selectivity for the linear aldehyde is not sacrificed with a l:b ratio of 1.56. The increase in pressure allows the

activity of the catalyst to increase with an increase in selectivity for the linear aldehyde when increasing from 200 psi to 300 psi with **L1**. The data also suggests that the *m*-terphenyl catalyst series shows a preference for more steric hindrance around the phosphine to achieve a higher selectivity towards linear aldehydes as seen by the increase from a l:b ratio of 1.18 for **L1** to 1.52 for **L4** which contains an additional methyl substituent on the phenyl rings. The preference for electron donation to the metal center from the phosphines shows an increase in activity as seen by the large improvement in activity of ^cPn (**L5**) to 36.4 % conversion.

These initial studies show the utility and flexibility of the *m*-terphenyl scaffold as a design for ligands in catalysis. The synthetic ease in which different functionalization can be designed makes the *m*-terphenyl scaffold an ideal candidate for catalytic applications as well as the ability for *m*-terphenyl catalysts to perform at comparable activities and selectivity's to that of Xantphos. This preliminary study serves as a great proof of principle step towards designing more sophisticated catalysts that can serve the growing needs of the current market.

4.3 Conclusions

The use of a versatile ligand that has the ability to preferentially form linear aldehydes is currently in large demand. These ligands must be flexible and accommodate a diequatorial geometry within a trigonal bipyramidal geometry as well as the *trans*-square planar. The *m*-terphenyl scaffold has been shown to have flexibility and was isolated in both of the geometries required for increase selectivity. The X-ray structure of [IrCl(COD)(**L1**)] has a P-Ir-P bite angle of 104.6° while [RhCl(CO)(**L1**)] (Chapter 2) shows the ability for the *trans*-square planar geometry. The catalytic ability of the ligands explored was comparable to the commercial Xantphos ligand. The continued improvement of this system would be expected as electronic and steric influences are optimized.

4.4 Experimental Details

All syntheses were carried out in an inert atmosphere of nitrogen using an MBraun dry or with standard Schlenk techniques. The materials used in the synthetic schemes **1**,^{43,44} **L1**,⁴⁵ **L2**,⁴⁶ **L3**⁴⁶ and Rh(CO)₂(dpm) (dpm = dipivaloylmethanoate)⁴⁷ were all prepared as reported previously. All phosphine reagents were used as received from Strem and the solvents were all purified by passage through alumina columns under a N₂ atmosphere employing an MBraun solvent purification system. Styrene was passed through activated alumina immediately before use to remove the stabilizer. All other reagents were used as received from TCI and Alfa Aesar. ³¹P, ¹H and ¹³C NMR spectra were collected using a Bruker Avance 300 instrument operating at 121.4, 300 and 75.4 MHz, respectively. A Parr micro pressure reactor model 4591 equipped with a model 4843 temperature controller was utilized for hydroformylation studies. Syngas was purchased from National Welders and was certified to be a 50/50 ratio of H₂/CO within 0.1% error.

Preparation of L4

To a solution of 0.600 g (2.40 mmol) of di-*o*-tolylchlorophosphine in 15 mL of tetrahydrofuran 0.040 g (5.80 mmol) of freshly cut lithium was added and allowed to stir overnight. The red solution was then decanted and cooled in a dry ice acetone bath to -78 °C. To this solution 0.489 g (1.17 mmol) 2,2'-bis(bromomethyl)-*m*-terphenyl (DotpH-Br) in 10 mL of tetrahydrofuran was added slowly over 30 minutes. The solution was then allowed to slowly warm to room temperature and then stirred overnight. The solution was then concentrated in vacuo and washed with 20 mL of degassed water to afford the thick oil as the crude product. Purification was achieved by washing the crude

product with acetonitrile then isolating 0.608 g (76.2 % yield) of the insoluble substance as a fine white powder. X-ray quality crystals were achieved by the slow diffusion of pentane into a saturated solution of **L4** in CH₂Cl₂. ¹H NMR (300 MHz, CDCl₃): δ 2.08 (s, 12H), 3.37 (s, 4H), 6.95-7.28 (m, 28H, overlapping with CDCl₃). ³¹P NMR (121.4 MHz, CDCl₃): δ -30.7. ¹³C NMR (75.4 MHz, CDCl₃): δ 20.8, 21.1, 32.0, 32.2, 125.7, 125.8, 126.0, 126.9, 127.6, 127.8, 127.9, 128.4, 129.7, 129.8, 130.3, 130.4, 131.4, 134.6, 134.7, 136.7, 136.9, 141.0, 142.2, 142.3, 142.5, 142.8.

Preparation of [IrCl(COD)(L1)]

To 0.021 g (0.031 mmol) of chloro(1,5-cyclooctadiene)iridium(I) dimer a solution of 0.037 g (0.060 mmol) **L1** in 10mL of toluene was added dropwise with rapid stirring. The solution was then allowed to stir overnight at room temperature followed by the removal of the volatile organics in vacuo. The resulting oil was then washed with pentane to give 0.031 g (54.9% yield) of a yellowish orange solid. X-ray quality crystals were obtained by the slow evaporation of a solution of [IrCl(COD)(**L1**)] in CH₂Cl₂. ¹H NMR (300 MHz, CDCl₃): δ 1.28-1.60 (m, 8H, overlapping with residual H₂O), 3.09 (bs, 2H), 4.59 (bs, 2H), 6.74-6.81 (m, 3H), 7.01 (t, 2H), 7.17-7.38 (m, 9H overlapping with CDCl₃). ³¹P NMR (121.4 MHz, CDCl₃): δ 30.2.

Preparation of L5

To a solution of 1.00 g (2.40 mmol) of DotpH-Br in 15 mL of acetone 0.951 g (5.60 mmol) of dicyclopentylphosphine was added and then refluxed overnight. The solution was then dried in vacuo and then dissolved in 15 mL of tetrahydrofuran followed by the addition of 2.00 g (24.4 mmol) of sodium acetate. The resulting solution was then stirred overnight followed by filtration. The filtrate was then concentrated in vacuo to

afford the crude product. Purification was afforded by washing the crude product with acetonitrile to give 1.43 g (63.8 % yield) of an isolated pure oil. ^1H NMR (300 MHz, CDCl_3): δ 1.21-1.71 (m, 32H, overlapping with residual H_2O), 2.93 (s, 4H), 7.23-7.35 (m, 9H overlapping with CDCl_3) 7.45-7.54 (m, 3H) ppm. ^{31}P NMR (121.4 MHz, CDCl_3): δ 4.9.

General conditions for catalysis

5.01 g of styrene was purified through a small column of activated alumina and then placed in the Parr reactor. To this 2.0 mL of a pre-made solution of 5.0×10^{-6} M $\text{Rh}(\text{dpm})(\text{CO})_2$ solution with 1.2:1.0 ratio of Rh to ligand (**L1**, **L2**, etc...) in toluene was then added. The reactor was then pressurized with 1:1 H_2/CO and then heated to the desired temperature and stirred for the corresponding time. A small amount of this was then analyzed using ^1H NMR at different time intervals to monitor the reaction. The dwell time of the NMR was set to be on a 5 second delay to ensure full relaxation of the Fourier transform.

X-ray crystallography

Intensity data were collected using a Rigaku Mercury CCD detector and an AFC8S diffractometer. Data reduction and absorbance corrections were achieved using CrystalClear.⁴⁸ The structure was solved by direct methods and subsequent Fourier difference techniques, and refined anisotropically, by full-matrix least squares, on F^2 using SHELXTL 6.10.⁴⁹ The structure of $[\text{IrCl}(\text{COD})(\text{L1})]$ exhibits disorder within the COD however partial occupancies were not used.

4.5 Selected Spectra

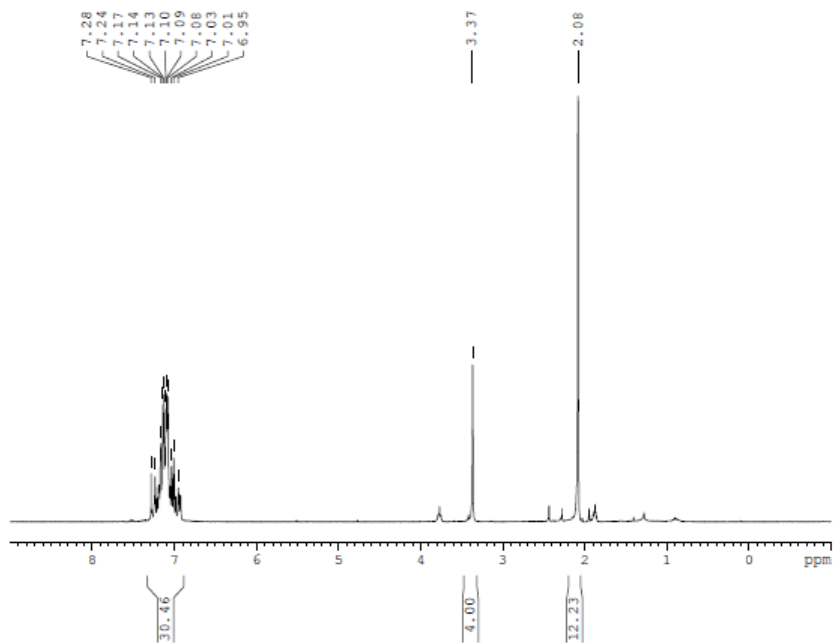


Figure 4.7 Proton NMR spectrum of **L4** (CDCl₃, 300 MHz) referenced to residual CHCl₃.

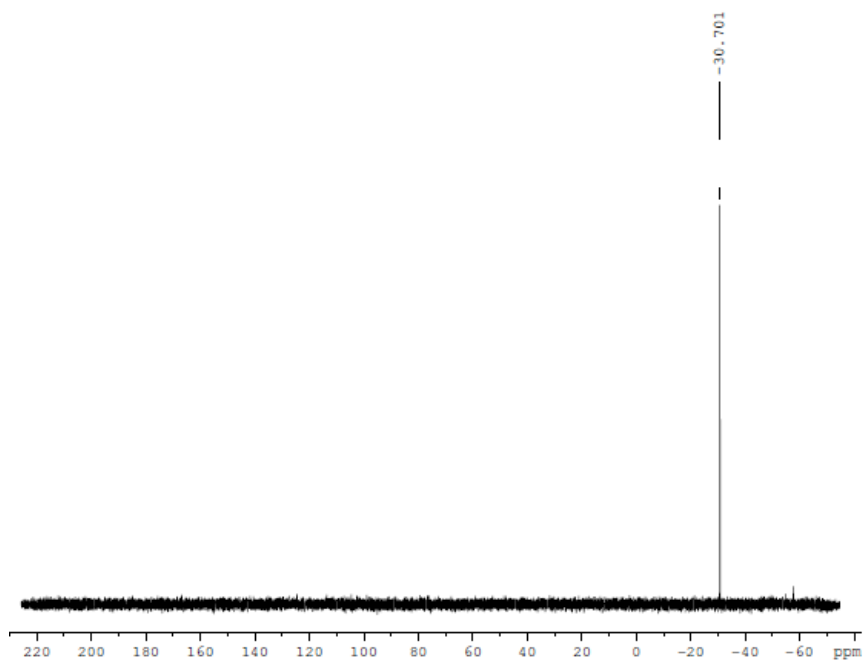


Figure 4.8 Phosphorus-31 NMR spectrum of **L4** (CDCl₃, 121 MHz).

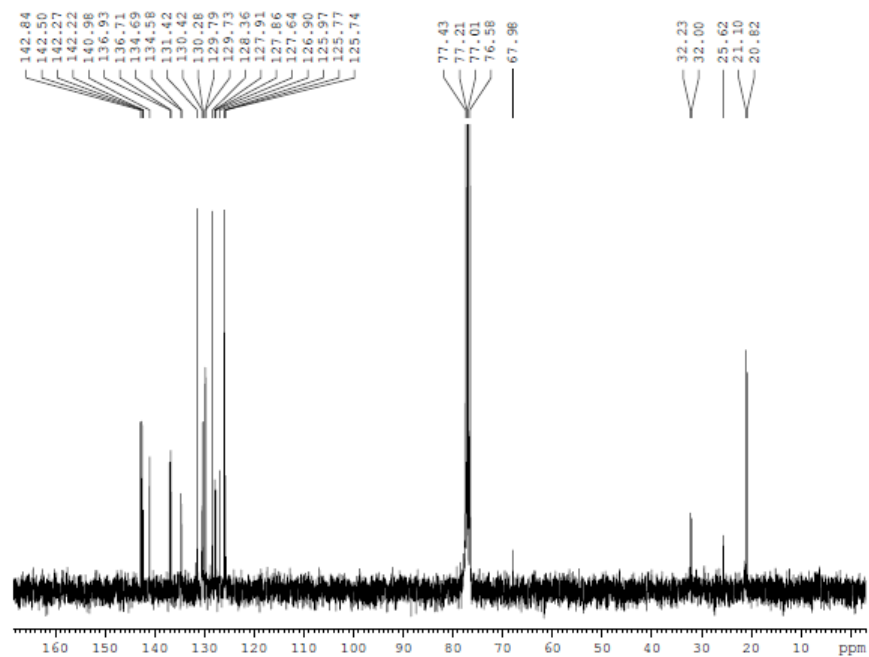


Figure 4.9 Carbon-13 NMR spectrum of **L4** (CDCl_3 , 75 MHz). Referenced to CDCl_3 .

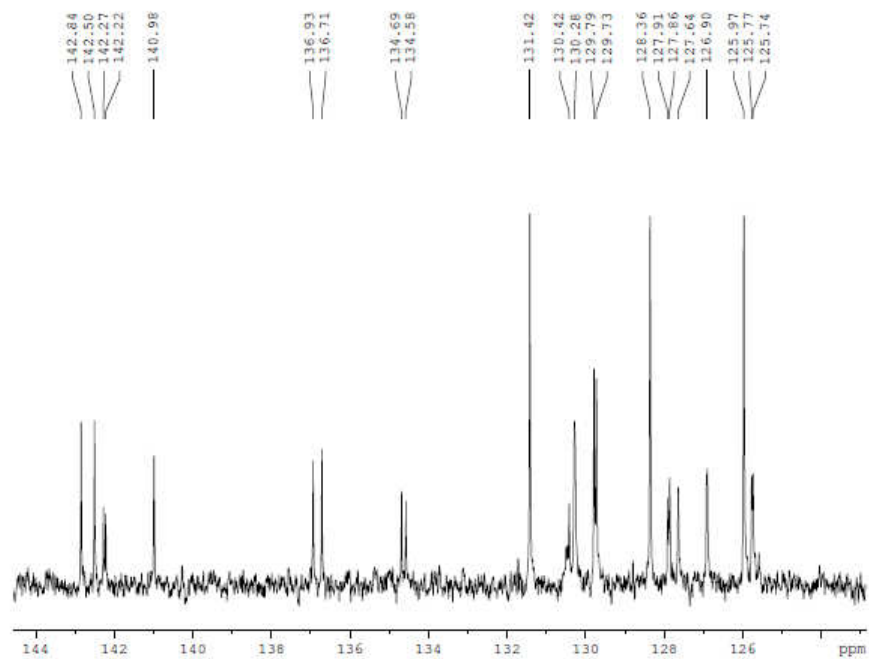


Figure 4.10 Aromatic region, carbon-13 NMR spectrum of **L4** (CDCl_3 , 75 MHz).

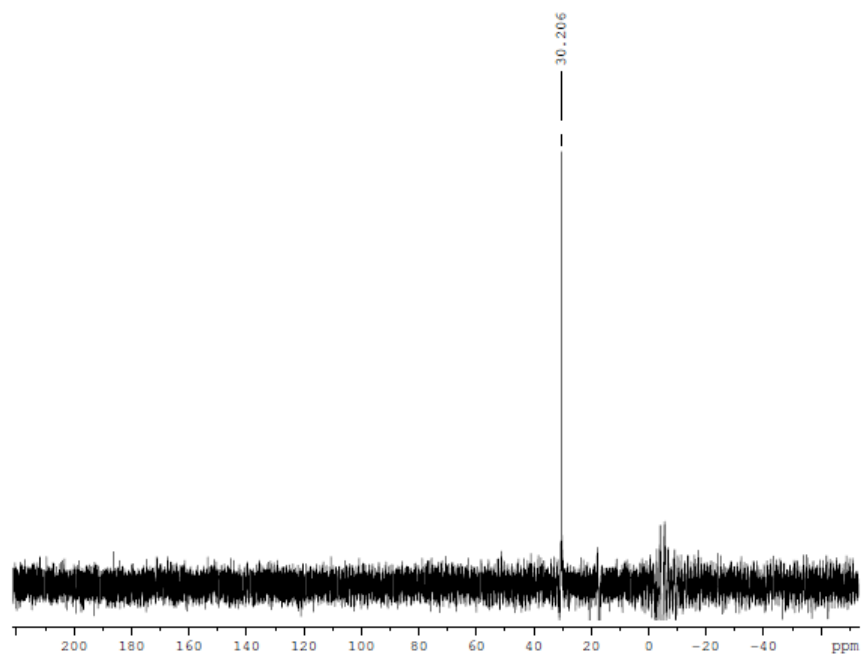


Figure 4.11 Phosphorus-31 NMR spectrum of $[\text{IrCl}(\text{COD})(\text{L1})]$ (CDCl_3 , 121 MHz).

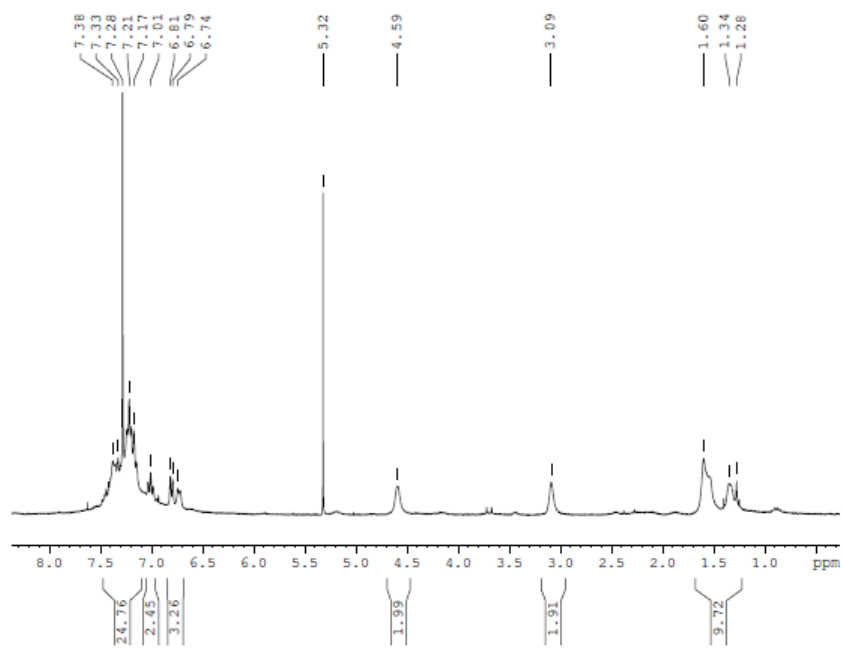


Figure 4.12 Proton NMR spectrum of $[\text{IrCl}(\text{COD})(\text{L1})]$ (CDCl_3 , 300 MHz) referenced to residual CHCl_3 .

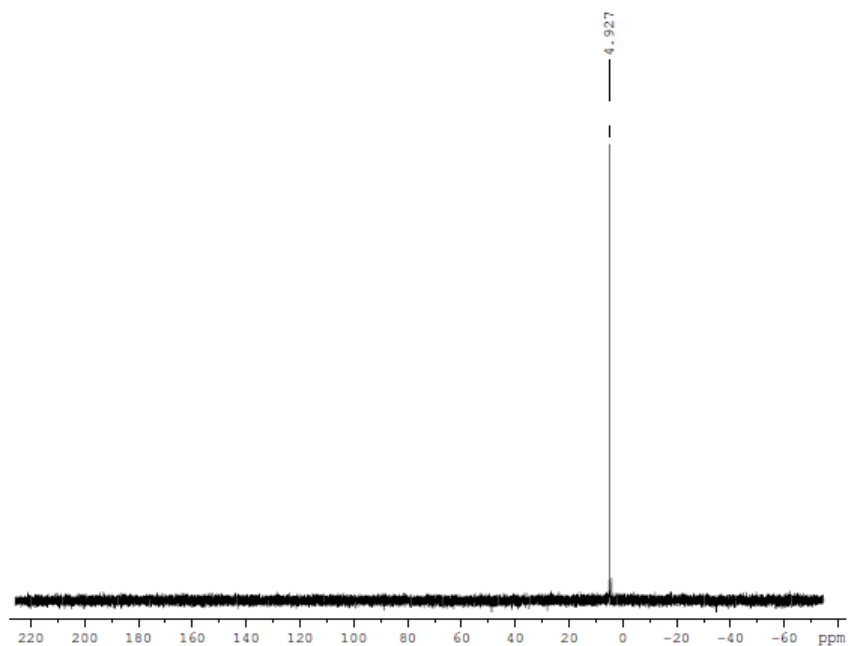


Figure 4.13 Phosphorus-31 NMR spectrum of **L5** (CDCl₃, 121 MHz).

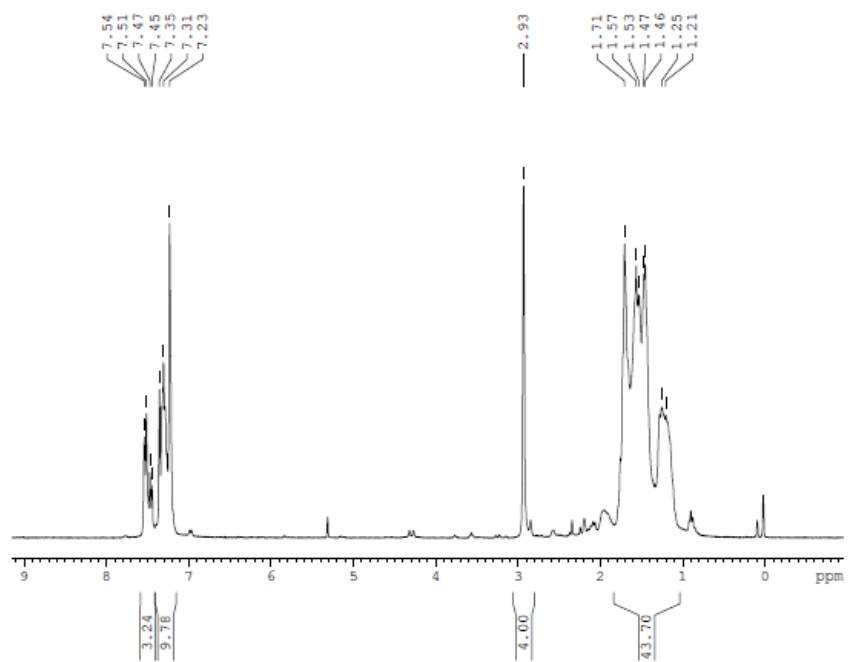


Figure 4.14 Proton NMR spectrum of **L5** (CDCl₃, 300 MHz) referenced to residual CHCl₃.

4.6 References

1. Reppe, W.; Sweckendiek, W. J., *Justus Liebigs Annalen der Chemie* **1948**, 560, 104-116.
2. Slauch, L. H.; Mullineaux, R. D., *Journal of Organometallic Chemistry* **1968**, 13, 469-477.
3. Slauch, L. H.; Mullineaux, R. D. *Hydroformylation of olefins*. 3239569, 19660308, 1966.
4. Brown, E. S., *Aspects of Homogeneous Catalysis* **1974**, 2, 57-78.
5. Drinkard, W. C., Jr. *Catalytic hydrocyanation of olefins*. 3655723, 19720411, 1972.
6. Tolman, C. A., *Chemical Reviews* **1977**, 77, 313-348.
7. Cramer, R. D.; Jenner, E. L.; Lindsey, R. V., Jr.; Stolberg, U. G., *Journal of the American Chemical Society* **1963**, 85, 1691-1692.
8. Sanger, A. R., *Journal of the Chemical Society, Chemical Communications* **1975**, 893-894.
9. Adams, D. M.; Brus, L.; Chidsey, C. E. D.; Creager, S.; Creutz, C.; Kagan, C. R.; Kamat, P. V.; Lieberman, M.; Lindsay, S.; Marcus, R. A.; Metzger, R. M.; Michel-Beyerle, M. E.; Miller, J. R.; Newton, M. D.; Rolison, D. R.; Sankey, O.; Schanze, K. S.; Yardley, J.; Zhu, X., *Journal of Physical Chemistry B* **2003**, 107, 6668-6697.
10. Knowles, W. S.; Sabacky, M. J.; Vineyard, B. D.; Weinkauff, D. J., *Journal of the American Chemical Society* **1975**, 97, 2567-2568.
11. Kawabata, Y.; Hayashi, T.; Ogata, I., *Journal of the Chemical Society, Chemical Communications* **1979**, 462-463.

12. Fernandez, A.; Reyes, C.; Wilson, M. R.; Woska, D. C.; Prock, A.; Giering, W. P., *Organometallics* **1997**, *16*, 342-348.
13. Dierkes, P.; Ramdeehul, S.; Barloy, L.; De Cian, A.; Fischer, J.; Kamer, P. C. J.; Van Leeuwen, P. W. N. M.; Osborn, J. A., *Angewandte Chemie, International Edition* **1998**, *37*, 3116-3118.
14. *Rhodium catalyzed hydroformylation*. Kluwer Academic Publishers: Dordrecht, Netherlands; Boston, 2000 p. 135.
15. Hirota, M.; Sakakibara, K.; Komatsuzaki, T.; Akai, I., *Computers and Chemistry* **1991**, *15*, 241-248.
16. Tour, J. M.; Jones, L., II; Pearson, D. L.; Lamba, J. J. S.; Burgin, T. P.; Whitesides, G. M.; Allara, D. L.; Parikh, A. N.; Atre, S., *Journal of the American Chemical Society* **1995**, *117*, 9529-9534.
17. Lee, T. R.; Carey, R. I.; Biebuyck, H. A.; Whitesides, G. M., *Langmuir* **1994**, *10*, 741-749.
18. Niksch, T.; Goerls, H.; Weigand, W., *European Journal of Inorganic Chemistry* **2010** 95-105.
19. Koide, Y.; Bott, S. G.; Barron, A. R., *Organometallics* **1996**, *15*, 2213-2226.
20. Brown, T. L., *Inorganic Chemistry* **1992**, *31*, 1286-1294.
21. Cha, J. S.; Brown, H. C., *Journal of Organic Chemistry* **1993**, *58*, 4727-4731.
22. Angermund, K.; Baumann, W.; Dinjus, E.; Fornika, R.; Goerls, H.; Kessler, M.; Krueger, C.; Leitner, W.; Lutz, F., *Chemistry--A European Journal* **1997**, *3*, 755-764.
23. Richards, F. M., *Annual Review of Biophysics and Bioengineering* **1977**, *6*, 151-176.

24. Connolly, M. L., *Journal of Applied Crystallography* **1983**, *16*, 548-558.
25. Connolly, M. L., *Journal of Molecular Graphics* **1993**, *11*, 139-141.
26. Casey, C. P.; Whiteker, G. T., *Israel Journal of Chemistry* **1990**, *30*, 299-304.
27. Kamer, P. C. J.; Reek, J. N. H.; Van Leeuwen, P. W. N. M., *Chemtech* **1998**, *28*, 27-33.
28. Dierkes, P.; van Leeuwen, P. W. N. M., *Journal of the Chemical Society, Dalton Transactions* **1999**, 1519-1530.
29. Roelen, O., *Oel und Kohle* **1938**, *14*, 1077-1079.
30. Van der Veen, L. A.; Kamer, P. C. J.; Van Leeuwen, P. W. N. M., *Angewandte Chemie, International Edition*. **1999**, *38*, 336-338.
31. Wittig, G.; Geissler, G., *Justus Liebigs Annalen der Chemie* **1953**, *580*, 44-57.
32. Beller, M.; Krauter, J. G. E., *Journal of Molecular Catalysis A: Chemical* **1999**, *143*, 31-39.
33. Unruh, J. D.; Christenson, J. R., *Journal of Molecular Catalysis* **1982**, *14*, 19-34.
34. Van der Veen, L. A.; Boele, M. D. K.; Bregman, F. R.; Kamer, P. C. J.; Van Leeuwen, P. W. N. M.; Goubitz, K.; Fraanje, J.; Schenk, H.; Bo, C., *Journal of the American Chemical Society* **1998**, *120*, 11616-11626.
35. Brown, J. M.; Kent, A. G., *Journal of the Chemical Society, Perkin Transactions 2* **1987**, 1597-1607.
36. Buisman, G. J. H.; Vos, E. J.; Kamer, P. C. J.; van Leeuwen, P. W. N. M., *Journal of the Chemical Society, Dalton Transactions* **1995**, 409-417.
37. van Leeuwen, P.; Kamer, P. C. J.; Reek, J. N. H., *Pure and Applied Chemistry* **1999**, *71*, 1443-1452.

38. Freixa, Z.; Van Leeuwen, P. W. N. M., *Dalton Transactions* **2003**, 1890-1901.
39. Kamer, P. C. J.; van Leeuwen, P. W. N. M.; Reek, J. N. H., *Accounts of Chemical Research* **2001**, *34*, 895-904.
40. Morgan, B. P.; Smith, R. C., *Journal of Organometallic Chemistry* **2008**, *693*, 11-16.
41. Morgan, B. P.; Galdamez, G. A.; Gilliard, R. J., Jr.; Smith, R. C., *Dalton Transactions* **2009**, 2020-2028.
42. Clark, T. P.; Landis, C. R.; Freed, S. L.; Klosin, J.; Abboud, K. A., *Journal of the American Chemical Society* **2005**, *127*, 5040-5042.
43. Vinod, T. K.; Hart, H., *Journal of Organic Chemistry* **1990**, *55*, 5461-5466.
44. Saednya, A.; Hart, H., *Synthesis* **1996**, 1455-1458.
45. Smith, R. C.; Protasiewicz, J. D., *Organometallics* **2004**, *23*, 4215-4222.
46. Smith, R. C.; Bodner, C. R.; Earl, M. J.; Sears, N. C.; Hill, N. E.; Bishop, L. M.; Sizemore, N.; Hehemann, D. T.; Bohn, J. J.; Protasiewicz, J. D., *Journal of Organometallic Chemistry* **2005**, *690*, 477-481.
47. Coolen, H. K. A. C.; van Leeuwen, P. W. N. M.; Nolte, R. J. M., *Journal of Organic Chemistry* **1996**, *61*, 4739-4747.
48. Hart, H.; Takehira, Y., *Journal of Organic Chemistry* **1982**, *47*, 4370-4372.
49. Hart, H.; Ward, D. L.; Tanaka, K.; Toda, F., *Tetrahedron Letters* **1982**, *23*, 2125-2128.

CHAPTER 5

PHOSPHORUS OXYANION DETECTION BASED ON CANOPIES WITH SCAFFOLDED DIMETALLIC SITES FOR SENSING APPLICATIONS[#]

5.1 Overview of Phosphorus Oxyanions

The utility of inorganic phosphates (IPs) and organophosphorus species (OPs) in physiology and pathophysiology have been a vital part of chemical biology. The understanding of this demand for IPs and OPs has been exemplified by the large number of phosphoester linkages that make up DNA and RNA backbones while also serving a vital role in adenosine phosphates which serve as the primary source of energy in the body.¹ Numerous biological processes rely upon phosphorus oxyanions such as IPs and OPs including metabolism, muscle contraction, ion pumps, signaling, energy capture and cell cycles.

Phosphorus acquisition is important for an organism's survival. A vast portion of naturally occurring phosphorus is present as oxyanions, both in biological systems and in mineral form. The two most common forms of inorganic phosphorus oxyanions are phosphate (P_i) and pyrophosphate (PP_i). (**Figure 5.1**) Phosphate is one of the three key components in fertilizers in conjunction with nitrogen and potassium. The deficiency of phosphate in soil content has been a growing concern due to large amounts of insoluble phosphate mineral production, which occupies phosphate from its normal cycle. The urbanization of man has amplified this effect by excessive waste productions and attendant leaching of phosphates into groundwater. Metals are able to complex water

[#] Adapted from Morgan, B. P.; He, S.; Smith, R. C. *Inorg. Chem.* **2007**, *46*, 9262-9266

soluble phosphates to form insoluble salts. These salts are usually taken back into the cycle through enzymes; however, naturally prevailing enzyme levels have been unable to keep pace with the urbanization of man. This creates the need to incorporate phosphorus containing fertilizers to balance the cycle.

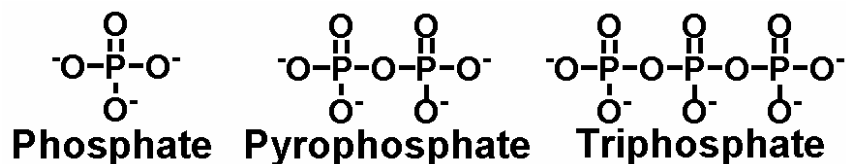


Figure 5.1 Examples of some phosphorus oxyanions.

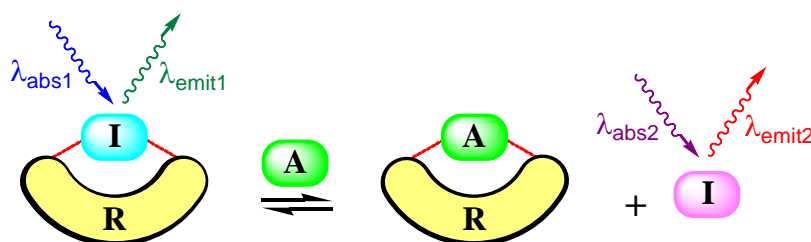
Farmers use up to four times the amount of fertilizer normally needed to accommodate for the lack of phosphate. It has also been predicted that, with such a high usage of fertilizer enriched in phosphates, the commercially available sources of phosphate will be depleted within 90 years. Phosphate deficiency in plants can lead to a number of undesirable outcomes including the secretion of organic acids, change in photosynthesis, and various enzymatic processes can be perturbed.²

Phosphate is also a biological buffer, notably intracellularly, in the urinary tract, and in saliva where it buffers against bacterial acid-induced tooth decay.^{3,4} Pyrophosphate ($\text{P}_2\text{O}_7^{4-}$, often abbreviated PP_i) is the product of ATP hydrolysis, the hallmark reaction of bioenergetics and metabolism, which regulates numerous enzymatic reactions.⁵ Phosphorylation is an important post-translational modification affecting protein structure and function through allosteric activation.^{6,7} Phospholipids are also key cell membrane components. Many senescence theories and associated preventative medicines focus on phospholipid bilayer deterioration as a primary cause of aging.⁸⁻¹⁰

Pathophysiological responses can also result from xenobiotic OPs. Organophosphorus pesticides and nerve agents of chemical warfare are among the most toxic substances ever isolated.^{11,12} These OPs induce toxic effects primarily by phosphorylation of a serine residue within the active site of acetylcholinesterase, leading to excess cholinergic stimulation within the synaptic cleft.¹³ Environmentally, phosphate is an essential soil nutrient for healthy plant growth and is a common component in agricultural supplementation.¹⁴⁻¹⁶

The multifaceted roles of inorganic phosphates and their phosphoester derivatives in biology and the environment have lead researchers to develop various means of detecting these species. UV-vis and fluorescence-based optical methods have been particularly pursued due to the convenient visual ('by eye') detection provided by colorimetric assays and the high sensitivity of fluorescence methods. The indicator displacement assay (IDA) strategy is a simple and increasingly-popular approach to optical detection. In this strategy (**Scheme 5.1**), a receptor is designed to bind a target analyte with a desired affinity, and an indicator is selected having a weaker affinity for the receptor than does the target analyte. The indicator must also exhibit a notable optical change upon displacement, thereby providing a means of assessing analyte presence and quantifying concentration spectroscopically.

The IDA strategy has emerged as an attractive alternative to covalently-tethered receptor-reporter constructs due to synthetic simplification and applicability of a single receptor to differentiation of various analytes.^{17, 18} Anslyn has pioneered IDAs for amino acids^{19,20} and carboxylates present in beverages,²¹⁻²⁶ for example. Other groups developing IDAs for similar analytes have focused on metal complexes as receptors.²⁷⁻³² Fluorescent IDAs for detecting nitric oxide (NO)³³⁻³⁶ exhibiting emission enhancement upon displacement of fluorogenic ligands from quenching transition metal centers have proven effective under physiological conditions, and have even been used to image NO synthesis by living cells.³⁵ IDAs for phosphate derivatives, the analytes of interest in the current study, have also been explored.^{31,37} Neutral organophosphorus nerve agent stimulants can be detected via metal ion displacement from fluorogenic 2,6-bis(1'-methylbenzimidazolyl)pyridine ligands,³⁸ while IDAs for anionic phosphate derivatives^{39,40} often utilize dizinc complexes as the receptor module. Dizinc phosphohydrolase model complexes supported by **L1** (**Figure 5.2**) have proven to be particularly useful receptors for IDAs.⁴⁰⁻⁴⁷ Chemosensors using the Zn₂L1 receptor or a derivative thereof have demonstrated stability *in vivo*, as exemplified by a recent application to imaging bacterial infection in live mice.³⁹ Complexometric indicators are



Scheme 5.1. Generalized representation of the signal transduction mechanism for indicator displacement assays (IDAs). I = indicator, A = analyte, R = receptor. Emission or absorption intensity or wavelength maxima may change between bound and unbound states.

well-known for their dramatic color changes in response to metal ions and are widely used for metal ion detection. As such, they are also obvious candidates to serve as displaceable chromophores from metal complex receptors in IDAs. Preliminary studies in this vein have used pyrocatechol violet (PV) or other indicator molecules binding the Zn_2L1 center via a catecholate moiety⁴⁸ as the displaced indicator.⁴⁹⁻⁵¹ Although the interaction of complexometric indicators with single metal ions in solution has been well-studied,⁵²⁻⁵⁸ knowledge of analogous binding interactions between these indicators and bimetallic centers remains incomplete. The current work examines in detail the binding of eleven well-known, commercially-available complexometric indicators (**Figure 5.2**) with the dizinc phosphohydrolase model compound Zn_2L1 . Subsequent displacement of the indicators by phosphate and pyrophosphate is explored to test the viability of each indicator as a displaceable reporter. These data should assist in the rational design of future indicator displacement sensors.

Inorganic phosphates are important for cellular function and biomineralization. Inorganic phosphates are useful in the metabolism of energetic pathways, phospholipid membranes, photosynthesis, respiration, regulation of enzymes, and production of nucleic acids. Inorganic phosphates are produced in glycolysis, phosphatases and the production of cholesterol.

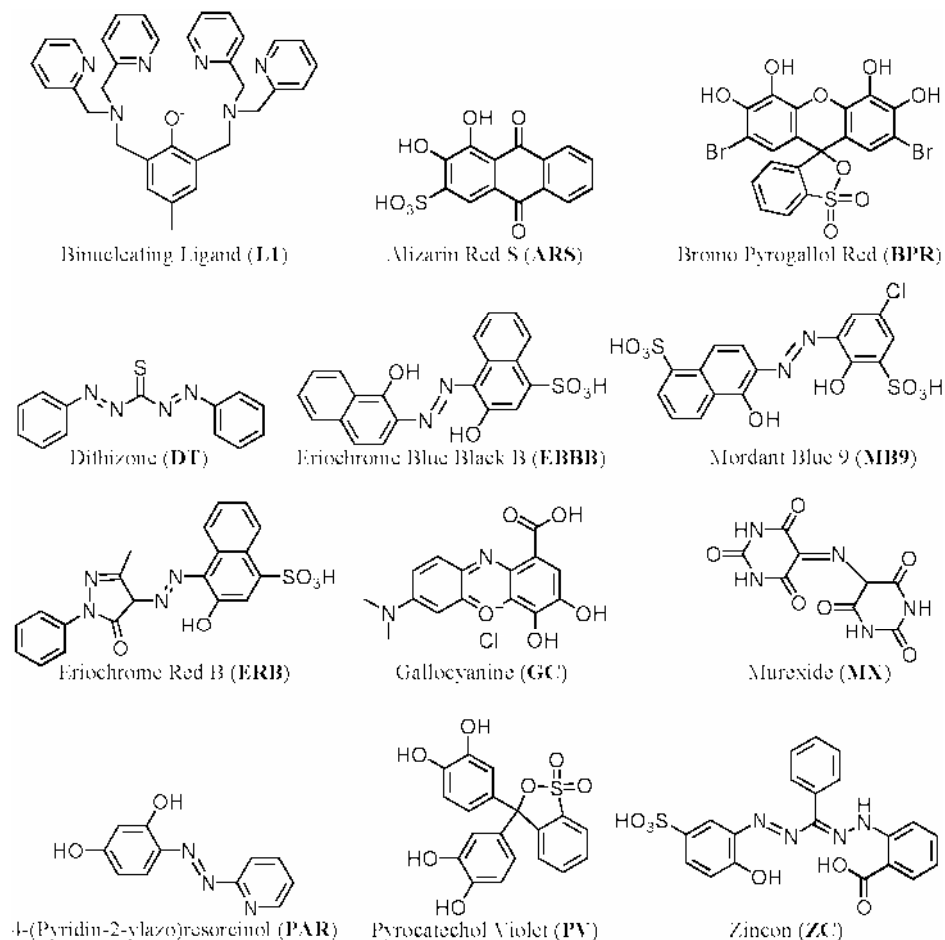


Figure 5.2. Dinucleating ligand and complexometric dyes used in the current study. Only one protonation state and resonance structure is shown in each case. Ligand **L1** is shown in the phenolate form present in the Zn_2L1 complex.

For the ecosystem to properly function plants must acquire the proper amount of phosphate to allow organisms to function properly. Phosphate is also used in food preservatives and the amount of these preservatives has been gradually increasing. The amount of phosphate consumed was 1,243 mg per day in 1960, 1,332 mg in 1975, and 1,421 mg in 1995, which agrees with the general consensus of phosphate intake. An over abundance of phosphate in the body can cause hormonal changes and hyperparathyroidism. More commonly is hypophosphataemia which is approximately 3

percent of hospitalized patients with 28 percent of those in critical condition. Hypophosphataemia is a phosphate deficiency that manifests as one of five diseases: X-linked hypophosphataemia (XLH), Autosomal dominant hypophosphataemia rickets (ADHR), Craniofacial dysplasia with hypophosphataemia (CFDH), Tumor induced rickets/osteomalacia (TIO), and Type II sodium dependent phosphate transporter (NPT2a) deficiency.

Phosphates are noteworthy anions in biology and have many functions in biological systems. Phosphates occur in two primary categories, inorganic phosphates and organic phosphates/esters. Inorganic phosphates come in the form of salts of phosphoric acid. The protonation state of phosphate varies from three to zero with acid dissociation constants (pK_a) of 2.1, 7.2, and 12.7. Phosphate can also form oligomeric ions, such as pyrophosphate and triphosphate. Pyrophosphate is of particular importance due to the hydrolysis of ATP into AMP which releases a pyrophosphate anion. The hydrolysis of pyrophosphate occurs rapidly to form phosphate.

Phosphate esters are common in biological systems and include and form the phosphate backbone of both DNA and RNA. Phosphagens, which are common in muscle tissue, act as a reserve of high energy phosphates that can be used during glycolysis or oxidative phosphorylation. Glycolysis consumes two phosphate molecules to convert glucose to pyruvate. Oxidative phosphorylation consumes one phosphate anion to convert ADP to ATP.

Biological systems use phosphate in many roles in the body, whether it is transportation or consumption to form a higher order of structure, phosphate has an important role. With such an important dependency of phosphate many researchers have

attempted to detect phosphate. Various detection methods have been used to determine phosphate concentration. Some of the earliest detection methods have included Ammonium molybdate colorimetric methods. These methods require harsh conditions and several days for preparation of samples. The accepted solvents used in ammonium molybdate determinations include, isopropanol, isobutanol, and ammonia. This method has remained the standard clinical evaluation method for phosphate since the 1920's. Detection of anions in general has required organic solvents and relies upon electrostatic forces for detection. The human body does not contain these organic solvents making previous methods unsuitable for biochemical applications. A renewed interest in detection of anions in water based solvents has begun with a focus towards in vitro techniques.⁵⁹

A common detection method for phosphorus oxyanions is to use bimetallic receptors. These receptors use different scaffolds to increase or decrease the bimetallic distance. Sometimes the scaffold is rigid while other times scaffolds can be more flexible. A recent scaffold was determined using a previously synthesized complex. In 1981, Suzuki, et. al. reported a binuclear Cobalt (II) complex based upon a 2,6-bis (bis(2-pyridylmethyl)aminomethyl)-4-methylphenol (Hbpmp). This complex has been studied and investigated thoroughly. Hbpmp has known redox activity, oxygen transport and adduct mechanisms, magnetic properties, hemocyanin and other bioinorganic applications such as phosphatases and hydroxylation.⁶⁰

It was not until 2002 when Han and Kim reported the first use of Hbpmp as a detection method for phosphate. Pyrocatechol violet (PV) dye was used as an indicator where its bound state to the bimetallic complex is a different color than the free PV. The

principle method used for this sensor is a displacement of pyrocatechol violet with phosphate, therefore phosphate must bind the bimetallic complex more readily than the PV. Kim reported the association constants of both phosphate and pyrocatechol violet using isothermal titration calorimetry (ITC). Phosphate was $11.2 \times 10^4 \text{ M}^{-1}$ and pyrocatechol violet was $5.3 \times 10^4 \text{ M}^{-1}$. This method was considered to be selective for phosphate over other anions.⁵⁰ In 2003 Kim reported the detection of AMP using the same system. The use of a cyclic nucleotide phosphodiesterase (PDE) was studied using cAMP as the substrate. The cleavage of the phosphoester bond resulted in complexation to the bimetallic sensor. Pyrocatechol violet was used as the chemosensor with displacement occurring due to AMP production. This technique was also employed to determine the activity of inhibitors of PDE, like 3-isobutyl-1-methylxanthine (IBMX). The IC_{50} value of IBMX was determined to be $36 \mu\text{M}$.⁶¹

In 2003, Hong reported the detection of pyrophosphate based upon a Hbpm scaffold with an azophenol chromophore attached where the methyl normally is. Hong reported the selective detection of pyrophosphate even in the presence of phosphate anions. The detection method was a fluorescent emission increase at 465 nm due to the bathochromic shift from 417 nm to 465 nm upon addition of pyrophosphate. The association constant of pyrophosphate was $6.6 \times 10^8 \text{ M}^{-1}$. The binding mode of pyrophosphate was determined by Hong using X-ray analysis which showed a four oxygen donation to the two zinc atoms.⁶² In 2004, Hong also reported the detection of pyrophosphate in water with high selectivity over ATP. In this study a naphthyl based chromophore was used instead of the previous azophenol. The bathochromic shift was from 305 nm to 316 nm upon addition of pyrophosphate. However, ATP gave a 5 nm

bathochromic shift while ADP only gave a 2 nm shift. AMP or phosphate however gave no spectral change upon addition.⁶³

In 2004 Bradley D. Smith et. al. reported the binding of the same bimetallic complex to pyrophosphate. The association constant for pyrophosphate was 60 times greater than phosphate. Smith reported the association constant of pyrophosphate to be $67 \times 10^4 \text{ M}^{-1}$ and phosphate to be $11 \times 10^4 \text{ M}^{-1}$.⁶⁴ In 2005 Smith reported the association constant of Hbpmp to pyrocatechol violet using UV-vis methods. The calculated association constant was $5.6 \times 10^4 \text{ M}^{-1}$. He also used a coumarin methylsulfinate with Hbpmp which gave an association constant of $17.8 \times 10^4 \text{ M}^{-1}$. Smith used the displacement of PV and coumarin methylsulfinate to detect phosphatidylcholine vesicles containing as little as 5 percent phosphatidylserine which could be detected.⁴⁹

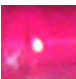
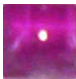
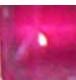

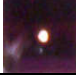





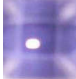






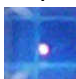

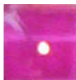
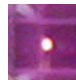


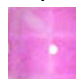




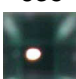
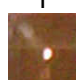

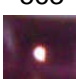
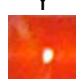
5.2 Results and Discussion

The ligand **L1** was selected for the current study because this ligand set and its derivatives have been utilized in indicator displacement and other sensing schemes under physiological conditions. **L1** was prepared by the condensation of di(2-picolyl)amine and 2,6-bis(chloromethyl)-4-methylphenol in THF in the presence of triethylamine following the reported procedure,⁶⁰ and its identity was confirmed by ¹H and ¹³C NMR spectroscopy (**Figure 5.15** and **Figure 5.16** respectively). The Zn₂**L1** complex used in complexometric and displacement studies was prepared *in situ* by addition of 2 equiv ZnCl₂ to **L1** in 10 mM HEPES buffer at pH 7.4. Among the various metals that may bind the di(2-picolyl)amino (DPA) ligating group in **L1**, zinc is the logical choice for a physiological, reversibly binding receptor due to its air stability and the relatively high kinetic lability of its complexes. Furthermore, phenolate/DPA-supported complexes display high affinity (on the nanomolar range in some cases) for Zn²⁺ in living tissue.⁶⁵⁻⁶⁷ These features suggest that while the indicator may be displaced, Zn₂**L1** itself will not be readily demetallated in biological contexts and is thus a stable scaffold for biosensor applications.

A set of eleven commercially available complexometric indicators were selected for screening (**Figure 5.2**). Each indicator shown in **Figure 5.2** was titrated with a solution of preformed Zn₂**L1** complex in HEPES (10 mM, pH 7.4), and absorption changes were monitored by UV-vis spectroscopy. Spectra for one titration (using **ZC**) are presented in **Figure 5.3**, while the complete set of titration spectra is provided in Chapter 5.4. A modification of the classic Benesi-Hildebrand method⁶⁸ was used to extract dissociation constants (K_d) from titration data for each indicator (**Table 5.1**; all plots and

linear fits are provided in Chapter 5.4). Among the indicators screened, K_d values cover two orders of magnitude, from 2.8×10^{-4} M to 2.7×10^{-6} M (**Table 5.1**). Significant variation due to steric and electronic influences is noted even for indicators that presumably bind to Zn_2L1 through the same ligating unit. For example, indicators binding through a catecholate (**ARS**, **BPR**, **GC**, and **PV**) have K_d values ranging from 2.8×10^{-4} M to 2.7×10^{-6} M, and the values for Eriochrome dyes **ERB** and **EBBB** are 4.0×10^{-5} M and 8.2×10^{-6} M, respectively. Among the indicators examined, the only K_d previously reported was for the **PV**- Zn_2L1 complex. The reported value of 1.9×10^{-5} M, determined from calorimetric and UV-vis data in HEPES at pH 7.0⁵⁰ (also reported in TES buffer at pH 7.4),⁴⁹ is in good agreement with that determined in the current study (3.0×10^{-5} M). The variation of binding constant with small pH/buffer changes is the likely origin of the difference between the two values. **BPR** and **ZC** bind to Zn_2L1 most strongly and approximately an order of magnitude more strongly than does **PV**, compared with the weakest binding, observed for **ARS**, an order of magnitude less strongly binding than **PV**. The availability of a wide range of K_d values is invaluable for the design of IDAs with specified responses (*vide infra*). Another parameter of interest in the design of colorimetric IDAs is the extent to which the color changes upon exposure to analyte. Photographs are provided in **Table 5.1** for bound and free forms of the indicators, demonstrating the range of wavelengths available within the indicator series. **EBBB** exhibits the greatest change in λ_{max} between free and Zn_2L1 -bound states ($\Delta\lambda = 195$ nm, **Table 5.1**), making it very easy to follow binding and displacement events by eye. The smallest shift is observed for **MB9**, with $\Delta\lambda_{max}$ of only 12 nm between bound

Table 5.1. Absorption data and photos demonstrating the range of colorimetric responses observed in free, bound and pyrophosphate-displaced states. Absorption spectra for these experiments and errors are provided in Chapter 5.4.

Indicator	K_d μM	λ_{free} nm	λ_{bound} nm	$\Delta\lambda$ nm	Displacement ^a	
					HPO_4^{2-}	$\text{H}_2\text{P}_2\text{O}_7^{2-}$
ARS	280	516 	541 	25	Y	Y 
BPR	2.7	554 	578 	24	N	Y 
DT	13	471 	487 	16	N	Y ^b 
EBBB	8.2	649 	454 	195	Y	Y 
ERB	40	469 	510 	41	Y	Y 
GC	18	621 	563 	58	Y	Y 
MB9	5.1	532 	544 	12	N	Y 
MX	21	520 	480 	40	Y	Y 
PAR	18	412 	490 	78	Y	Y 
PV	30	443 	635 	192	Y	Y 
ZC	2.9	467 	563 	96	Y	Y 

a) Displacement is considered to take place when there is a >50% return in absorbance at λ_{bound} to the absorbance at that wavelength for the unbound form.

b) Displacement requires ~1 min before it can be observed, whereas all other positive displacement events are observed immediately upon mixing.

and unbound states. This change is still visible to the naked eye in a side by side comparison, but is considerably less pronounced than that for some of the other dyes.

Once the binding of indicators to Zn_2L1 had been quantitated, phosphate and pyrophosphate were selected as test analytes to gauge their ability to displace indicators with restoration of the “unbound” color. These analytes were selected to allow comparison of the series of indicators screened in this study with previous IDAs for these analytes utilizing the Zn_2L1 receptor. Furthermore, previous studies have already demonstrated little or no binding affinity of other common anions such as nitrate, sulfate, acetate, or halides to this receptor.⁴⁹ Pyrophosphate ($K_d = 1.5 \times 10^{-6}$ M) is bound about six times more strongly than phosphate ($K_d = 9.1 \times 10^{-6}$ M) in 1:1 complexes with Zn_2L1 .⁶⁴ On the basis of equilibrium considerations, displacement of >50% of indicator by 1 equiv of analyte will occur when $K_{d, \text{indicator}} > K_{d, \text{analyte}}$. Assuming that indicator binding is reversible and that there is no significant kinetic barrier to displacement, a colorimetric response corresponding to at least partial restoration of the indicator to its uncomplexed form would be expected in such cases. An indicator that binds to Zn_2L1 with a K_d significantly higher than both analytes should be easily displaced by either of them, so selectivity cannot be accomplished in these cases. This prediction holds true for six of the seven indicators in this category (**ARS**, **ERB**, **GC**, **MX**, **PAR**, and **PV**), all of which immediately return to the color of the unbound indicator upon addition of phosphate or pyrophosphate. The exception is **DT**, which requires ~1 min for displacement following anion addition.

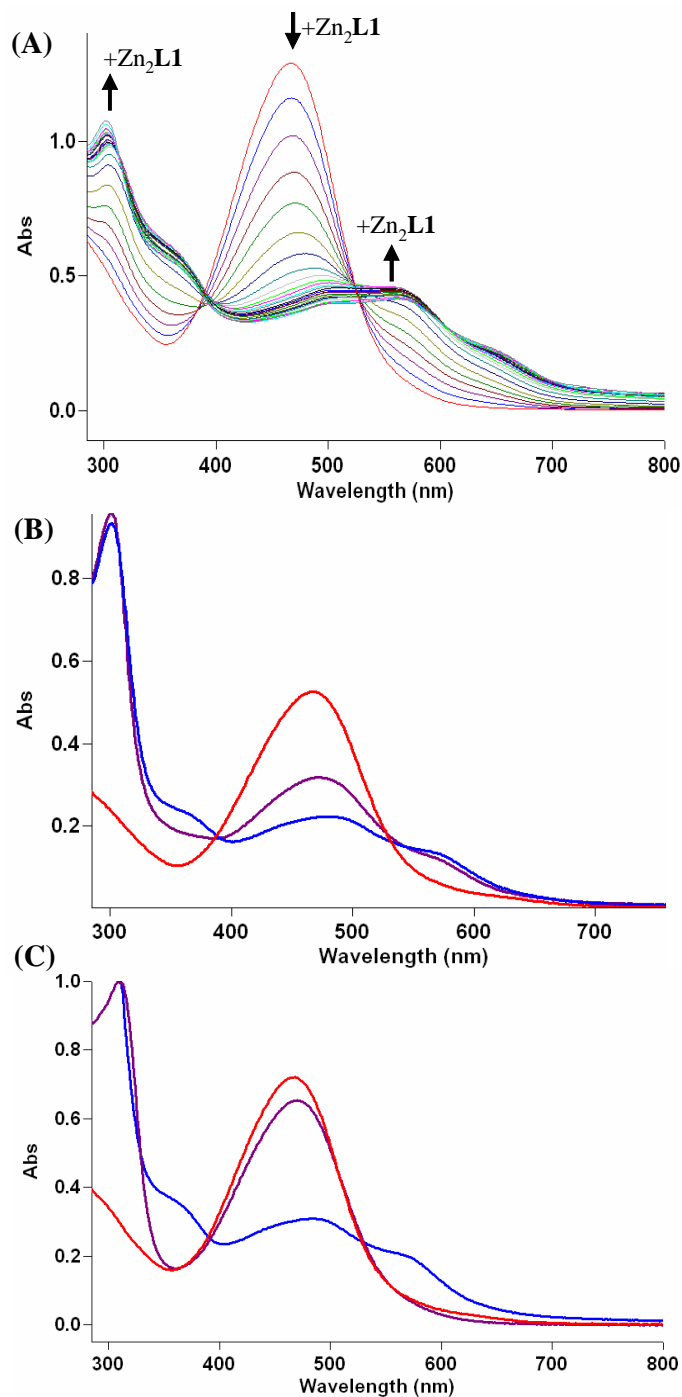


Figure 5.3. (A) Titration of **ZC** with **Zn₂L1**, followed by UV-vis spectroscopy (the solvent is 10 mM HEPES at pH 7.4). (B) Phosphate displacement test; the red trace corresponds to **ZC**, the blue trace to the **ZC-Zn₂L1** complex, and the purple trace **ZC-Zn₂L1** complex in the presence of HPO_4^{2-} . (C) Pyrophosphate displacement test; the red trace corresponds to **ZC**, the blue trace to the **ZC-Zn₂L1** complex, and the purple trace **ZC-Zn₂L1** complex in the presence of $\text{H}_2\text{P}_2\text{O}_7^{2-}$.

Although an IDA for phosphate employing **PV-Zn₂L1** was previously noted,⁴⁹ pyrophosphate was not tested as a competing analyte, and this IDA cannot distinguish between the two anions at physiological pH. In order to accomplish selective detection of the more strongly binding pyrophosphate from an equal concentrations of phosphate, the indicator selected must bind to **Zn₂L1** with K_d between the values for phosphate and pyrophosphate (between 1.5 and 9.1 μ M). The narrow range afforded by these analytes makes selective detection a challenge. In the current series, **BPR**, **MB9** and **ZC** have appropriate K_d values expected to facilitate such a selective response.³¹ The binding constant for **EBBB** is in this range as well but is nearly identical to that of phosphate, and we were not able to observe selectivity in this case. A selective response to 1 equiv pyrophosphate over equimolar phosphate is evident, both visually and spectroscopically, when **BPR**, **MB9**, or **ZC** is used as the indicator. The selectivity of the **ZC**-based IDA for pyrophosphate (**Figure 5.3C**) over phosphate (**Figure 5.3B**) is evident from the absorption spectra as well as by eye. The violet **ZC-Zn₂L1** complex changes to the orange color typical of free **ZC** immediately upon addition of pyrophosphate, but changes little in upon addition of phosphate. The phosphate/pyrophosphate displacement described herein is another illustrative example of the IDA strategy's simplicity; a single receptor can be utilized with a range of indicators to give different responses and selectivities that depend on the relative binding affinities of the analyte and indicator selected. The dissociation constants determined in the current study for this set of commercially available indicators should guide their application in future IDAs.

5.3 Conclusions

A series of eleven complexometric indicators was investigated for spectral response to a dizinc phosphohydrolase model complex Zn_2L1 . Dissociation constants determined these complexes span two orders of magnitude. These eleven indicators were tested for displacement by phosphate and pyrophosphate anions in HEPES buffer at physiological pH of 7.4. Selective indicator displacement assays for pyrophosphate were discovered using **BPR**, **MB9**, or **ZC** as displaceable indicators. Differentiation of analytes relies heavily on the relative binding constants of the indicator and analyte(s) of interest. The binding data presented herein will guide our future application of biologically-applicable sensors utilizing this set of dyes. Work to expand upon these data and to prepare more selective dizinc receptors for anion detection by indicator displacement are currently underway in our laboratory.

5.4 Experimental Details

General procedures for absorption spectroscopy

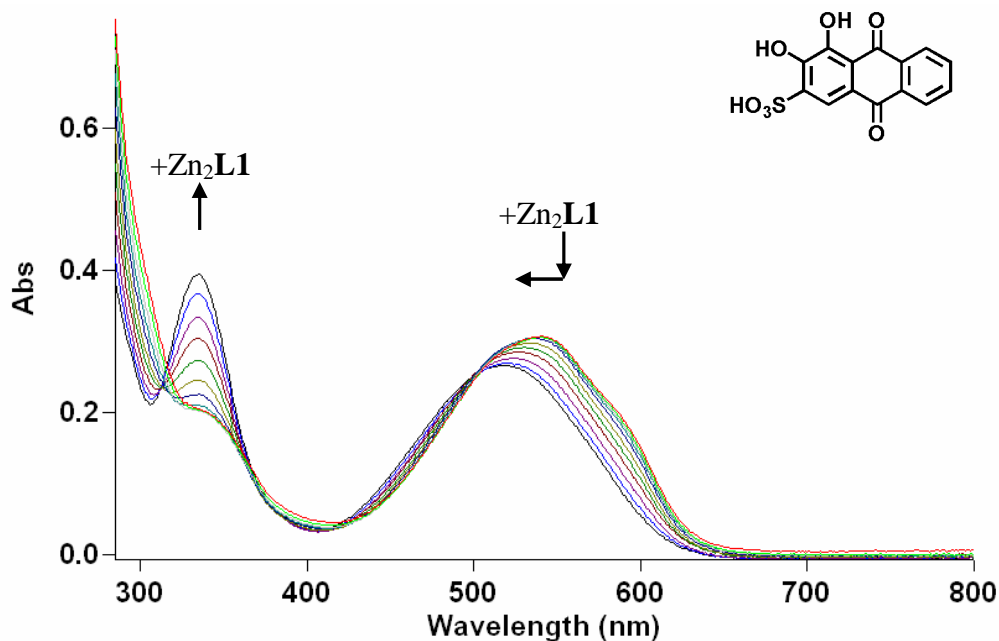
Absorption spectra were collected using a Varian Cary-50 Bio spectrophotometer in poly(methylmethacrylate) cuvettes with a pathlength of 1 cm. Titrations of indicators, monitored by UV-vis spectroscopy (**Figures 5.4-5.14**) were carried out by progressively adding aliquots of Zn₂L1 (0.1 equiv at a time) to $\sim 5 \times 10^{-5}$ M solutions of the indicator in HEPES (10 mM, pH 7.4). The titration was monitored up to 2 equiv Zn₂L1 were added in each case. Displacement of indicators from a 1:1 indicator:Zn₂L1 solution (also $\sim 5 \times 10^{-5}$ M) involved addition of 1 equiv phosphate, and up to 10 equiv of anion was added in some cases to confirm low responsiveness.

Materials

Ligand L1 was prepared as reported previously⁶⁰ and its identity confirmed by ¹H and ¹³C NMR spectra (**Figure 5.15** and **Figure 5.16** respectively) obtained using a Bruker Avance 300 operating at 300 MHz for proton and 75 MHz for carbon-13 at 25 °C. Peaks are reported in ppm with reference to TMS or residual CDCl₃ solvent signal. Other reagents and indicators were used as received from the suppliers without further purification. Buffer pH was measured using a Corning CHEK-MITE pH 25 sensor equipped with a symphony Ag/AgCl pH electrode, and adjusted to the target value by addition of HCl(aq) and NaOH(aq) solutions. Binding constants were determined using variations of the Benesi-Hildebrand method recommended by Hammond.⁶⁸

5.5 Selected Spectra

(A)



(B)

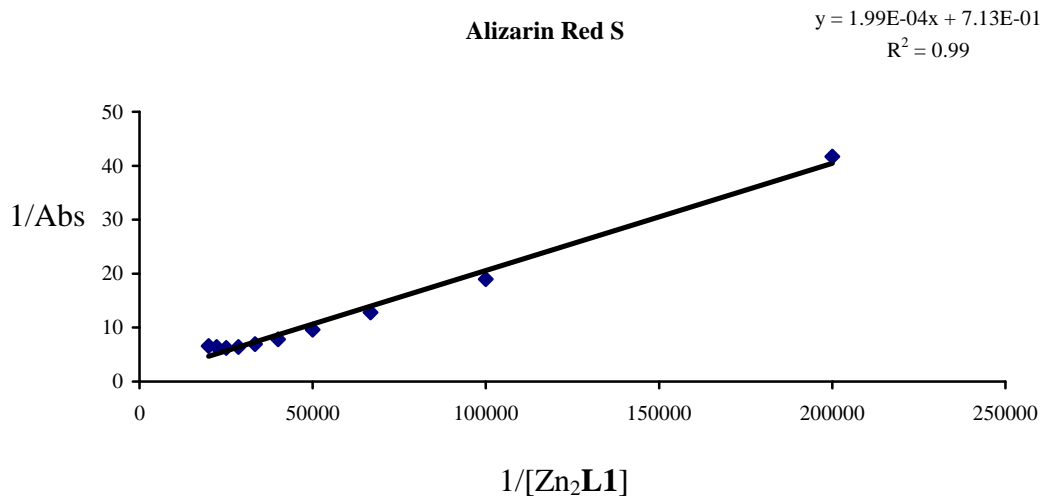


Figure 5.4. Titration of alizarin red S (ARS). (A) Structure of the indicator superimposed on UV-vis spectra collected as the indicator was titrated with Zn_2L1 , and (B) Benesi-Hildebrand plot of spectral data points (blue diamonds) and the linear fit (black line) used to calculate K_d . The equation and R^2 value for the linear fit are displayed in the upper right hand corner of the plot. This variation of the classic Benesi-Hildebrand method is based on a treatment described in reference 68 (note that slope does not equal K_d directly).

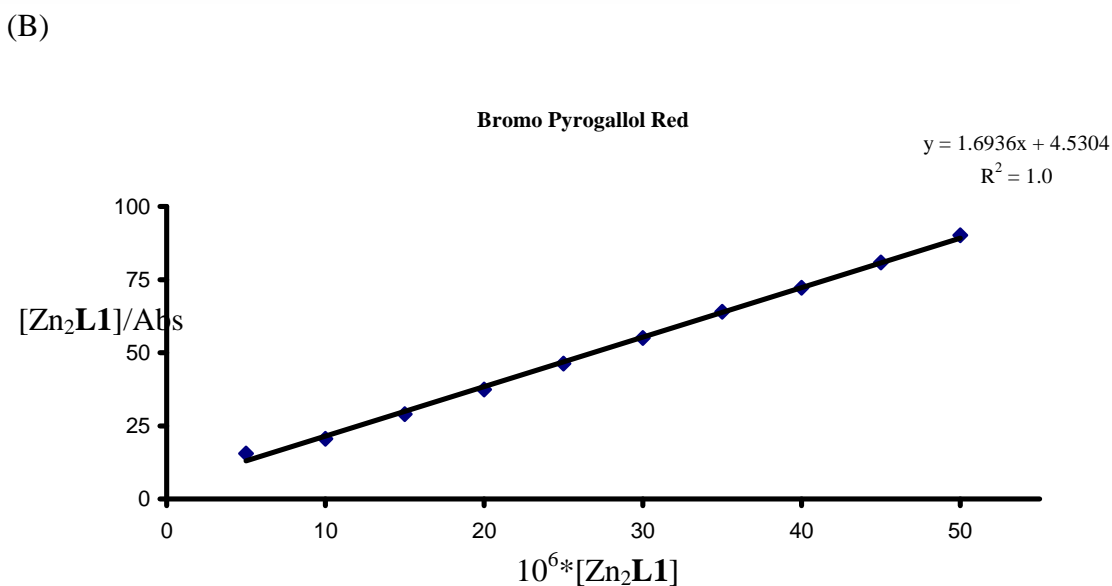
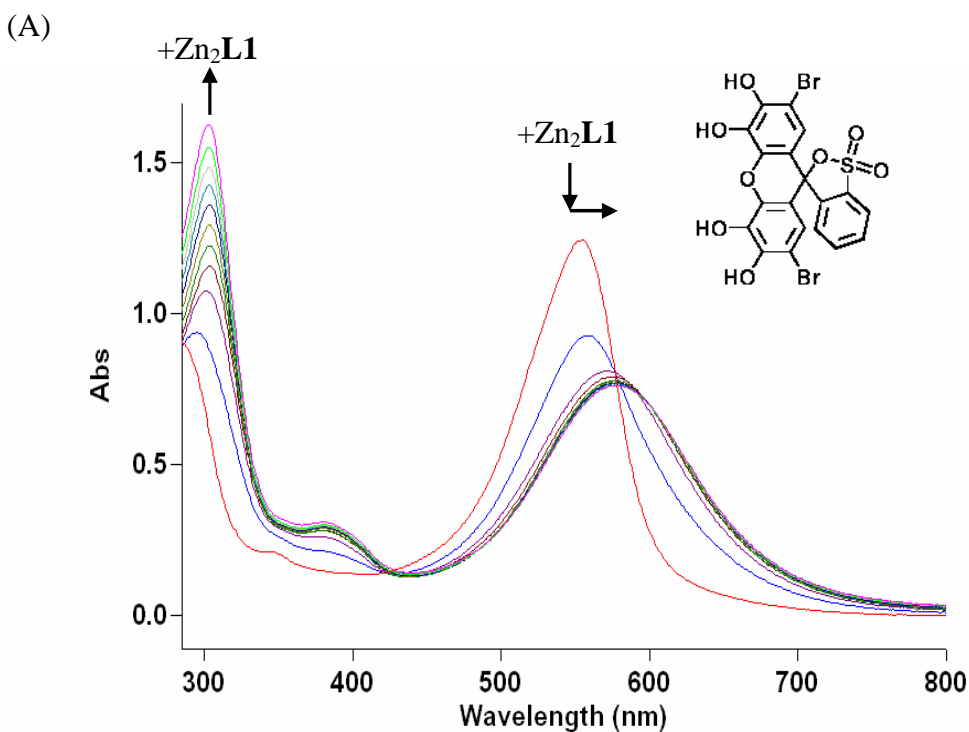


Figure 5.5. Titration of bromo pyrogallol red (**BPR**). (A) Structure of the indicator superimposed on UV-vis spectra collected as the indicator was titrated with Zn_2L1 , and (B) Benesi-Hildebrand plot of spectral data points (blue diamonds) and the linear fit (black line) used to calculate K_d . The equation and R^2 value for the linear fit are displayed in the upper right hand corner of the plot. This variation of the classic Benesi-Hildebrand method is based on a treatment described in reference 68 (note that slope does not equal K_d directly).

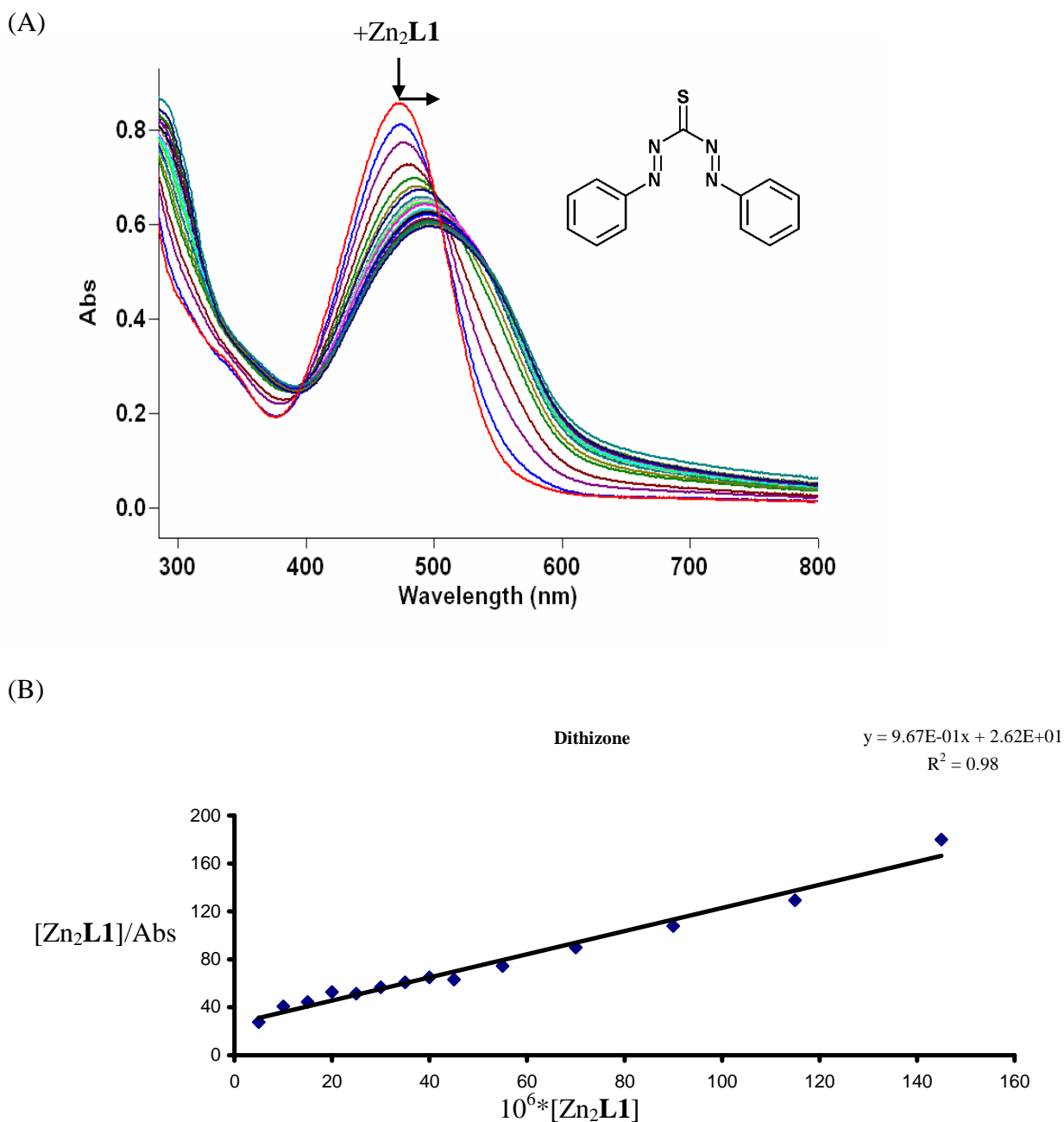
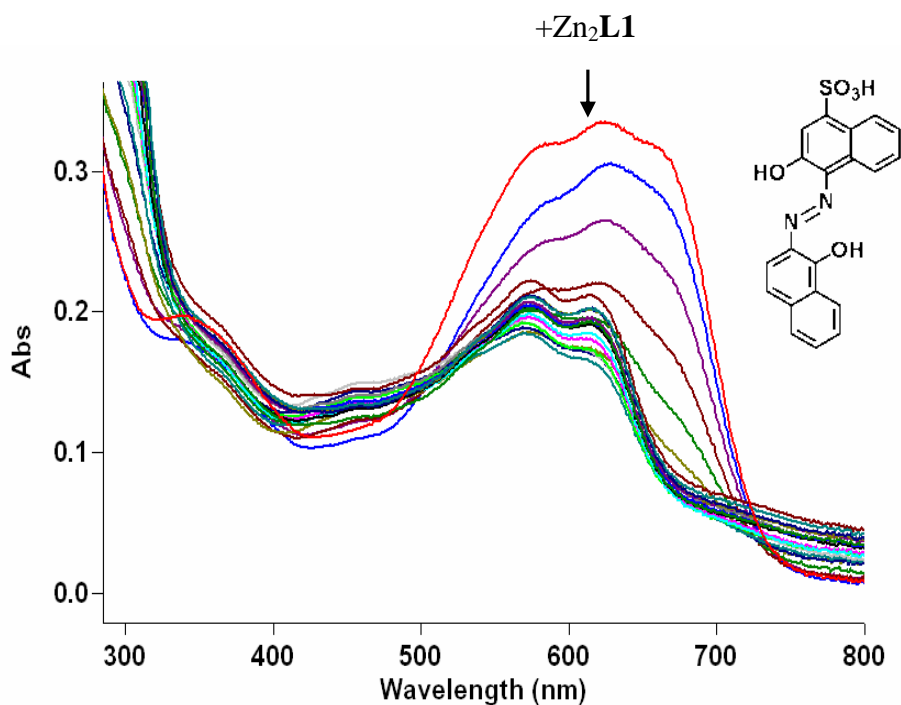


Figure 5.6. Titration of dithizone (DT). (A) Structure of the indicator superimposed on UV-vis spectra collected as the indicator was titrated with Zn_2L1 , and (B) Benesi-Hildebrand plot of spectral data points (blue diamonds) and the linear fit (black line) used to calculate K_d . The equation and R^2 value for the linear fit are displayed in the upper right hand corner of the plot. This variation of the classic Benesi-Hildebrand method is based on a treatment described in reference 68 (note that slope does not equal K_d directly).

(A)



(B)

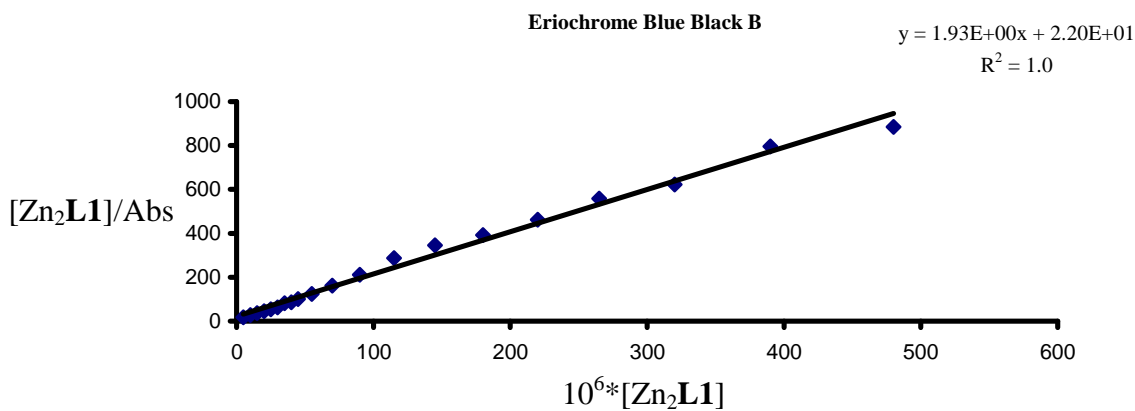


Figure 5.7. Titration of Eriochrome Blue Black B (EBBB). (A) Structure of the indicator superimposed on UV-vis spectra collected as the indicator was titrated with Zn_2L1 , and (B) Benesi-Hildebrand plot of spectral data points (blue diamonds) and the linear fit (black line) used to calculate K_d . The equation and R^2 value for the linear fit are displayed in the upper right hand corner of the plot. This variation of the classic Benesi-Hildebrand method is based on a treatment described in reference 68 (note that slope does not equal K_d directly).

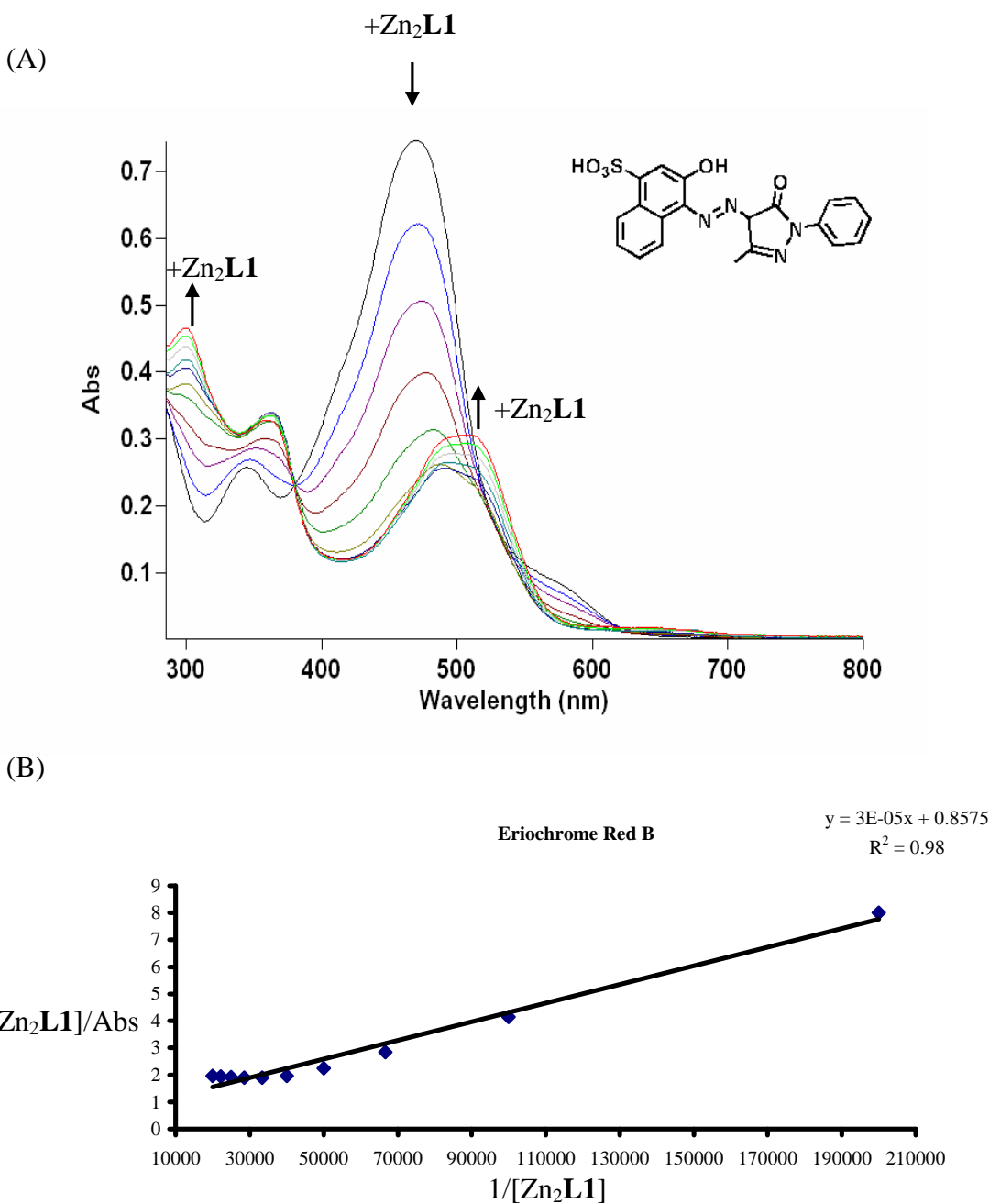


Figure 5.8. Titration of eriochrome red B (**ERB**). (A) Structure of the indicator superimposed on UV-vis spectra collected as the indicator was titrated with Zn_2L1 , and (B) Benesi-Hildebrand plot of spectral data points (blue diamonds) and the linear fit (black line) used to calculate K_d . The equation and R^2 value for the linear fit are displayed in the upper right hand corner of the plot. This variation of the classic Benesi-Hildebrand method is based on a treatment described in reference 68 (note that slope does not equal K_d directly).

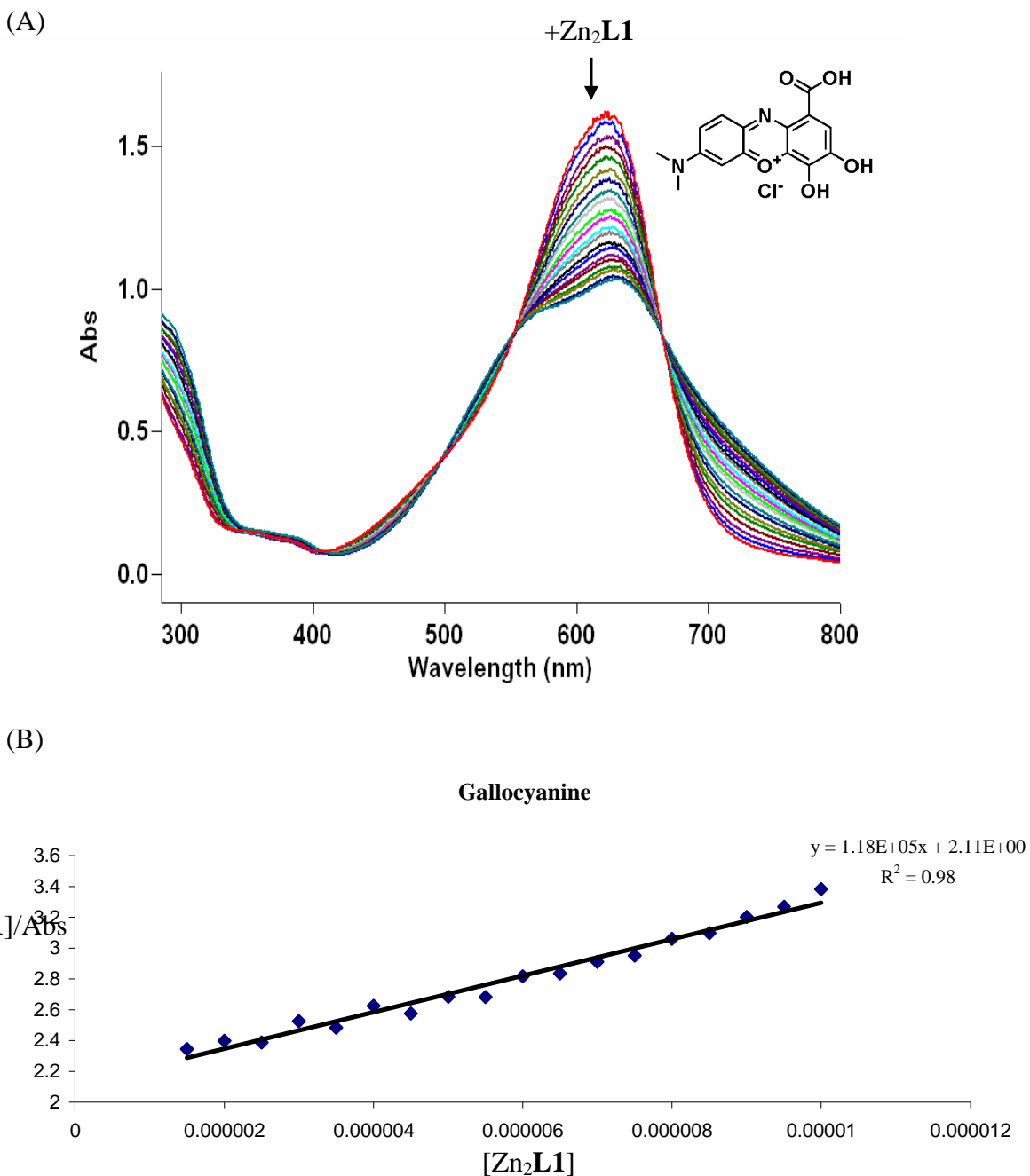
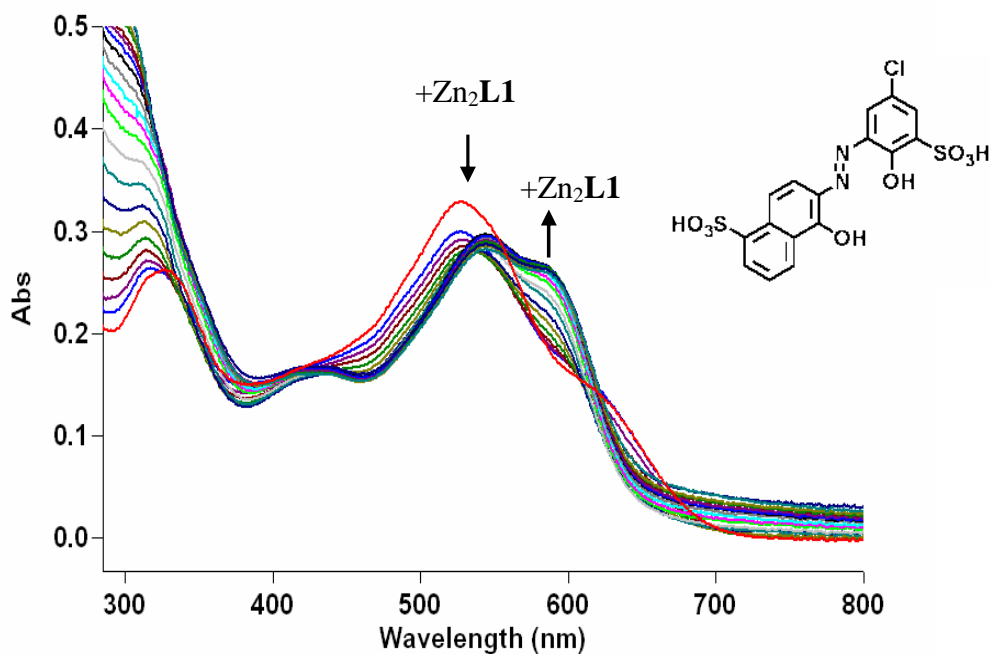


Figure 5.9. Titration of gallocyanine (GC). (A) Structure of the indicator superimposed on UV-vis spectra collected as the indicator was titrated with Zn_2L1 , and (B) Benesi-Hildebrand plot of spectral data points (blue diamonds) and the linear fit (black line) used to calculate K_d . The equation and R^2 value for the linear fit are displayed in the upper right hand corner of the plot. This variation of the classic Benesi-Hildebrand method is based on a treatment described in reference 68 (note that slope does not equal K_d directly).

(A)



(B)

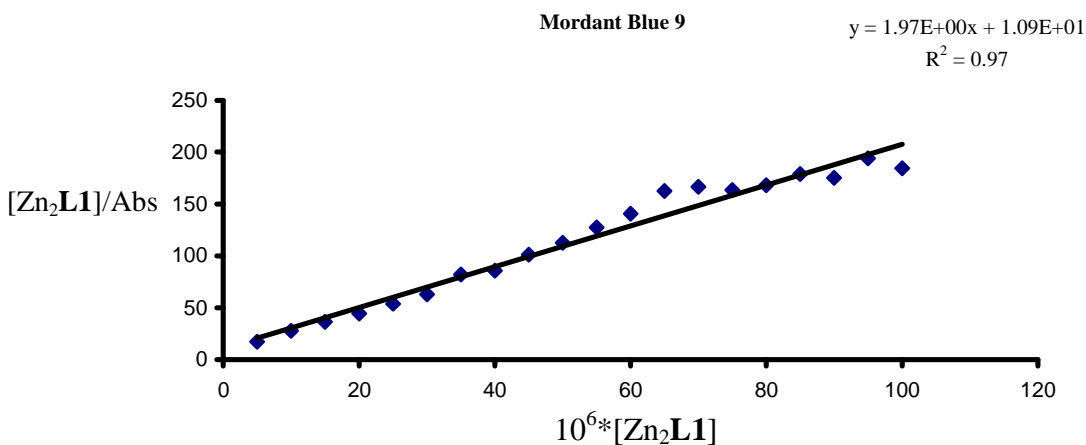
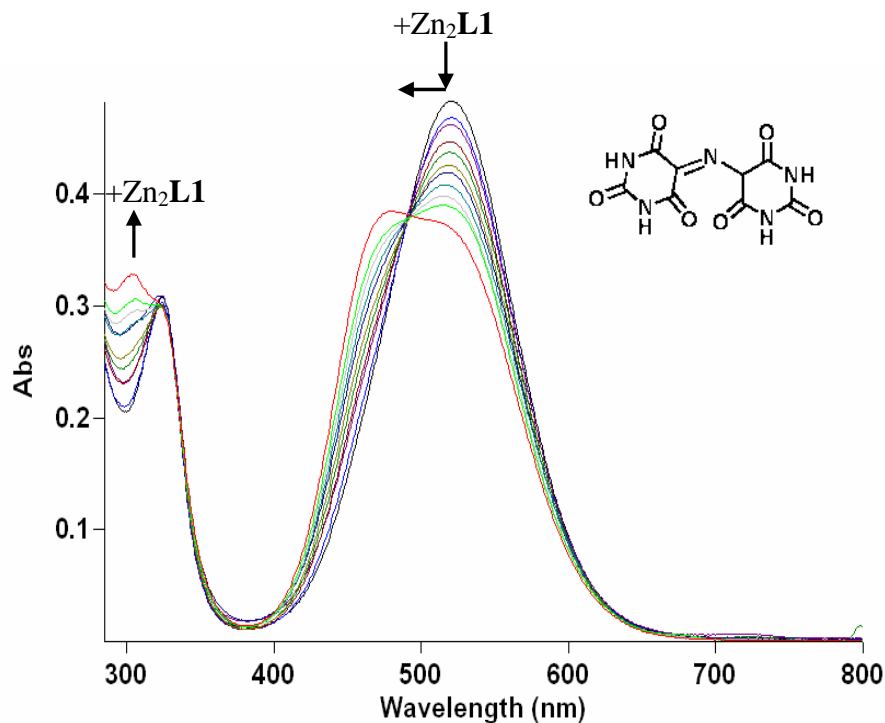


Figure 5.10. Titration of mordant blue 9 (MB9). (A) Structure of the indicator superimposed on UV-vis spectra collected as the indicator was titrated with Zn_2L1 , and (B) Benesi-Hildebrand plot of spectral data points (blue diamonds) and the linear fit (black line) used to calculate K_d . The equation and R^2 value for the linear fit are displayed in the upper right hand corner of the plot. This variation of the classic Benesi-Hildebrand method is based on a treatment described in reference 68 (note that slope does not equal K_d directly).

(A)



(B)

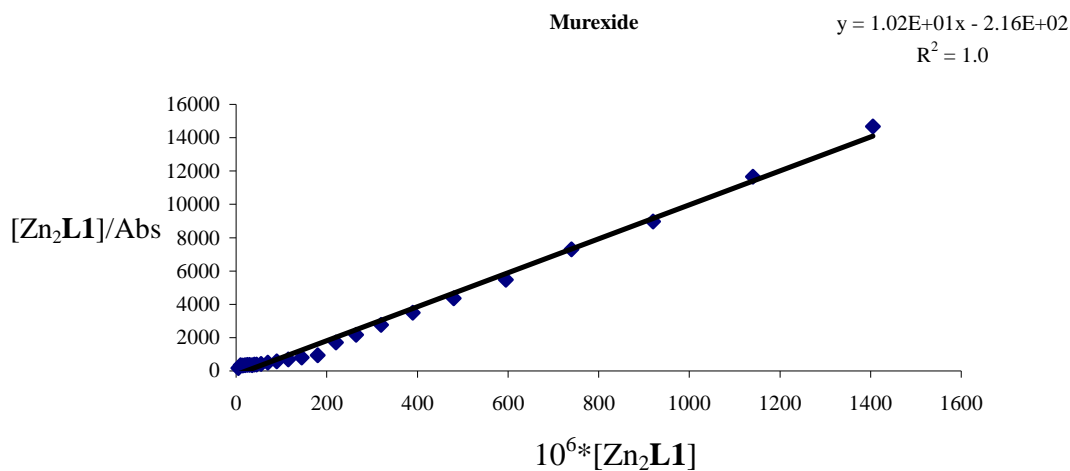


Figure 5.11. Titration of murexide (MX). (A) Structure of the indicator superimposed on UV-vis spectra collected as the indicator was titrated with Zn₂L1, and (B) Benesi-Hildebrand plot of spectral data points (blue diamonds) and the linear fit (black line) used to calculate K_d . The equation and R^2 value for the linear fit are displayed in the upper right hand corner of the plot. This variation of the classic Benesi-Hildebrand method is based on a treatment described in reference 68 (note that slope does not equal K_d directly).

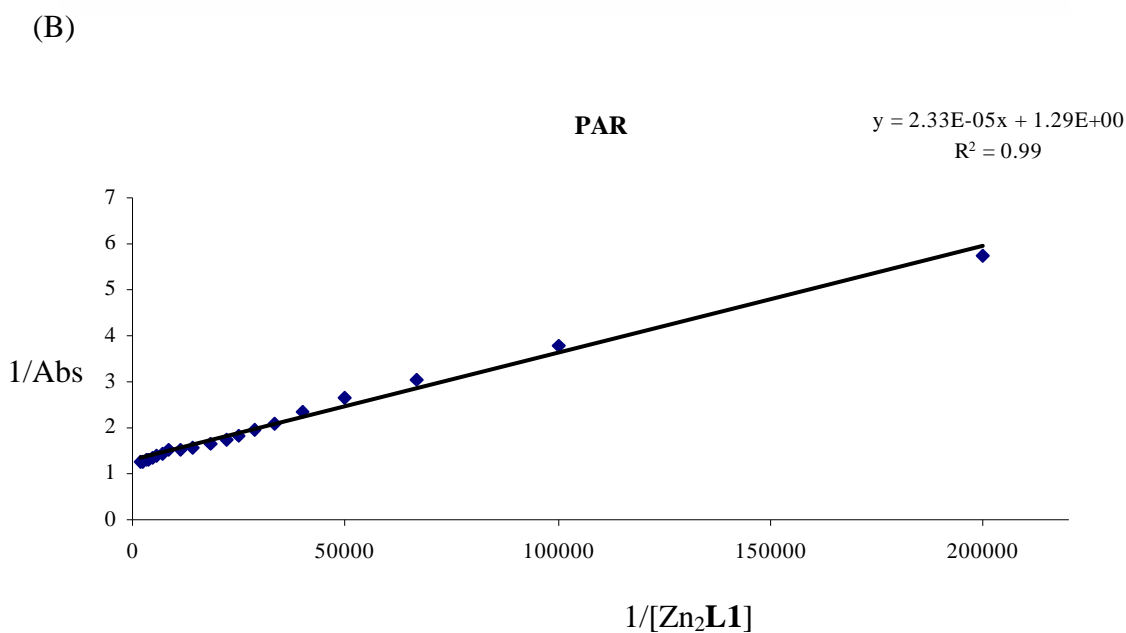
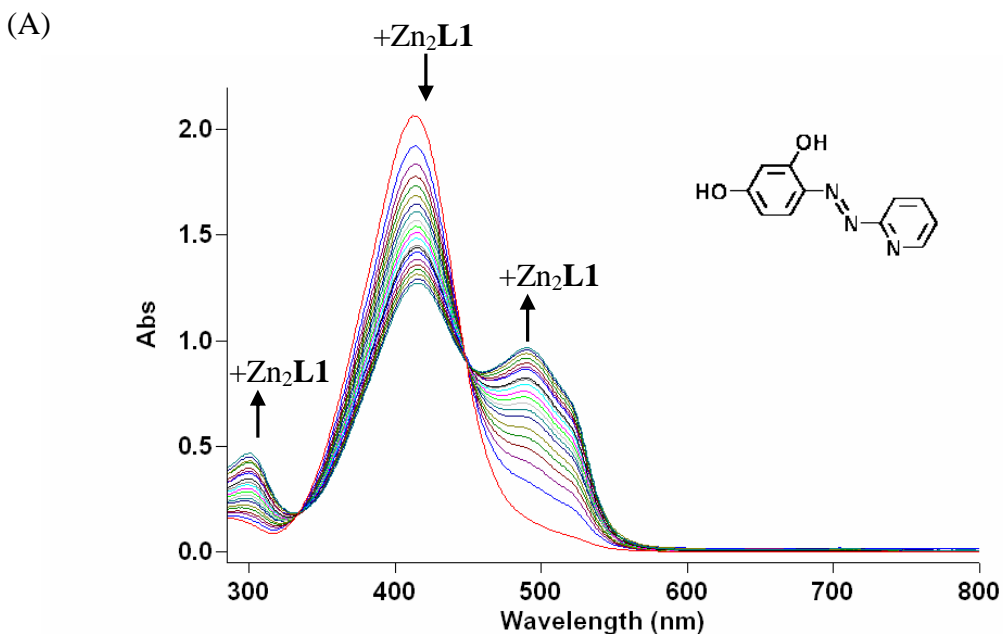


Figure 5.12. Titration of 4-(pyridin-2-ylazo)resorcinol (**PAR**). (A) Structure of the indicator superimposed on UV-vis spectra collected as the indicator was titrated with Zn_2L1 , and (B) Benesi-Hildebrand plot of spectral data points (blue diamonds) and the linear fit (black line) used to calculate K_d . The equation and R^2 value for the linear fit are displayed in the upper right hand corner of the plot. This variation of the classic Benesi-Hildebrand method is based on a treatment described in reference 68 (note that slope does not equal K_d directly).

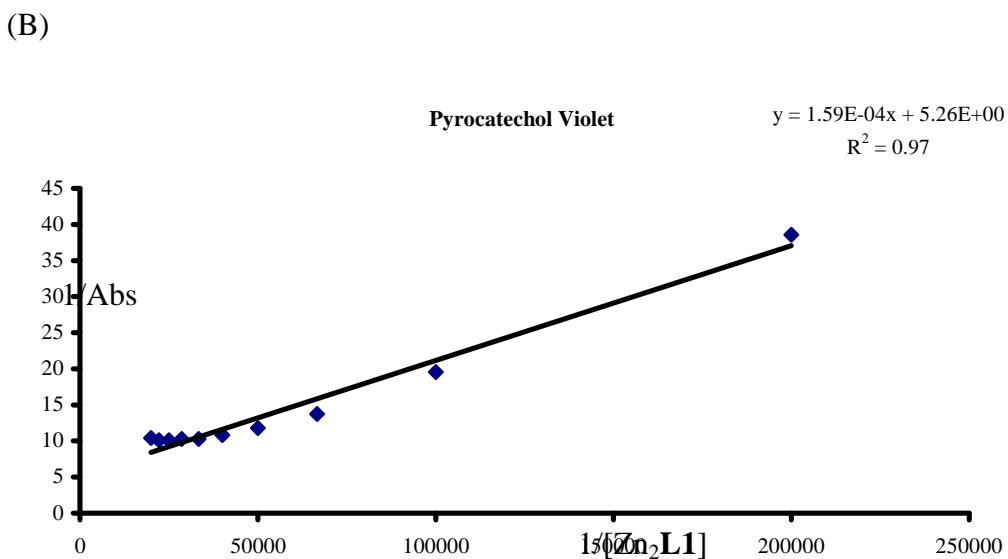
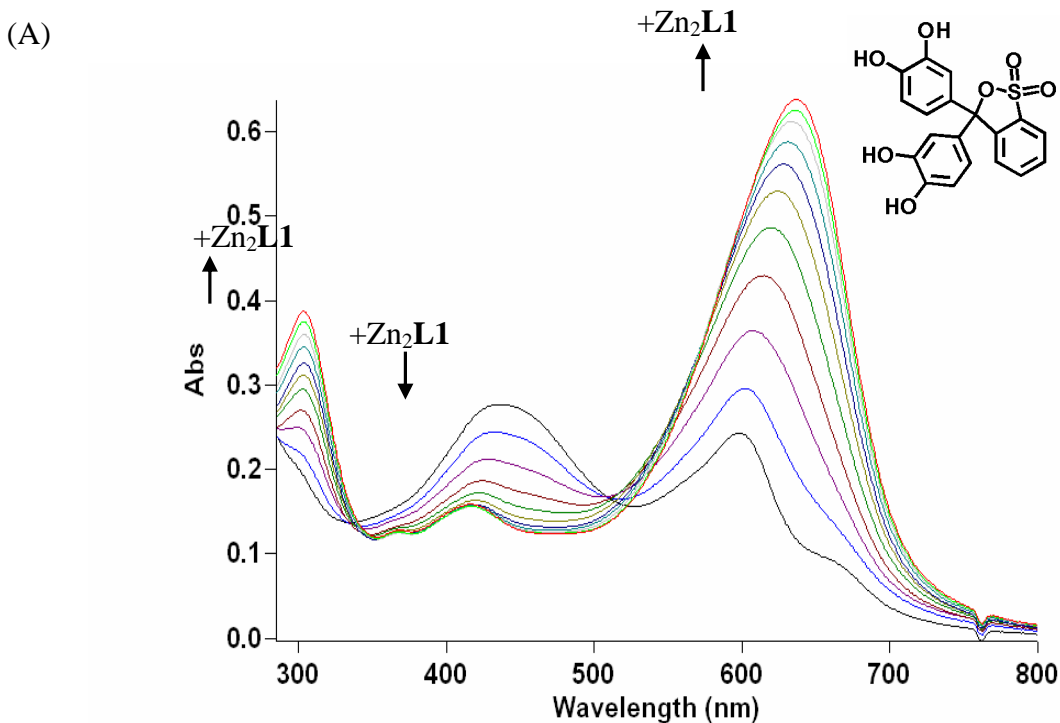
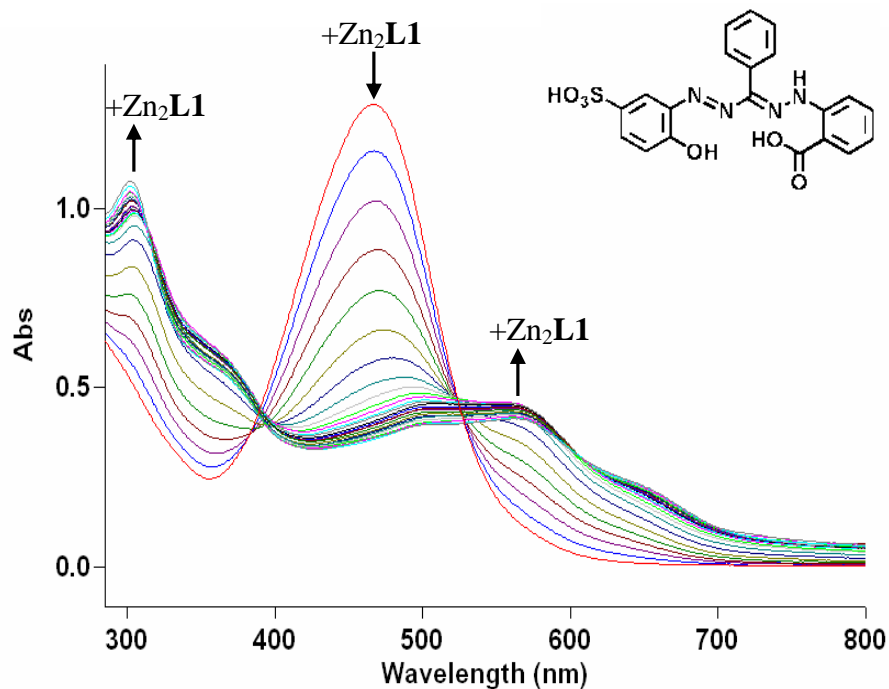


Figure 5.13. Titration of pyrocatechol violet (PV). (A) Structure of the indicator superimposed on UV-vis spectra collected as the indicator was titrated with $\text{Zn}_2\text{L1}$, and (B) Benesi-Hildebrand plot of spectral data points (blue diamonds) and the linear fit (black line) used to calculate K_d . The equation and R^2 value for the linear fit are displayed in the upper right hand corner of the plot. This variation of the classic Benesi-Hildebrand method is based on a treatment described in reference 68 (note that slope does not equal K_d directly).

(A)



(B)

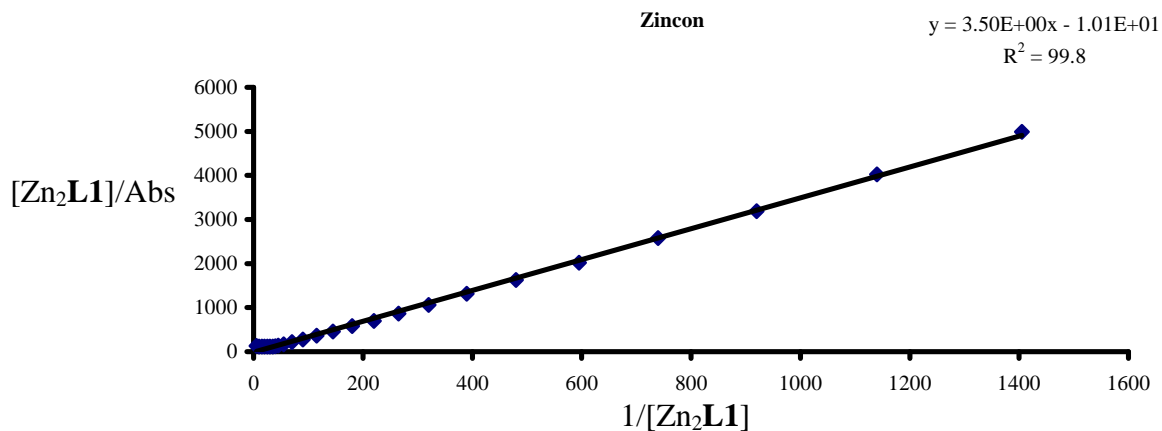


Figure 5.14. Titration of zincon (ZC). (A) Structure of the indicator superimposed on UV-vis spectra collected as the indicator was titrated with Zn₂L1, and (B) Benesi-Hildebrand plot of spectral data points (blue diamonds) and the linear fit (black line) used to calculate K_d . The equation and R^2 value for the linear fit are displayed in the upper right hand corner of the plot. This variation of the classic Benesi-Hildebrand method is based on a treatment described in reference 68 (note that slope does not equal K_d directly).

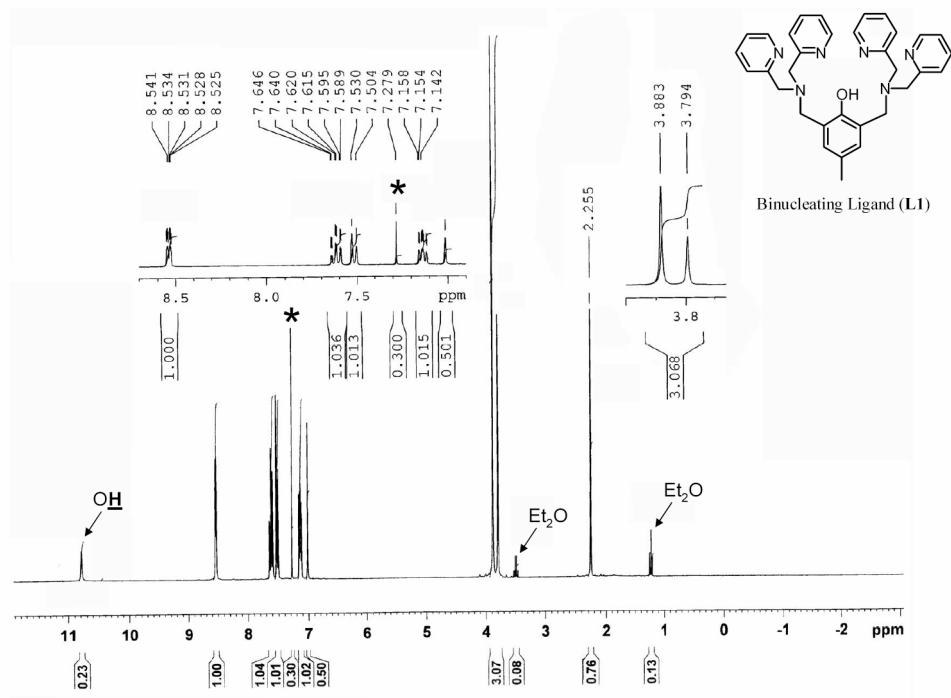


Figure 5.15. Proton NMR spectrum of H-L1 (CDCl_3 , 300 MHz). Peak marked with an asterisk is due to residual solvent signal. Some residual diethyl ether from recrystallization is also present.

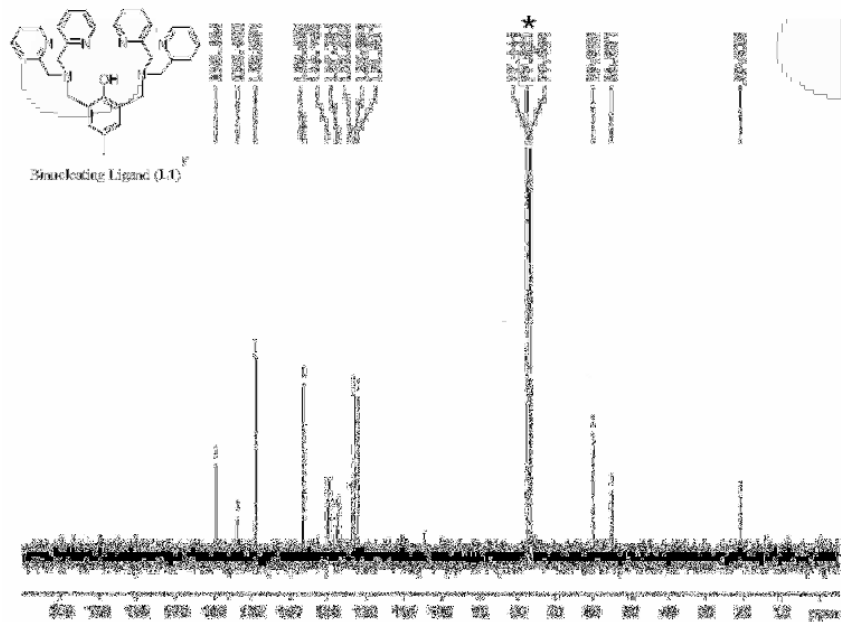


Figure 5.16. Carbon-13 NMR spectrum of H-L1 (CDCl_3 , 75 MHz). The peak labeled with an asterisk is due to CDCl_3 .

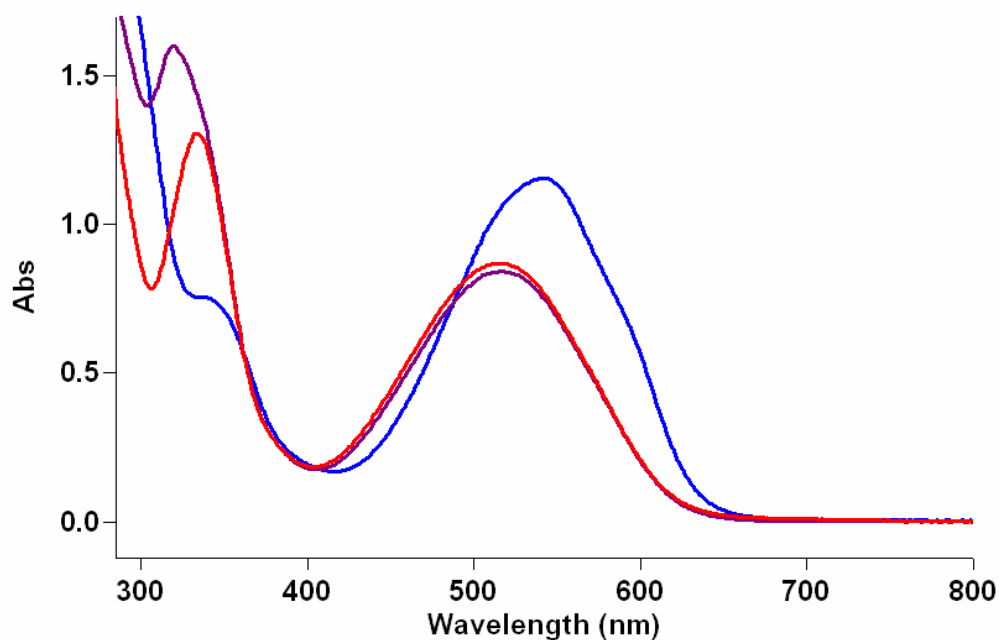
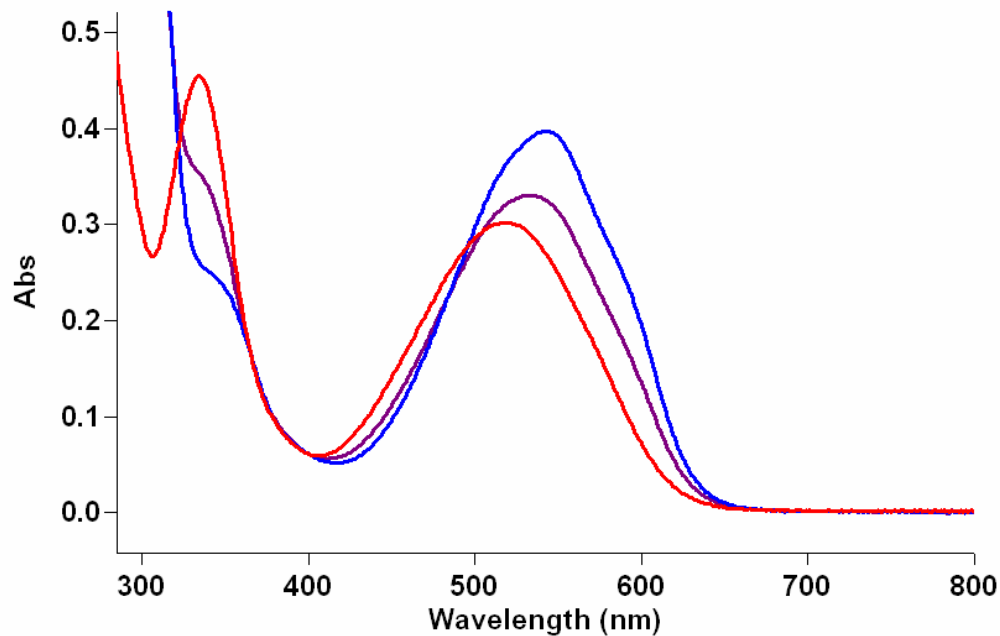


Figure 5.17. Phosphate (top) and pyrophosphate (bottom) displacement tests for alizarin red S (**ARS**). The red trace corresponds to the indicator alone, the blue trace corresponds to the (indicator)- Zn_2L1 complex, and the purple trace corresponds to (indicator)- Zn_2L1 complex plus the anion.

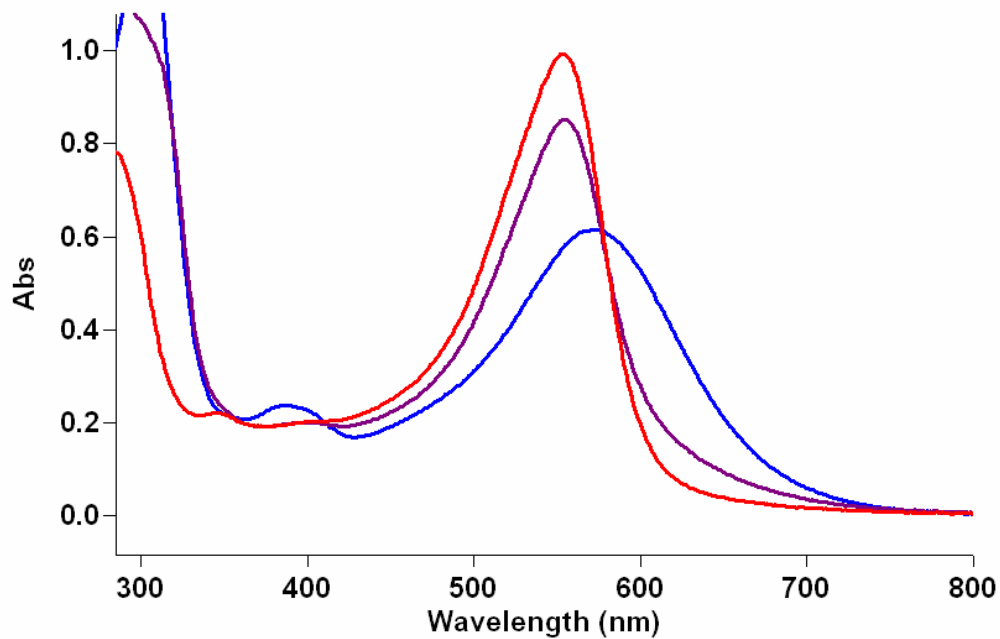
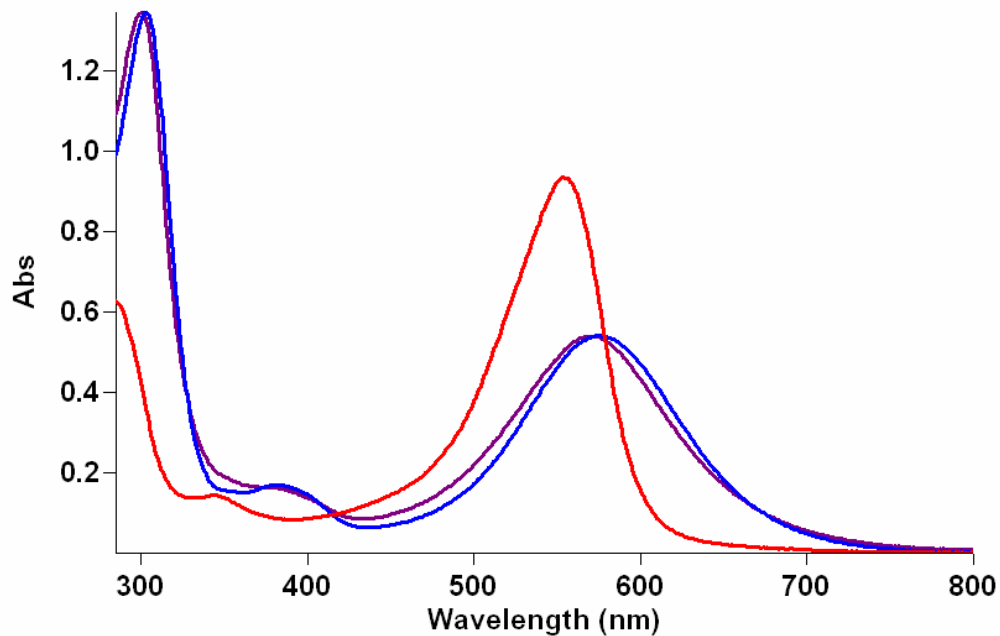


Figure 5.18. Phosphate (top) and pyrophosphate (bottom) displacement tests for bromo pyrogallol red (**BPR**). The red trace corresponds to the indicator alone, the blue trace corresponds to the (indicator)- Zn_2L1 complex, and the purple trace corresponds to (indicator)- Zn_2L1 complex plus the anion.

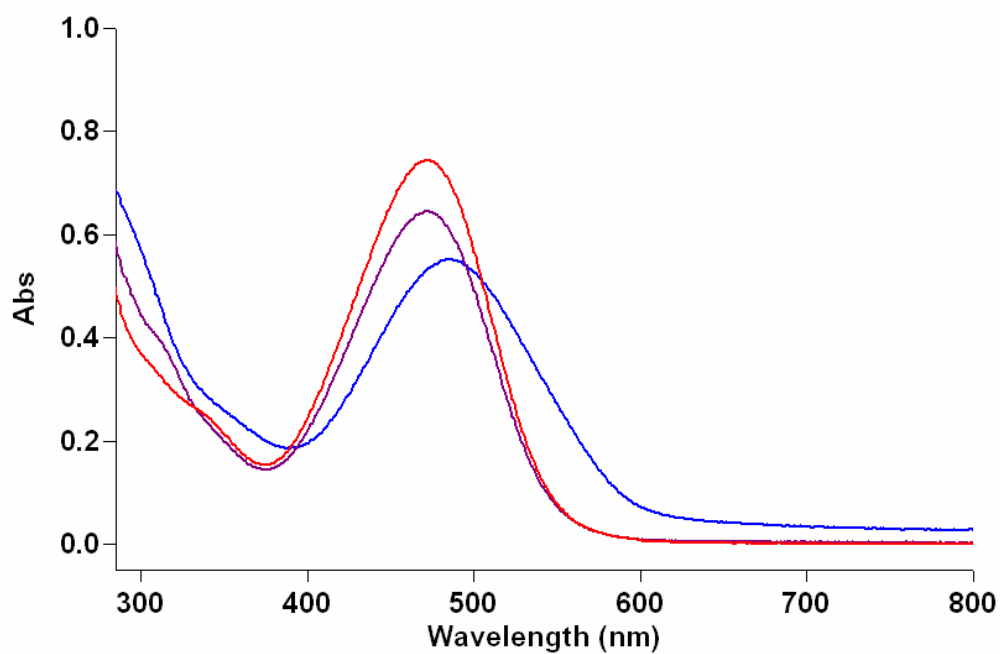
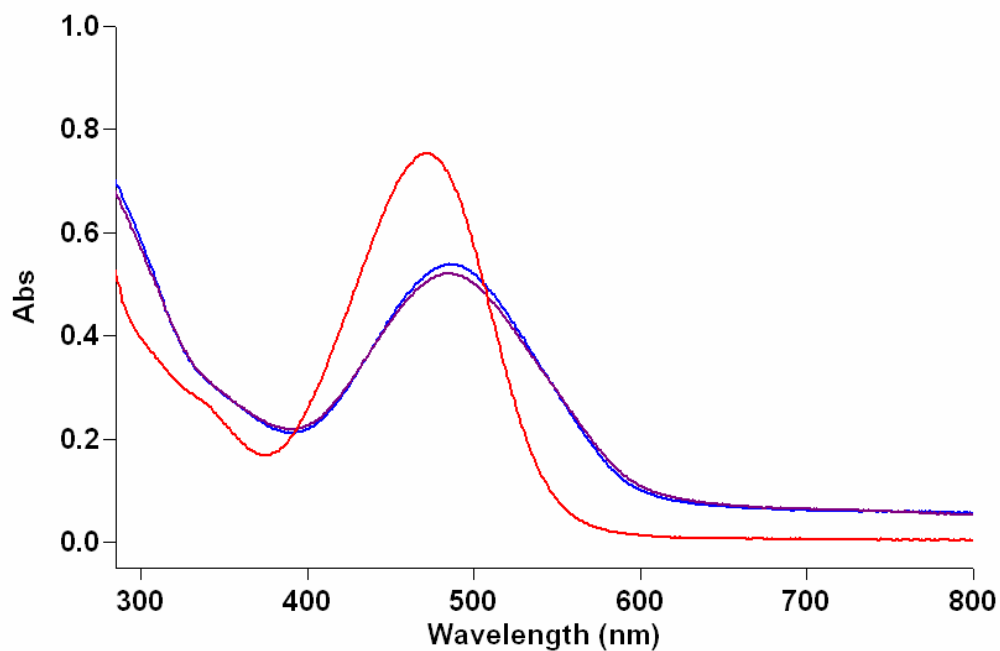


Figure 5.19. Phosphate (top) and pyrophosphate (bottom) displacement tests for dithizone (**DT**). The red trace corresponds to the indicator alone, the blue trace corresponds to the (indicator)- Zn_2L1 complex, and the purple trace corresponds to (indicator)- Zn_2L1 complex plus the anion. Approximately 1 min is required for displacement to reach equilibrium.

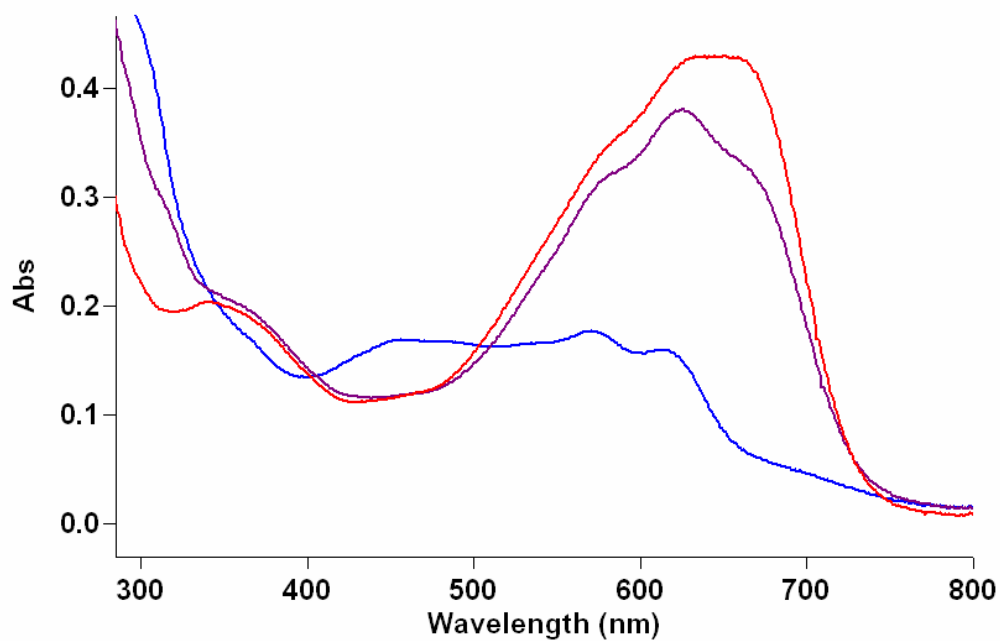
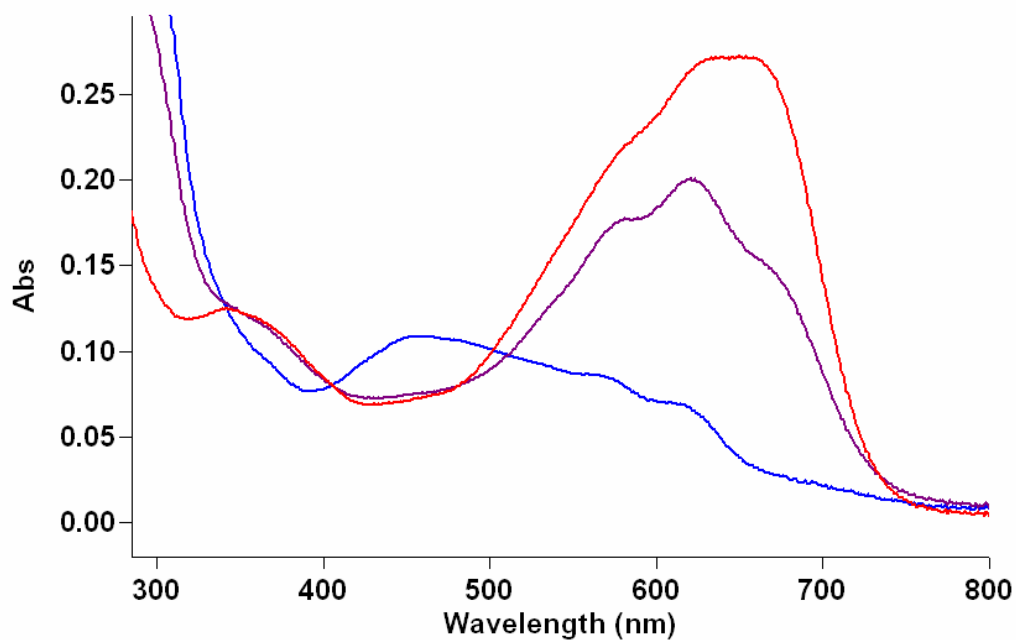


Figure 5.20. Phosphate (top) and pyrophosphate (bottom) displacement tests for eriochrome blue black B (**EBBB**). The red trace corresponds to the indicator alone, the blue trace corresponds to the (indicator)- Zn_2L1 complex, and the purple trace corresponds to (indicator)- Zn_2L1 complex plus the anion.

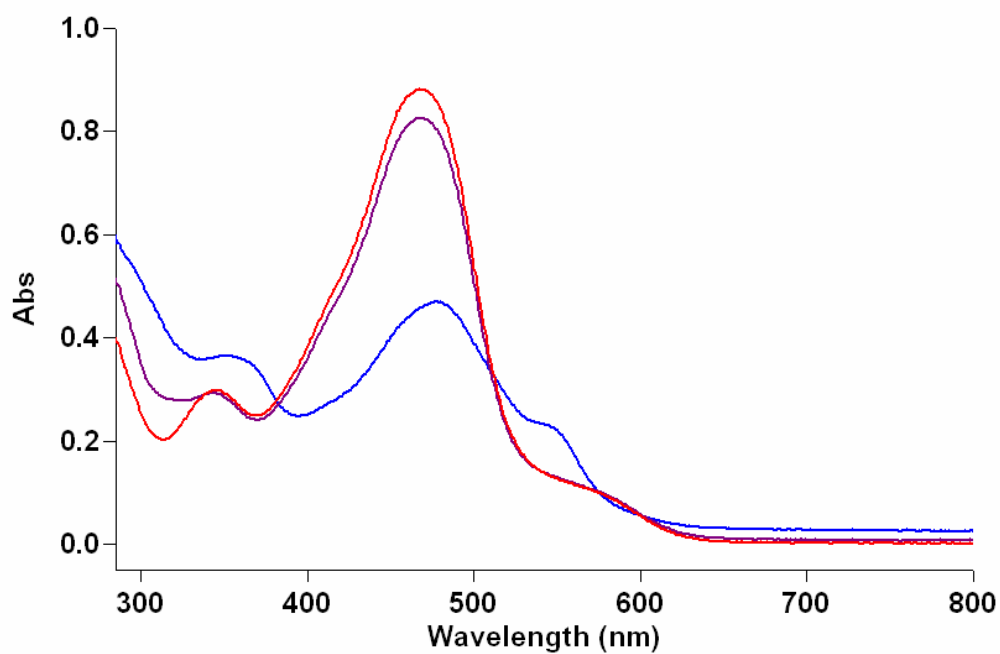
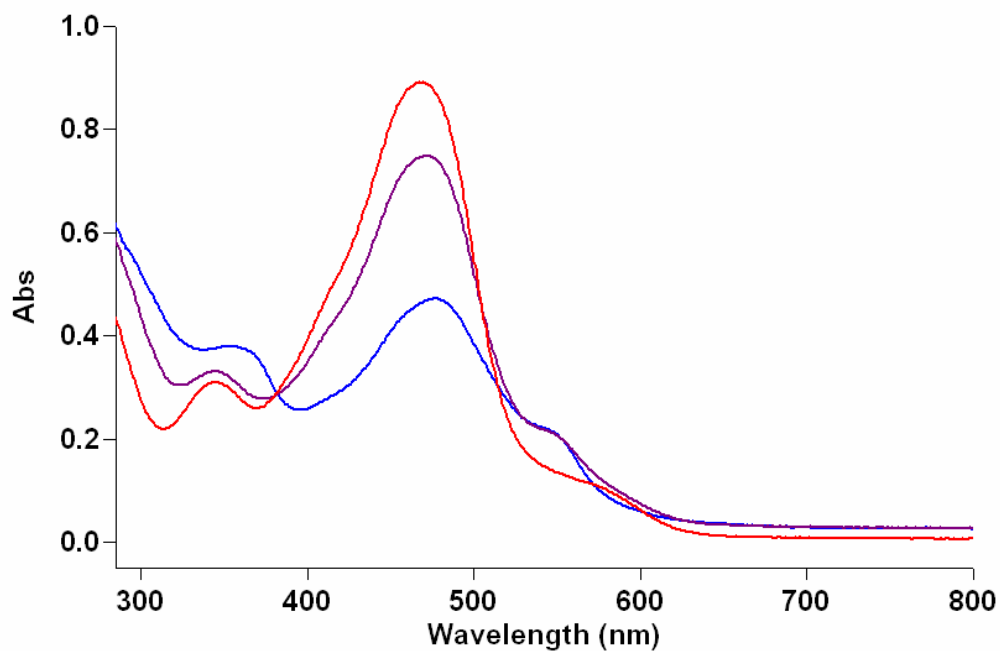


Figure 5.21. Phosphate (top) and pyrophosphate (bottom) displacement tests for eriochrome red B (**ERB**). The red trace corresponds to the indicator alone, the blue trace corresponds to the (indicator)-Zn₂L1 complex, and the purple trace corresponds to (indicator)-Zn₂L1 complex plus the anion.

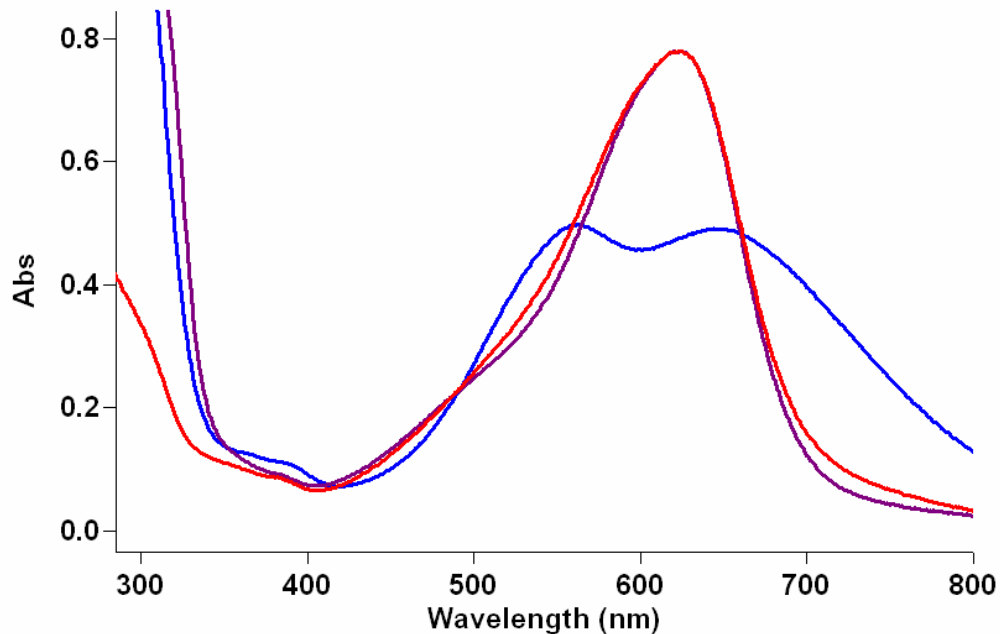
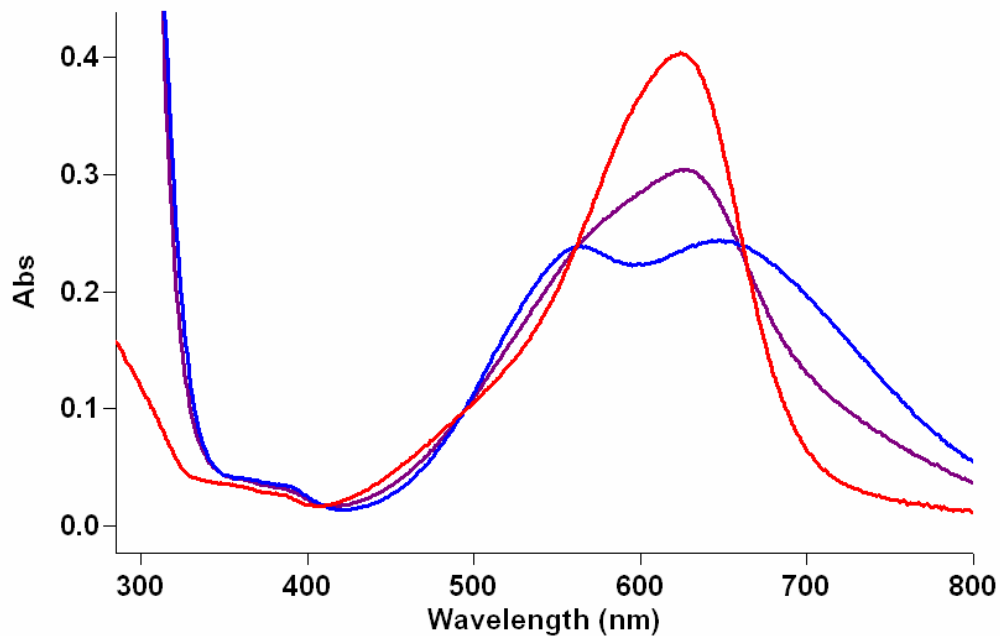


Figure 5.22. Phosphate (top) and pyrophosphate (bottom) displacement tests for gallocyanine (**GC**). The red trace corresponds to the indicator alone, the blue trace corresponds to the (indicator)- $\text{Zn}_2\text{L1}$ complex, and the purple trace corresponds to (indicator)- $\text{Zn}_2\text{L1}$ complex plus the anion.

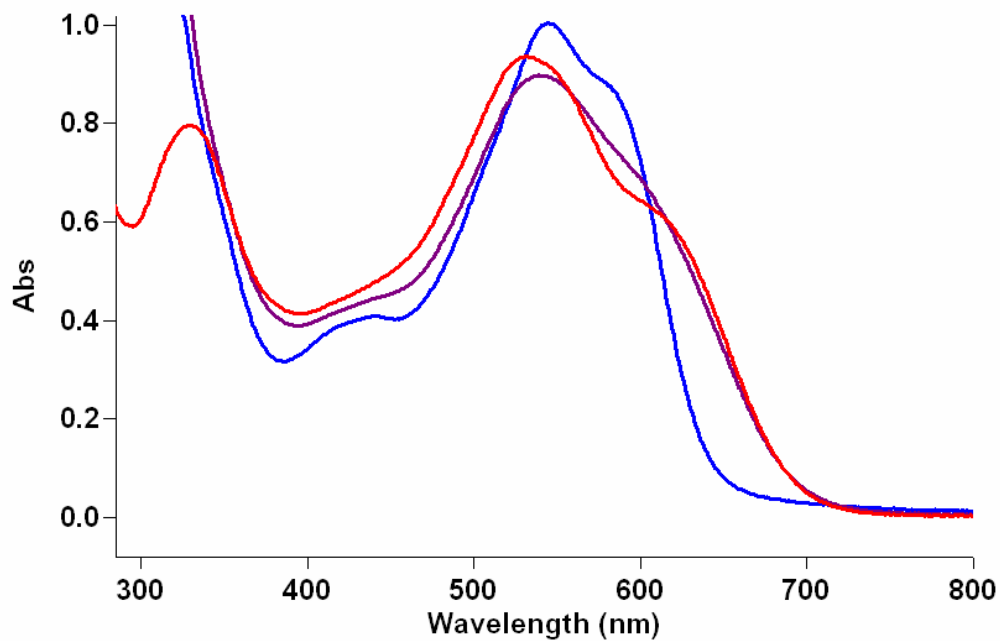
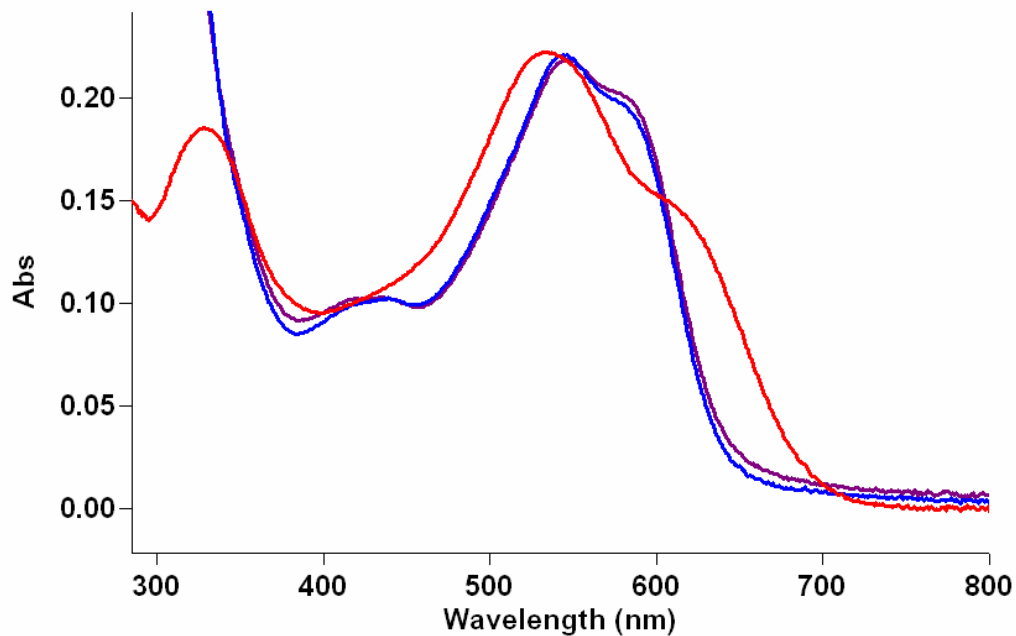


Figure 5.23. Phosphate (top) and pyrophosphate (bottom) displacement tests for mordant blue 9 (**MB9**). The red trace corresponds to the indicator alone, the blue trace corresponds to the (indicator)- Zn_2L1 complex, and the purple trace corresponds to (indicator)- Zn_2L1 complex plus the anion.

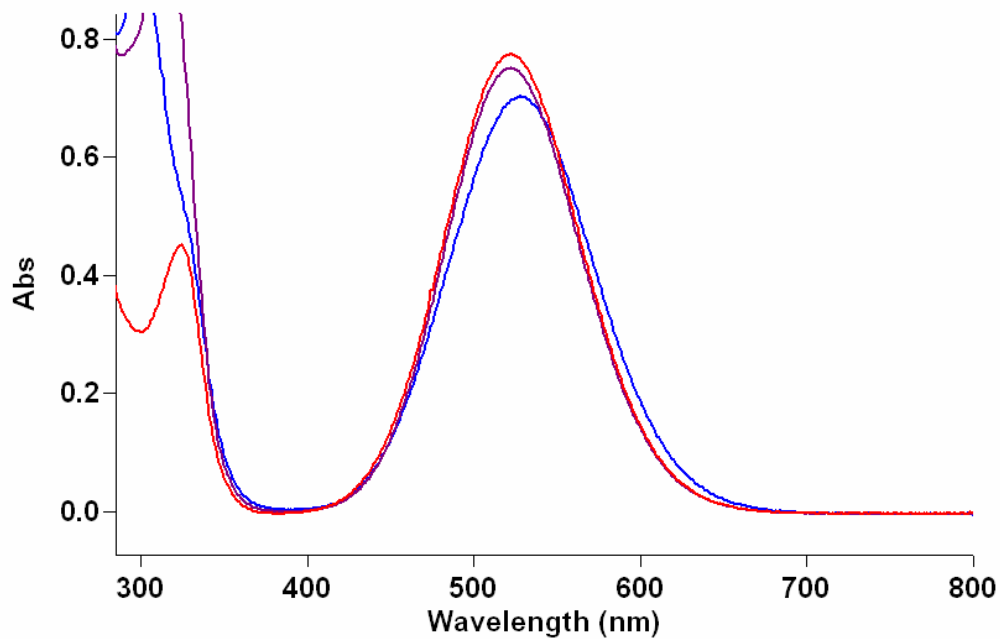
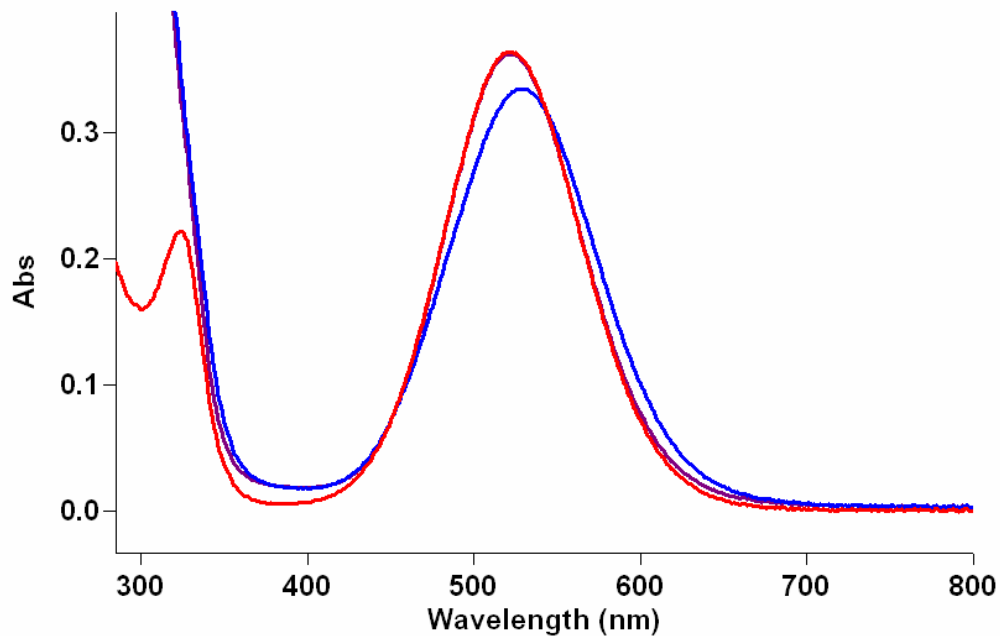


Figure 5.24. Phosphate (top) and pyrophosphate (bottom) displacement tests for murexide (**MX**). The red trace corresponds to the indicator alone, the blue trace corresponds to the (indicator)- Zn_2L1 complex, and the purple trace corresponds to (indicator)- Zn_2L1 complex plus the anion.

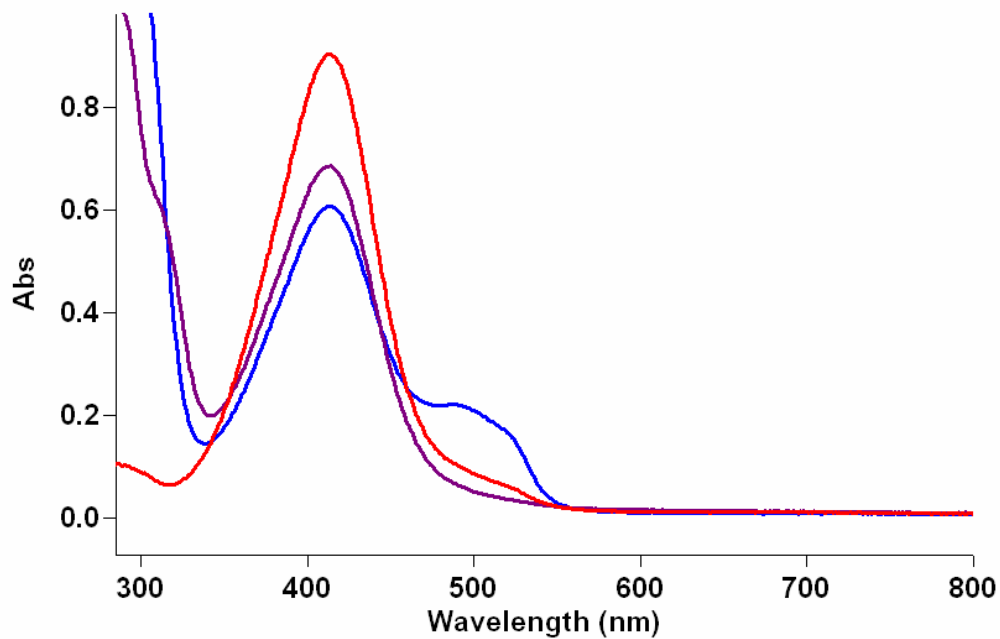
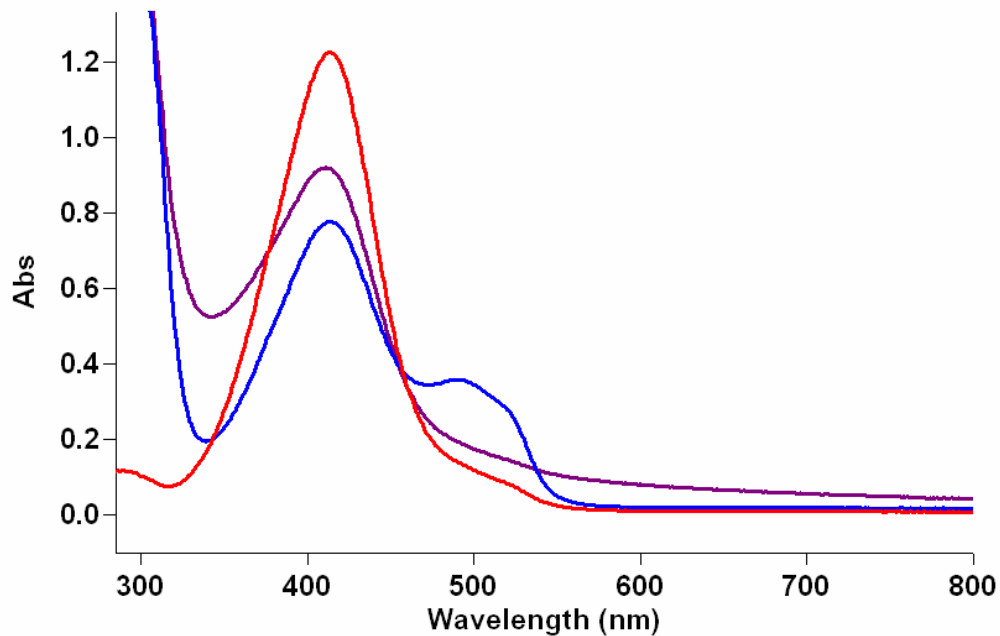


Figure 5.25. Phosphate (top) and pyrophosphate (bottom) displacement tests for 4-(pyridin-2-ylazo)resorcinol (**PAR**). The red trace corresponds to the indicator alone, the blue trace corresponds to the (indicator)-Zn₂L₁ complex, and the purple trace corresponds to (indicator)-Zn₂L₁ complex plus the anion.

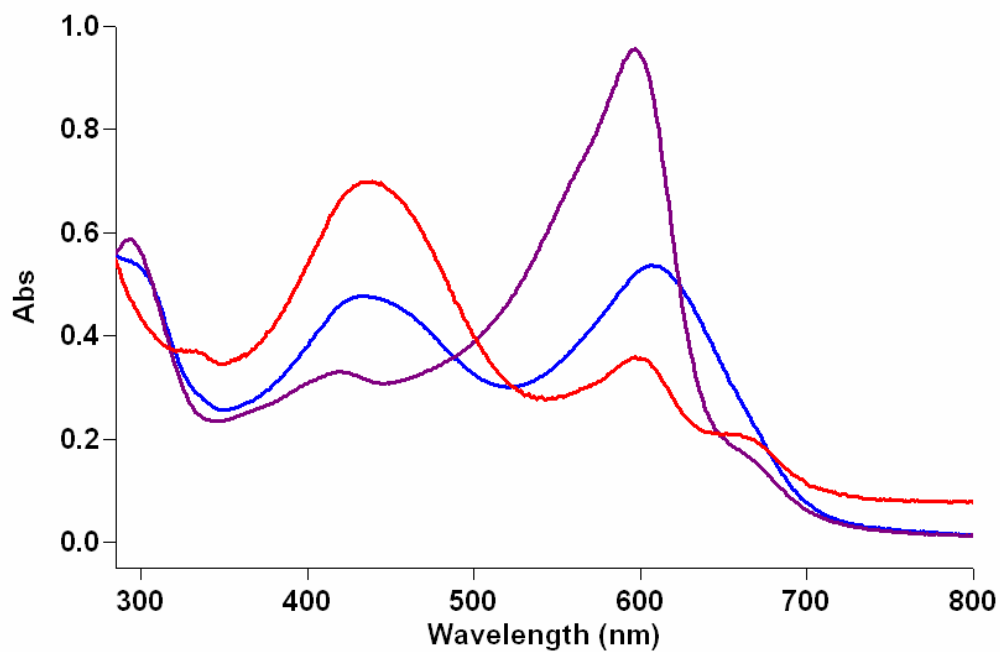
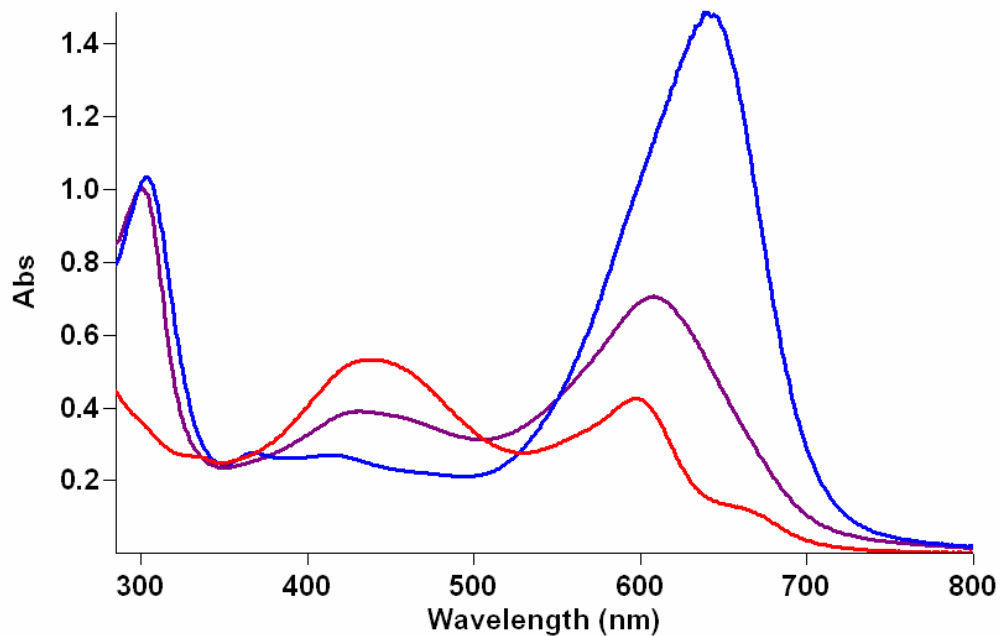


Figure 5.26. Phosphate (top) and pyrophosphate (bottom) displacement tests for pyrocatechol violet (**PV**). The red trace corresponds to the indicator alone, the blue trace corresponds to the (indicator)- Zn_2L1 complex, and the purple trace corresponds to (indicator)- Zn_2L1 complex plus the anion.

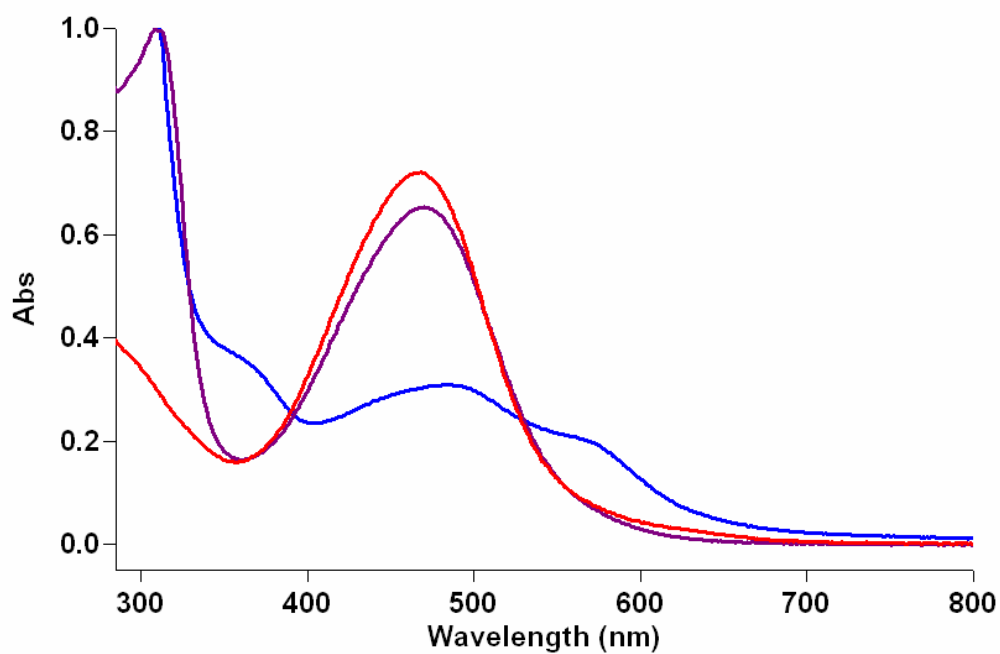
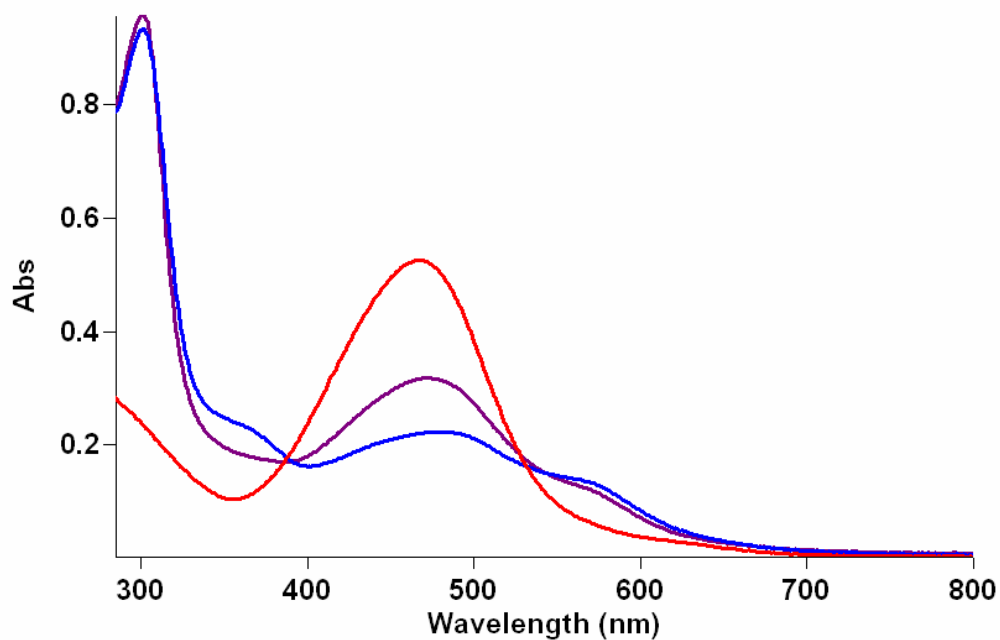


Figure 5.27. Phosphate (top) and pyrophosphate (bottom) displacement tests for zincon (**ZC**). The red trace corresponds to the indicator alone, the blue trace corresponds to the (indicator)- $\text{Zn}_2\text{L1}$ complex, and the purple trace corresponds to (indicator)- $\text{Zn}_2\text{L1}$ complex plus the anion.

5.6 References

1. Berg, J. M.; Tymoczko, J. L.; Stryer, L.; Stryer, L., *Biochemistry*. 5th ed.; W.H. Freeman: New York, **2002** p 4.
2. Raghothama, K. G., *Annual Review of Plant Physiology and Plant Molecular Biology* **1999**, *50*, 665-693.
3. Lagerlof, F.; Oliveby, A., *Advances in Dental Research* **1994**, *8*, 229-238.
4. Haub, M. D., *Nutritional Ergogenic Aids* **2004**, 257-273.
5. Horton, H. R.; Moran, L. A.; Scrimgeour, K. G.; Perry, M. D.; Rawn, J. D., *Principles of Biochemistry*. 4 ed.; Pearson Prentice Hall, : Upper Saddle River, NJ, 2006 p 27.
6. Deutscher, J.; Editor, *Ser/Thr/Tyr Protein Phosphorylation in Bacteria, A Written Symposium*. [In: *J. Mol. Microbiol. Biotechnol.*; 2005, 9(3-4)]. 2005; p 112.
7. Uchida, T.; Editor, *Protein Phosphorylation: Dysregulation and Diseases*. [In: *Mol. Med. (Tokyo, Jpn.)*, 2004; 41(5)]. 2004; p 89.
8. Soederberg, M.; Edlund, C.; Kristensson, K.; Dallner, G., *Lipids* **1991**, *26*, 421-425.
9. Calderini, G.; Aporti, F.; Bonetti, A. C.; Zanotti, A.; Toffano, G., *Progress in Clinical and Biological Research* **1985**, *192*, 383-386.
10. Mattson, M. P.; Editor, *Protein Phosphorylation in Aging and Age-Related Disease*. 2004; p 178.
11. Yang, Y.-C., *Accounts of Chemical Research* **1999**, *32*, 109-115.
12. Yang, Y.-C.; Baker, J. A.; Ward, J. R., *Chemical Reviews* **1992**, *92*, 1729-1743.

13. Pope, C.; Karanth, S.; Liu, J., *Environmental Toxicology and Pharmacology* **2005**, *19*, 433-446.
14. Sierra, M., *Environmental Science and Pollution Control Series* **1994**, *10*, 145-149.
15. Rajan, S. S. S.; Marwaha, B. C., *Fertilizer Research* **1993**, *35*, 47-59.
16. Chien, S. H.; Sale, P. W. G.; Friesen, D. K., *Fertilizer Research* **1990**, *24*, 149-157.
17. Wiskur, S. L.; Ait-Haddou, H.; Lavigne, J. J.; Anslyn, E. V., *Accounts of Chemical Research* **2001**, *34*, 963-972.
18. Nguyen, B. T.; Anslyn, E. V., *Coordination Chemistry Reviews* **2006**, *250*, 3118-3127.
19. Folmer-Andersen, J. F.; Lynch, V. M.; Anslyn, E. V., *Chemistry A European Journal* **2005**, *11*, 5319-5326.
20. Aiet-Haddou, H.; Wiskur, S. L.; Lynch, V. M.; Anslyn, E. V., *Journal of the American Chemical Society* **2001**, *123*, 11296-11297.
21. Wiskur, S. L.; Lavigne, J. J.; Metzger, A.; Tobey, S. L.; Lynch, V.; Anslyn, E. V., *Chemistry A European Journal* **2004**, *10*, 3792-3804.
22. Lavigne, J. J.; Anslyn, E. V., *Angewandte Chemie, International Edition*. **1999**, *38*, 3666-3669.
23. Wiskur, S. L.; Anslyn, E. V., *Journal of the American Chemical Society* **2001**, *123*, 10109-10110.
24. McCleskey, S. C.; Floriano, P. N.; Wiskur, S. L.; Anslyn, E. V.; McDevitt, J. T., *Tetrahedron* **2003**, *59*, 10089-10092.

25. Piatek, A. M.; Bomble, Y. J.; Wiskur, S. L.; Anslyn, E. V., *Journal of the American Chemical Society* **2004**, *126*, 6072-6077.
26. Nguyen, B. T.; Wiskur, S. L.; Anslyn, E. V., *Organic Letters* **2004**, *6*, 2499-2501.
27. Bonizzoni, M.; Fabbrizzi, L.; Piovani, G.; Taglietti, A., *Tetrahedron* **2004**, *60*, 11159-11162.
28. Fabbrizzi, L.; Foti, F.; Taglietti, A., *Organic Letters* **2005**, *7*, 2603-2606.
29. Hortala, M. A.; Fabbrizzi, L.; Marcotte, N.; Stomeo, F.; Taglietti, A., *Journal of the American Chemical Society* **2003**, *125*, 20-21.
30. Fabbrizzi, L.; Licchelli, M.; Taglietti, A., *Dalton Transactions* **2003**, 3471-3479.
31. Fabbrizzi, L.; Marcotte, N.; Stomeo, F.; Taglietti, A., *Angewandte Chemie, International Edition* **2002**, *41*, 3811-3814.
32. Boiocchi, M.; Bonizzoni, M.; Fabbrizzi, L.; Piovani, G.; Taglietti, A., *Angewandte Chemie, International Edition*. **2004**, *43*, 3847-3852.
33. Lim, M. H.; Lippard, S. J., *Inorganic Chemistry* **2004**, *43*, 6366-6370.
34. Hilderbrand, S. A.; Lim, M. H.; Lippard, S. J., *Journal of the American Chemical Society* **2004**, *126*, 4972-4978.
35. Lim, M. H.; Xu, D.; Lippard, S. J., *Nature Chemical Biology* **2006**, *2*, 375-380.
36. Lim, M. H.; Lippard, S. J., *Journal of the American Chemical Society* **2005**, *127*, 12170-12171.
37. Tobey, S. L.; Anslyn, E. V., *Organic Letters* **2003**, *5*, 2029-2031.
38. Knapton, D.; Burnworth, M.; Rowan, S. J.; Weder, C., *Angewandte Chemie, International Edition* **2006**, *45*, 5825-5829.

39. Leevy, W. M.; Gammon, S. T.; Jiang, H.; Johnson, J. R.; Maxwell, D. J.; Jackson, E. N.; Marquez, M.; Piwnica-Worms, D.; Smith, B. D., *Journal of the American Chemical Society* **2006**, *128*, 16476-16477.
40. Leevy, W. M.; Johnson, J. R.; Lakshmi, C.; Morris, J.; Marquez, M.; Smith, B. D., *Chemical Communications* **2006**, 1595-1597.
41. Hanshaw, R. G.; Lakshmi, C.; Lambert, T. N.; Johnson, J. R.; Smith, B. D., *ChemBioChem* **2005**, *6*, 2214-2220.
42. Hanshaw, R. G.; Smith, B. D., *Bioorganic Medicinal Chemistry* **2005**, *13*, 5035-5042.
43. Lee, H. N.; Swamy, K. M. K.; Kim, S. K.; Kwon, J.-Y.; Kim, Y.; Kim, S.-J.; Yoon, Y. J.; Yoon, J., *Organic Letters* **2007**, *9*, 243-246.
44. Jang, Y. J.; Jun, E. J.; Lee, Y. J.; Kim, Y. S.; Kim, J. S.; Yoon, J., *Journal of Organic Chemistry* **2005**, *70*, 9603-9606.
45. Shiraishi, H.; Jikido, R.; Matsufuji, K.; Nakanishi, T.; Shiga, T.; Ohba, M.; Sakai, K.; Kitagawa, H.; Okawa, H., *Bulletin of the Chemical Society of Japan* **2005**, *78*, 1072-1076.
46. Matsufuji, K.; Shiraishi, H.; Miyasato, Y.; Shiga, T.; Ohba, M.; Yokoyama, T.; Okawa, H., *Bulletin of the Chemical Society of Japan* **2005**, *78*, 851-858.
47. Adams, H.; Bradshaw, D.; Fenton, D. E., *Inorganic Chimica Acta* **2002**, *332*, 195-200.
48. Karlin, K. D.; Gultneh, Y.; Nicholson, T.; Zubieta, J., *Inorganic Chemistry* **1985**, *24*, 3727-3729.

49. Hanshaw, R. G.; O'Neil, E. J.; Foley, M.; Carpenter, R. T.; Smith, B. D., *Journal of Materials Chemistry* **2005**, *15*, 2707-2713.
50. Han, M. S.; Kim, D. H., *Angewandte Chemie, International Edition* **2002**, *41*, 3809-3811.
51. O'Neil, E. J.; Smith, B. D., *Coordination Chemistry Reviews* **2006**, *250*, 3068-3080.
52. Schwarzenbach, G., *Complexometric Titrations*. . Interscience Publishers: London, 1957 p 138.
53. Surak, J. G.; Herman, M. F.; Haworth, D. T., *Analytical Chemistry* **1965**, *37*, 428-429.
54. Cano-Raya, C.; Fernandez-Ramos, M. D.; Capitan-Vallvey, L. F., *Analytical Chimica Acta* **2006**, *555*, 299-307.
55. Islam, M.; Khanin, M.; Sadik, O. A., *Biomacromolecules* **2003**, *4*, 114-121.
56. Drennan, C. E.; Hughes, R. J.; Reinsborough, V. C.; Soriyan, O. O., *Canadian Journal of Chemistry* **1998**, *76*, 152-157.
57. Andac, M.; Asan, A.; Isildak, I., *Journal of Chemical Crystallography* **2003**, *33*, 599-603.
58. Biswas, S.; Chowdhury, B.; Ray, B. C., *Analytical Letters* **2004**, *37*, 1965-1979.
59. Bell, R. D.; Doisy, E. A., *Journal of Biological Chemistry* **1920**, *44*, 55-67.
60. Suzuki, M.; Kanatomi, H.; Murase, I., *Chemistry Letters* **1981**, 1745-1748.
61. Han, M. S.; Kim, D. H., *Bioorganic & Medicinal Chemistry Letters* **2003**, *13*, 1079-1082.
62. Freixa, Z.; Van Leeuwen, P. W. N. M., *Dalton Transactions* **2003**, 1890-1901.

63. Lee, H. M.; Lu, C. Y.; Chen, C. Y.; Chen, W. L.; Lin, H. C.; Chiu, P. L.; Cheng, P. Y., *Tetrahedron* **2004**, *60*, 5807-5825.
64. Hanshaw, R. G.; Hilkert, S. M.; Jiang, H.; Smith, B. D., *Tetrahedron Letters* **2004**, *45*, 8721-8724.
65. Nolan, E. M.; Ryu, J. W.; Jaworski, J.; Feazell, R. P.; Sheng, M.; Lippard, S. J., *Journal of the American Chemical Society* **2006**, *128*, 15517-15528.
66. Walkup, G. K.; Burdette, S. C.; Lippard, S. J.; Tsien, R. Y., *Journal of the American Chemical Society* **2000**, *122*, 5644-5645.
67. Burdette, S. C.; Walkup, G. K.; Spingler, B.; Tsien, R. Y.; Lippard, S. J., *Journal of the American Chemical Society* **2001**, *123*, 7831-7841.
68. Hammond, P. R., *Journal of the Chemical Society* **1964**, 479-484.

CHAPTER 6

POLY(PARA-PHENYLENE ETHYNYLENE) INCORPORATING STERICALLY ENSHROUDING META-TERPHENYL OXACYCLOPHANE CANOPIES[#]

6.1 Introduction

The use of π -conjugated polymers (CPs)¹ as organic semiconductors have received a large flux in interest due to their wide variety of optoelectronic applications including organic light emitting diodes (OLEDs),² photovoltaics^{3,4} and sensing.⁵ The advantage of utilizing organic materials is their ease of synthetic manipulation. The large

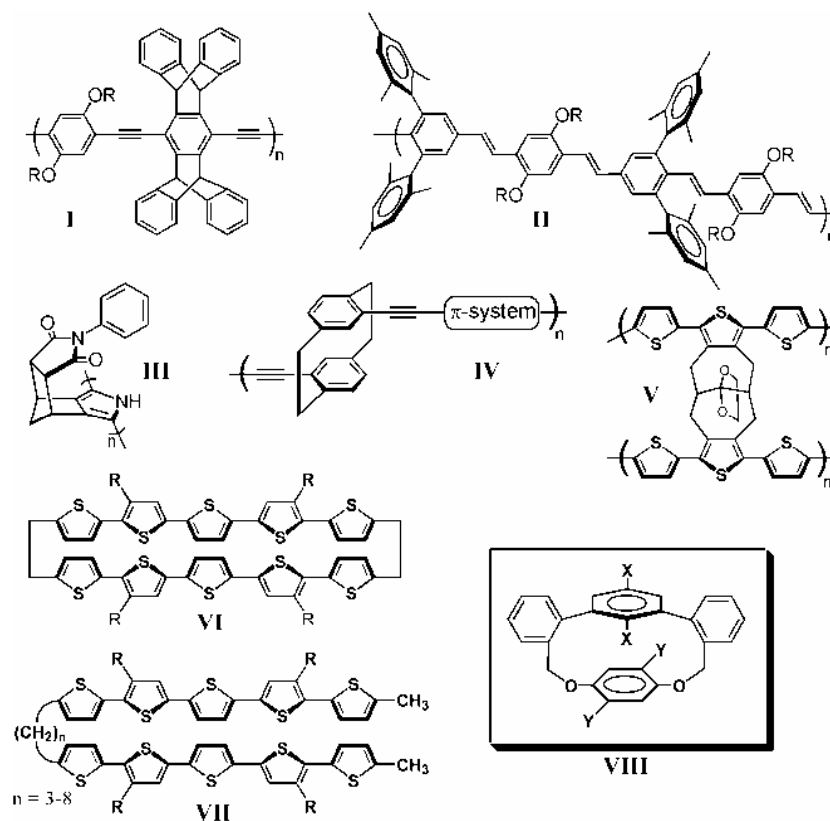


Figure 6.1 Examples of sterically-insulated CPs (I-III) and of covalently-scaffolded π -systems (IV-VII), and the oxacyclophane scaffold VIII used in the current work.

[#] Adapted from Morgan, B. P.; Gilliard, R. J.; Loungani, R. S.; Smith, R. C. *Macromol Rapid Commun.* **2009**, *30*, 2067-2078.

amount of synthetic knowledge allows for chemists to achieve target properties that allow for cost-effective polymer processing techniques.²

An array of optoelectronic properties including but not limited to band gap, charge carrier mobility, electrochemical potentials, as well as the absorption and photoluminescence profiles are all controlled by various morphological effects within polymers. These morphologies can be very difficult to control due to strong inter- and intra-chain effects. This gives rise to inconsistent measurements and has been a primary reason CPs have not progressed as initially anticipated.

The change in morphology from solution to solid state has been of particular interest and a vast amount of effort has been focused on this area. A great deal of effort has been focused on altering and carefully designing specific monomers that can translate their unique properties to CP's. One of the most difficult obstacles to overcome has been the control of interchain interactions and a commonly employed solution to this is to use bulky substituents to control the amount of these interactions. Specific target applications rely on the ability to achieve these interchain effects.

The limitation of exciton diffusion by charge transfer processes that depend on molecular morphology between the donor and acceptor elements are an example of a process in which interchain effects are desired as seen by bulk heterojunction-type organic solar cells (photovoltaics). OLEDs and various fluorescent sensors rely on the ability of CPs to exhibit high emission efficiencies and quantum yields however interchain interactions can lead to significant quenching of luminescence prohibiting these compounds from use towards these applications. To completely understand these interchain interactions a systematic approach is needed to fully understand how specific

changes in morphology effect optoelectronic properties. One approach has been the attachment of sterically encumbered sidechains such as bulky iptycene (**I**)⁶ or *m*-terphenyl subunits (**II**)⁷ and a polypyrrole derivative (**III**)⁸ featuring a sterically-encumbered “canopy” (**Figure 6.1**) to insulate these CPs and control these interchain interactions.

A large amount of the control of these interchain interactions arises from specific geometries in solution or solid state and the development of covalent or supramolecular⁹,¹⁰ scaffolds have been another approach to control interchain effects. These scaffolded CPs can have much more controlled interchain and intrachain interactions that dictate charge transfer/mobility and optical profiles of materials. These effects can also provide additional information into the formation of π -dimers which have been of recent interest. Small molecular models incorporating [2.2]paracyclophane¹¹ and related units (i.e., **IV**¹² and **VI**¹³ **Figure 6.1**) have been one of the most studied π -conjugated polymers that incorporate the covalently scaffolded approach. The ability for cyclophane scaffolds to have a constrained nature can be seen as an obstacle that must be avoided to prevent the distortion of their constituent π -systems. This can cause the inter- π -system distances to no longer reflect those likely to be observed in films of organic CPs in the ground state. To alleviate this additional distortion from cyclophane structures, less constrained systems have been designed (i.e., **V**¹⁴ and **VII**,¹⁵ **Figure 6.1**) in which more flexibility scaffolds were used. This additional flexibility allows inter- π -system distances and geometries to more accurately replicate properties observed for unscaffolded materials.

The difference in π -dimers formed upon oxidation of bis(oligothiophene)s scaffolded by different linkers (**VI** and **VII**, **Figure 6.1**)¹⁵ is a great example of how a

scaffold influences photophysics. The use of flexible alkyl linkers in materials of type **VII** demonstrate chain conformations in spectroelectrochemical responses that resemble those of untethered oligothiophenes. The use of two linkers as seen in **VI** gives rise to a more constrained system with greater inter- π -system interactions than the use of free oligo- and polythiophene derivatives (i.e., those used in devices). To correctly study the effects of interchain interactions in organic semiconductors the use of unstrained scaffolds is an essential part to give accurate models. The inter- π -system interaction distances must also be controlled to provide precise conclusions. The use of *m*-terphenyl-scaffolded oxacyclophanes (i.e., **VIII**, **Figure 6.1**),¹⁶⁻²¹ appeared to be a viable candidate for studying these interchain interactions. The ability for these oxacyclophanes to form π - π interaction distances of around 3.4–4.0 Å was of specific interest due to the similarity in distances in films of poly(*p*-phenylene vinylene) (PPV) and poly(*p*-phenylene ethynylene) (PPE) derivatives.²²⁻²⁵

The preparation of a sterically encumbered *m*-terphenyl oxacyclophane substituted with two aryl iodide substituents is a good example of a versatile monomer for π -conjugated polymers. The usage of aryl iodides allows for the easy preparation of a wide variety of compounds through C-C bond formation coupling reactions. A commonly employed reaction of that type is the Sonogashira-Hagihara coupling in which a poly(*p*-phenylene ethynylene) derivative can be synthesized. The incorporation of oxacyclophane units as canopies that shield one side of the π -system from interchain interactions gives rise to a unique polymer (**P1**) that has interesting photophysical properties. In dilute solution the photoluminescence spectra of (**P1**) compares well to a similar π -conjugated polymer that lacks a canopy (**P2**). The similarities in **P1** and **P2**

come about as a result of both consisting of a poly(*p*-phenylene ethynylene) derivative which is not disturbed by the presence of a steric canopy. This steric canopy however does lead to the diminished interchain interactions in the solid state. The increased permeability of **P1** can be envisioned over that of **P2** which enhances the kinetic response of **P1** to vapors of nitroorganics such as TNT.

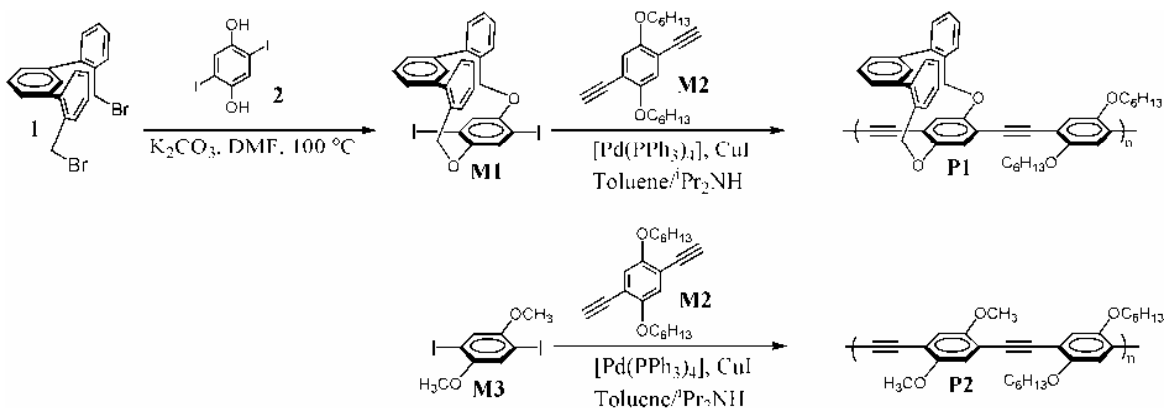
Novel canopies comprised by a *m*-terphenyl oxacyclophane units have been installed about a π -conjugated polymers backbone to shield one side of the π -system from interchain interactions and to scaffold π -stacking between the polymer and a canopy aryl ring. The photophysical properties of **P1** in dilute solution compare well to those of a poly(*p*-phenylene ethynylene) derivative (**P2**) that lacks the canopy, indicating little solution state influence of the voluminous macrocyclic subunits. In the solid state, however, the influence of the canopies is dramatic. Canopied **P1** exhibits an enhanced kinetic response to vapors of explosives and explosive stimulant nitroorganics such as TNT due to enhanced permeability of the films. This property portends utility of canopied fluorescent polymers for the detection of improvised explosive devices and in other security applications.

We envisioned that scaffold **VIII** could be modified to include π -systems at any of the sites X and Y. The presence of *m*-terphenyl substituents should also insulate appended π -systems from extraneous undesired interchain interactions (cf. **II**). Furthermore, this class of oxacyclophanes includes cuppedophanes and cappedophanes^{16-18,26} that were developed as hosts for inclusion compounds, suggesting that their incorporation into CPs could provide a new class of stimuli-responsive materials.

As a first step towards developing CPs featuring *m*-terphenyl oxacyclophanes, we sought to incorporate the oxacyclophane core **VIII** into a PPE derivative in which the PPE polymer was appended to sites Y. This involved the development of a *m*-terphenyl oxacyclophane canopied monomer and initial testing of **P1** films for response to nitroaromatic vapors.

6.2 Results and Discussion

The reaction of 1,3-bis(2-bromomethylphenyl)benzene (**1**) and 2,5-diiodohydroquinone (**2**) in the presence of a stirred suspension of K_2CO_3 in DMF at $90^\circ C$ yielded the key monomer **M1** (Scheme 6.1) at a 64% yield following a modification of the oxacyclophane preparation reported by Hart.²¹ The formation of macrocyclic ring structures such as **M1** have been shown to be difficult if the ring size does not allow for the correct accommodation of molecular geometries and creates strain within the ring. The formation of the 15-membered ring in **M1** was driven towards completion by the use of a syringe pump to add a solution of **1** and **2** over 100 h to the suspension of K_2CO_3 at $100^\circ C$ which increased the yield by more than 54 % over similar reactions at room temperature.



Scheme 6.1 Synthetic route to **P1** and **P2**.

This is in contrast to what was observed by Hart in which he was able to obtain good yields (~40-80%) for the oxacyclophanes he prepared at room temperature. The main difference in the oxacyclophanes prepared by Hart was that they did not contain any bulky iodo substituents that were incorporated in **M1**. It was thus anticipated that more thermal energy may be required to assist in the formation of the more hindered

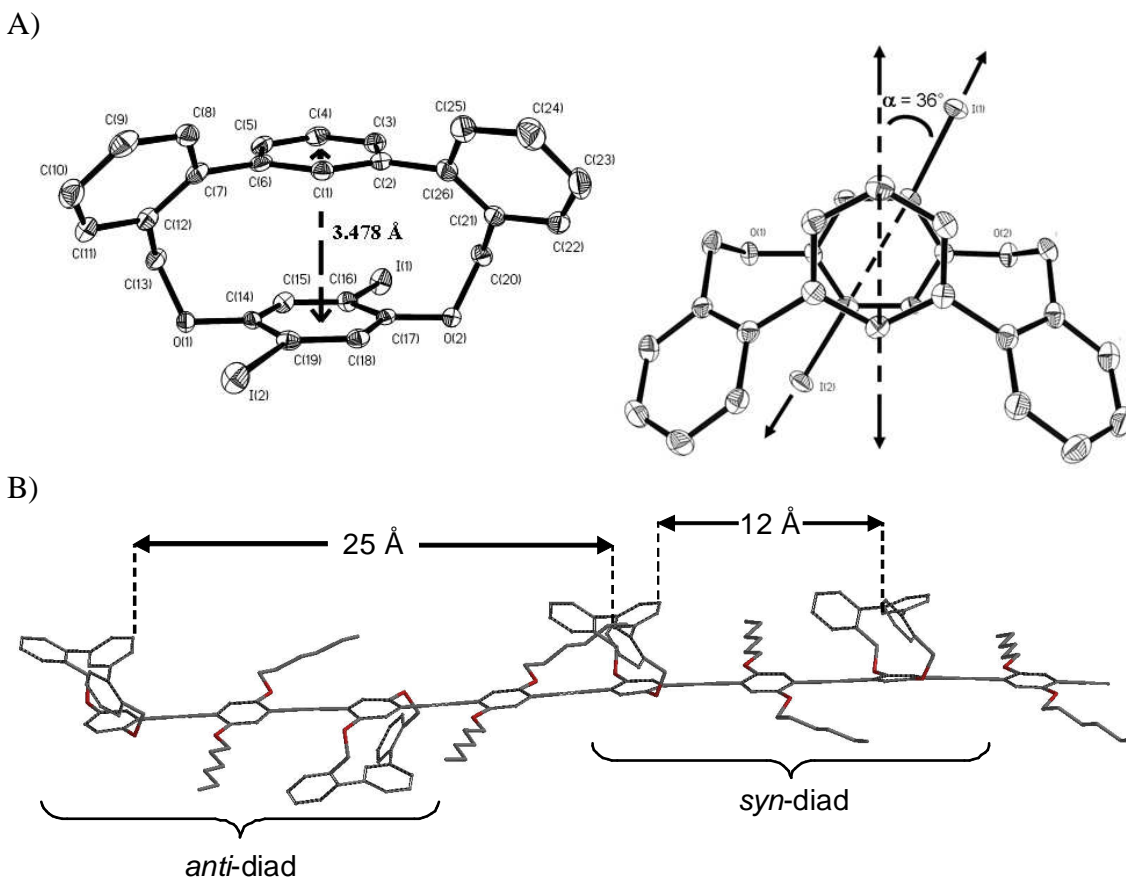


Figure 6.2. A) ORTEP drawing (left) and numbering scheme for **M1** (50% probability ellipsoids) H atoms are omitted for clarity. **M1** is chiral, with the two enantiomers present in a 1:1 ratio in the unit cell, but only one of the two isomers is shown here. An alternate rendering of **M1** as viewed looking down through the upper ring, demonstrating the offset angle between upper arene and lower arene is shown on the right. B) Optimized geometry (semi-empirical PM3-level) indicating possible arrangements of canopy substituents around the backbone in a section of polymer **P1** demonstrating the size of molecular clefts and structure of *syn*- and *anti*-diads.

macrocycle. Indeed, a notable improvement to 62% yield was accomplished when the reaction was repeated at 100 °C. The diffusion of pentane into a saturated CH_2Cl_2 solution of **M1** at room temperature gave analytically pure, X-ray quality crystals which were then characterized by ^1H and ^{13}C NMR spectrometry, single crystal X-ray diffraction and elemental combustion analysis.

The single crystal X-ray diffraction of the colorless plates of **M1** that formed from solvent diffusion gave a final R1 indices from $I > 2\sigma(I)$ of 0.0334 and a wR2 of 0.0777. An ORTEP drawing of **M1** is shown in **Figure 6.2A** and one of the features of interest in the current context are the absence of π -system distortion as seen by the lack of excess strain in this scaffold. Another salient feature of **M1** are the nearly parallel planes of the upper aryl ring (comprised of C(1)–C(6)) and the lower aryl ring (comprised of C(14)–C(19)), with a centroid-centroid distance of 3.478 Å. The ability for π -stacking effects is well within the centroid-centroid distance observed in **M1** and the geometry indicates a face-to-face stacking interaction between rings. This was also evident within the aromatic resonances in the ^1H NMR spectrum of **M1** from 6.4 to 7.7 ppm in which there was a wide distribution of resonances due to the π -stacking effect between the two aryl rings

Table 6.1 Select photophysical properties of **P1** and **P2** solutions in tetrahydrofuran.

	Absorbance		Photoluminescence		
	$\lambda_{\text{max}}^{\text{a}}$	$\log \epsilon^{\text{b}}$	$\lambda_{\text{ex}}^{\text{a}}$	$\lambda_{\text{em}}^{\text{a}}$	Φ
P1	427	4.65	430	462	0.57
P2	427	4.69	430	472	0.50

^a in units of nm

^b in units of $\text{M}^{-1} \text{cm}^{-1}$

The ability for the oxacyclophane canopy to sterically shield derived polymers utilizing **M1** is also highlighted by the ORTEP drawing in which the polymer chain would be appended at I(1) and I(2) sites as in the current case. The canopy which would be comprised of C(1)–C(6) as well as the flanking aryl rings (C(7) – C(12) and C(21) – C(26)) of the *m*-terphenyl moiety would allow for inter/intrachain interactions through steric blocking.

The preparation of the PPE derivative polymer **P1** was achieved following a Sonogashira-Hagihara coupling reaction of **M1** with **M2**, which includes *n*-hexyloxy substituents for solubility. **P1** was a bright yellow-orange solid that was obtained in a 90% yield and was calculated to have an average degree of polymerization of 20. The GPC of **P1** in CHCl₃ relative to polystyrene gave a monomodal distribution of $M_n = 13,400$ with a PDI (M_w/M_n) of 3.2. The preparation of **P2** which lacks the oxacyclophane canopy was carried out in the same manner as **P1** using side-by-side Sonogashira-Hagihara coupling reactions to ensure the same reaction conditions. The preparation of **P2** as a more traditional *n*-alkoxy sidechain substituted material was then used for direct comparison to **P1**. The ability for **P2** to achieve a somewhat higher average degree of polymerization (29) than did **P1** was attributed to the less steric encumbrance of the monomers for **P2**. The GPC of **P2** in CHCl₃ relative to polystyrene gave a monomodal distribution of $M_n = 12,800$ with a PDI (M_w/M_n) of 2.3.

The photophysical properties of **P1** and **P2** in solution are very similar to each other as seen in **Table 6.1** and **Figure 6.3A** which shows the UV-vis absorbance and photoluminescence spectra. Specifically, the absorption maxima (λ_{max}), extinction coefficients (ϵ), emission maxima (λ_{em}) and fluorescence quantum yields (Φ) were all very similar between **P1** and **P2** (**Table 6.1**) which suggests that the addition of the oxacyclophane canopy in **P1** did not affect or perturb the π -system of the PPE backbone. The aptitude for **P1** and **P2** to exhibit similar photophysical parameters also suggests that the sterically encumbered unit does not deflect adjacent chain segments from coplanarity in solution. The ability for the coplanarity to remain in solution would then advocate the

lack of a decrease in the effective conjugation length which would be expected to cause a hypsochromic shift of spectra if this were occurring.

The possibility for different relative conformations adjacent repeat units (diads) must be considered. The presence of the oxacyclophane canopy in **P1** allows for two possible configurations of repeat units. When the two repeat units have canopies on the same side this is typically referred to as a *syn*-diad, however, when the two repeat units are on the opposite sides it is typically referred to as an *anti*-diad within the polymer chain (**Figure 6.2B**).

The difference in molecular cleft size between adjacent canopies is directly influenced by the orientation of the specific diad. If the diad exists as an *anti*-diad the ability for the material to pack within solid state will allow for a larger amount of porosity. This additional porosity will allow for the ability for different types of analytes to interact with the π -conjugated backbone. To evaluate the ability for **P1** to exhibit additional porosity as a result of molecular clefts as semi empirical, PM3-level theory optimized geometry was calculated and shown in **Figure 6.2B**. The calculated geometry indicated that indeed the ability for **P1** to display diads was observed and the ground state energies in steric interactions did not show a noticeable difference between the two. The allowed spacing between canopies of adjacent units in the *syn*-diad were calculated to be 11 Å however, the calculation for *anti*-diads were seen as 25 Å. Other noteworthy features of **P1** that are crucial to the utility of **P1** are the ability for the central π -system to remain essentially coplanar without significant distortion.

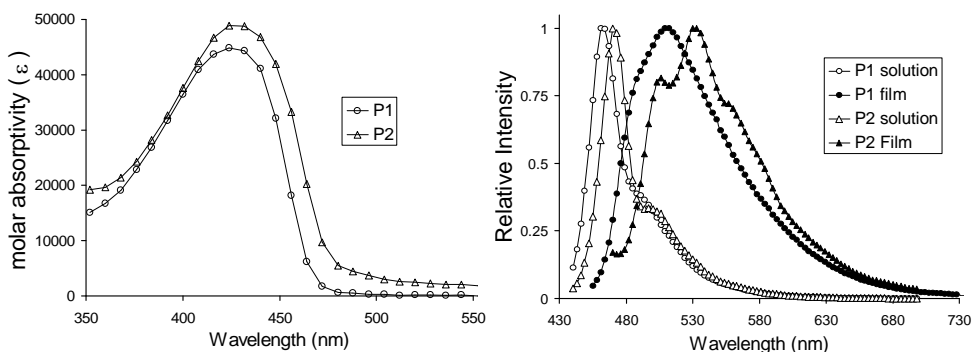
The utility of polymers with designed porosity within them has seen a wide variety of applications including membranes as well as molecular sensing. The design of

these pockets of free space within **P1** were a salient feature to exploit. A specific interest was the ability to facilitate analyte entry by the use of sterically encumbered substituents that allow interactions with the CPs in the solid state.^{5,27-29} Initial tests in this realm for **P1** showed the response to vapors of nitro-substituted organics as seen by the solid state emission response. The interest in nitroorganics as analytes is of the utmost need due to their use in landmines and explosives.^{6, 27, 30-33} The ability for CPs that include sterically enshrouding units to exhibit emission quenching effects upon the addition of such analytes has seen recent interest in where iptycene derivatives^{27, 30, 34} have been used. Preliminary studies were first explored using 2,6-dinitrotoluene (DNT) to investigate the ability of **P1** and **P2** to respond to these vapors. After seeing much success in this area the use of 2,4,6-trinitrotoluene (TNT) and 2,3-dimethyl-2,3-dinitrobutane (DMDNB, a taggant for explosives) vapor were explored to evaluate their photoluminescence response to films of **P1** and **P2**.

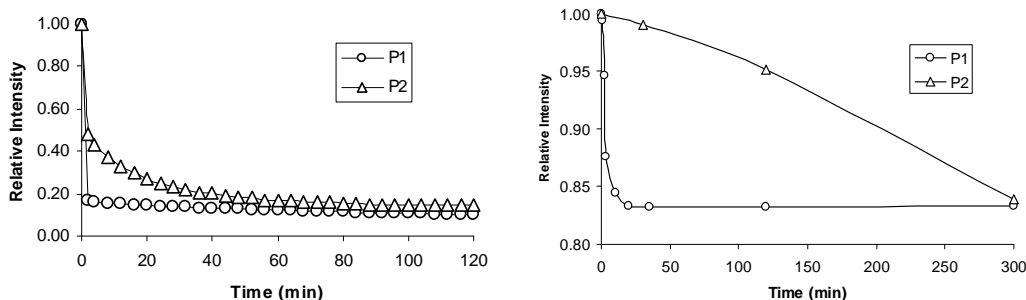
A thorough investigation of the luminescence sensing abilities of a film of **P1** drop cast from a THF solution onto a quartz substrate was explored using DNT vapor. The film of **P1** displayed an 83% quenching of integrated emission intensity within 30 sec of exposure to 140 ppb DNT. This was in contrast to that of **P2** which lacked the steric canopy in which it took 65 min to reach this level of quenching under identical conditions (**Figure 6.3B**, left). The large difference in the kinetic response of DNT vapors between **P1** and **P2** result from the additional porosity of the oxacyclophane canopy in **P1**. The ability for **P1** to exhibit similar response times and quenching percentages as compared to pentyptycene-derivatized PPE reported by Swager previously (91% quenching after 30 s) is very promising.^[35] The ability for **P1** to exhibit

reversibility was limited in that only a ~30% return of its photoluminescence upon a nitrogen purge was seen in which the pentiptycene-PPE exhibited reversibility over many exposure cycles. The advantage of having a reversible process has some applications it has also been seen where irreversible uptake can be advantageous in sensor designs.³⁵

A)



B)



C)

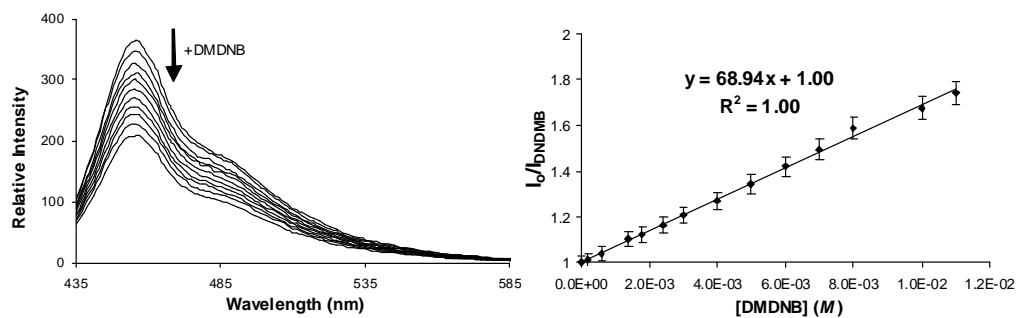


Figure 6.3 A) Absorption spectra in THF (1.0×10^{-6} M, left); and photoluminescence spectra of both films and THF solutions (right) for **P1** and **P2**. B) Solid state photoluminescence kinetic study exhibiting quenching effects of P1 and P1 in the presence of (left) DNT and (right) TNT C) Photoluminescence spectra (left) showing the progressive quenching of **P1** (1.0×10^{-6} M in THF) upon titration with up to 11 mM DMDNB and Stern-Volmer plot (right) derived from the titration (solid line is a linear fit of data points; equation and R^2 value for the linear fit are displayed on the graph).

The successful kinetic enhancement **P1** offered over **P2** to nitro-organic vapors encouraged the study of TNT vapor sensing. The ability for **P1** to achieve a maximum quenching of 16 % when exposed to 10 ppb of TNT vapor within 35 minutes was a severe improvement compared to **P2** which took 300 minutes to obtain the same maximum quenching level (**Figure 6.3B**, right). This large rate enhancement demonstrates the ability for the oxacylophane canopy to enhance the capability for **P1** to sense nitro-organics much better than that of **P2**. The lower quenching ability of TNT compared to DNT was attributed to the ca. 18-fold lower volatility of TNT versus DNT. The ability for **P1** to exhibit emission quenching upon the expose of 2.7 ppm of the taggant DMDNB vapors revealed minimal quenching even with the three order of magnitude vapor pressure of DMDNB in comparison to TNT. This indicated that **P1** was selective for nitroaromatic compounds in the solid state however the ability for **P1** to observe emission quenching in solution was still of interest. The ability for nitroaromatics to π -stack has been cited as the origin to this selectivity in other CPs that exhibit this nitroaromatics selectivity.³⁴ The initial investigation into the solution based sensing ability of **P1** was tested using THF solutions of both **P1** and DMDNB. In contrast to the solid state abilities for **P1** to sense DMDNB a 43 % emission quenching was observed for a 1.0×10^{-6} M **P1** solution in THF that was titrated with 11 mM DMDNB in THF up to 11,000 equivalents (**Figure 6.3C**). The Though a relatively low Stern-Volmer quenching constant of 69 M^{-1} (**Figure 6.3C**) was determined from a photoluminescence quenching titration, this value is still somewhat higher than that observed in several other CPs whose quenching constants have been determined, though these constants can be quite solvent dependent.³⁴ The ability for emission quenching of **P1** with DMDNB suggests that the

selectivity of **P1** for nitroaromatics in the solid state is not due to a difference in permeability to DMDNB, but to the innately low quenching efficiency of DMDNB. The ability for other canopy functionalized CPs is of current interest and efforts to improve the capability for these polymers to sense nitroorganic materials are currently being explored. Some of the possible ways to improve on the current scaffold and design might be to allow for modification of the linker size or electronic effect on the PPE backbone as well as attaching the polymer linkers at different positions.

6.3 Experimental Details

All reagents were used as received without further purification from Alfa Aesar, Acros and TCI America. The materials 2,5-dimethoxy-1,4-diodobenzene,³⁶ 2,5-diiodohydroquinone,³⁷ 1,3-bis(2-bromomethylphenyl)benzene³⁸ and 1,4-diethynyl-2,5-dihexyloxybenzene³⁹ were prepared as previously reported and their identity confirmed by ¹H and ¹³C NMR spectroscopy and melting points. Solvents were purified via an MBraun solvent purification system using alumina-packed columns under nitrogen. Air sensitive reactions were carried out employing an MBraun dry box or standard Schlenk techniques under an inert nitrogen atmosphere. NMR spectra were obtained using a Bruker Avance 500 instrument operating at 500 MHz for proton and 125.7 MHz for ¹³C and referenced to residual solvent signal.

Absorption and photoluminescent spectroscopy

UV-vis absorption spectra were collected using a Varian Cary-50 Bio spectrophotometer and photoluminescence (PL) spectra were collected utilizing a Varian Cary Eclipse spectrofluorimeter. All solution absorbance and PL spectra were collected in tetrahydrofuran (THF) in airtight screwcap-sealed Spectrosil quartz cuvettes having a path length of 1 cm. Photoluminescence quantum yields (Φ) were measured relative to quinine bisulfate in 0.1 N aqueous sulfuric acid ($\Phi = 0.564$).⁴⁰

Response of polymer films to nitroorganics

A solution of the corresponding polymer (**P1** or **P2**) was drop cast as a film onto a quartz substrate. The film was sealed in the cuvette with the film facing the excitation source at a 45° angle. The intensity of fluorescence was verified to be within the working range of the fluorimeter. A solid sample of the analyte in the cuvette with the film (but

not in contact with the film), the cuvette was sealed with a screwcap, and the fluorescence spectrum was then acquired every few seconds until the intensity had stabilized for at least 2 h. The analytes examined were 2,6-dinitrotoluene, 2,4,6-trinitrotoluene and 2,3-dimethyl-2,3-dinitro-*n*-butane. Each analyte was run at least twice to verify reproducibility.

Titration of P1 with DMDNB

A 3.0 mL aliquot of a **P1** solution (1.0×10^{-6} M in THF) was added to a cuvette and an initial photoluminescence spectrum was acquired. Aliquots (100 μ L) of a DMDNB solution in THF were added to the cuvette, where each aliquot represented 400 equiv of DMDNB per **P1** repeat unit. After the addition of each aliquot, the cuvette was sealed with a screwcap and inverted to mix the contents, and a photoluminescence spectrum was acquired. A total of 11000 equiv of DMDNB were added, with progressive decrease in fluorescence emission observed after each addition as shown in **Figure 6.3C**.

Synthesis of oxacyclophane M1

To a solution of 0.103 g (0.250 mmol) of 1,3-bis(2-bromomethylphenyl)benzene in 10 mL of dry *N,N*-dimethylformamide (DMF) was added 0.089 g (0.250 mmol) of 2,5-Diodohydroquinone. The resulting solution was then added dropwise over a 100 h period to a solution of 1.15 g (8.32 mmol) of anhydrous K_2CO_3 in 10 mL of anhydrous DMF preheated to 100 °C under nitrogen. The solution was heated at 100 °C for 48 h then concentrated under reduced pressure to afford a dark brown residue. This was then passed through a short silica gel column using CH_2Cl_2 as the eluting solvent. The solution was concentrated under reduced pressure then washed with pentane to afford 0.096 g (62.0%) of **M1** as a white solid. 1H NMR (500 MHz, $CDCl_3$): δ 4.90 (d, 1H, $J = 12.5$ Hz), 5.14 (d,

1H, $J = 12.0$ Hz), 5.46 (d, 1H, $J = 12.0$ Hz), 5.71 (d, 1H, $J = 12.0$ Hz), 6.39 (s, 1H), 6.71 (s, 1H), 7.00 (s, 1H), 7.08 (d, 1H, $J = 7.5$ Hz), 7.16 (d, 1H, $J = 7.5$ Hz), 7.26 - 7.27 (m, 1H), 7.33 (t, 2H, $J = 7.5$ Hz), 7.46 - 7.51 (m, 4H), 7.62 - 7.67 (m, 2H) ppm ^{13}C NMR (125.7 MHz, CDCl_3): δ 71.8, 75.6, 89.49, 91.86, 125.9, 126.4, 127.1, 128.2, 128.4, 129.0, 129.5, 130.7, 130.8, 131.0, 131.9, 132.0, 132.5, 132.7, 133.2, 134.2 ppm. Anal. Calcd for $\text{C}_{26}\text{H}_{18}\text{I}_2\text{O}_2$ C, 50.68; H, 2.94; N, 0.00. Found C, 50.84; H, 2.98; N, 0.00. NMR spectra are provided in **Figures 6.4-6.7**.

Synthesis of P1

To a solution of 0.100 g (0.160 mmol) of **M1** in 10 mL of toluene was added 0.009 g (0.008 mmol) $\text{Pd}(\text{PPh}_3)_4$ and the mixture was allowed to stir for 30 min under nitrogen. To the resulting solution 0.001 g (0.005 mmol) of copper iodide was added followed by dropwise addition of a diisopropylamine (5 mL) solution of 0.0530 g (0.160 mmol) 1,4-diethynyl-2,5-bis(hexyloxy)benzene. The solution was stirred for 24 h at 25 °C under an inert atmosphere. To the resulting bright yellow solution 30 mL of diethyl ether was added followed by washing with water (3×20 mL). The organic layer was then dried using anhydrous sodium sulfate and concentrated under reduced pressure. The residue was then purified by dissolving in a minimal amount of CH_2Cl_2 followed by dropwise addition of this concentrated solution to 5 mL of methanol, upon which a bright yellow-orange solid precipitated. The solid was collected by filtration and dried in vacuo to afford 0.097 g (90 %) of **P1**. ^1H NMR (500 MHz, CDCl_3): δ 0.74-1.03 (m, 6H), 1.13-2.15 (m, 16H), 3.62-4.33 (m, 4H), 4.81-5.29 (m, 2H), 5.39-5.87 (m, 1H), 6.06-6.37 (m, 1H), 6.37-7.26 (m, 8H), 7.29-7.91 (m, 8H) ppm. The ^1H NMR spectrum is provided as **Figure 6.8**. GPC in CHCl_3 relative to polystyrene gave a monomodal distribution of

M_n 13,400 ($M_w/M_n = 3.2$). UV-vis: $\lambda_{\max} = 427$ nm, $\log(\epsilon) = 4.65$ Photoluminescence: $\lambda_{\text{ex}} = 430$ nm, $\lambda_{\text{em}} 462$ nm, $\Phi = 0.57$.

Synthesis of P2

To a solution of 0.050 g (0.13 mmol) of 2,5-dimethoxy-1,4-diiodobenzene in 10 mL of toluene was added 0.007 g (0.006 mmol) $\text{Pd}(\text{PPh}_3)_4$ and allowed to stir for 30 minutes under nitrogen. To the resulting solution 0.001 g (0.006 mmol) of copper iodide was added followed by dropwise addition of a solution of 0.042 g (0.13 mmol) 1,4-diethynyl-2,5-bis(hexyloxy)benzene dissolved in 5 mL of diisopropylamine. The solution was allowed to stir for 24 hours at 25 °C under an inert atmosphere. To the resulting bright yellow solution 30 mL of diethyl ether was added followed by washing with water (3×20 mL). The organic layer was then dried using anhydrous sodium sulfate and concentrated under reduced pressure. The residue was then purified by dissolving in a minimal amount of CH_2Cl_2 followed by dropwise addition to 5 mL of methanol. A bright yellow solid formed which was isolated and dried in vacuo to afford 0.055 g (98 %) of the desired product. ^1H NMR (500 MHz, CDCl_3): δ 0.81-0.97 (m, 6H), 1.29-1.46 (m, 8H), 1.46-1.68 (m, 4H), 1.79-1.98 (m, 4H), 3.84-3.97 (m, 6H), 3.97-4.18 (m, 4H), 7.01-7.12 (m, 4H). The ^1H NMR spectrum is provided as **Figure 6.8**. GPC in CHCl_3 relative to polystyrene gave a monomodal distribution of M_n 12,800 ($M_w/M_n = 2.3$). UV-vis: $\lambda_{\max} = 427$ nm, $\log(\epsilon) = 4.69$ Photoluminescence: $\lambda_{\text{ex}} = 430$ nm, $\lambda_{\text{em}} = 472$ nm, $\Phi = 0.50$.

6.4 Conclusions

The synthesis of a *m*-terphenyl scaffolded oxacyclophane-containing monomer **M1** was followed and its successful application to the synthesis of PPE derivative **P1** has been undertaken as the first step in studies on a wide range of CPs containing such oxacyclophane subunits. The oxacyclophane canopy in **P1** provides defined molecular clefts and areas of free space about the π -conjugated backbone that seem to facilitate analyte entry and molecular sensing of molecules such as nitro-substituted organics, as demonstrated by the up to 100-fold emission quenching rate enhancement in response to these analytes. These early proof-of-principle studies lay the foundation for more sophisticated materials incorporating additional chromophore and stimuli-responsive subunits appended to the versatile oxacyclophane canopies that are currently under investigation in our labs.

6.5 Selected Spectra

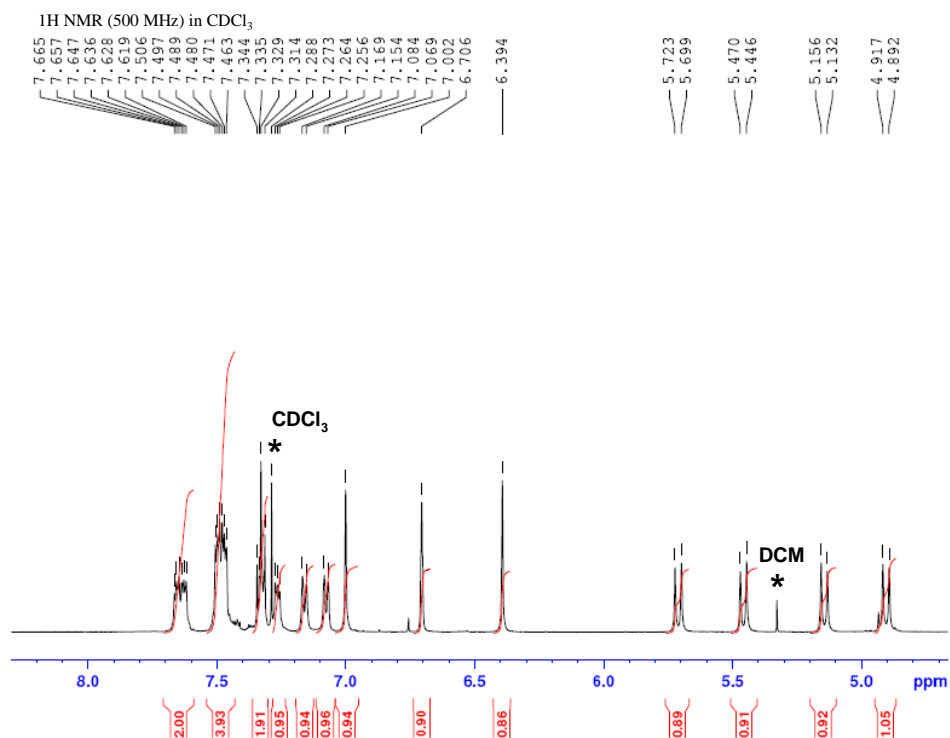


Figure 6.4 ¹H NMR spectra of **M1** in CDCl₃ at 500 MHz.

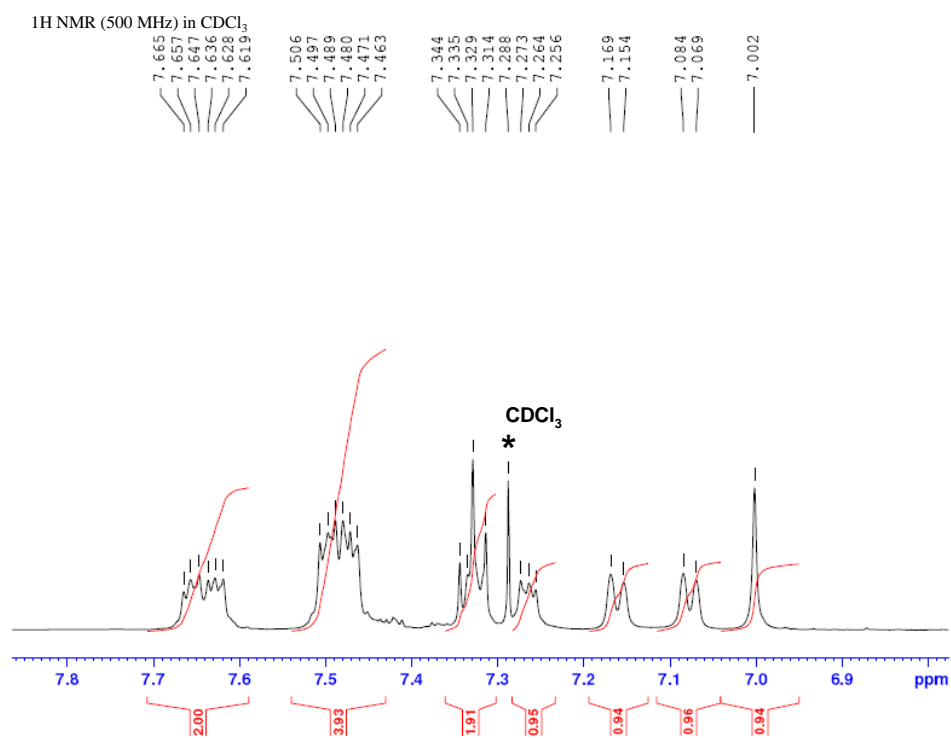


Figure 6.5 Aromatic region of ¹H NMR spectra of **M1** in CDCl₃ at 500 MHz.

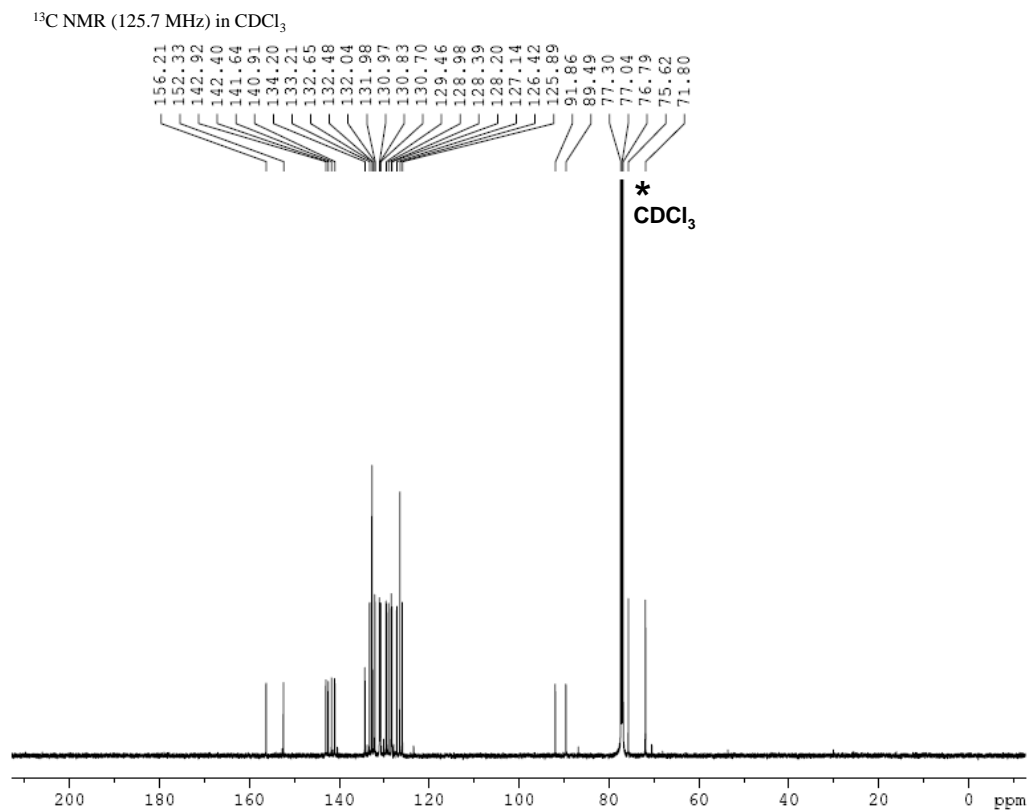


Figure 6.6 ^{13}C NMR spectra of **M1** in CDCl_3 at 125.7 MHz.

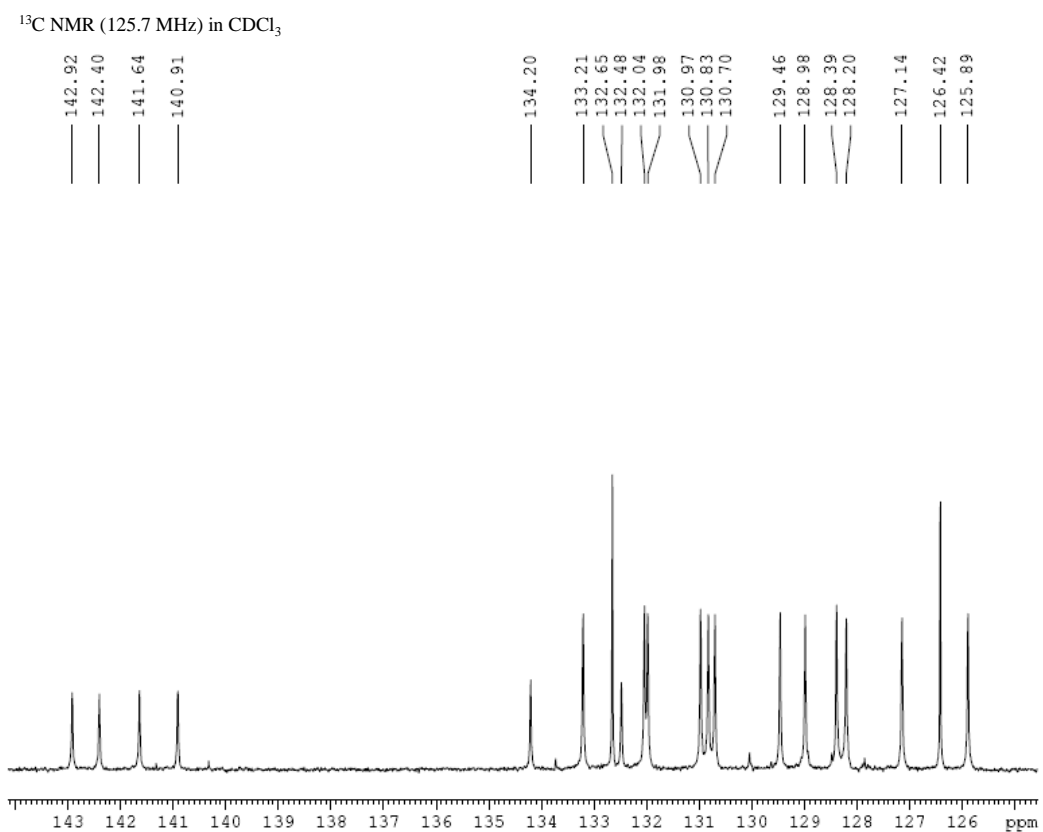


Figure 6.7 Aromatic region of ^{13}C NMR spectra of **M1** in CDCl_3 at 125.7 MHz.

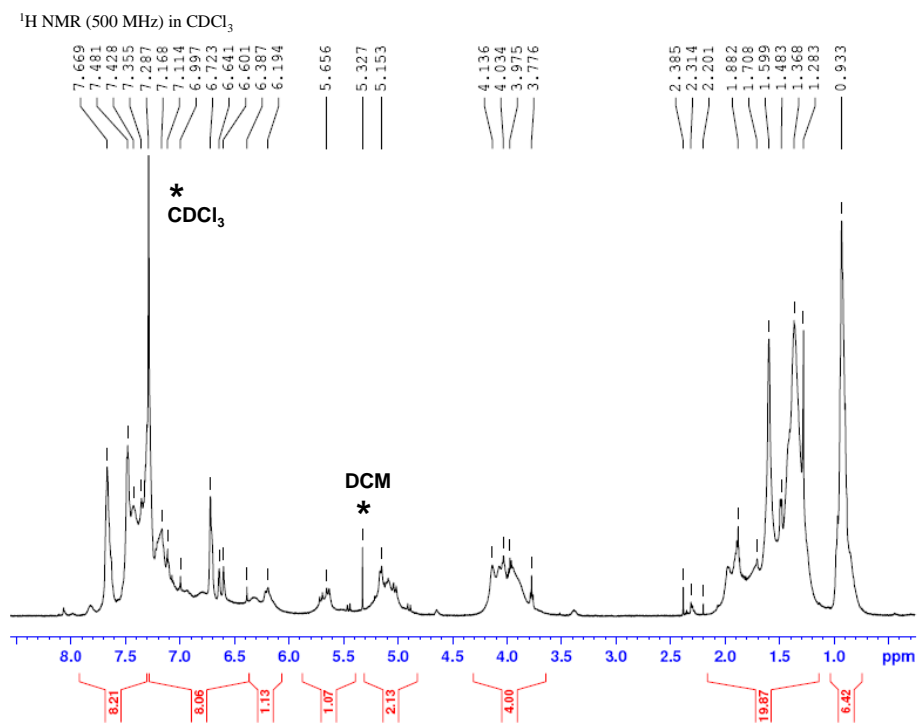


Figure 6.8 ¹H NMR spectra of **P1** in CDCl₃ at 500 MHz.

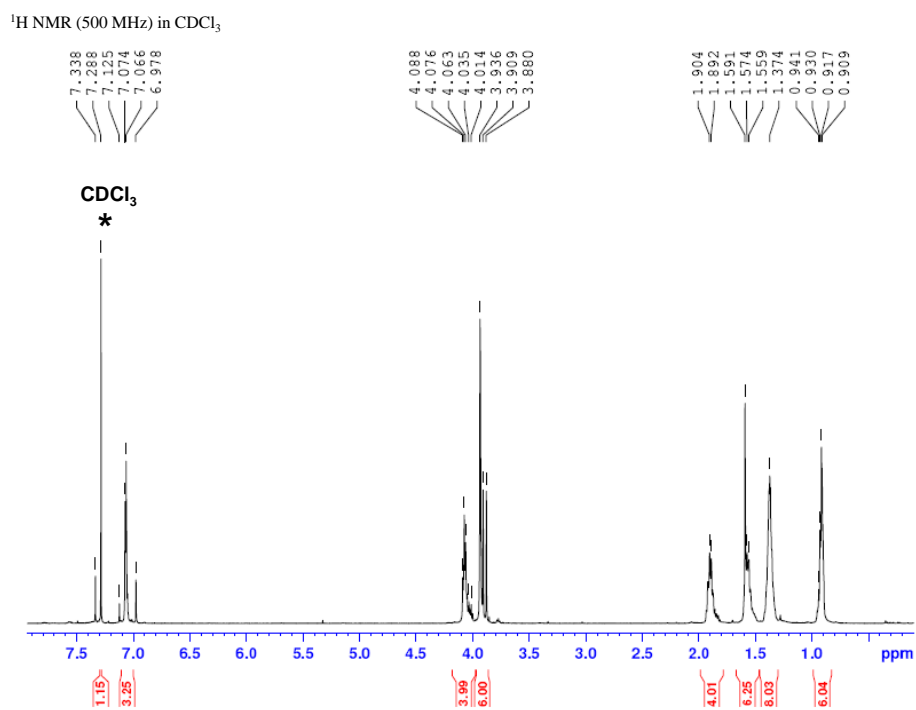


Figure 6.9 ¹H NMR spectra of **P2** in CDCl₃ at 500 MHz.

Table 6.2 Refinement details for **M1**.

Empirical formula	C ₂₆ H ₁₈ I ₂ O ₂
Formula weight (g/mol)	616.20
Temperature (K)	153 (2)
Wavelength (Å)	0.71073
Crystal system	Monoclinic
Space group	P2 ₁ /c (#14)
Unit cell dimensions	
<i>a</i> (Å)	13.146(3)
<i>b</i> (Å)	8.2785(17)
<i>c</i> (Å)	20.265(4)
<i>α</i> (deg)	90.00
<i>β</i> (deg)	103.91(3)
<i>γ</i> (deg)	90.00
Volume (Å ³)	2140.7(7)
<i>Z</i>	4
Calculated density (Mg/m ³)	1.912
Absorption coefficient (mm ⁻¹)	2.959
<i>F</i> (000)	1184
Crystal size (mm)	0.36 × 0.24 × 0.19
Crystal color and shape	colorless chip
θ range for data collection (deg)	2.93 - 25.10
Limiting indices	-15 < <i>h</i> < 15 -9 < <i>k</i> < 9 -24 < <i>l</i> < 21
Reflections collected	13664
Independent reflections	3772
Completeness to θ	25.10 (99.1 %)
Max. transmission	0.6033
Min. transmission	0.4156
Refinement method	Full-matrix least-squares on <i>F</i> ²
Data / restraints / parameters	3772/0/271
Goodness of fit on <i>F</i> ²	1.146
Final R indices (<i>I</i> > 2σ(<i>I</i>))	
R1	0.0334
wR2	0.0777
R indices (all data)	
R1	0.0364
wR2	0.0809

6.6 References

1. *Handbook of Conducting Polymers*. 3 ed.; CRC Press: New York, 2007; Vol. 1 p 1.
2. Kraft, A.; Grimsdale, A. C.; Holmes, A. B., *Angewandte Chemie, International Edition* **1998**, *37*, 403-428.
3. Guenes, S.; Neugebauer, H.; Sariciftci, N. S., *Chemical Reviews* **2007**, *107*, 1324-1338.
4. Thompson, B. C.; Frechet, J. M. J., *Angewandte Chemie, International Edition* **2008**, *47*, 58-77.
5. Nonnenmacher, M.; Kunz, D.; Rominger, F.; Oeser, T., *Journal of Organometallic Chemistry* **2007**, *692*, 2554-2563.
6. Yang, J.-S.; Swager, T. M., *Journal of the American Chemical Society* **1998**, *120*, 11864-11873.
7. Smith, R. C.; Gleason, L. B.; Protasiewicz, J. D., *Journal of Materials Chemistry* **2006**, *16*, 2445-2452.
8. Lee, D.; Swager, T. M., *Journal of the American Chemical Society* **2003**, *125*, 6870-6871.
9. Smaldone, R. A.; Moore, J. S., *Chemistry - A European Journal* **2008**, *14*, 2650-2657.
10. Smith, R. C.; Bodner, C. R.; Earl, M. J.; Sears, N. C.; Hill, N. E.; Bishop, L. M.; Sizemore, N.; Hehemann, D. T.; Bohn, J. J.; Protasiewicz, J. D., *Journal of Organometallic Chemistry* **2005**, *690*, 477-481.
11. Bazan, G. C., *Journal of Organic Chemistry* **2007**, *72*, 8615-8635.

12. Morisaki, Y.; Chujo, Y., *Angewandte Chemie, International Edition* **2006**, *45*, 6430-6437.
13. Kaikawa, T.; Takimiya, K.; Aso, Y.; Otsubo, T., *Organic Letters* **2000**, *2*, 4197-4199.
14. Knoblock, K. M.; Silvestri, C. J.; Collard, D. M., *Journal of the American Chemical Society* **2006**, *128*, 13680-13681.
15. Satou, T.; Sakai, T.; Kaikawa, T.; Takimiya, K.; Otsubo, T.; Aso, Y., *Organic Letters* **2004**, *6*, 997-1000.
16. Vinod, T. K.; Hart, H., *Topics in Current Chemistry* **1994**, *172*, 119-178.
17. Vinod, T. K.; Hart, H., *Journal of Organic Chemistry* **1991**, *56*, 5630-5640.
18. Vinod, T.; Hart, H., *Journal of Organic Chemistry* **1990**, *55*, 881-890.
19. Grewal, R. S.; Hart, H., *Tetrahedron Letters* **1990**, *31*, 4271-4274.
20. Vinod, T. K.; Hart, H., *Journal of the American Chemical Society* **1990**, *112*, 3250-3252.
21. Grewal, R. S.; Hart, H.; Vinod, T. K., *Journal of Organic Chemistry* **1992**, *57*, 2721-2726.
22. Beljonne, D.; Cornil, J.; Silbey, R.; Millie, P.; Bredas, J. L., *Journal of Chemical Physics* **2000**, *112*, 4749-4758.
23. Bredas, J.-L.; Cornil, J.; Beljonne, D.; Dos Santos, D. A.; Shuai, Z., *Accounts of Chemical Research* **1999**, *32*, 267-276.
24. Cornil, J.; dos Santos, D. A.; Crispin, X.; Silbey, R.; Bredas, J. L., *Journal of the American Chemical Society* **1998**, *120*, 1289-1299.

25. Cornil, J.; Beljonne, D.; Calbert, J.-P.; Bredas, J.-L., *Advanced Materials* **2001**, *13*, 1053-1067.
26. Vinod, T. K.; Hart, H., *Journal of the American Chemical Society* **1988**, *110*, 6574-6575.
27. Yang, J.-S.; Swager, T. M., *Journal of the American Chemical Society* **1998**, *120*, 5321-5322.
28. Lee, D.; Swager, T. M., *Synlett* **2004**, 149-154.
29. Swager, T. M., *Accounts of Chemical Research* **2008**, *41*, 1181-1189.
30. Zyryanov, G. V.; Palacios, M. A.; Anzenbacher, P., Jr., *Organic Letters* **2008**, *10*, 3681-3684.
31. Narayanan, A.; Varnavski, O. P.; Swager, T. M.; Goodson, T., III, *Journal of Physical Chemistry C* **2008**, *112*, 881-884.
32. Andrew, T. L.; Swager, T. M., *Journal of the American Chemical Society* **2007**, *129*, 7254-7255.
33. Rose, A.; Zhu, Z.; Madigan, C. F.; Swager, T. M.; Bulovic, V., *Nature* **2005**, *434*, 876-879.
34. Thomas, S. W., III; Amara, J. P.; Bjork, R. E.; Swager, T. M., *Chemical Communications* **2005**, 4572-4574.
35. Walker, N. R.; Linman, M. J.; Timmers, M. M.; Dean, S. L.; Burkett, C. M.; Lloyd, J. A.; Keelor, J. D.; Baughman, B. M.; Edmiston, P. L., *Analytica Chimica Acta* **2007**, *593*, 82-91.
36. Wariishi, K.; Morishima, S.; Inagaki, Y., *Organic Process Research and Development* **2003**, *7*, 98-100.

37. Ramey, M. B.; Hiller, J. A.; Rubner, M. F.; Tan, C.; Schanze, K. S.; Reynolds, J. R., *Macromolecules* **2005**, *38*, 234-243.
38. Vinod, T. K.; Hart, H., *Journal of Organic Chemistry* **1990**, *55*, 5461-5466.
39. Pu, K.-Y.; Chen, Y.; Qi, X.-Y.; Qin, C.-Y.; Chen, Q.-Q.; Wang, H.-Y.; Deng, Y.; Fan, Q.-L.; Huang, Y.-Q.; Liu, S.-J.; Wei, W.; Peng, B.; Huang, W., *Journal of Polymer Science, Part A: Polymer Chemistry* **2007**, *45*, 3776-3787.
40. *Handbook of Photochemistry*. 3rd ed.; CRC Press: Boca Raton, 2006.

CHAPTER 7

CONCLUSIONS AND FURTHER DIRECTIONS

The ease with which the *m*-terphenyl building block has been incorporated into a diverse set of molecules described throughout the previous chapters lends to their application in a number of applications requiring a multifunctional, rationally designed scaffold. As noted in Chapter 1, the potential for practical application are enhanced by the availability of high yield, one pot syntheses of functionalized *m*-terphenyls, ease of purification and relatively inexpensive materials required.

The facile functionalization of *m*-terphenyls allows for the design of compounds that have functional groups on both the central aryl ring and the flanking aryl rings. Functional groups can, for example, serve as donor atoms for binding to metals. The ability to prepare *m*-terphenyl scaffolded metal complexes lends to their utility in catalytic applications discussed in Chapters 3-5, and the sensor applications discussed in Chapter 2. Functionalization with polymerizable units can allow for design of the specialized organic materials discussed in Chapter 6.

The success of the materials presented in this dissertation is accentuated by the ability of materials in Chapters 4 and 6 to produce results comparable to some commercial catalysts and sensing polymers. By further optimizing these systems, it is anticipated that they may even exceed the performance of existing state of the art. The incorporation of chiral metal binding domains into the *m*-terphenyl unit could also extend application to applications such as pharmaceuticals, where chirality is crucial.

BIBLIOGRAPHY

1. *Rhodium catalyzed hydroformylation*. Kluwer Academic Publishers: Dordrecht, Netherlands ; Boston, 2000.
2. *Handbook of Photochemistry*. 3rd ed.; CRC Press: Boca Raton, 2006.
3. N-Heterocyclic Carbenes in Transition Metal Catalysis. In Glorius, F., Ed. 2007; p 21.
4. *Handbook of Conducting Polymers*. 3 ed.; CRC Press: New York, 2007; Vol. 1.
5. Abbass, M.; Kuehl, C.; Manthey, C.; Mueller, A.; Luening, U., *Collection of Czechoslovak Chemical Communications* **2004**, *69*, 1325-1344.
6. Adams, D. M.; Brus, L.; Chidsey, C. E. D.; Creager, S.; Creutz, C.; Kagan, C. R.; Kamat, P. V.; Lieberman, M.; Lindsay, S.; Marcus, R. A.; Metzger, R. M.; Michel-Beyerle, M. E.; Miller, J. R.; Newton, M. D.; Rolison, D. R.; Sankey, O.; Schanze, K. S.; Yardley, J.; Zhu, X., *Journal of Physical Chemistry B* **2003**, *107*, 6668-6697.
7. Adams, H.; Bradshaw, D.; Fenton, D. E., *Inorganica Chimica Acta* **2002**, *332*, 195-200.
8. Aiet-Haddou, H.; Wiskur, S. L.; Lynch, V. M.; Anslyn, E. V., *Journal of the American Chemical Society* **2001**, *123*, 11296-11297.
9. Andac, M.; Asan, A.; Isildak, I., *Journal of Chemical Crystallography* **2003**, *33*, 599-603.
10. Andres, J. M.; Martinez, M. A.; Pedrosa, R.; Perez-Encabo, A., *Tetrahedron: Asymmetry* **2001**, *12*, 347-353.
11. Andrew, T. L.; Swager, T. M., *Journal of the American Chemical Society* **2007**, *129*, 7254-7255.

12. Angermund, K.; Baumann, W.; Dinjus, E.; Fornika, R.; Goerls, H.; Kessler, M.; Krueger, C.; Leitner, W.; Lutz, F., *Chemistry--A European Journal* **1997**, *3*, 755-764.
13. Annan, K. O.; Scherf, U.; Mullen, K., *Synthetic Metals* **1999**, *99*, 9-16.
14. Antonisse, M. M. G.; Reinhoudt, D. N., *Chemical Communications* **1998**, 443-448.
15. Arduengo, A., *Journal of the American Chemical Society* **1991**, *113*, 361-362.
16. Armstrong, N.; Hoft, R. C.; McDonagh, A.; Cortie, M. B.; Ford, M. J., *Nano Letters* **2007**, *7*, 3018-3022.
17. Baker, M. V.; Skelton, B. W.; White, A. H.; Williams, C. C., *Journal of the Chemical Society, Dalton Transactions* **2001**, 111-120.
18. Baker, M. V.; Brown, D. H.; Simpson, P. V.; Skelton, B. W.; White, A. H.; Williams, C. C., *Journal of Organometallic Chemistry* **2006**, *691*, 5845-5855.
19. Bazan, G. C., *Journal of Organic Chemistry* **2007**, *72*, 8615-8635.
20. Bedford, R. B.; Welch, S. L., *Chemical Communications* **2001**, 129-130.
21. Bedford, R. B.; Hazelwood, S. L.; Horton, P. N.; Hursthouse, M. B., *Dalton Transactions* **2003**, 4164-4174.
22. Bedford, R. B.; Hazelwood, S. L.; Limmert, M. E.; Brown, J. M.; Ramdeehul, S.; Cowley, A. R.; Coles, S. J.; Hursthouse, M. B., *Organometallics* **2003**, *22*, 1364-1371.
23. Beer, P. D.; Gale, P. A., *Angewandte Chemie, International Edition* **2001**, *40*, 486-516.
24. Behr, J.-P. Y. O. N.; Ed. By Jean-Paul, B., *The lock-and-key principle : the state of the art--100 years on*. Wiley & Sons: Chichester; New York, 1994; p ix, 325.

25. Beljonne, D.; Cornil, J.; Silbey, R.; Millie, P.; Bredas, J. L., *J. Chem. Phys.* **2000**, *112*, 4749-4758.
26. Bell, R. D.; Doisy, E. A., *Journal of Biological Chemistry* **1920**, *44*, 55-67.
27. Beller, M.; Krauter, J. G. E., *Journal of Molecular Catalysis A: Chemical* **1999**, *143*, 31-39.
28. Berg, J. M.; Tymoczko, J. L.; Stryer, L.; Stryer, L., *Biochemistry*. 5th ed.; W.H. Freeman: New York, 2002; p 1.
29. Biswas, S.; Chowdhury, B.; Ray, B. C., *Analytical Letters* **2004**, *37*, 1965-1979.
30. Boehme, C.; Frenking, G., *Journal of the American Chemical Society* **1996**, *118*, 2039-2046.
31. Boiocchi, M.; Bonizzoni, M.; Fabbrizzi, L.; Piovani, G.; Taglietti, A., *Angewandte Chemie, International Edition* **2004**, *43*, 3847-3852.
32. Boiteau, J.-G.; Imbos, R.; Minnaard, A. J.; Feringa, B. L., *Organic Letters* **2003**, *5*, 681-684.
33. Boiteau, J.-G.; Minnaard, A. J.; Feringa, B. L., *Journal of Organic Chemistry* **2003**, *68*, 9481-9484.
34. Bondi, A., *Journal of Physical Chemistry* **1964**, *68*, 441-451.
35. Bonizzoni, M.; Fabbrizzi, L.; Piovani, G.; Taglietti, A., *Tetrahedron* **2004**, *60*, 11159-11162.
36. Bourissou, D.; Guerret, O.; Gabbaie, F. P.; Bertrand, G., *Chemical Reviews* **2000**, *100*, 39-91.
37. Boydston, A. J.; Williams, K. A.; Bielawski, C. W., *Journal of the American Chemical Society* **2005**, *127*, 12496-12497.
38. Boydston, A. J.; Bielawski, C. W., *Dalton Transactions* **2006**, 4073-4077.

39. Bredas, J.-L.; Cornil, J.; Beljonne, D.; Dos Santos, D. A.; Shuai, Z., *Accounts of Chemical Research* **1999**, *32*, 267-276.
40. Brown, E. S., *Aspects of Homogeneous Catalysis* **1974**, *2*, 57-78.
41. Brown, J. M.; Kent, A. G., *Journal of the Chemical Society, Perkin Trans. 2* **1987**, 1597-1607.
42. Brown, T. H.; Green, P. J., *Journal of the American Chemical Society* **1970**, *92*, 2359-2362.
43. Brown, T. L., *Inorganic Chemistry* **1992**, *31*, 1286-1294.
44. Brown, T. L., *Inorganic Chemistry* **1994**, *33*, 367-372.
45. Buisman, G. J. H.; Vos, E. J.; Kamer, P. C. J.; van Leeuwen, P. W. N. M., *Journal of the Chemical Society, Dalton Transactions* **1995**, 409-417.
46. Burdette, S. C.; Walkup, G. K.; Spingler, B.; Tsien, R. Y.; Lippard, S. J., *Journal of the American Chemical Society* **2001**, *123*, 7831-7841.
47. Burling, S.; Mahon, M. F.; Reade, S. P.; Whittlesey, M. K., *Organometallics* **2006**, *25*, 3761-3767.
48. Calderini, G.; Aporti, F.; Bonetti, A. C.; Zanotti, A.; Toffano, G., *Progress in Clinical and Biological Research* **1985**, *192*, 383-386.
49. Cano-Raya, C.; Fernandez-Ramos, M. D.; Capitan-Vallvey, L. F., *Analytical Chimica Acta* **2006**, *555*, 299-307.
50. Cao, D. R.; Schollmeyer, D.; Meier, H., *Eur. Journal of Organic Chemistry* **1999**, 791-795.
51. Carre, F.; Chuit, C.; Corriu, R. J. P.; Fanta, A.; Mehdi, A.; Reye, C., *Organometallics* **1995**, *14*, 194-198.
52. Casey, C. P.; Whiteker, G. T., *Israel Journal of Chemistry* **1990**, *30*, 299-304.

53. Casey, C. P.; Whiteker, G. T.; Melville, M. G.; Petrovich, L. M.; Gavney, J. A., Jr.; Powell, D. R., *Journal of the American Chemical Society* **1992**, *114*, 5535-5543.
54. Cha, J. S.; Brown, H. C., *Journal of Organic Chemistry* **1993**, *58*, 4727-4731.
55. Chan, K. L.; Watkins, S. E.; Mak, C. S. K.; McKiernan, M. J.; Towns, C. R.; Pascu, S. I.; Holmes, A. B., *Chemical Communications* **2005**, 5766-5768.
56. Chen, W.; Liu, F., *Journal of Organometallic Chemistry* **2003**, *673*, 5-12.
57. Chien, S. H.; Sale, P. W. G.; Friesen, D. K., *Fertilizer Research* **1990**, *24*, 149-157.
58. Chiu, J. J.; Hart, H.; Ward, D. L., *Journal of Organic Chemistry* **1993**, *58*, 964-966.
59. Chiu, P. L.; Lai, C.-L.; Chang, C.-F.; Hu, C.-H.; Lee, H. M., *Organometallics* **2005**, *24*, 6169-6178.
60. Choi, M.-G.; White, D.; Brown, T. L., *Inorganic Chemistry* **1994**, *33*, 5591-5594.
61. Churruca, F.; SanMartin, R.; Ines, B.; Tellitu, I.; Dominguez, E., *Advanced Synthesis and Catalysis* **2006**, *348*, 1836-1840.
62. Clark, T. P.; Landis, C. R.; Freed, S. L.; Klosin, J.; Abboud, K. A., *Journal of the American Chemical Society* **2005**, *127*, 5040-5042.
63. Clyburne, J. A. C.; McMullen, N., *Coordination Chemistry Reviews* **2000**, *210*, 73-99.
64. Clyburne, J. A. C.; McMullen, N., *Coordination Chemistry Reviews* **2003**, *213*, 145-162.
65. Clyne, D. S.; Jin, J.; Genest, E.; Gallucci, J. C.; RajanBabu, T. V., *Organic Letters* **2000**, *2*, 1125-1128.

66. Connolly, M. L., *Journal of Applied Crystallography* **1983**, *16*, 548-558.
67. Connolly, M. L., *Journal of Molecular Graphics* **1993**, *11*, 139-141.
68. Coolen, H. K. A. C.; van Leeuwen, P. W. N. M.; Nolte, R. J. M., *Journal of Organic Chemistry* **1996**, *61*, 4739-4747.
69. Corberan, R.; Ramirez, J.; Poyatos, M.; Peris, E.; Fernandez, E., *Tetrahedron: Asymmetry* **2006**, *17*, 1759-1762.
70. Cornil, J.; dos Santos, D. A.; Crispin, X.; Silbey, R.; Bredas, J. L., *Journal of the American Chemical Society* **1998**, *120*, 1289-1299.
71. Cornil, J.; Beljonne, D.; Calbert, J.-P.; Bredas, J.-L., *Advanced Materials* **2001**, *13*, 1053-1067.
72. Cottrell, I. F.; Hands, D.; Houghton, P. G.; Humphrey, G. R.; Wright, S. H. B., *J. Heterocyclic Chemistry* **1991**, *28*, 301-304.
73. Cowley, A. H.; Norman, N. C.; Pakulski, M., *Journal of the Chemical Society, Dalton Transactions* **1985**, 383-386.
74. Crabtree, R. H., *The organometallic chemistry of the transition metals*. 4th ed.; John Wiley: Hoboken, NJ, 2005; p xiii, 546.
75. Cram, D. J.; Cram, J. M., *Accounts of Chemical Research* **1978**, *11*, 8-14.
76. Cramer, R. D.; Jenner, E. L.; Lindsey, R. V., Jr.; Stolberg, U. G., *Journal of the American Chemical Society* **1963**, *85*, 1691-1692.
77. De Fremont, P.; Scott, N. M.; Stevens, E. D.; Ramnial, T.; Lightbody, O. C.; Macdonald, C. L. B.; Clyburne, J. A. C.; Abernethy, C. D.; Nolan, S. P., *Organometallics* **2005**, *24*, 6301-6309.
78. Desimoni, G.; Faita, G.; Jorgensen, K. A., *Chemical Reviews* **2006**, *106*, 3561-3651.

79. Deutscher, J.; Editor, *Ser/Thr/Tyr Protein Phosphorylation in Bacteria, A Written Symposium*. 2005; p 112 pp.
80. Dierkes, P.; Ramdeehul, S.; Barloy, L.; De Cian, A.; Fischer, J.; Kamer, P. C. J.; Van Leeuwen, P. W. N. M.; Osborn, J. A., *Angewandte Chemie, International Edition* **1998**, *37*, 3116-3118.
81. Dierkes, P.; van Leeuwen, P. W. N. M., *Journal of the Chemical Society, Dalton Transactions* **1999**, 1519-1530.
82. Diesveld, J. W.; Menger, E. M.; Edzes, H. T.; Veeman, W. S., *Journal of the American Chemical Society* **1980**, *102*, 7935-7936.
83. Dinares, I.; Garcia de Miguel, C.; Font-Bardia, M.; Solans, X.; Alcalde, E., *Organometallics* **2007**, *26*, 5125-5128.
84. Drennan, C. E.; Hughes, R. J.; Reinsborough, V. C.; Soriyan, O. O., *Canadian Journal of Chemistry* **1998**, *76*, 152-157.
85. Drinkard, W. C., Jr. Catalytic hydrocyanation of olefins. 3655723, 19720411, **1972**.
86. Du, C. J. F.; Hart, H.; Ng, K. K. D., *Journal of Organic Chemistry* **1986**, *51*, 3162-3165.
87. Fabbrizzi, L.; Marcotte, N.; Stomeo, F.; Taglietti, A., *Angewandte Chemie, International Edition* **2002**, *41*, 3811-3814.
88. Fabbrizzi, L.; Licchelli, M.; Taglietti, A., *Dalton Transactions* **2003**, 3471-3479.
89. Fabbrizzi, L.; Foti, F.; Taglietti, A., *Organic Letters* **2005**, *7*, 2603-2606.
90. Fairlamb, I. J. S.; Grant, S.; Tommasi, S.; Lynam, J. M.; Bandini, M.; Dong, H.; Lin, Z.; Whitwood, A. C., *Advanced Synthesis and Catalysis* **2006**, *348*, 2515-2530.
91. Fan, Q.-H.; Li, Y.-M.; Chan, A. S. C., *Chemical Reviews* **2002**, *102*, 3385-3465.

92. Fernandez, A.; Reyes, C.; Wilson, M. R.; Woska, D. C.; Prock, A.; Giering, W. P., *Organometallics* **1997**, *16*, 342-348.
93. Fielding, L., *Tetrahedron* **2000**, *56*, 6151-6170.
94. Fischer, E., *Ber.* **1894**, *27*, 2985-2993.
95. Folmer-Andersen, J. F.; Lynch, V. M.; Anslyn, E. V., *Chemistry A European Journal* **2005**, *11*, 5319-5326.
96. Frank, M.; Maas, G.; Schatz, J., *European Journal of Organic Chemistry* **2004**, 607-613.
97. Freixa, Z.; Van Leeuwen, P. W. N. M., *Dalton Transactions* **2003**, 1890-1901.
98. Freixa, Z.; Kamer, P.C.J.; Lutz, M.; Spek, A. L.; van Leeuwen, P.W.N.M., *Angewandte Chemie, International Edition* **2005**, *44*, 4385-4388.
99. Frenzel, U.; Weskamp, T.; Kohl, F. J.; Schattenmann, W. C.; Nuyken, O.; Herrmann, W. A., *Journal of Organometallic Chemistry* **1999**, *586*, 263-265.
100. Frisch, A. C.; Rataboul, F.; Zapf, A.; Beller, M., *Journal of Organometallic Chemistry* **2003**, *687*, 403-409.
101. Garrison, J. C.; Youngs, W. J., *Chemical Reviews* **2005**, *105*, 3978-4008.
102. Gevorgyan, V.; Radhakrishnan, U.; Takeda, A.; Rubina, M.; Rubin, M.; Yamamoto, Y., *Journal of Organic Chemistry* **2001**, *66*, 2835-2841.
103. Goel, R. G.; Ogini, W. O., *Organometallics* **1982**, *1*, 654-658.
104. Green, D. P.; Balcom, B. J.; Lees, T. J., *Review of Scientific Instruments* **1996**, *67*, 102-107.
105. Green, M. L. H., *Journal of Organometallic Chemistry* **1995**, *500*, 127-148.

106. Grewal, R. S.; Hart, H., *Tetrahedron Letters* **1990**, *31*, 4271-4274.
107. Grewal, R. S.; Hart, H.; Vinod, T. K., *Journal of Organic Chemistry* **1992**, *57*, 2721-2726.
108. Guenes, S.; Neugebauer, H.; Sariciftci, N. S., *Chemistry Reviews* **2007**, *107*, 1324-1338.
109. Hahn, F. E.; Langenhahn, V.; Luegger, T.; Pape, T.; Le Van, D., *Angewandte Chemie, International Edition* **2005**, *44*, 3759-3763.
110. Hahn, F. E.; Jahnke, M. C.; Pape, T., *Organometallics* **2007**, *26*, 150-154.
111. Hammond, P. R., *Journal of the Chemical Society* **1964**, 479-484.
112. Han, M. S.; Kim, D. H., *Angewandte Chemie, International Edition* **2002**, *41*, 3809-3811.
113. Han, M. S.; Kim, D. H., *Bioorganic & Medicinal Chemistry Letters* **2003**, *13*, 1079-1082.
114. Hannig, F.; Kehr, G.; Froehlich, R.; Erker, G., *Journal of Organometallic Chemistry* **2005**, *690*, 5959-5972.
115. Hanshaw, R. G.; Hilkert, S. M.; Jiang, H.; Smith, B. D., *Tetrahedron Letters* **2004**, *45*, 8721-8724.
116. Hanshaw, R. G.; Lakshmi, C.; Lambert, T. N.; Johnson, J. R.; Smith, B. D., *ChemBioChem* **2005**, *6*, 2214-2220.
117. Hanshaw, R. G.; O'Neil, E. J.; Foley, M.; Carpenter, R. T.; Smith, B. D., *Journal of Material Chemistry* **2005**, *15*, 2707-2713.
118. Hanshaw, R. G.; Smith, B. D., *Bioorg. Med. Chem.* **2005**, *13*, 5035-5042.
119. Hart, H.; Takehira, Y., *Journal of Organic Chemistry* **1982**, *47*, 4370-4372.

120. Hart, H.; Ward, D. L.; Tanaka, K.; Toda, F., *Tetrahedron Letters* **1982**, 23, 2125-2128.
121. Hart, H., *Pure and Applied Chemistry* **1993**, 65, 27-34.
122. Hart, H.; Rajakumar, P., *Tetrahedron* **1995**, 51, 1313-1336.
123. Hartley, J. H.; James, T. D.; Ward, C. J., *Perkin 1* **2000**, 3155-3184.
124. Hassan, J.; Sevignon, M.; Gozzi, C.; Schulz, E.; Lemaire, M., *Chemical Reviews* **2002**, 102, 1359-1470.
125. Haub, M. D., *Nutritional Ergogenic Aids* **2004**, 257-273.
126. Hayashi, T.; Konishi, M.; Kumada, M., *Tetrahedron Letters* **1979**, 1871-1874.
127. Hayashi, T.; Konishi, M.; Kobori, Y.; Kumada, M.; Higuchi, T.; Hirotsu, K., *Journal of the American Chemical Society* **1984**, 106, 158-163.
128. Hayashi, T.; Takahashi, M.; Takaya, Y.; Ogasawara, M., *Journal of the American Chemical Society* **2002**, 124, 5052-5058.
129. Hayashi, T.; Yamasaki, K., *Chemical Reviews* **2003**, 103, 2829-2844.
130. Heinemann, C.; Mueller, T.; Apeloig, Y.; Schwarz, H., *Journal of the American Chemical Society* **1996**, 118, 2023-2038.
131. Herrmann, W. A.; Elison, M.; Fischer, J.; Koecher, C.; Artus, G. R. J., *Angewandte Chemie, International Edition* **1995**, 34, 2371-2374.
132. Herrmann, W. A.; Reisinger, C.-P.; Spiegler, M., *Journal of Organometallic Chemistry* **1998**, 557, 93-96.
133. Herrmann, W. A.; Bohm, V. P. W.; Gstottmayr, C. W. K.; Grosche, M.; Reisinger, C. P.; Weskamp, T., *Journal of Organometallic Chemistry* **2001**, 617-618, 616-628.

134. Hilderbrand, S. A.; Lim, M. H.; Lippard, S. J., *Journal of the American Chemical Society* **2004**, *126*, 4972-4978.
135. Hill, J. E.; Nile, T. A., *Journal of Organometallic Chemistry* **1977**, *137*, 293-300.
136. Hillier, A. C.; Grasa, G. A.; Viciu, M. S.; Lee, H. M.; Yang, C.; Nolan, S. P., *Journal of Organometallic Chemistry* **2002**, *653*, 69-82.
137. Hirota, M.; Sakakibara, K.; Komatsuzaki, T.; Akai, I., *Computers & Chemistry* **1991**, *15*, 241-248.
138. Hortala, M. A.; Fabbrizzi, L.; Marcotte, N.; Stomeo, F.; Taglietti, A., *Journal of the American Chemical Society* **2003**, *125*, 20-21.
139. Horton, H. R.; Moran, L. A.; Scrimgeour, K. G.; Perry, M. D.; Rawn, J. D., *Principles of Biochemistry*. 4 ed.; Pearson Prentice Hall, : Upper Saddle River, NJ, 2006.
140. Hsu, J.-H.; Fann, W.; Tsao, P.-H.; Chuang, K.-R.; Chen, S.-A., *Journal of Physical Chemistry A* **1999**, *103*, 2375-2380.
141. Hu, X.; Castro-Rodriguez, I.; Meyer, K., *Journal of the American Chemical Society* **2003**, *125*, 12237-12245.
142. Huheey, J. E.; Keiter, E. A.; Keiter, R. L., *Inorganic Chemistry*. 4th ed.; Harper Collins College Publishers: New York, 1993.
143. Ingleson, M.; Patmore, N. J.; Ruggiero, G. D.; Frost, C. G.; Mahon, M. F.; Willis, M. C.; Weller, A. S., *Organometallics* **2001**, *20*, 4434-4436.
144. Islam, M.; Khanin, M.; Sadik, O. A., *Biomacromolecules* **2003**, *4*, 114-121.
145. Itooka, R.; Iguchi, Y.; Miyaura, N., *Journal of Organic Chemistry* **2003**, *68*, 6000-6004.
146. Jacobson, R. *REQAB*, 1.1; Molecular Structure Corporation, The Woodlands, Texas, USA, 1998.

147. Jang, Y. J.; Jun, E. J.; Lee, Y. J.; Kim, Y. S.; Kim, J. S.; Yoon, J., *Journal of Organic Chemistry* **2005**, *70*, 9603-9606.
148. Kaikawa, T.; Takimiya, K.; Aso, Y.; Otsubo, T., *Organic Letters* **2000**, *2*, 4197-4199.
149. Kamer, P. C. J.; Reek, J. N. H.; Van Leeuwen, P. W. N. M., *Chemtech* **1998**, *28*, 27-33.
150. Kamer, P. C. J.; van Leeuwen, P. W. N. M.; Reek, J. N. H., *Accounts of Chemical Research* **2001**, *34*, 895-904.
151. Kamplain, J. W.; Bielawski, C. W., *Chemical Communications* **2006**, 1727-1729.
152. Karlin, K. D.; Gultneh, Y.; Nicholson, T.; Zubieta, J., *Inorganic Chemistry* **1985**, *24*, 3727-3729.
153. Kawabata, Y.; Hayashi, T.; Ogata, I., *Journal of the Chemical Society, Chemical Communications* **1979**, 462-463.
154. Kazuhiro Yoshida, T. H., Rhodium(I)-Catalyzed Asymmetric Addition of Organometallic Reagents to Electron-Deficient Olefins. In *Modern Rhodium-Catalyzed Organic Reactions*, Prof, P. A. E., Ed. 2005; pp 55-77.
155. Khramov, D. M.; Boydston, A. J.; Bielawski, C. W., *Angewandte Chemie, International Edition* **2006**, *45*, 6186-6189.
156. Knapton, D.; Burnworth, M.; Rowan, S. J.; Weder, C., *Angewandte Chemie, International Edition* **2006**, *45*, 5825-5829.
157. Knoblock, K. M.; Silvestri, C. J.; Collard, D. M., *Journal of the American Chemical Society* **2006**, *128*, 13680-13681.
158. Knowles, W. S.; Sabacky, M. J.; Vineyard, B. D.; Weinkauff, D. J., *Journal of the American Chemical Society* **1975**, *97*, 2567-2568.
159. Koide, Y.; Bott, S. G.; Barron, A. R., *Organometallics* **1996**, *15*, 2213-2226.

160. Kraft, A.; Grimsdale, A. C.; Holmes, A. B., *Angewandte Chemie, International Edition* **1998**, *37*, 403-428.
161. Kranenburg, M.; Kamer, P. C. J.; Vanleeuwen, P.; Vogt, D.; Keim, W., *Journal of the Chemical Society-Chemical Communications* **1995**, 2177-2178.
162. Kranenburg, M.; Kamer, P. C. J.; Van Leeuwen, P. W. N. M., *European Journal of Inorganic Chemistry* **1998**, 155-157.
163. Kranenburg, M.; Kamer, P. C. J.; Van Leeuwen, P. W. N. M., *European Journal of Inorganic Chemistry* **1998**, 25-27.
164. Kress, T. H.; Leanna, M. R., *Synthesis* **1988**, 803-805.
165. Kuriyama, M.; Tomioka, K., *Tetrahedron Letters* **2001**, *42*, 921-923.
166. Kuriyama, M.; Nagai, K.; Yamada, K.; Miwa, Y.; Taga, T.; Tomioka, K., *Journal of the American Chemical Society* **2002**, *124*, 8932-8939.
167. Kutzelnigg, W., *Angewandte Chemie* **1984**, *96*, 262-286.
168. Kyba, E. P.; Helgeson, R. C.; Madan, K.; Gokel, G. W.; Tarnowski, T. L.; Moore, S. S.; Cram, D. J., *Journal of the American Chemical Society* **1977**, *99*, 2564-2571.
169. Laeng, F.; Breher, F.; Stein, D.; Gruetzmacher, H., *Organometallics* **2005**, *24*, 2997-3007.
170. Lagerlof, F.; Oliveby, A., *Advances in Dental Research* **1994**, *8*, 229-238.
171. Lavigne, J. J.; Anslyn, E. V., *Angewandte Chemie, International Edition* **1999**, *38*, 3666-3669.
172. Lee, C. K.; Lee, K. M.; Lin, I. J. B., *Organometallics* **2002**, *21*, 10-12.
173. Lee, C. K.; Vasam, C. S.; Huang, T. W.; Wang, H. M. J.; Yang, R. Y.; Lee, C. S.; Lin, I. J. B., *Organometallics* **2006**, *25*, 3768-3775.

174. Lee, D.; Swager, T. M., *Journal of the American Chemical Society* **2003**, *125*, 6870-6871.
175. Lee, D.; Swager, T. M., *Synlett* **2004**, 149-154.
176. Lee, H. M.; Lu, C. Y.; Chen, C. Y.; Chen, W. L.; Lin, H. C.; Chiu, P. L.; Cheng, P. Y., *Tetrahedron* **2004**, *60*, 5807-5825.
177. Lee, H. N.; Swamy, K. M. K.; Kim, S. K.; Kwon, J.-Y.; Kim, Y.; Kim, S.-J.; Yoon, Y. J.; Yoon, J., *Organic Letters* **2007**, *9*, 243-246.
178. Lee, T. R.; Carey, R. I.; Biebuyck, H. A.; Whitesides, G. M., *Langmuir* **1994**, *10*, 741-749.
179. Leevy, W. M.; Gammon, S. T.; Jiang, H.; Johnson, J. R.; Maxwell, D. J.; Jackson, E. N.; Marquez, M.; Piwnica-Worms, D.; Smith, B. D., *Journal of the American Chemical Society* **2006**, *128*, 16476-16477.
180. Leevy, W. M.; Johnson, J. R.; Lakshmi, C.; Morris, J.; Marquez, M.; Smith, B. D., *Chemical Communications* **2006**, 1595-1597.
181. Levy, S. M.; Kohout, F. J.; Guha-Chowdhury, N.; Kiritsy, M. C.; Heilman, J. R.; Wefel, J. S., *Journal of dental research* **1995**, *74*, 1399-1407.
182. Li, G. Y., *Angewandte Chemie, International Edition* **2001**, *40*, 1513-1516.
183. Liang, T.-T.; Naitoh, Y.; Horikawa, M.; Ishida, T.; Mizutani, W., *Journal of the American Chemical Society* **2006**, *128*, 13720-13726.
184. Lim, M. H.; Lippard, S. J., *Inorganic Chemistry* **2004**, *43*, 6366-6370.
185. Lim, M. H.; Lippard, S. J., *Journal of the American Chemical Society* **2005**, *127*, 12170-12171.
186. Lim, M. H.; Xu, D.; Lippard, S. J., *Nature Chemical Biology* **2006**, *2*, 375-380.
187. Lin, I. J. B.; Vasam, C. S., *Coordination Chemistry Reviews* **2007**, *251*, 642-670.

188. Liu, T.; Han, W.-G.; Himo, F.; Ullmann, G. M.; Bashford, D.; Touthkine, A.; Hahn, K. M.; Noodleman, L., *Journal of Physical Chemistry A* **2004**, *108*, 3545-3555.
189. Loch, J. A.; Albrecht, M.; Peris, E.; Mata, J.; Faller, J. W.; Crabtree, R. H., *Organometallics* **2002**, *21*, 700-706.
190. Luening, U.; Baumgartner, H., *Synlett* **1993**, 571-572.
191. Luening, U.; Baumstark, R.; Wangnick, C.; Mueller, M.; Schyja, W.; Gerst, M.; Gelbert, M., *Pure and Applied Chemistry* **1993**, *65*, 527-532.
192. Luening, U.; Baumbartner, H.; Wangnick, C., *Tetrahedron* **1996**, *52*, 599-604.
193. Luening, U.; Baumgartner, H.; Manthey, C.; Meynhardt, B., *Journal of Organic Chemistry* **1996**, *61*, 7922-7926.
194. Luening, U., *Journal of Materials Chemistry* **1997**, *7*, 175-182.
195. Ma, L.; Woloszynek, R. A.; Chen, W.; Ren, T.; Protasiewicz, J. D., *Organometallics* **2006**, *25*, 3301-3304.
196. Ma, L. Synthesis and Characterization of Ligands and Transition Metal Complexes Containing m-Terphenyl Scaffolds. Ph.D. Dissertation, Case Western Reserve University, Cleveland, OH, 2007.
197. Ma, L.; Imbesi, P. M.; Updegraff, J. B., III; Hunter, A. D.; Protasiewicz, J. D., *Inorganic Chemistry* **2007**, *46*, 5220-5228.
198. Ma, L.; Wobser, S. D.; Protasiewicz, J. D., *Journal of Organometallic Chemistry* **2007**, *692* 5331-5338
199. Ma, Y.; Song, C.; Ma, C.; Sun, Z.; Chai, Q.; Andrus, M. B., *Angewandte Chemie, International Edition* **2003**, *42*, 5871-5874.
200. Maerten, E.; Hassouna, F.; Couve-Bonnaire, S.; Mortreux, A.; Carpentier, J.-F.; Castanet, Y., *Synlett* **2003**, 1874-1876.

201. Magill, A. M.; McGuinness, D. S.; Cavell, K. J.; Britovsek, G. J. P.; Gibson, V. C.; White, A. J. P.; Williams, D. J.; White, A. H.; Skelton, B. W., *Journal of Organometallic Chemistry* **2001**, 617-618, 546-560.
202. Marcone, J. E.; Moloy, K. G., *Journal of the American Chemical Society* **1998**, 120, 8527-8528.
203. Mas-Marza, E.; Segarra, A. M.; Claver, C.; Peris, E.; Fernandez, E., *Tetrahedron Letters* **2003**, 44, 6595-6599.
204. Matsufuji, K.; Shiraishi, H.; Miyasato, Y.; Shiga, T.; Ohba, M.; Yokoyama, T.; Okawa, H., *Bulletin of the Chemical Society of Japan* **2005**, 78, 851-858.
205. Mattson, M. P.; Editor, *Protein Phosphorylation in Aging and Age-Related Disease*. 2004; p 178.
206. McCleskey, S. C.; Floriano, P. N.; Wiskur, S. L.; Anslyn, E. V.; McDevitt, J. T., *Tetrahedron* **2003**, 59, 10089-10092.
207. McGuinness, D. S.; Cavell, K. J., *Organometallics* **2000**, 19, 741-748.
208. Metivier, R.; Amengual, R.; Leray, I.; Michelet, V.; Genet, J.-P., *Organic Letters* **2004**, 6, 739-742.
209. Michael, A., *Journal für Praktische Chemie* **1887**, 35, 349-356.
210. Michael, A., *Journal für Praktische Chemie* **1894**, 49, 20-25.
211. Miyaura, N.; Suzuki, A., *Chemical Reviews* **1995**, 95, 2457-2483.
212. Morgan, B. P.; Smith, R. C., *Journal of Organometallic Chemistry* **2008**, 693, 11-16.
213. Morgan, B. P.; Galdamez, G. A.; Gilliard, R. J., Jr.; Smith, R. C., *Dalton Transactions* **2009**, 2020-2028.

214. Morisaki, Y.; Chujo, Y., *Angewandte Chemie, International Edition* **2006**, *45*, 6430-6437.
215. Moss, R. J.; Wadsworth, K. J.; Chapman, C. J.; Frost, C. G., *Chemical Communications* **2004**, 1984-1985.
216. Narayanan, A.; Varnavski, O. P.; Swager, T. M.; Goodson, T., III, *Journal of Physical Chemistry C* **2008**, *112*, 881-884.
217. Nguyen, B. T.; Wiskur, S. L.; Anslyn, E. V., *Organic Letters* **2004**, *6*, 2499-2501.
218. Nguyen, B. T.; Anslyn, E. V., *Coordination Chemistry Reviews* **2006**, *250*, 3118-3127.
219. Niksch, T.; Goerls, H.; Weigand, W., *European Journal of Inorganic Chemistry*, 95-105.
220. Nolan, E. M.; Ryu, J. W.; Jaworski, J.; Feazell, R. P.; Sheng, M.; Lippard, S. J., *Journal of the American Chemical Society* **2006**, *128*, 15517-15528.
221. Nolan, S. P., *N-Heterocyclic Carbenes in Synthesis*. Wiley-VCH: Weinheim, Germany, 2006.
222. Nonnenmacher, M.; Kunz, D.; Rominger, F.; Oeser, T., *Journal of Organometallic Chemistry* **2007**, *692*, 2554-2563.
223. Nonnenmacher, M.; Kunz, D.; Rominger, F.; Oeser, T., *Journal of Organometallic Chemistry* **2007**, *692*, 2554-2563.
224. O'Neil, E. J.; Smith, B. D., *Coordination Chemistry Reviews* **2006**, *250*, 3068-3080.
225. Oefele, K., *Journal of Organometallic Chemistry* **1968**, *12*, P42-P43.
226. Okada, T.; Katou, K.; Hirose, T.; Yuasa, M.; Sekine, I., *Chemistry Letters* **1998**, 841.

227. Otomaru, Y.; Senda, T.; Hayashi, T., *Organic Letters* **2004**, *6*, 3357-3359.
228. Otomaru, Y.; Kina, A.; Shintani, R.; Hayashi, T., *Tetrahedron: Asymmetry* **2005**, *16*, 1673-1679.
229. Otomaru, Y.; Okamoto, K.; Shintani, R.; Hayashi, T., *Journal of Organic Chemistry* **2005**, *70*, 2503-2508.
230. Parshall, G. W., *Accounts of Chemical Research* **1970**, *3*, 139-144.
231. Pauling, L., *The nature of the chemical bond, and the structure of molecules and crystals : an introduction to modern structural chemistry*. 2nd ed.; Cornell University Press: Ithaca, N.Y., 1948; p xvi, 450.
232. Peris, E.; Crabtree, R. H., *Coordination Chemistry Reviews* **2004**, *248*, 2239-2246.
233. Perry, M. C.; Cui, X.; Burgess, K., *Tetrahedron: Asymmetry* **2002**, *13*, 1969-1972.
234. Piatek, A. M.; Bomble, Y. J.; Wiskur, S. L.; Anslyn, E. V., *Journal of the American Chemical Society* **2004**, *126*, 6072-6077.
235. Poater, A.; Ragone, F.; Giudice, S.; Costabile, C.; Dorta, R.; Nolan, S. P.; Cavallo, L., *Organometallics*, **2008**, *27*, 2679-2681.
236. Pope, C.; Karanth, S.; Liu, J., *Environmental Toxicology and Pharmacology* **2005**, *19*, 433-446.
237. Portnoy, M.; Milstein, D., *Organometallics* **1993**, *12*, 1655-1664.
238. Power, P. P., *Chemical Reviews* **1999**, *99*, 3463-3503.
239. Pryjomska, I.; Bartosz-Bechowski, H.; Ciunik, Z.; Trzeciak, A. M.; Zi'olkowski, J. o. J., *Dalton Transactions* **2006**, 213-220.

240. Pu, K.-Y.; Chen, Y.; Qi, X.-Y.; Qin, C.-Y.; Chen, Q.-Q.; Wang, H.-Y.; Deng, Y.; Fan, Q.-L.; Huang, Y.-Q.; Liu, S.-J.; Wei, W.; Peng, B.; Huang, W., *Journal of Polymer Science, Part A: Polymer Chemistry* **2007**, *45*, 3776-3787.
241. Pucheault, M.; Darses, S.; Genet, J.-P., *Tetrahedron Letters* **2002**, *43*, 6155-6157.
242. Raghothama, K. G., *Annual Review of Plant Physiology and Plant Molecular Biology* **1999**, *50*, 665-693.
243. Rajan, S. S. S.; Marwaha, B. C., *Fertilizer Research* **1993**, *35*, 47-59.
244. Ramey, M. B.; Hiller, J. A.; Rubner, M. F.; Tan, C.; Schanze, K. S.; Reynolds, J. R., *Macromolecules* **2005**, *38*, 234-243.
245. Ramirez, J.; Corberan, R.; Sanau, M.; Peris, E.; Fernandez, E., *Chemical Communications* **2005**, 3056-3058.
246. Reetz, M. T.; Moulin, D.; Gosberg, A., *Organic Letters* **2001**, *3*, 4083-4085.
247. Reppe, W.; Sweckendiek, W. J., *Justus Liebigs Annalen der Chemie* **1948**, *560*, 104-116.
248. Richards, F. M., *Annual Review of Biophysics and Bioengineering* **1977**, *6*, 151-176.
249. Rigaku/MSD *CrystalClear*, MSD, The Woodlands, Texas, USA, and Rigaku Corporation, Tokyo, Japan, 2006.
250. Roelen, O., *Oel und Kohle* **1938**, *14*, 1077-1079.
251. Rose, A.; Zhu, Z.; Madigan, C. F.; Swager, T. M.; Bulovic, V., *Nature* **2005**, *434*, 876-879.
252. Roseblade, S. J.; Ros, A.; Monge, D.; Alcarazo, M.; Alvarez, E.; Lassaletta, J. M.; Fernandez, R., *Organometallics* **2007**, *26*, 2570-2578.
253. Rossiter, B. E.; Swingle, N. M., *Chemical Reviews* **1992**, *92*, 771-806.

254. Rothfuss, H.; Barry, J. T.; Huffman, J. C.; Caulton, K. G.; Chisholm, M. H., *Inorganic Chemistry* **1993**, *32*, 4573-4577.
255. Saednya, A.; Hart, H., *Synthesis* **1996**, 1455-1458.
256. Saito, S.; Yamaguchi, H.; Muto, H.; Makino, T., *Tetrahedron Letters* **2007**, *48*, 7498-7501.
257. Sakai, M.; Hayashi, H.; Miyaura, N., *Organometallics* **1997**, *16*, 4229-4231.
258. Sanger, A. R., *Journal of the Chemical Society, Chemical Communications* **1975**, 893-894.
259. Satou, T.; Sakai, T.; Kaikawa, T.; Takimiya, K.; Otsubo, T.; Aso, Y., *Organic Letters* **2004**, *6*, 997-1000.
260. Schlosser, M., *Organometallics in synthesis : a manual*. John Wiley & Sons: Chichester, West Sussex, England ; New York, 1994; p 603.
261. Schmidtchen, F. P.; Berger, M., *Chemical Reviews* **1997**, *97*, 1609-1646.
262. Schmitz, M.; Leininger, S.; Bergstrasser, U.; Regitz, M., *Heteroatom Chemistry* **1998**, *9*, 453-460.
263. Scholl, M.; Ding, S.; Lee, C. W.; Grubbs, R. H., *Organic Letters* **1999**, *1*, 953-956.
264. Scholl, M.; Trnka, T. M.; Morgan, J. P.; Grubbs, R. H., *Tetrahedron Letters* **1999**, *40*, 2247-2250.
265. Scholl, R.; Seer, C., *Monatshefte fuer Chemie* **1912**, *33*, 1-8.
266. Schwarzenbach, G., *Complexometric Titrations*. . Interscience Publishers: London, 1957.
267. Serp, P.; Hernandez, M.; Richard, B.; Kalck, P., *European Journal of Inorganic Chemistry* **2001**, 2327-2336.

268. Shah, S.; Eichler, B. E.; Smith, R. C.; Power, P. P.; Protasiewicz, J. D., *New Journal of Chemistry* **2003**, *27*, 442-445.
269. Shaw, B. L.; Mann, B. E.; Masters, C., *Journal of the Chemical Society A: Inorganic, Physical, Theoretical* **1971**, 1104-1106.
270. Sheldrick, G. M., *Acta Crystallography, Sect. A: Foundation of Crystallography* **2008**, *A64*, 112-122.
271. Shi, M.; Qian, H.-X., *Applied Organometallic Chemistry* **2005**, *19*, 1083-1089.
272. Shiraishi, H.; Jikido, R.; Matsufuji, K.; Nakanishi, T.; Shiga, T.; Ohba, M.; Sakai, K.; Kitagawa, H.; Okawa, H., *Bulletin of the Chemical Society of Japan* **2005**, *78*, 1072-1076.
273. Sierra, M., *Environmental Science and Pollution Control Series* **1994**, *10*, 145-149.
274. Silvestri, M. A.; Bromfield, D. C.; Lepore, S. D., *Journal of Organic Chemistry* **2005**, *70*, 8239-8241.
275. Slauch, L. H.; Mullineaux, R. D. *Hydroformylation of olefins*. 3239569, 19660308, **1966**.
276. Slauch, L. H.; Mullineaux, R. D., *J. Organometal. Chem.* **1968**, *13*, 469-477.
277. Smaldone, R. A.; Moore, J. S., *European Journal of Chemistry* **2008**, *14*, 2650-2657.
278. Smith, R. C.; Protasiewicz, J. D., *Organometallics* **2004**, *23*, 4215-4222.
279. Smith, R. C.; Bodner, C. R.; Earl, M. J.; Sears, N. C.; Hill, N. E.; Bishop, L. M.; Sizemore, N.; Hehemann, D. T.; Bohn, J. J.; Protasiewicz, J. D., *Journal of Organometallic Chemistry* **2005**, *690*, 477-481.
280. Smith, R. C.; Gleason, B.; Protasiewicz, J. D., *Journal of Material Chemistry* **2006**, *16*, 2445-2452.

281. Smith, R. C. *Macromolecules Rapid Communication* **2010**, *30*, 2067-2078.
282. Soederberg, M.; Edlund, C.; Kristensson, K.; Dallner, G., *Lipids* **1991**, *26*, 421-425.
283. Solov'ev, V. P.; Strakhova, N. N.; Raevsky, O. A.; Ruediger, V.; Schneider, H.-J., *Journal of Organic Chemistry* **1996**, *61*, 5221-5226.
284. Sonogashira, K.; Tohda, Y.; Hagihara, N., *Tetrahedron Letters* **1975**, 4467-4470.
285. Stille, J. K., *Angewandte Chemie, International Edition* **1986**, *98*, 504-519.
286. Surak, J. G.; Herman, M. F.; Haworth, D. T., *Analytical Chemistry* **1965**, *37*, 428-429.
287. Suzuki, M.; Kanatomi, H.; Murase, I., *Chemistry Letters* **1981**, 1745-1748.
288. Swager, T. M., *Accounts of Chemical Research* **2008**, *41*, 1181-1189.
289. Tamao, K.; Sumitani, K.; Kumada, M., *Journal of the American Chemical Society* **1972**, *94*, 4374-4376.
290. Taton, T. A.; Chen, P., *Angewandte Chemie International Edition* **1996**, *35*, 1011-1013.
291. Thayer, J. S., *Advances in Organometallic Chemistry* **1975**, *13*, 1-45.
292. Thomas, S. W., III; Amara, J. P.; Bjork, R. E.; Swager, T. M., *Chemical Communications* **2005**, 4572-4574.
293. Thompson, B. C.; Frechet, J. M. J., *Angewandte Chemie, International Edition* **2008**, *47*, 58-77.
294. Tobey, S. L.; Anslyn, E. V., *Organic Letters* **2003**, *5*, 2029-2031.
295. Tolman, C. A., *Journal of the American Chemical Society* **1970**, *92*, 2956-2965.

296. Tolman, C. A., *Journal of the American Chemical Society* **1970**, *92*, 2953-2956.
297. Tolman, C. A.; Meakin, P. Z.; Lindner, D. I.; Jesson, J. P., *Journal of the American Chemical Society* **1974**, *96*, 2762-2774.
298. Tolman, C. A., *Chemical Reviews* **1977**, *77*, 313-348.
299. Tolman, W. B.; Que, L., Jr., *Journal of the Chemical Society, Dalton Transactions* **2002**, 653-660.
300. Tour, J. M.; Jones, L., II; Pearson, D. L.; Lamba, J. J. S.; Burgin, T. P.; Whitesides, G. M.; Allara, D. L.; Parikh, A. N.; Atre, S., *Journal of the American Chemical Society* **1995**, *117*, 9529-9534.
301. Trost, B. M.; Breit, B.; Peukert, S.; Zambrano, J.; Ziller, J. W., *Angewandte Chemie, International Edition* **1995**, *34*, 2386-2388.
302. Tsuboyama, A.; Iwawaki, H.; Furugori, M.; Mukaide, T.; Kamatani, J.; Igawa, S.; Moriyama, T.; Miura, S.; Takiguchi, T.; Okada, S.; Hoshino, M.; Ueno, K., *Journal of the American Chemical Society* **2003**, *125*, 12971-12979.
303. Tu, T.; Assenmacher, W.; Peterlik, H.; Weisbarth, R.; Nieger, M.; Doetz, K. H., *Angewandte Chemie, International Edition* **2007**, *46*, 6368-6371.
304. Uchida, T.; Editor, *Protein Phosphorylation: Dysregulation and Diseases..* **2004**; p 89 pp.
305. Unruh, J. D.; Christenson, J. R., *Journal of Molecular Catalysis* **1982**, *14*, 19-34.
306. Van der Veen, L. A.; Boele, M. D. K.; Bregman, F. R.; Kamer, P. C. J.; Van Leeuwen, P. W. N. M.; Goubitz, K.; Fraanje, J.; Schenk, H.; Bo, C., *Journal of the American Chemical Society* **1998**, *120*, 11616-11626.
307. Van der Veen, L. A.; Kamer, P. C. J.; Van Leeuwen, P. W. N. M., *Angewandte Chemie, International Edition* **1999**, *38*, 336-338.
308. van der Veen, L. A.; Keeven, P. K.; Kamer, P. C. J.; van Leeuwen, P. W. N. M., *Dalton Transactions* **2000**, 2105-2112.

309. Van Haaren, R. J.; Oevering, H.; Coussens, B. B.; Van Strijdonck, G. P. F.; Reek, J. N. H.; Kamer, P. C. J.; Van Leeuwen, P. W. N. M., *European Journal of Inorganic Chemistry* **1999**, 1237-1241.
310. van Leeuwen, P.; Kamer, P. C. J.; Reek, J. N. H., *Pure and Applied Chemistry* **1999**, *71*, 1443-1452.
311. van Leeuwen, P. W. N. M.; Kamer, P. C. J.; Reek, J. N. H.; Dierkes, P., *Chemical Reviews* **2000**, *100*, 2741-2769.
312. Verkade, J. G.; Quin, L. D., *Phosphorus-31 NMR Spectroscopy in Stereochemical Analysis*. VCH: Deerfield Beach, 1987; Vol. 8, p 717.
313. Vinod, T. K.; Hart, H., *Journal of the American Chemical Society* **1988**, *110*, 6574-6575.
314. Vinod, T. K.; Hart, H., *Journal of Organic Chemistry* **1990**, *55*, 5461-5466.
315. Vinod, T. K.; Hart, H., *Journal of the American Chemical Society* **1990**, *112*, 3250-3252.
316. Vinod, T. K.; Hart, H., *Journal of Organic Chemistry* **1991**, *56*, 5630-5640.
317. Vinod, T. K.; Hart, H., *Topics in Current Chemistry* **1994**, *172*, 119-178.
318. Walker, N. R.; Linman, M. J.; Timmers, M. M.; Dean, S. L.; Burkett, C. M.; Lloyd, J. A.; Keelor, J. D.; Baughman, B. M.; Edmiston, P. L., *Analytical Chimica Acta* **2007**, *593*, 82-91.
319. Walkup, G. K.; Burdette, S. C.; Lippard, S. J.; Tsien, R. Y., *Journal of the American Chemical Society* **2000**, *122*, 5644-5645.
320. Wang, J.-W.; Li, Q.-S.; Xu, F.-B.; Song, H.-B.; Zhang, Z.-Z., *Eur. Journal of Organic Chemistry* **2006**, 1310-1316.
321. Wanzlick, H. W.; Schoenherr, H. J., *Angewandte Chemie, International Edition* **1968**, *7*, 141-142.

322. Wariishi, K.; Morishima, S.; Inagaki, Y., *Organic Process Research & Development* **2003**, *7*, 98-100.
323. Weskamp, T.; Bohm, V. P. W.; Herrmann, W. A., *Journal of Organometallic Chemistry* **1999**, *585*, 348-352.
324. Williams, K. A.; Boydston, A. J.; Bielawski, C. W., *J. R. Soc. Interface* **2007**, *4*, 359-362.
325. Wiskur, S. L.; Ait-Haddou, H.; Lavigne, J. J.; Anslyn, E. V., *Accounts of Chemical Research* **2001**, *34*, 963-972.
326. Wiskur, S. L.; Anslyn, E. V., *Journal of the American Chemical Society* **2001**, *123*, 10109-10110.
327. Wiskur, S. L.; Lavigne, J. J.; Metzger, A.; Tobey, S. L.; Lynch, V.; Anslyn, E. V., *Chemistry A European Journal* **2004**, *10*, 3792-3804.
328. Withers, H. P., Jr.; Seyferth, D.; Fellmann, J. D.; Garrou, P. E.; Martin, S., *Organometallics* **1982**, *1*, 1283-1288.
329. Wittig, G.; Geissler, G., *Justus Liebigs Annalen der Chemie* **1953**, *580*, 44-57.
330. Wolf, C.; Lerebours, R., *Journal of Organic Chemistry* **2003**, *68*, 7077-7084.
331. Xu, Q.; Duan, W.-L.; Lei, Z.-Y.; Zhu, Z.-B.; Shi, M., *Tetrahedron* **2005**, *61*, 11225-11229.
332. Yang, J.-S.; Swager, T. M., *Journal of the American Chemical Society* **1998**, *120*, 11864-11873.
333. Yang, J.-S.; Swager, T. M., *Journal of the American Chemical Society* **1998**, *120*, 5321-5322.
334. Yang, Y.-C.; Baker, J. A.; Ward, J. R., *Chemical Reviews* **1992**, *92*, 1729-1743.
335. Yang, Y.-C., *Accounts of Chemical Research* **1999**, *32*, 109-115.

336. Yuan, W.-C.; Cun, L.-F.; Gong, L.-Z.; Mi, A.-Q.; Jiang, Y.-Z., *Tetrahedron Letters* **2005**, *46*, 509-512.
337. Zhang, T.; Wang, W.; Gu, X.; Shi, M., *Organometallics* **2008**, *27*, 753-757.
338. Zou, G.; Wang, Z.; Zhu, J.; Tang, J., *Chemical Communications* **2003**, 2438-2439.
339. Zyryanov, G. V.; Palacios, M. A.; Anzenbacher, P., Jr., *Organic Letters* **2008**, *10*, 3681-3684.